Evaluation and comparison of the ability of three industrially relevant adsorbents to remove alcohol contaminants from an alkane solvent

by

Jomaré Groenewald

Thesis presented in partial fulfilment
of the requirements for the Degree

of

MASTER OF ENGINEERING
(CHEMICAL ENGINEERING)

in the Faculty of Engineering
at Stellenbosch University

Supervisor

Professor C.E. Schwarz

Co-Supervisor

Professor A.J. Burger

April 2019

DECLARATION

By submitting this thesis electronically, I declare that the entirety of the work contained therein is my own, original work, that I am the sole author thereof (save to the extent explicitly otherwise stated), that reproduction and publication thereof by Stellenbosch University will not infringe any third party rights and that I have not previously in its entirety or in part submitted it for obtaining any qualification.

Date: *April 2019*

PLAGIARISM DECLARATION

1. Plagiarism is the use of ideas, material and other intellectual property of another's work and to present is as my own.
2. I agree that plagiarism is a punishable offence because it constitutes theft.
3. I also understand that direct translations are plagiarism.
4. Accordingly all quotations and contributions from any source whatsoever (including the internet) have been cited fully. I understand that the reproduction of text without quotation marks (even when the source is cited) is plagiarism.
5. I declare that the work contained in this assignment, except where otherwise stated, is my original work and that I have not previously (in its entirety or in part) submitted it for grading in this module/assignment or another module/assignment.

Student number: ……..

Initials and surname: ……..

Signature: ……..

Date: ……..

Abstract

Adsorption has been used successfully in many industries and has replaced the use of processes such as distillation in some cases.

The adsorption process is influenced by many factors and its efficiency is largely dependent on the regeneration of the spent adsorbent. Adsorption is system specific and requires experimental adsorption and regeneration data for the system to be separated. A better understanding of adsorbent regeneration and its effects on the adsorption process also aids in improving the overall efficiency of the process.

The aims of this project were to investigate the adsorption of alcohol solutes from an alkane solvent using three industrially used adsorbents and to evaluate the effects of regeneration on each adsorbent. This was achieved through the following objectives: (1) designing and constructing batch adsorption and regeneration experimental setups; (2) performing equilibrium and kinetic adsorption tests to evaluate the effect of the type of adsorbent, type of adsorbate and temperature on the adsorption process, (3) modelling this data with existing equilibrium and kinetic models; (4) Perform cyclic adsorption-regeneration batch tests.

Objective one was met by designing and constructing two batch experimental setups. The adsorption setup consisted of a heated water bath housing 10 tall form beakers in which the adsorption experiments were run. The column type regeneration system included three regeneration columns, a condenser, a liquid trap and activated carbon trap. Nitrogen gas was used as the carrier gas in the system and electric heat tracing on the column inlet tubing and regeneration columns was used to heat the system to the required regeneration temperatures.

Adsorption tests investigating the alcohol adsorbing capabilities were performed using 3 types of adsorbates (1-hexanol, 1-octanol and 1-decanol), 3 types of adsorbents (activated alumina F-220, Selexsorb® CD and Selexsorb® CDx) and 3 temperatures (25, 30 and 35 °C). Overall, the activated alumina F-220 adsorbent performed better than the other two adsorbents. Generally, the 1-hexanol showed higher adsorbent loadings compared to those of 1-octanol and 1-decanol. The performance of the adsorption systems appeared to favour the slightly higher adsorption temperatures, showing the largest adsorbent loadings at 35 °C.

The third objective was met by applying three isotherm and three kinetic models to the equilibrium and kinetic adsorption data respectively. The isotherm modelling confirmed that all adsorption systems exhibited favourable adsorption with physical bonds formed between adsorbate and

adsorbent. The kinetic modelling gave insight into the rate-limiting step of each kinetic system, indicating that the rate-limiting step of each adsorption system could not be solely defined as intra-particle diffusion or adsorption reaction, but was rather a combination of the two.

Lastly, the effects of two regeneration temperatures (185 and 205 °C) were tested on the three adsorbents in 8 adsorption-regeneration cycles. All three adsorbents remained thermally stable for all 8 cycles and the activated alumina F-220 adsorbent showed the lowest decline in alcohol removal efficiency for both regeneration temperatures. At a regeneration temperature of 185 °C the adsorbents showed slightly higher initial adsorbent loadings, but a greater decline in adsorbent loading over the 8 cycles than at the 205 °C regeneration temperature.

Recommended future work suggestions included investigating higher adsorption temperatures to find the optimal temperature and investigating the effect of regeneration duration on the regeneration process.

Opsomming

Adsorpsie word suksesvol in baie industrieë gebruik en het die gebruik van prosesse soos distillasie in sommige gevalle vervang.

Die adsorpsieproses word beïnvloed deur vele faktore en sy doeltreffendheid steun grootliks op die regenerasie van die gebruikte adsorbeermiddel. Adsorpsie is stelsel-spesifiek en vereis eksperimentele adsorpsie- en regenerasie-data vir die stelsel om geskei te word. ’n Beter begrip van adsorpsie regenerasie en sy effek op die adsorpsieproses help ook met die verbetering van die algehele doeltreffendheid van die proses.

Die doel van hierdie projek was om die adsorpsie van alkohol opgeloste stowwe vanuit ’n alkaan oplosmiddel te ondersoek deur drie adsorbeermiddels wat in die industrie gebruik word, te gebruik en die effek van regenerasie op elke adsorbeermiddel te evalueer. Dit is bereik deur die volgende doelstellings: (1) die ontwerp en bou van lotadsorpsie en regenerasie eksperimentele opstellings; (2) uitvoering van ewewig en kinetiese adsorpsietoetse om die effek van die tipe adsorbeermiddel, tipe adsorbaat en temperatuur op die adsorpsieproses te evalueer; (3) modellering van hierdie data met bestaande ewewigs- en kinetiese modelle; (4) uitvoering van sikliese adsorpsie-regenerasie lottoetse.

Die eerste doel is behaal deur twee loteksperimentele opstellings te ontwerp en te bou. Die adsorpsie opstelling het uit ’n verhitte waterbad bestaan, wat tien lang vorm bekers huisves waarin adsorpsie eksperimente gedoen is. Die kolomtipe regenerasiestelsel het drie regenerasie kolomme, ’n kondensator, ’n vloeistofvanger en geaktiveerde koolstofvanger ingesluit. Stikstofgas is gebruik as die draergas in die stelsel en elektriese hitte opsporing op die kolominlaatpype en regenerasiekolomme is gebruik om die stelsel na die vereiste regenerasie temperature te verhit.

Adsorpsietoetse wat die alkohol adsorbering vermoë ondersoek, is uitgevoer deur drie tipes adsorbate (1-heksanol, 1-oktanol en 1-dekanol), drie tipes adsorbeermiddels (geaktiveerde alumina F-220, Selexsorb® CD en Selexsorb® CDx) en drie temperature (25 °C, 30 °C en 35 °C) te gebruik. Oor die algeheel het die geaktiveerde alumina beter doeltreffendheid as die ander twee adsorbeermiddels gehad. Gewoonlik het die 1-heksanol hoër adsorbeermiddellading in vergelyking met dié van 1-oktanol en 1-dekanol, gehad. Die werkverrigting van die adsorpsiestelsel lyk of dit die effens hoër adsorpsie temperature verkies, met die grootste adsorbeermiddelladings by 35 °C.

Die derde doel is bereik deur drie isotermiese en drie kinetiese modelle op die ewewig en kinetiese adsorpsie data onderskeidelik toe te pas. Die isoterm modellering het bevestig dat alle adsorpsiestelsels gunstige adsorpsie vertoon met fisiese verbindings wat gevorm is tussen adsorbate

en adsorbeermiddels. Die kinetiese modellering het insig gebied in die tempo-beperkende stap van elke kinetiese stelsel, wat aandui dat die tempo-beperkende stap van elke adsorpsiestelsel nie alleenlik gedefinieer kan word as intra-partikel diffusie of adsorpsie reaksie nie, maar dat dit eerder ’n kombinasie van die twee is.

Laastens is die effek van twee regenerasie temperature (185 °C en 205 °C) op die drie adsorbsie-regenerasiesiklusse getoets. Al drie adsorbeermiddels het termies stabiel gebly vir al agt siklusse en die geaktiveerde alumina F-220 adsorbeermiddel het die laagste vermindering in alkohol-verwydering-doeltreffendheid vir beide regenerasie temperature gewys. By ’n regenerasie temperatuur van 185 °C het die adsorbeermiddels effens hoër aanvanklike adsorbeermiddellading gewys, maar ’n groter afname in adsorbeermiddellading oor die agt siklusse as by die 205 °C regenerasie temperatuur.

Voorstelle vir toekomstige werk sluit in die ondersoek van hoër adsorpsie temperature om die optimale temperatuur te vind en die ondersoek van die effek van regenerasie duur op die regenerasieproses.

Acknowledgements

I would like to thank my supervisors, Prof. Schwarz and Prof. Burger, for their support, guidance, understanding and financial support throughout my masters.

My parents, John and Komien. Thank you for always believing in me and supporting me. Thank you for always being there to listen to me and give me hugs when I needed them. Thank you for helping me in any way you could to get through my masters.

Kirsten and Stefan Heusser. Thank you so much for providing me with a place to stay, food, wisdom and support. You two are truly a blessing and your help really took some of the weight off my shoulders. I can never thank you enough.

My brother and sister, Jordan and Tiffany, thanks for keeping me laughing and just being there for me.

My cousin, Matthew. Cuz, you are the greatest and I can't imagine life without you. Thank you for everything.

Thank you to my absolute best, Jolene, for all the coffee dates and sanity checks. Thanks for believing in me, keeping me positive and making sure I knew I could do it. Your support means the world.

Carla, dankie vir alles wat jy oor die laaste twee jaar vir my gedoen het. Dankie vir al die wyn sessies, die lag sessies, die dans sessies en chat sessies. Dankie dat jy altyd daar was, ek sal nooit genoeg kan dankie sê nie.

My other two besties, Elisa and Zantel. You two are amazing and I really appreciate you both. Thank you for always believing in my abilities and being convinced that I am super smart. Thank you for all the coffee, cake and late night chats.

I would like to thank Oom Anton, Oom Jos, Bevan and Brent for all the help with the building of my various experimental parts. Oom Anton, dankie vir al die braai's, die werk wat Oom gedoen het op my setup en die drukkies. Ek waardeer dit, dankie.

Dankie Calizé en Sunel vir al die wyn en lag sessies.Thank you Uncle Damian for all the help with the electrical stuff and all the bottles of wine.

Dankie Jandre vir al die koffie en chat sessies.

Dankie Heinrich vir al die hulp en onderstening.

Dankie aan Tannie Hanlie vir die hulp met die GC. Dankie Jaco vir al die geselsies. Dankie Levine vir jou mooi gimlag waarop ek altyd kon staat maak.

Dankie Ollie dat jy altyd die gas bottels so gou as moontlik omgeruil het vir my en dankie dat jy altyd bereid was om my te help.

Dankie Alvin vir al die advies en hulp.

Dankie Riccardo vir al die naweek buddy sessies.

Lastly, I'd like to thank God for never leaving my side and carrying me through these past few years.

Contents

Nomenclature

Roman symbols

Symbol	Definition
Δq	relative error
C_f	Initial adsorbate concentration
C_t	adsorbate concentration at time t
C_e	Equilibrium adsorbate concentration
q_e	equilibrium adsorption capacity
R^2	coefficient of determination
t	time
T	temperature
V	solution volume
W	adsorbent mass

Isotherm and Kinetic Model symbols

Symbol	Definition	Symbol	Definition
Langmuir isotherm model		Weber-Morris kinetic model	
K_L	Langmuir constant	B	initial adsorption constant
q_m	maximum adsorption capacity	k_{id}	intra-particle diffusion rate constant
R_L	Langmuir dimensionless constant	Pseudo-1st-Order kinetic model	
Freundlich isotherm model		k_1	first order rate constant
K_f	Freundlich constant	Pseudo-2nd-Order kinetic model	
n_f	Freundlich constant	k_2	second order rate constant
Dubinin-Radushkevich isotherm model			
ε	Concentration dependent variable		
k_{ad}	Dubinin-Radushkevich constant		
q_s	Dubinin-Radushkevich constant		

Physical constants

Symbol	Description	Value
R	Universal gas constant	8,314 $J\cdot(mol\cdot K)^{-1}$

Abbreviations

Abbreviation	Description
F-220	Activated alumina F-220 adsorbent
SCD	Selexsorb® CD adsorbent
SCDx	Selexsorb® CDx adsorbent
RMSE	Root Mean Square Error
Fr	Freundlich
D-R	Dubinin-Radushkevich
W-M	Weber-Morris

Chapter 1: Introduction

Separation is often defined as the process by which a mixture is transformed into two or more product streams that differ from one another in composition (Yang, 2003). Separation is often difficult to achieve and generally accounts for the majority of operation costs in industrial processes. Separation processes form an essential part of the chemical, petrochemical and materials processing industries by reducing waste, improving energy efficiency and improving efficiency of raw materials usage (National Research Council, 1998). The types of separation techniques used in these industries include distillation, membrane separations, crystallization, precipitation, absorption and stripping and adsorption (National Research Council, 1998).

Distillation has a dominant role in the separation technology industry due to its wide applicability and simplicity, providing the standard to which most other separation technologies are measured (Ruthven, 1984). However, due to the rise in energy costs and the energy usage associated with distillation alternative, more attractive, separation techniques are being employed.

Adsorption, is one such technique considered as an alternative to distillation. It offers more energy efficient separation and can often be used in cases where distillation fails due to components with similar boiling points.

Adsorption separates gas or liquid components (adsorbates) from a bulk solution using a microporous solid material (adsorbent) with an affinity for the specific components, allowing the components to bond to the adsorbent's surface creating a superficial layer of adsorbed molecules (Green & Perry, 2008).

An adsorption process is characterized by the type of adsorbent used, the adsorbate(s) removed and the temperature and pressure at which the system is operated. These characteristics influence the equilibrium and kinetics of the process which affect the design of an adsorption column, its process operating values and the process efficiency.

The efficiency of the adsorption process is also influenced by the regeneration technique used. Adsorption is, in many cases, a reversible process and adsorbates are removed from the adsorbent surface using a regeneration technique. These techniques include pressure, temperature, displacement or purge-gas regeneration (Ruthven, 1984). The regeneration of adsorbents naturally causes adsorbents to lose adsorption capacity over time resulting in a decrease in adsorption efficiency.

The selection of adsorbent, adsorption system temperature, regeneration technique and its associated variables is consequently vitally important to ensuring an economically viable and efficient adsorption process and can be done through experimental investigations.

1.1 Project Background

The adsorption technique has been used extensively in industrial separation processes over the past few decades for separations of paraffins and olefins, C_8 aromatics and light gases (Cavalcante Jr., 2000). Adsorption processes are used in industries such as the natural gas industry for drying gases and carbon dioxide removal, the waste water treatment industry for removing organic contaminants, many chemical plants use adsorption to remove NOx from various gas streams and refineries apply the technique for the removal of chloride and water from hydrogen amongst other things.

In the petrochemical industry, adsorption is used for drying gases and cracked liquids, purifying alkene streams prior to polymerisation and for solvent purification in downstream processing. Solvent purification is performed to recover spent solvents to minimise waste and purify chemical end-products that are to be sold. It generally involves the removal of organic compounds such as alcohols and ketones from alkane solvent streams. Adsorption is successfully used in solvent purification, however due to the numerous contaminants in the solvent streams and various factors affecting the adsorption process, a better understanding of the adsorption system in this context could lead to an improved process efficiency.

This project therefore focuses on adsorption systems present within the petrochemical industry and aims to form the basis of adsorption research within the Process Engineering Department at Stellenbosch University. The complexity of adsorption systems within this industry requires the knowledge of simpler systems in order to aid in understanding the behaviour of more complex systems. The lack of open literature data and the need for system specific data within an adsorption system, meant focusing this research project on investigating single adsorbate systems involving the removal of alcohol contaminants from an alkane solvent.

1.2 Aims and Objectives

The aims of this project are to investigate the adsorption of alcohol solutes from an alkane solvent using three industrially used adsorbents and to evaluate the effects of regeneration on each adsorbent.

To achieve these aims the following objectives need to be fulfilled:

1. Design and develop a batch adsorption and regeneration experimental setup
2. Perform equilibrium and kinetic adsorption tests
    a. Determine the effects of the type of adsorbate, temperature and type of adsorbent on the adsorption process
3. Model measured equilibrium and kinetic data using existing models
4. Perform cyclic adsorption – regeneration tests to compare the effects of regeneration on the three adsorbents tested

1.3 Project Scope

Adsorption systems found in the petrochemical industry are fairly complex and due to a lack of literature and data, it is important to start with simplified systems to build upon in future studies. Therefore the scope of this project is limited to the investigation of single adsorbate systems.

i. Adsorbates and Solvent

Alkanes form the bulk of many streams within the petrochemical industry, specifically detergent range alkanes. Therefore *n*-decane was chosen as the solvent in this study due to economic and relevance reasons.

Alcohols are also often found in the petrochemical industry, but usually in small amounts. Therefore a series of 1-alcohols were considered as adsorbates. These were 1-hexanol, 1-octanol and 1-decanol. These three alcohols were chosen in order to investigate the influence of molecule size on adsorption. Their availability and price made them ideal for the proposed project.

ii. Adsorbents

The adsorbents chosen were done so based on their product specifications and availability. It was seen that the activated alumina series of adsorbents were generally well suited to the removal of polar components. There has also been a vast development in activated alumina adsorbents producing adsorbents for the specific removal of various organic compounds.

It was therefore useful to investigate the adsorption capabilities of a standard activated alumina adsorbent to those developed more specifically for systems such as these being investigated in this project. The three adsorbents chosen in this study were from the BASF range of activated alumina adsorbents and included the activated alumina F-220 adsorbent, the Selexsorb® CD adsorbent and the Selexsorb® CDx adsorbent.

1.4 Thesis Overview

Chapter 2 gives insight into an extensive literature study covering the adsorption process and the numerous factors affecting it. The types of adsorbents are discussed followed by a discussion of the adsorption equilibrium and kinetic models. Lastly the topic of adsorbent regeneration is investigated and the different types and their applications explained.

Chapter 3 discusses detailed adsorption and regeneration equipment development and the respective experimental designs and methodologies fulfilling objective one of this study.

Chapter 4 presents the adsorption data collected and discusses the influence of the three factors affecting the adsorption process investigated in partial fulfilment of objective two.

Chapter 5 presents the equilibrium and kinetic data of the systems investigated. Furthermore the modelling of the data is presented and discussed fulfilling objective two of this study.

Chapter 6 presents the regeneration results for the systems investigated fulfilling objective three of this study.

Chapter 7 concludes this study, highlighting the main findings and providing recommendations for future studies.

Chapter 2: Literature Study

This chapter discusses the adsorption separation process and all its associated topics.

Firstly, the basics of the adsorption phenomenon are discussed and the factors affecting the process are highlighted and explained. The different types of adsorbents are then elaborated on and their different uses discussed followed by details of the adsorbents chosen in this study. Previous literature on organic adsorption systems are identified and the gap in literature highlighted.

The reason for collecting adsorption experimental data is to ultimately model the various systems. Modelling of adsorption systems include both equilibrium and kinetic modelling. Therefore the several equilibrium and kinetic models used in this study are discussed in the second section of this chapter.

Lastly, in order to ensure the overall economic efficiency and improve the environmental impact of the adsorption process, the adsorbents are regenerated. The different regeneration techniques and the general areas of application are discussed.

2.1 Adsorption Fundamentals

Adsorption is a term used to describe the transfer of a molecule from a bulk fluid to a solid surface. It is deemed a physical-chemical separations technique because the bonds formed between the molecule and solid can either be physical or chemical depending on the characteristics of each component (Green & Perry, 2008).

The solid particles onto which the molecules adsorb are referred to as the adsorbent, while the molecules adsorbed are referred to as the adsorbate (Seader, et al., 2011).

2.1.1. Adsorption types

Molecules adsorb onto porous solids, filling their pores by moving from the bulk fluid and bonding to their surface either physically or chemically.

2.1.1.1 Physisorption

Physisorption describes the physical adsorption of adsorbates onto an adsorbent's surface. It involves relatively weak intermolecular (or van der Waals) forces between the molecules and the adsorbent's surface (Ruthven, 1984). Due to these weaker bonds the adsorption process is fairly easily reversed and the adsorbent can be regenerated.

Physical adsorption usually causes the formation of multiple layers of adsorbate on the surface of the adsorbent, is associated with a low enthalpy of adsorption and is favoured by low adsorption temperatures (Ruthven, 1984).

2.1.1.2 Chemisorption

Chemisorption involves the formation of chemical bonds between the adsorbate and adsorbent (Ruthven, 1984). These are much stronger bonds and therefore adsorbent regeneration is more difficult and often results in the significant decreases in adsorbent capacity.

Chemisorption causes a uniform layer of adsorbate on the adsorbent surface. High adsorption enthalpies are associated with it and an increase in adsorption temperatures favours chemisorption. Chemisorption is, however, highly specific and will only occur if there is a possibility of a chemical bond forming between adsorbent and adsorbate (Ruthven, 1984).

2.1.2. Factors affecting the adsorption process

There are several factors affecting the adsorption process. These include; the type of adsorbent, the type of adsorbate, process parameters such as temperature and pressure and the presence of more than one solute in the solution.

2.1.2.1 Type of adsorbent

Adsorbents are developed for specific applications and have a certain affinity for specific molecules. An adsorbent's physiochemical characteristics, such as surface functional groups and structure, affect both adsorption rate and capacity.

The functional groups present on an adsorbent's surface affect both the physical and chemical interactions between adsorbate and adsorbent. The surface polarity of an adsorbent affects its affinity for various adsorbates (Suzuki, 1990), for example polar adsorbents are classified as hydrophilic adsorbents and non-polar adsorbents are hydrophobic adsorbents. Activated alumina, silica gels, and zeolites are examples of polar adsorbents, while carbonaceous and silicate adsorbents are non-polar adsorbents (Suzuki, 1990).

The structure of the adsorbent's surface refers to the pores present, including macro-, meso- and micro-pores, with their size determining which molecules can be adsorbed. Large specific surfaces areas are preferable for adsorbents to increase their adsorption capacity and the presence of micropores within an adsorbent particle enhance the internal specific area of an adsorbent while ensuring a small particle volume is maintained (Suzuki, 1990). The size of the micropores also

determine the accessibility of various adsorbate molecules to the internal surface area of the adsorbent (Suzuki, 1990).

According to the IUPAC classification of pores, micropores are pores with sizes smaller than 20 Å, mesopores have sizes ranging between 20 and 500 Å, while macropores are pores with sizes greater than 500 Å (Sing, et al., 1982).

Generally mesoporous adsorbents (pore sizes > 30 Å) are preferred for liquid adsorption systems, while more microporous adsorbents (pore sizes between 10 and 25 Å) are preferred for vapour adsorption systems (Yang, 2003). Larger pore sizes are required for liquid systems due to the larger adsorbate molecule sizes and the slower rate of diffusion in a liquid (Yang, 2003).

Activated carbon adsorbents generally present with polymodal pore size distributions with small pores branching off of bigger pores, while activated alumina and silica gel are more mesoporous adsorbents presenting with a large portion of the surfaces areas in pore sizes larger than 50 and 20 Å respectively (Yang, 2003).

2.1.2.2 Type of adsorbate

Specific properties of the adsorbate will determine the type of adsorbent to be used for the process. Properties such as polarity, molecule size and solubility are some of the properties of adsorbates that need to be considered when deciding on an adsorbent.

The more polar a molecule, the more polar the adsorbent of choice should be. The size of a molecule will influence the choice of adsorbent because the adsorbate needs to be able to access the active surface of the adsorbent and penetrate its pores (Yang, 2003). The solubility of an adsorbate in solvent has a significant influence on the adsorption process. Adsorption decreases with an increase of adsorbate solubility in the solvent and therefore solubility acts as a controlling factor in adsorption equilibrium.

2.1.2.3 Process parameters

Temperature and pressure are process parameters that affect the adsorption process. Pressure plays much more of a significant role in gas phase adsorption, with an increase in pressure generally leading to an increase in adsorption up until a certain extent at which adsorbent saturation is achieved.

Most adsorption processes are exothermic and therefore lower system temperatures are preferred (Suzuki, 1990). However, when chemisorption takes place, a slightly higher temperature is usually favoured due to the higher activation energies required for the adsorbate-adsorbent interactions to occur (Saha & Chowdhury, 2011).

2.1.2.4 Two or more solutes

The presence of more than one solute in a solvent will affect the adsorption process. These solutes may mutually enhance the adsorption of one or the other or there could be competition between the solutes (Yang, 2003). The solutes might have to compete for surface area or the one could be more soluble than the other in the solvent, pushing the other to adsorb more easily.

2.1.3. Quantification of an adsorption system

The adsorption system is quantified to give an indication of adsorption efficiency and the amount of adsorption taking place in a specific system,

At any time, t, in an adsorption system, the amount of adsorption is quantified using equation [2-1] (Vijayakumar, et al., 2012):

$$q_t = \frac{(C_i - C_t)V}{W} \quad [2\text{-}1]$$

Where q_t [mg/g] represents the quantity adsorbed at time t, C_i [mg/mL] is the initial concentration of adsorbate in solution, C_t [mg/mL] is the adsorbate concentration at time t, V [mL] represents the volume of the solution and W [g] is the adsorbent mass. A plot of q_t versus t represents adsorption kinetic data and is used in the kinetic modelling of the system.

At equilibrium, the amount adsorbed is calculated using equation [2-2] (Vijayakumar, et al., 2012):

$$q_e = \frac{(C_i - C_e)V}{W} \quad [2\text{-}2]$$

Where q_e [mg/g] and C_e [mg/mL] represent the quantity adsorbed at equilibrium and the adsorbate equilibrium concentration respectively. A plot of q_e versus C_e represents adsorption equilibrium data and is used in the equilibrium modelling of the system.

The variable q is also referred to as the adsorption capacity and adsorbent loading.

The efficiency of an adsorption system relies on the removal of the adsorbate. The adsorbate removal percentage is therefore a required quantification of the system and is calculated using [2-3] (Vijayakumar, et al., 2012):

$$adsorbate\ removal\ \% = \frac{C_i - C_e}{C_i} * 100 \quad [2\text{-}3]$$

2.2 Adsorbents

The type of adsorbent used in the adsorption process plays a vital role in the efficiency of the process. It is important to find or develop the right adsorbent with a large specific surface area and pores sizes suitable for the adsorbate which must be removed. The properties characterizing an adsorbent are discussed below. The four generic adsorbents are then discussed, leading into more specific adsorbents developed for particular industrial purposes.

2.2.1. Adsorbent characterization properties

Physical adsorption occurs due to forces between molecules and the atoms making up an adsorbent's surface. Adsorbents, therefore, need to be characterised by their surface properties such as, surface polarity, surface area, pore size distribution and surface chemistry (Yang, 2003).

2.2.1.1 Surface polarity

The polarity of an adsorbent's surface determines it's affinity for polar or non-polar molecules. Polar attracts polar. Therefore polar adsorbents are generally called hydrophilic adsorbents and non-polar adsorbents hydrophobic. Adsorbents such as zeolites, activated alumina and silica gel are classified as hydrophilic adsorbents, while activated carbons and polymer adsorbents are examples of hydrophobic adsorbents (Suzuki, 1990).

2.2.1.2 Surface area

Adsorption is a surface phenomenon and therefore the specific surface area of an adsorbent needs to be as large as possible while maintaining a small particle volume. Specific surface area is defined as the portion of the total area available for adsorption. A large specific surface area results in a large amount of adsorption relative to the weight of the adsorbent and a higher adsorption capacity.

2.2.1.3 Pore size distribution

A large internal surface area in a limited volume results in the development of micropores, the size of which limits accessibility of certain adsorbate molecules to the adsorbate internal surface. The size distribution of these pores is therefore important in determining which solute molecules will adsorb and which will not.

Some adsorbent materials also contain macropores which are several micrometers in size. Macropores are formed when fine powders or crystals are transformed into pellets or granules. They act as diffusion paths for adsorbate molecules to move from the surface of the adsorbent to the micropores within the internal surface area structure.

2.2.1.4 Surface chemistry

Surface chemistry determines the nature and type of bonds formed between adsorbent and adsorbate molecules. An adsorbent's surface presents with functional groups which determine the basic or acidic nature of the adsorbent's surface. This, in turn, influences the reactions and bonds formed between adsorbate molecules and the adsorbent's surface. The surface chemistry of an adsorbent can often be modified by treatment with an acid or base or controlled thermal treatment (Yang, 2003).

2.2.2. Types of adsorbents

There are 4 generic types of adsorbents used on an industrial scale namely activated carbon, silica gel, zeolites and activated alumina.

2.2.2.1 Activated carbon

Commercial activated carbon adsorbents are made from carbonaceous materials such as coal, lignite, wood, coconut and nut shell, peat and petroleum residues, to name a few (Yang, 2003). The quality of an activated carbon adsorbent is influenced by the starting material as well as the carbonising and activation process used.

The preparation of activated carbon adsorbents involves carbonization of the raw material and an activation process. There are two standard activation processes used, gas activation and chemical activation. Figure 2-1 shows the two general processes used to prepare activated carbons (Yang, 2003). The activation process of the carbonised material is what causes the formation of macro- and micropores in activated carbon adsorbents, giving it its large internal surface area.

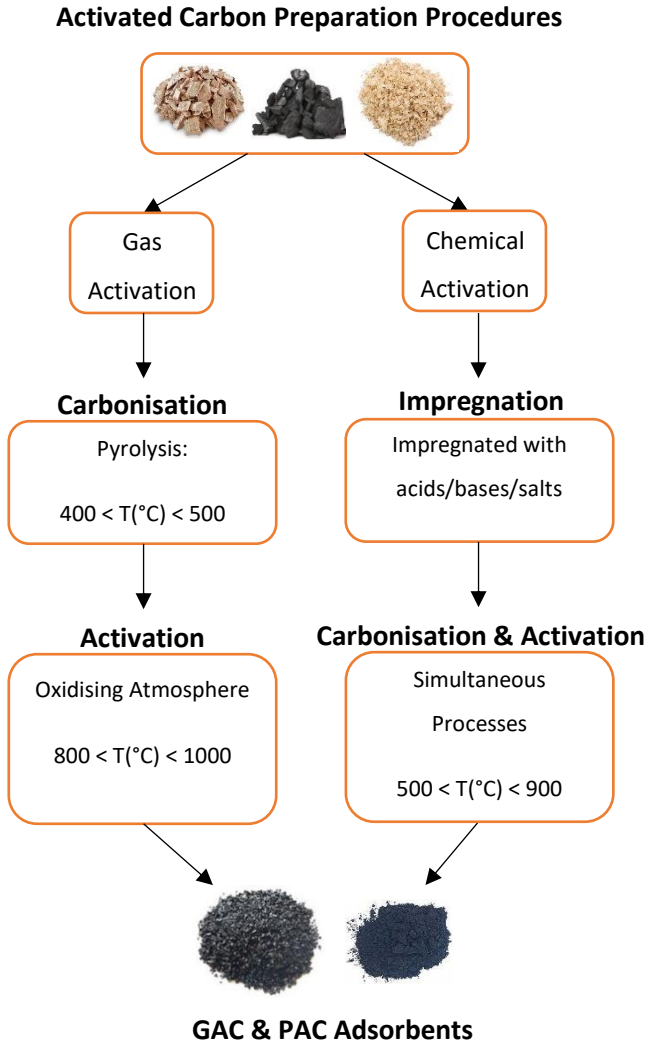

Figure 2-1: Activated carbon adsorbent preparation processes

Activated carbons are nonpolar, however, a slight polarity is possible due to surface oxides present on the adsorbent's surface. Activated carbons are thus generally considered to be hydrophobic and organophilic (Ruthven, 1984). These adsorbents are therefore widely used to remove organics in waste water purification, decolourising sugar and solvent recovery (Ruthven, 1984). Activated carbons are also used in air purification, flue gas desulphurisation and gas separations (Suzuki, 1990).

2.2.2.2 Silica gel

Silica gel can be described as a rigid three-dimensional grid of connecting particles of colloidal silica. Pure silica is a naturally inert, non-polar compound, however, with the addition of a hydroxyl functional group, its surface becomes extremely polar and hydrophilic (Suzuki, 1990).

Silica gel can be manufactured either through polymerisation of silicic acid or aggregation of colloidal silica particles (Yang, 2003). Commercially, silica gel is manufactured using the polymerization technique – shown in Figure 2-2.

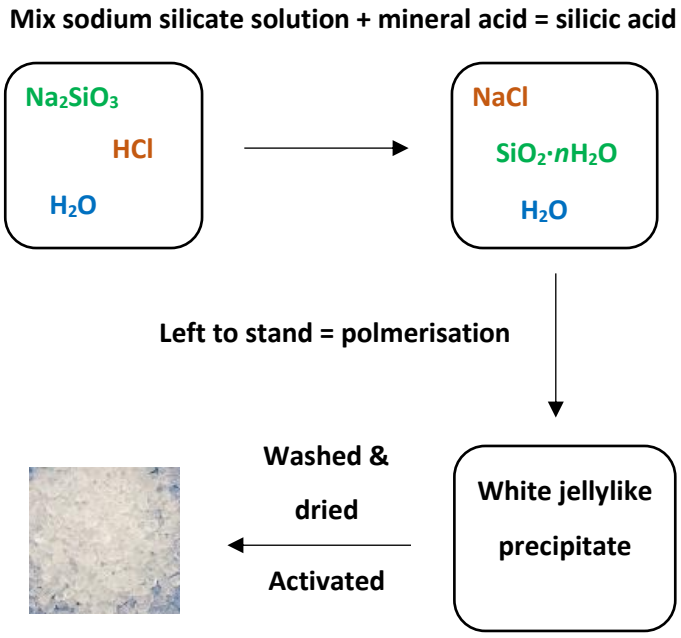

Figure 2-2: Commercial preparation process of silica gel adsorbents

The properties of silica gel, such as pore size, strength and surface area, can be altered by controlling the temperature, pH and silica concentration in the process depicted in Figure 2-2 (Yang, 2003). Silica gels are most commonly used as desiccants due to their hydrophilic nature and large pore volume (Yang, 2003). Their polar nature and hydrogen bonding capabilities also make them excellent for removing polar compounds and unsaturated hydrocarbons from various solvents.

2.2.2.3 Zeolites

Zeolites are a group of hydrated aluminosilicate minerals. They are nanoporous minerals with well-defined pore structures determined by their precisely uniform crystal lattice. This crystal structure means zeolites have no pore size distribution and can therefore be used to separate molecules purely on size alone. It's this feature that distinguishes zeolite adsorbents from the rest of the microporous adsorbents available.

The types of zeolites available range from naturally occurring minerals to synthetic adsorbent frameworks (Yang, 2003). Zeolites contain alumina and silica, the content of which varying between

different types of zeolites based on the separation need. The Si/Al ratio is never less than one, alumina rich zeolites are generally more polar with very high affinities for water, while silica rich zeolites are hydrophobic and preferentially adsorb n-paraffins (Ruthven, 1984).

Zeolites are used to separate hydrocarbons and to dry gases and liquids. They are widely used in the petroleum industry, specifically for refining feedstocks used in isomerisation, alkylation and reforming processes.

2.2.2.4 Activated alumina

Activated alumina is a dehydrated, highly porous form of aluminium oxide (Ruthven, 1984). Alumina particles are generally prepared by dehydrating aluminium hydrates, specifically aluminium trihydrate, at elevated temperatures using air (Yang, 2003). The γ-alumina is the most commonly used alumina as an adsorbent (Suzuki, 1990). It has a good resistance to high temperatures and shows an inert yet highly active surface.

The process with which the activated alumina is prepared determines the specific surface area and pore size of the adsorbent. Activated alumina adsorbents have very high surface area to weight ratios due to their 'tunnel-like' pores. Their surface is characterised as strongly polar and has both basic and acidic characteristics (Ruthven, 1984). The pore structure and surface chemistry of activated alumina can be manipulated and controlled to provide the specific characteristics needed for certain adsorption applications. The heat treatment of alumina determines pore sizes and acid treatment can alter surface chemistry (Ramaswamy, et al., 2013). This gives activated alumina versatility and enlarges the adsorbent applications.

Activated alumina adsorbents are generally used as desiccants, showing a higher capacity for water than silica gel at elevated temperatures (Ruthven, 1984). Through the tailoring of the activated alumina the adsorbent can then be used for removing compounds such as acidic gases from hydrocarbon streams, polar organic compounds, oxygenates, Lewis bases and various ions from water.

There are two ways of tailoring the activated alumina for specific applications; via the activation process and the use of doping. For example the alumina adsorbents used in removing acidic gases are alkalised to contain more sodium and therefore have a greater affinity for acids. The activated alumina adsorbents used for the removal of oxygenates generally have low sodium content and are tailored to have high Lewis acidity and low BrØnsted acidity (Yang, 2003). The high Lewis acidity attracts Lewis bases such as alcohols, ketones and aldehydes, while the low BrØnsted acidity minimises unwanted side reactions due to proton transfer during adsorption (Yang, 2003).

2.2.3. Project specific adsorbents

BASF is the largest chemical company in the world, with their headquarters in Germany. They represent themselves in numerous product and service sectors including, but not limited to, agriculture, energy and resources, paints, chemicals and plastics. They are also a leading manufacturer of adsorbents.

BASF's range of adsorbents include alumina, silica, alumina-silica gels and a range of base metal oxide guard beds. Their portfolio of adsorbents include many proprietary adsorbents specifically tailored for processes in the petrochemical, gas processing and chemical industries. The alumina range of adsorbents include the F-200 and Selexsorb® series of adsorbents, which are spherical activated alumina adsorbents with high crush strength and density.

Although activated alumina adsorbents have in the past mostly been used as desiccants, their ability to be tailored has allowed versatility in their applications and they have since developed into polar organic removing adsorbents, acidic gas removing adsorbents and sulphur removing adsorbents (Yang, 2003).

Based on the activated alumina's versatility, BASF's wide range of activated alumina adsorbents and what is known from industrial adsorbent applications (Scholtz, 26 Oct 2016), three activated alumina adsorbent's were chosen for this study. These are the activated alumina F-220, Selexsorb® CD and Selexsorb® CDx adsorbents.

2.2.3.1 Activated alumina F-220 (BASF, 2009)

The F-220 adsorbent is a spherical activated alumina adsorbent optimised for maximum capacity and hydrothermal stability. It is characterised by a uniform ball size, low abrasion and high crush strength and adsorptive capacity. The uniform ball size is important in minimising pressure drop in desiccant columns and preventing adsorbent segregation during pneumatic loading thereby minimising channeling within the columns. The high crush strength allows this pneumatic loading to occur rapidly, while the low abrasion property ensures very little dust occurring during loading, transportation and its service life. Its large surface area (355 m^2/g) and tailored pore size distribution enables a high adsorptive capacity and with proper adsorption process design and F-220's cyclic stability, the adsorbent will yield a long lifespan.

The F-220 adsorbent is used specifically for drying, acid removal, process stream purification and the purification of hydrocarbons. As a desiccant, the F-220 adsorbent can be used to dry almost all gases and liquids. F-220 removes the degradation acids formed during the use of lubricating oils, refrigerants and transformer acids. Its polar surface aids in the removal of polar compounds such as

alcohols, ethers and ketones, during process stream purifications and under the correct operating conditions, the F-220 adsorbent, can also separate various hydrocarbons from one another.

The F-220 adsorbent was therefore chosen because in theory it appears to hold the characteristics required to purify an alkane solvent and would be interesting to see its capabilities in organic stream purifications.

2.2.3.2 Selexsorb® CD (BASF, 2009)

The BASF Selexsorb® CD adsorbent is an alumina based adsorbent custom formulated to provide optimal adsorption capabilities for polar compounds including; oxygenated hydrocarbons, sulphides and nitrogen-based molecules. This adsorbent is an aluminium oxide with a promoter.

This adsorbent was custom made by BASF for the removal of oxygenated organic compounds from various process streams. It was therefore chosen for this study to test its ability in removing the various alcohols from the alkane solvent and comparing its behaviour to a more 'basic' activated alumina adsorbent like the activated alumina F-220 adsorbent.

2.2.3.3 Selexsorb® CDx (BASF, 2009)

The BASF Selexsorb® CDx adsorbent is also an alumina based adsorbent. Its proprietary modification allows it to adsorb numerous polar compounds such as sulphur- and nitrogen-based molecules, and oxygenated hydrocarbons. This adsorbent is an aluminium oxide containing a propriety modifier.

The Selexsorb® CDx adsorbent, also being custom formulated by BASF, shows similar removal capabilities to the Selexsorb® CD adsorbent. It was therefore chosen to compare its removal capabilities to that of the Selexsorb® CD adsorbent and in turn the activated alumina F-220 adsorbent.

2.3 Organic Adsorption Literature

Organic adsorption systems have been studied extensively in literature most specifically for waste water treatment applications, Behera, et al. (2007) investigated the removal of polyvinyl alcohol using powdered activated carbon to treat wastewater systems in the textile, pharmaceutical and emulsion paints industries. Another study involved removing phenolic compounds from water using various carbon adsorbents for application in the chemical, pharmaceutical and food and beverage industries (Moreno-Castilla, 2004).

Adsorption has also been used to study the purification of air streams specifically the removal of volatile organic compounds in air using activated alumina, zeolites and activated carbon (Diaz, et al.,

2004) and the remove of water vapour from air Selexsorb® CDx (Serbezov, et al., 2011). The technique has also been used in the recovery of butanol from a fermentation broth stream produced in the ABE fermentation process (Qureshi, et al., 2005).

The adsorption of alcohols has also appeared in literature, with several different adsorbents being used to remove specific alcohols from various solvents. In one investigation, a SBA-16 silica adsorbent was used in the adsorption of binary adsorption systems involving *n*-octane, 1-octanol and 1-ethanol (Rockmann & Kalies, 2007). In another study, a gamma alumina adsorbent was tested for the adsorption of methanol, 1-ethanol, 1-propanol and isopropanol (Cai & Sohlberg, 2003).

Focusing on the activated alumina adsorbents, the Selexsorb® CDx adsorbent has also been studied for its use in the desulphurization of fuel (Muzic, et al., 2012). The performance of both the Selexsorb® CD and Selexsorb® CDx adsorbents were compared to the adsorption capabilities of a metal-organic framework (MIL-101) adsorbent in the removal of nitrogen compounds from diesel feedstocks (Laredo, et al., 2016).

Literature shows that adsorption applications are extensive and that there is a need for system specific data. From this review of literature, no open data could be found specifically comparing the three activated alumina adsorbents investigated in this work in their removal of higher chained alcohol contaminants from an alkane solvent. Thus introducing the gap which this work could start to fill.

2.4 Adsorption Equilibrium

During the adsorption process, a dynamic equilibrium is recognised for the distribution of the solute between the fluid and solid phase. This equilibrium state is expressed in terms of the solute concentration (for liquids) or partial pressure (for gases) and the loading of the solute on the adsorbent. Solute loading is expressed as mass, moles or volume of solute per unit mass of adsorbent.

For vapour-liquid or liquid-liquid equilibrium systems a theory is applied to estimate the phase distribution in the form of K-values. There is, unfortunately, no well-established theory developed that can predict fluid-solid equilibrium data, thus making it necessary to obtain equilibrium data for specific adsorption systems (Green & Perry, 2008). An adsorption system is described by a specific solute(s), solvent and adsorbent material. The equilibrium data of an adsorption system taken over a range of solute concentrations at a specific adsorption temperature can be used to plot an adsorption isotherm. An adsorption isotherm is a plot of adsorbent solute loading, q_i, versus solute concentration or partial pressure in the fluid phase, C_i or p_i (Green & Perry, 2008). Each adsorption isotherm describes an adsorption system at one set of conditions and sets a limit of the extent of solute adsorption for

that specific system. The adsorption isotherm plays an important role in the modeling analysis, operational design and relevant practice of the adsorption system (Foo & Hameed, 2010).

Brunauer (1945) defined five principal groups of isotherms, labelling them type I through to V. Figure 2-3 below illustrates the five types of isotherm classes (Basmadjian, 1997).

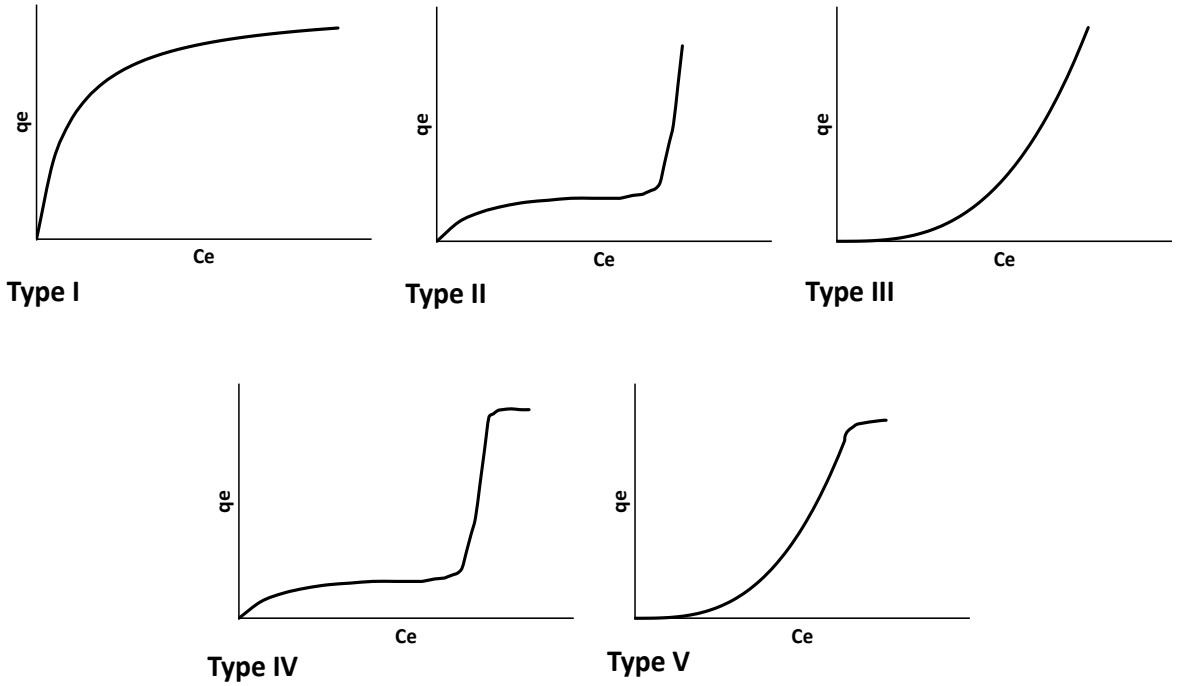

Figure 2-3: Brunauer isotherm classifications (Basmadjian, 1997)

Isotherm type I is typically characterised by the Langmuir isotherm, showing the approach of the system to a limiting value (maximum adsorption capacity) signifying the completion of a monolayer of adsorbed molecules (Chiou, 2002). Microporous adsorbents with relatively small external surfaces usually display type I isotherm behaviour. The micropore volume accessibility rather than the internal surface area governing the maximum adsorptive capacity. Systems exhibiting type I isotherm behaviour are preferred for cyclic adsorption operations (Ramaswamy, et al., 2013).

Type II describes adsorption for non-porous or macroporous adsorbents (Ramaswamy, et al., 2013). At low concentrations they exhibit monolayer adsorption and as concentrations increase multilayer adsorption begins to occur. Type II isotherms can usually described by the BET isotherm equation (Ramaswamy, et al., 2013).

The type III isotherm signifies weak interactions between adsorbate and adsorbent, but strong lateral interactions between adsorbed molecules causing the formation of multiple layers on the adsorbent surface. In this case, the adsorbate molecules are not effectively spread across the adsorbent surface and the adsorption is classified as unfavourable (Chiou, 2002).

The type IV isotherm is generally an indication of systems involving capillary condensation followed by multilayer adsorption. Mesoporous solids are known to display this type of isotherm behaviour.

The type V isotherm is also associated with capillary condensation adsorption, showing similar behaviour to type III isotherms, but where the adsorption reaches an asymptote as the equilibrium concentration is reached. Systems showing type V isotherm behaviour are also considered as unfavourable (Ramaswamy, et al., 2013).

2.4.1. Isotherm models

The modelling of an adsorption isotherm is used to predict and compare the performance of adsorption systems. It is critical for optimising the adsorption process, determining adsorption capacities and designing an adsorption system (Chen, 2015). Numerous isotherm models have been developed over the years (Foo & Hameed, 2010), however the most commonly applied and understood models are the Langmuir, Freundlich and Dubinin-Radushkevich models (Singh & Pant, 2004).

Langmuir was originally developed describing gas phase adsorption onto activated carbon adsorbents, while Freundlich was developed for animal charcoal adsorbents (Foo & Hameed, 2010). Both isotherm models assume a type of layering of adsorbate molecules onto either a homogeneous or heterogeneous adsorbent surface. The Dubinin-Radushkevich model is another empirical model assuming a rather a pore-filling adsorbate mechanism, originally developed to describe the adsorption of subcritical vapours (Foo & Hameed, 2010). All three of these models are two-parameter models with their parameters suggesting certain physical characteristics of the adsorption system.

Langmuir isotherm

The Langmuir isotherm is a flat surface model based on the following assumptions:

1. The adsorbent surface is homogeneous, i.e. all adsorption sites are identical
2. The adsorbed molecules do not interact with one another
3. Only a monolayer of adsorbed molecules is formed
4. All adsorption occurs with the same mechanism

In 1916, Irvin Langmuir, published an isotherm model for gaseous adsorption onto solids. Over the years, the model has been adapted for liquid systems and the non-linear expression of the Langmuir isotherm for liquid systems is shown in equation [2-4] (Foo & Hameed, 2010).

$$q_e = q_m K_L \frac{C_e}{1 + K_L C_e} \quad [2\text{-}4]$$

Where,

q_m = Langmuir constant representing maximum adsorption capacity [mg/g]

K_L = Langmuir constant related the net enthalpy of adsorption [L/mg]

Graphically, the Langmuir isotherm is characterised by a plateau representing the equilibrium saturation point. An essential characteristic of the Langmuir isotherm, is the ability to predict adsorbate-adsorbent affinity using a dimensionless constant incorporating the K_L Langmuir constant (Foo & Hameed, 2010). This dimensionless constant, R_L, is called the separation factor and is described as:

$$R_L = \frac{1}{(1 + K_L C_i)} \quad [2\text{-}5]$$

The R_L value indicates the nature of the adsorption to be either irreversible ($R_L = 0$), favourable ($0 < R_L < 1$), linear ($R_L = 1$) or unfavourable ($R_L > 1$).

Freundlich isotherm

The Freundlich isotherm is another flat surface model. It is the earliest known model describing non-ideal and irreversible adsorption systems. The empirical Freundlich model assumes (Vijayakumar, et al., 2012):

1. The adsorbent surface is heterogeneous (variable adsorption energies)
2. Multiple layers of adsorbed species
3. Non-uniform distributions of heats of adsorption and adsorption affinities

The Freundlich isotherm for liquid systems is characterised as (Chen, 2015):

$$q_e = K_f C_e^{\,1/n_f} \quad [2\text{-}6]$$

Where the K_f [mg/g] parameter is a measure of adsorption capacity and n_f, the adsorption intensity. The parameter n_f in mathematical terms is an indication of a degree of nonlinearity. If $n_f = 1$, then the adsorption process is seen as linear. If $n_f < 1$ then the adsorption process is classified as a

chemisorption process, while if n_f > 1, the adsorption process is of a physical nature. An n value between 1 and 10 represents an efficient adsorption system (Desta, 2013).

Dubinin-Radushkevich

The Dubinin-Radushkevich isotherm model is an empirical model and is generally suitable to adsorption systems with a Gaussian energy distribution on a heterogeneous surface (Ayawei, et al., 2017). Contrary to the Langmuir and Freundlich models, the DR model describes the mechanism of adsorption in micropores as pore-filling instead of mono- or multiple layers on the pore surface (Foo & Hameed, 2010).

The Dubinin-Radushkevich isotherm is expressed as follows:

$$q_e = q_s \exp(-k_{ad}\varepsilon^2) \quad [2\text{-}7]$$

Where q_s [mg/g] and $-k_{ad}$ [mol^2/J^2] are D-R constants, ε can be calculated with

$$\varepsilon = RT \ln\left(1 + \frac{1}{C_e}\right) \quad [2\text{-}8]$$

The parameter R is the universal gas constant (8,314 J.mol^{-1}.K^{-1}) and T is the absolute adsorption temperature (K). A mean free energy term is also associated with the Dubinin-Radushkevich model. The mean free energy of adsorption, E [J.mol^{-1}], is defined as the energy change when one mole of an adsorbate ion is transferred from an infinitive position in solution to the surface of the adsorbent. This energy is calculated using the k_{ad} parameter in equation [2-9] (Singh & Pant, 2004).

$$E = \frac{-1}{\sqrt{2k_{ad}}} \quad [2\text{-}9]$$

The mean free energy gives an indication of the type of adsorption. An E value between 8 and 16 kJ/mol, the adsorption type is explained by ion exchange, i.e. chemisorption, while if E < 8 kJ/mol then the adsorption is physical in nature (Mahramanlioglu, et al., 2002).

2.4.2. Isotherm model conclusions

Figure 2-4 shows the general isotherm shapes for each of the isotherms discussed above. The Langmuir and Dubinin-Radushkevich models show similar isotherm shapes differing from that seen for the Freundlich model. These models provide adsorption system characterisation information such as maximum adsorption capacity, the adsorption intensity and favourability of the adsorption system, as well as the type of adsorption occurring. The information required to evaluate and adsorption system and compare it to other adsorption systems, is provided by these models and therefore they were used in this study to model the equilibrium data.

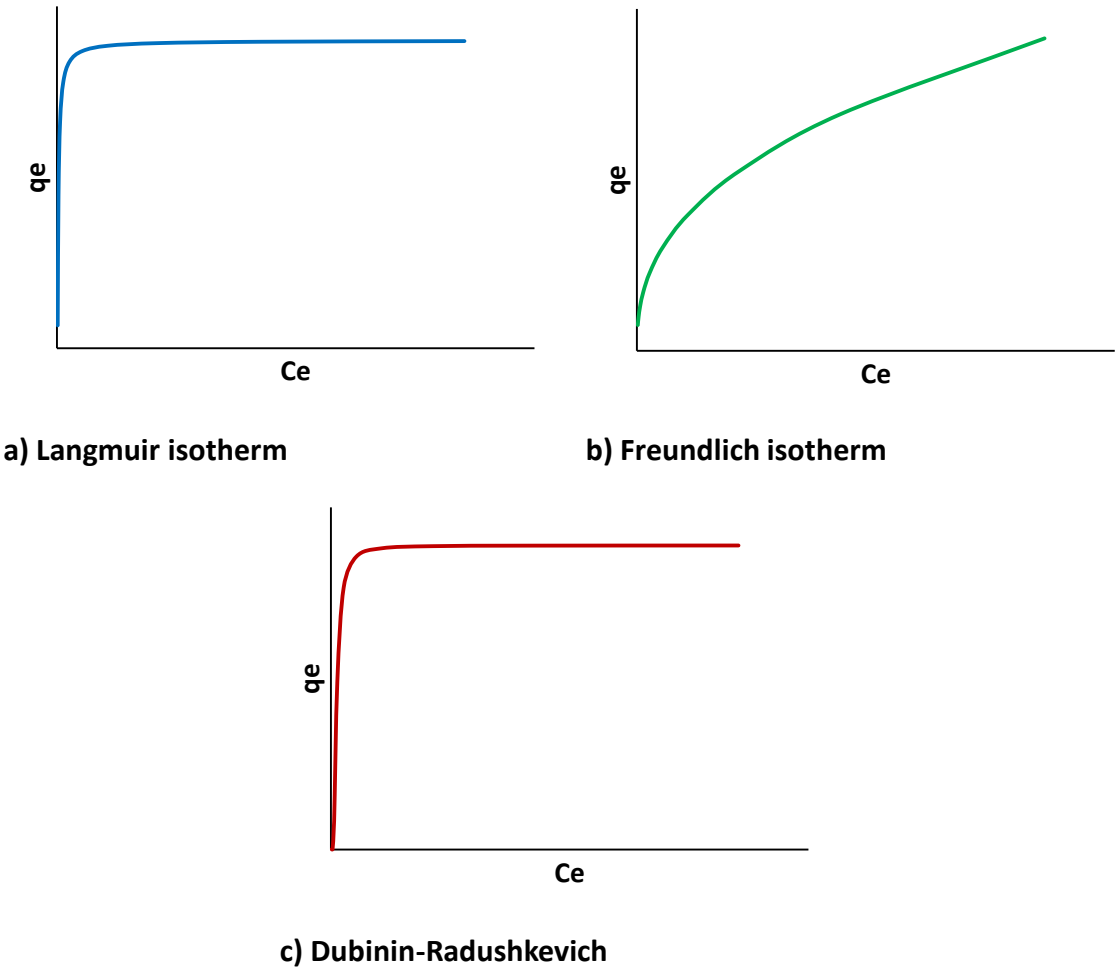

Figure 2-4: The general isotherm shapes for a) Langmuir, b) Freundlich and c) Dubinin-Radushkevich

2.5 Adsorption Kinetics

The design and scale-up of adsorption systems relies on both adsorption equilibrium and kinetics. Often the equilibrium data of an adsorption system does not give a complete picture of the mechanisms involved and performance of the adsorbent. The kinetic data is therefore used to fill in the details of an adsorption system and optimise the adsorption process through indications of the rate-controlling step and adsorption mechanisms (Largitte & Pasquier, 2016).

Adsorption kinetics are represented by a plot of adsorbent loading versus time, known as a kinetic isotherm (Tan & Hameed, 2017). The kinetic data is obtained experimentally by continuously sampling the solution at various time intervals during the adsorption experiment.

Kinetic data is important when scaling up an adsorption system and moving from a batch process to a continuous process as it determines the size of the adsorption unit and the residence time required. In a manner of speaking, the kinetic data of an adsorption system forms the basis for assessing the adsorption performance in a continuous fixed bed system (Tan & Hameed, 2017).

There are three steps in an adsorption process. On a molecular level the first step involves the external mass transfer of the adsorbate molecule from the bulk solution to the external adsorbent surface. The second step is the internal diffusion of the molecule to the actual adsorption site and finally, the third step is the act of adsorption of the molecule to the surface. Adsorption kinetic models are based on which of these steps is considered to be the rate-limiting step and are generally either classified as adsorption diffusion models or adsorption reaction models.

2.5.1. Adsorption diffusion models

Adsorption diffusion models assume the diffusion of the molecule to be the rate limiting step. The diffusion of molecules involves film diffusion, diffusion through the liquid film surrounding the adsorbent particle, and intra-particle diffusion (diffusion through the liquid in the pores and along the pore walls). The Weber Morris model is most commonly used in adsorption kinetic studies to determine whether the process is intra-particle diffusion rate limited.

Weber-Morris model

The Weber-Morris model is based on an adsorption process limited by intra-particle diffusion. The Weber-Morris model is shown below in equation [2-15] (Tan & Hameed, 2017).

$$q = k_{id}\sqrt{t} + B \qquad [2\text{-}15]$$

With constant k_{id} being the intra-particle diffusion rate constant [mg/(g·min^{0,5})] and B the initial adsorption [mg/g]. For kinetics controlled solely by intra-particle diffusion, B should equal zero (Tan & Hameed, 2017).

2.5.2. Adsorption reaction models

In adsorption reaction models, the adsorption step is considered to be the rate-limiting step. The two commonly used adsorption reaction models is the Pseudo-First-Order and Pseudo-Second-Order models.

Pseudo-First-Order model

The Pseudo-First-Order model was first proposed by Largergren and is shown in equation [2-16] (Tan & Hameed, 2017).

$$q = q_e(1 - e^{-k_1 t}) \quad [2\text{-}16]$$

Where constant, k_1, represents the first order rate constant [1/min]. The rate constant is a function of adsorption process conditions such as temperature and smaller particle sizes give rise to larger k_1 values (QIU, et al., 2009).

Pseudo-Second-Order model

The Pseudo-Second-Order model assumes the rate of adsorbate loading onto adsorbent particles is second order with respect to the available adsorption sites. It has been used to describe the kinetics of metal ion removal by adsorption onto peat and is shown in equation [2-17] (Simonin, 2016).

$$q = \frac{k_2 {q_e}^2 t}{1 + k_2 q_e t} \quad [2\text{-}17]$$

Where k_2 is the second order rate constant [g/(mg·min)]. Generally, a smaller adsorbent particle size produces a larger value for k_2 because of the reduced intra-particle diffusion resistance.

2.5.3. Kinetic model conclusions

Figure 2-5 show the general shapes described by the three kinetic models given above. Generally adsorption systems involve physisorption between adsorbent and adsorbate, and therefore, it is speculated that the adsorption kinetic systems investigated in this project will show diffusion rate limited behaviour. However, adsorption mechanisms are usually complex and a combination of steps might be rate-limiting.

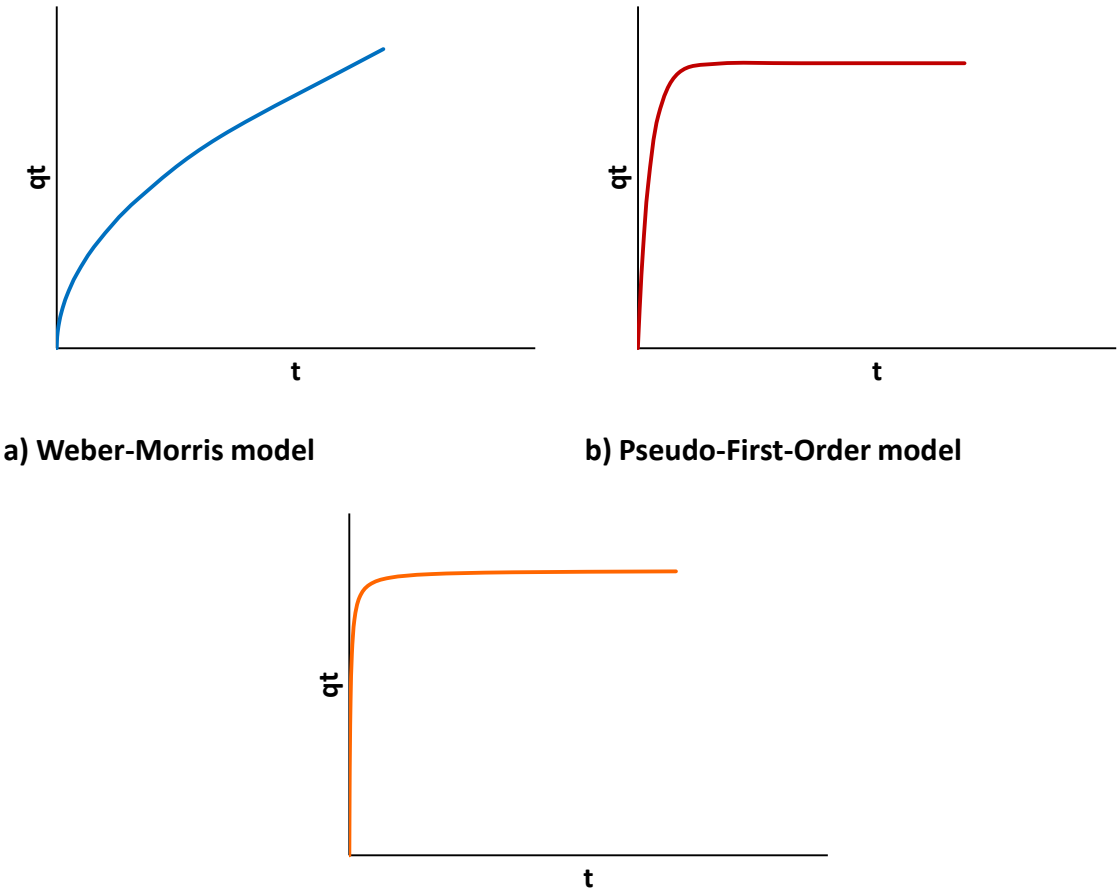

Figure 2-5: The general kinetic model shapes described by a) Weber-Morris, b) Pseudo-First-Order and c) Pseudo-Second-Order models

2.6 Regeneration

Regeneration is a term used to describe the process of reactivating spent adsorbent in order to reuse it in an adsorption cycle. The aim of the regeneration process is to return the adsorbent's capacity to its original state and in some cases the objective is also to recover valuable components that were adsorbed (Ruthven, 1984).

There are various adsorbent regeneration techniques used in industry, however some are still in the research phase. The four basic techniques are pressure-, displacement, purge gas- and temperature regeneration (Ruthven, 1984). Some other regeneration techniques include microwave, chemical and vacuum regeneration (Polaert, et al., 2010), (Martin & No, 1987) & (Pak & Jeon, 2016). Many adsorption systems use a combination of regeneration techniques. The choice of technique

depends on factors such as the type of adsorbent, the adsorption isotherm (giving details on the adsorbate-adsorbent interactions and layering), the regeneration aim (adsorbate recovery) and economic factors (Ruthven, 1984). The four basic regeneration techniques are explained below.

2.6.1. Pressure regeneration

Pressure regeneration involves dropping the pressure of an adsorption system at constant temperature (Ruthven, 1984). The regeneration pressure is much lower than the adsorption pressure thereby shifting the equilibrium of the system. Pressure regeneration is mostly only applicable to gaseous systems.

In a cyclic pressure swing system, rapid cycling between high and low pressure can be achieved thereby reducing the adsorbent inventory required and in turn reducing the capital costs of the system (Suzuki, 1990). Unless the product species is weakly adsorbed, the product recovered from the regeneration process generally has a low purity and therefore this technique is not suitable for high purity product recovery. Pressure regeneration is used in air separation processes and for hydrogen purification.

2.6.2. Displacement regeneration

At a constant pressure and temperature, the adsorbed molecules can be displaced by a competitively adsorbed component in a new fluid stream (Ruthven, 1984). The adsorbed molecules are therefore displaced and replaced by the new component introduced into the system. Displacement regeneration is applicable to gas and liquid systems.

Displacement regeneration is preferred over temperature regeneration when adsorbent stability and adsorbate reactivity are an issue, but the adsorbate is strongly adsorbed (Ruthven, 1984). Product recovery is complex and further separation steps are required. Therefore the choice of solvent in the desorption stream is crucial. The new adsorbed species should also not adsorb more strongly than the original species as this will introduce problems into the adsorption process.

2.6.3. Purge-gas regeneration

Purge-gas regeneration involves stripping the adsorbed species using a non-adsorbing inert gas at a constant temperature and pressure. This method is only applicable when dealing with weakly adsorbed species otherwise the quantity of purge gas required would be too large (Ruthven, 1984). The adsorbate is generally also only present in very low concentrations in the purge gas and therefore this method cannot be used when adsorbate recovery is required.

However, purge-gas regeneration, is commonly used in combination with a thermal regeneration technique. This allows for the desorption of more strongly adsorbed species using a smaller temperature change and therefore avoiding some of the disadvantages associated with temperature regeneration.

2.6.4. Temperature regeneration

Temperature regeneration uses heat to regenerate adsorbent particles. Temperature has a large impact on adsorption equilibrium and with adsorption being known as an exothermic process, an increase in temperature will favour the reverse reaction, i.e. the desorption of the adsorbed species (Ruthven, 1984).

Temperature alone is not usually used in industry as a regeneration technique, as the adsorbate needs to be removed from the adsorbent bed as well. A heated gas (and less commonly, a hot liquid) is used as a carrying fluid in a thermal swing process to remove the desorbed species from the adsorbent bed (Suzuki, 1990).

Thermal swing regeneration is well suited to systems where adsorbates are strongly adsorbed as, generally, a small change in temperature will result in the desorption of the adsorbed species (Ramaswamy, et al., 2013). It is also useful when product recovery is essential and relatively high purities need to be achieved. The time required to heat and cool adsorbent beds, makes thermal swing regeneration unsuitable for rapid cycling and therefore a large adsorbent inventory is required meaning a negative impact on adsorption system economics (Ramaswamy, et al., 2013). Repeated thermal exposure can also negatively impact the adsorbent lifespan and when dealing with reactive adsorbates, high temperatures can lead to coking on the adsorbent surface.

2.6.5. Choice of regeneration technique

On consideration of the four basic regenerations techniques explained, pressure and displacement regeneration are not ideal techniques for the systems studied in this project. This is due to the systems being liquid systems and the further separation processing required with displacement regeneration adding unnecessary complications and negative economic implications to the experimental work.

This leaves purge gas and temperature regeneration. Purge gas regeneration alone would require large quantities of gas adding negative economic impacts to the project. Combining temperature regeneration and purge gas regeneration is therefore the choice as regeneration technique that makes the most sense.

This combination of techniques is used in industry for organic chemical systems, as well as activated alumina systems (Scholtz, 26 Oct 2016). It is also the most common technique and would provide the energy to desorb the alcohol adsorbates from the activated alumina adsorbents.

2.7 Chapter Conclusions

It is clear that an adsorption system is influenced by many factors and the need for system specific adsorption data is evident and necessary to model adsorption systems. The lack of activated alumina – alcohol organic adsorption system data was also made evident and hence the need for this research arrived.

The BASF range of adsorbents provides adsorbents specific for the removal of oxygenated hydrocarbons which in theory should work in the removal of 1-alcohols from an *n*-decane solution and therefore a comparison on the effectiveness of these adsorbents (activated alumina F-220, Selexsorb® CD and Selexsorb® CDx) is done in this work.

Batch adsorption experiments can supply the data required to characterise an adsorption system through equilibrium and kinetic modelling. The regeneration technique will help improve the efficiency of the entire adsorption process, however its effects on each adsorbent's capacity is system specific and requires experimental investigation.

Chapter 3: Equipment Development and Experimental Design

To achieve the aim of this project and subsequently the three objectives, two experimental setups needed to be designed and constructed and batch experiments performed. All information pertaining to the equipment and experimental designs are presented in this chapter. Firstly, the materials used in this study are highlighted. The equipment specifications and designs of the adsorption and regeneration setups are then discussed. Next, the experimental designs and procedures for the adsorption and regenerations experiments are presented. Lastly, the sample preparation procedure and experimental errors are explained.

3.1 Materials

The details of the chemicals used in the experiments conducted are shown below in Table 3-1. The purities listed in the table are those indicated by the supplier. Gas chromatography analyses of these chemicals showed no impurities that would alter the results of the experiments being conducted and confirmed the purities specified by the supplier, therefore the chemicals were used as is.

Table 3-1: A list of the chemicals used in this project along with their suppliers, CAS numbers and supplier specified purities

Chemical	Supplier	CAS Number	Purity (wt%)
1-pentanol	Sigma Aldrich	71-41-0	≥ 99,0
1-hexanol	Sigma Aldrich	111-27-3	98,0
1-octanol	Sigma Aldrich	111-87-5	≥ 99,0
1-decanol	Sigma Aldrich	112-30-1	≥ 98,0
n-decane	Sigma Aldrich	124-18-5	≥ 95,0
methanol	Sigma Aldrich	67-56-1	≥ 99,9

The adsorbents used in this work, their supplier and the supplier specified particle sizes are given below in Table 3-2. The adsorbents were used as received.

Table 3-2: A list of the adsorbents used in this project, their suppliers and supplier specified particle sizes

Adsorbent	Supplier	Particle Size
Activated alumina F-220	BASF through UDEC	3,2 mm
Selexsorb® CD	BASF through UDEC	3,2 mm
Selexsorb® CDx	BASF through UDEC	3,2 mm

The adsorbents were characterized using nitrogen adsorption-desorption isotherms at 77,343 K on a Micrometrics® BET analyser. Table 3-3 below lists the structural characterization of each adsorbent. The surface area and average pore diameter was determined using the Brumauer-Emmett-Teller (BET) method. The total pore volume was determined using desorption data and Barrett-Joyner-Halanda (BJH) formula. The crush strength and bulk density were obtained from the specifications sheets available on the BASF website.

Table 3-3: Structural characterisation of the adsorbents used in this project

Adsorbent	Activated alumina F-220	Selexsorb® CD	Selexsorb® CDx
BET surface area [m^2/g]	334,34	408,28	466,01
Total pore volume [cm^3/g]	0,4189	0,4109	0,4051
Average pore diameter [Å]	48,179	46,104	42,890
Crush strength [kg]	15	11	11
Bulk density [kg/m^3]	785	697	665

The nitrogen gas used as the carrier gas, in the regeneration experiments, was a baseline nitrogen with a supplier specified purity of ≥ 99,999 %, supplied by Afrox.

3.2 Equipment Specifications and Design

The equipment specifications for both the adsorption and regeneration experimental setups were based on mode of operation, previous experimental setups used in literature and the adsorption systems investigated. Their subsequent design was then based on these specifications and physical laboratory constraints.

3.2.1. Adsorption Experimental Setup

For this study, the adsorption setup had to provide a means for performing batch adsorption tests during which both equilibrium and kinetic data could be collected, i.e. continuous sampling. The regeneration testing also had to be kept in mind when designing the adsorption setup, as the adsorbents had to be easily cycled between the two experimental setups.

Previous equilibrium adsorption experiments were carried out in Schott bottles or flasks placed in heated water baths (Ezeh, et al., 2017), (Ozkaya, 2006) & (Oguz & Keskinler, 2005). The adsorbent and solution were mixed in these bottles or flasks, which were closed and left in a water bath for the duration of the experiment. The adsorbent was then filtered out and subsequent solution testing and

adsorbent weighing performed. Numerous experiments were also run at the same time, as the water baths were large enough to house several bottles or flasks at a time.

Based on literature and previous experimental adsorption setups used at the Process Engineering Department at Stellenbosch University, a heated water bath design was chosen for the batch adsorption experimental setup. Figure 3-1 gives a depiction of the water bath experimental setup and the elements involved are discussed below.

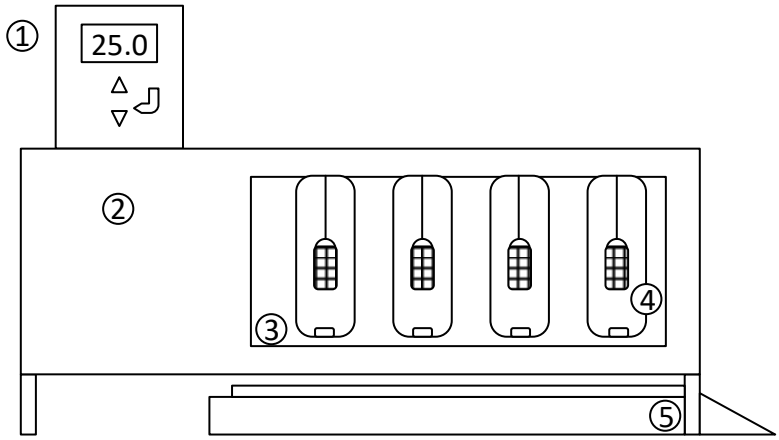

Figure 3-1: Schematic of the adsorption water bath experimental setup. 1) Water bath heating unit, 2) Stainless steel water bath, 3) Tall form glass beakers, 4) Adsorbent mesh baskets and 5) Magnetic stirrer plate.

Equipment design

The adsorption water bath was designed to house ten 500 mL tall form beakers, each representing one adsorption experiment. The bath was designed with 'legs' to give sufficient space underneath for a magnetic stirrer plate and a space on the left to house the heating unit. The water bath was constructed using stainless steel 316 material and a Perspex window was inserted into the front of the bath. The reader is referred to Appendix 8.1 for a detailed drawing of the water bath.

The beakers were held in place in the water bath by a hold plate which allowed the rim of each beaker to rest on it and remain in place above its magnetic stirrer plate section. The reader is referred to Appendix 8.1 for the hold plate detailed drawing.

Alternating the adsorbent from the adsorption setup to the regeneration setup required the adsorbent to be contained and yet still accessible to the solution and carrier gas in the adsorption and regeneration steps, respectively. A mesh basket design was chosen to hold the adsorbent particles during experimentation. Figure 3-2 gives an example of the mesh basket holder and the reader is

referred to Appendix 8.2 for a detailed drawing of the mesh basket. A stainless steel 2,5 mm mesh was used to make the mesh baskets to ensure durability after prolonged exposure to organic chemicals and allow the adsorption solutions sufficient access to the adsorbent particles.

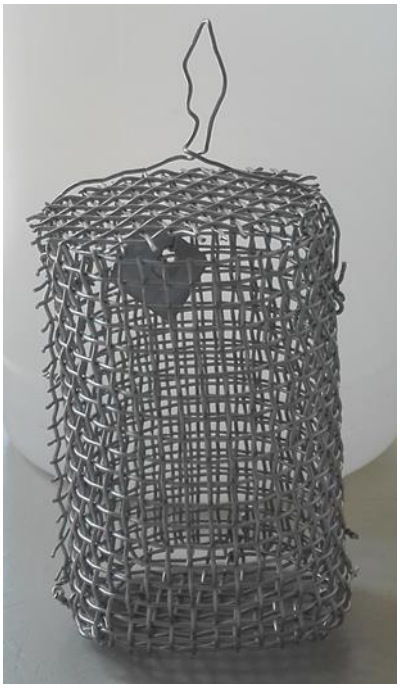

Figure 3-2: Mesh basket holder for adsorbent particles

The mesh baskets were held in place in the beakers using a water bath lid. Figure 3-3 gives the schematic of the water bath lid. The reader is referred to appendix 8.3 for a detailed water bath lid drawing. Sample ports in the lid allowed for continuous sampling during each adsorption experiment using a pipette, while the hooks attached to the bottom of the lid allowed the mesh baskets to hang in the adsorption solution.

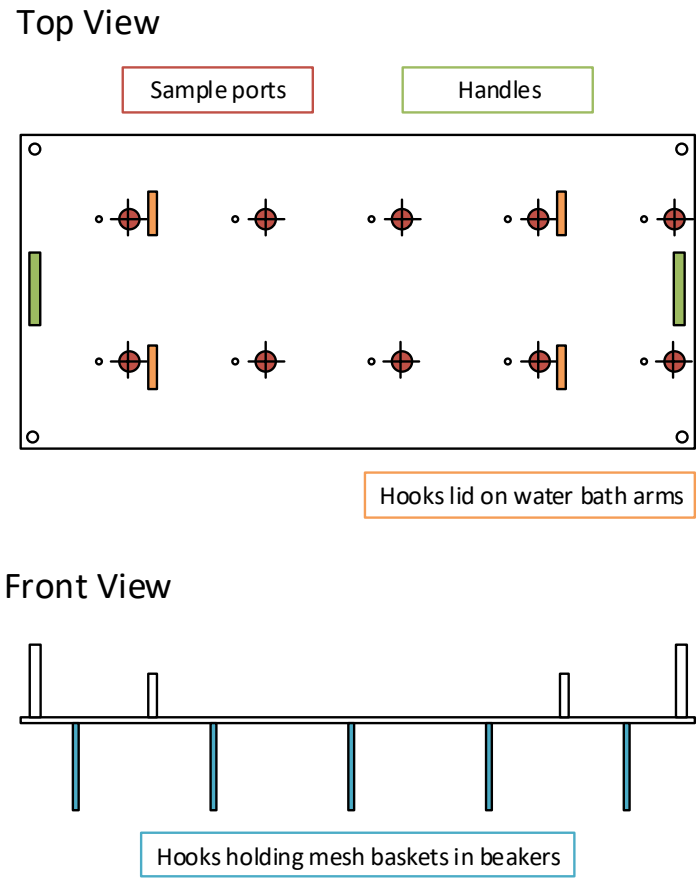

Figure 3-3: Water bath lid schematic showing the sample ports, mesh basket hooks and hooks holding the lid above the bath before experimentation

3.2.2. Regeneration Experimental Setup

The regeneration experimental setup was required to perform batch regeneration tests. Adsorbents had to be cycled between the adsorption setup and regeneration setup after each respective test. From literature findings in section 2.5, a temperature regeneration technique using a purge gas was chosen for the adsorption systems investigated in this study.

This combination of techniques appears to be common in experimental adsorption studies using various types of adsorbents. Zhang and Wang (2017) investigated the desorption temperature during a thermal swing process for a water-activated alumina system conducted using a cylindrical adsorbent container. Temperature and a purge gas were used to regenerate the adsorbent bed. The column consisted of four Pt-100 temperature probes placed within the bed and the purge gas was heated

through electric wiring on the inlet tube. High purity nitrogen gas was used as the carrier gas and temperature control was used to control the temperature of the gas entering the column.

Lashaki, et al. (2012) investigated the effect of regeneration temperature on the irreversible adsorption of organic vapours on activated carbon also using a column-type adsorption-regeneration reactor. High purity nitrogen gas was again used as carrier gas and the system was heated using heating tape wrapped around the reactor. A type K thermocouple was placed in the centre of the reactor to monitor the bed temperature and this in combination with a control system and solid state relay was used to control the bed temperature.

Based on these studies and some general engineering design knowledge a column design was chosen for the regeneration setup. The basic batch regeneration process concept is shown in a simplified process flow diagram in Figure 3-4. Units V-101, V-102 and V-103 represent the regeneration columns containing the adsorbents. Unit E-101 is the condenser used to cool the hot gas exiting the regeneration columns. Units V-104 and V-105 are traps to remove the organic material carried in the nitrogen purge gas before releasing the gas to the atmosphere.

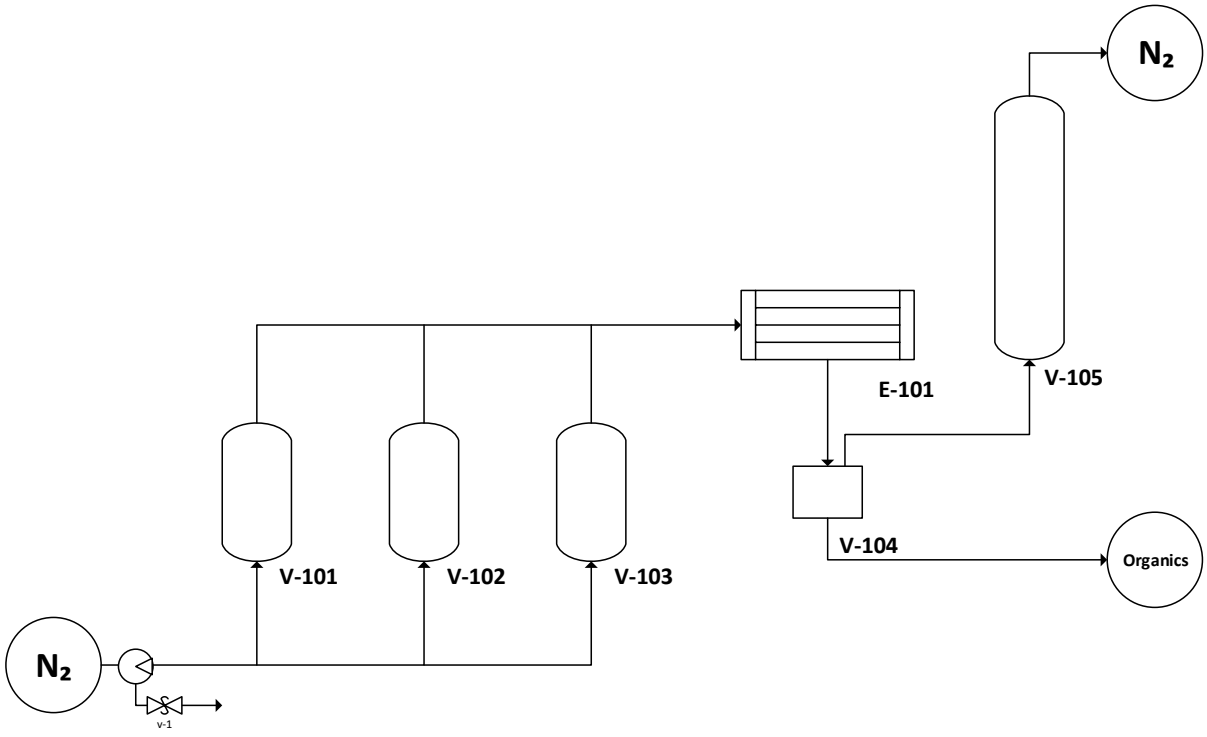

Figure 3-4: Simplified overview of the regeneration experimental setup

The design specifications for the regeneration experimental setup are shown in Table 3-4. A design temperature of 450 °C was chosen based on regeneration temperatures seen in literature (Lashaki, et al., 2012), boiling points of organic compounds and the heat rating of several available heat tracing wires. Although the system would operate at pressures close to atmospheric pressure, the system was designed to handle a slightly higher pressure for future studies and in the case of requiring a higher system pressure. Nitrogen is one of the commonly used purge gases in regeneration processes. It was also required as the purge gas for safety reasons as regeneration temperatures are often close to the auto-ignition temperatures of the chemical components in adsorption systems and therefore the entire system needs to be void of oxygen.

Table 3-4: Design specifications for specific process variables in the regeneration experimental setup

Process Variables	
Design Temperature	450 °C
Design Pressure	5 bar
Purge gas	Nitrogen
Chemical components	• Organic compounds • Alumina adsorbents

Regeneration setup detailed design

The reader is referred to Appendix 8.4 for a detailed process flow diagram for this regeneration process system. The designs of each process unit is discussed below and the reader is referred to appendices for detailed equipment drawings and specification sheets.

1. Regeneration columns (V-101, V-102 and V-103)

The regeneration columns functioned as the adsorbent holders during the regeneration process through which the purge gas flowed. They were required to be able to handle the temperatures applied to the system and needed to be resistant to the organics in the system. Due to the batch nature of the experiments, their accessibility and ability to be regularly opened and closed needed to be considered as well.

The choice of having 3 regeneration columns, instead of say 10 in relation to the number of batch adsorption experiments that could be run at one time, was due to physical space constraints. The regeneration equipment needed to fit in the fume hood next to the adsorption water bath.

Figure 3-5 below is a schematic of the regeneration column. The reader is referred to Appendix 8.5 for the equipment specification sheet and a detailed regeneration column drawing.

Stainless steel 316 was chosen as the material of construction for the body of the column. It provided the necessary resistance to the chemicals and could handle the design temperature. Gas flow through the column was from bottom to top.

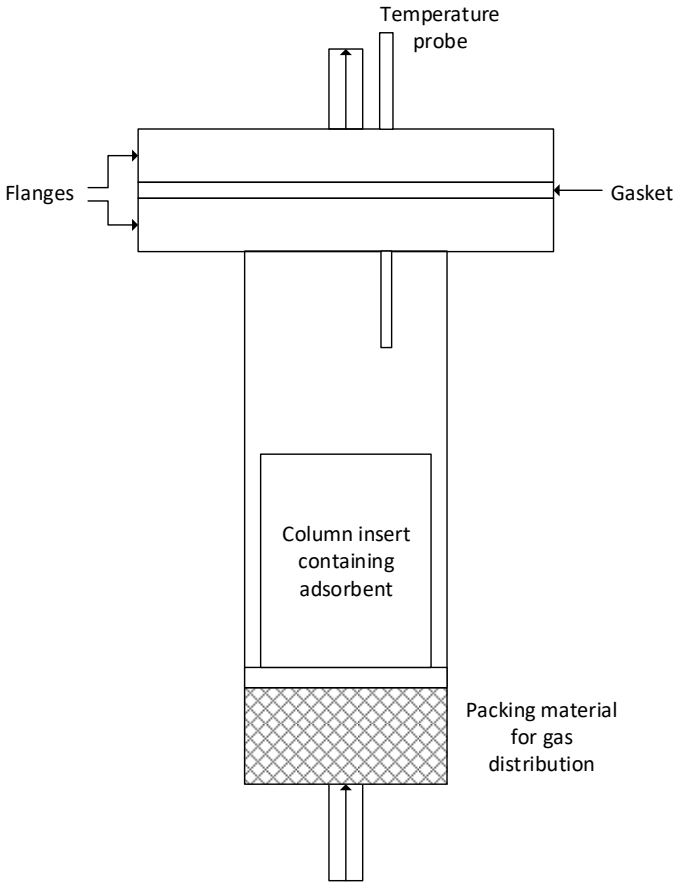

Figure 3-5: Schematic of the regeneration column

The bottom end of the column was sealed, i.e. no flanges were used, and the inlet tubing connected using a weld connection. The bottom of the column was packed with ¼" stainless steel 316 Dixon rings (shown in Figure 3-6) in order to ensure adequate gas distribution within the column.

Figure 3-6: Dixon rings used for gas distribution in the regeneration columns

Adsorbents were held in the columns using column inserts which could easily slide into and out of the columns and into which the adsorbents could easily be poured from the mesh baskets used in the adsorption experiments. The use of additional column inserts were due to difficulties experienced inserting the mesh baskets into the regeneration columns. A detailed drawing of the column insert can be found in Appendix 8.5. The column inserts consisted of a stainless steel base ring which fitted snuggly into the column, preventing the gas from bypassing the adsorbent bed and up the sides of the column. This base ring then held in place a 2,5 mm stainless steel mesh base plate underneath the cylindrical adsorbent holder. A 1 ¼" stainless steel tube cut into 60 mm lengths was used as the cylindrical wall of the column inserts.

The lids of the columns were formed using two stainless steel flanges with a graphite gasket wedged between them. The top flange of each column held the connection for the outlet tubing as well as for the temperature probe.

2. Condenser (E-101)

The condenser was required to cool down the hot nitrogen gas exiting the columns and condense the organic components desorbed from the adsorbents inside the columns. The reader is referred to Appendix 8.6 for the condenser equipment specification sheet and detailed drawing.

The condenser schematic can be seen in Figure 3-7. A counterflow condenser using cooling water was used in this regeneration process system. A large stainless steel column with a diameter of 130 mm and a length of 295 mm was used as the shell of the condenser. It was sealed at the bottom and two outlet connections were welded onto the base. One connection was the outlet port for the gas stream, the other formed the water drain pipe. Two other connections were inserted on the sides of

the column, one at the top and one at the bottom, forming the cooling water outlet and inlet points respectively. A large inlet port with a screw in top was welded into the top lid of the condenser. This was done to be able to fill up the condenser with water prior to start-up.

The gas process stream entered in through the top of the condenser, through a spiral copper tube inside the condenser and out the bottom into the organics trap. The spiral copper tubing in the condenser had a diameter of 80 mm and the tube was 1 m in length. This ensured adequate surface area for heat transfer and the slope associated with the spiral shape ensured the condensing organics were forced to flow down the tubing and out into the organics liquid trap.

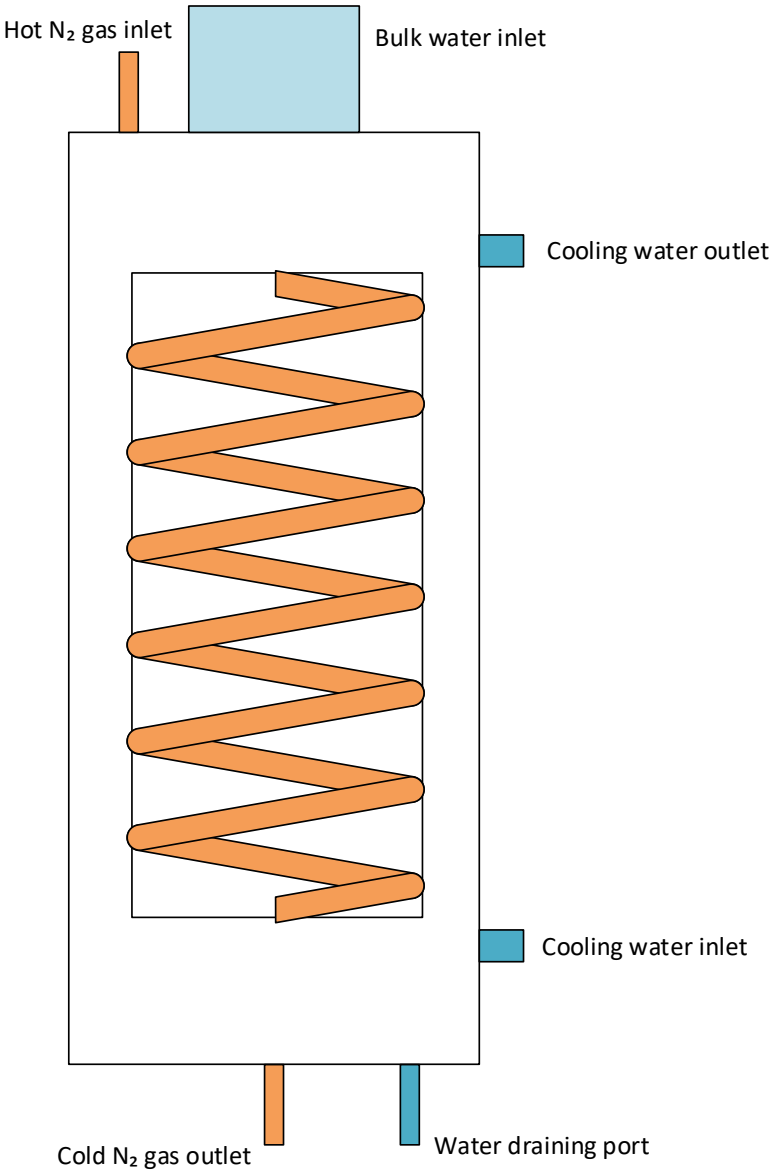

Figure 3-7: Schematic of the condenser (E-101) in the regeneration setup

3. Organics trap (V-104)

The organics trap was required to remove the condensed organic compounds from the nitrogen gas before releasing it to the atmosphere. The reader is referred to Appendix 8.7 for the organics trap equipment specification sheet and detailed drawing.

The organics trap is essentially a liquid-gas separator. The gas containing condensed organics is forced to bubble through water and then out again through the top of the trap. The inlet tube lies 30 mm into the organics trap to ensure the gas bubbles through the water. The bottom of the trap is a pyramid shape to ensure easy draining of the liquid from the trap through an outlet port at the pyramid point.

4. Activated carbon trap (V-105)

The activated carbon trap is the final step in cleaning the gas, ensuring no pollutants are released into the atmosphere. The reader is referred to Appendix 8.8 for the activated carbon trap equipment specification sheet and detailed drawing.

The trap is an adsorption column with an activated carbon bed height of 290 mm. Activated carbon is well-known for removing organic components from gaseous systems as well as water systems. It therefore acts as the last barrier for removing any organics still contained in the nitrogen stream.

The stainless steel column has an outer diameter of 70 mm and a bottom gas distribution section of 45 mm in height. A 1,5 mm stainless steel mesh acts as a hold plate to keep the adsorbent in place. Rubber gaskets ensure tight seals between the stainless steel flanges at the top and bottom of the column and an outlet valve can be found at the top of the column.

Piping and instrumentation

The piping and instrumentation diagram (P&ID) for the regeneration process is shown in Figure 3-8. The reader is also referred to Appendix 8.9 which gives the control design form for the regeneration system. The regeneration process required flow control, temperature control and pressure safety measures. All these aspects required certain instrumentation in order for them to be implemented. This instrumentation includes temperature probes, flowmeters, valves and pressure gauges.

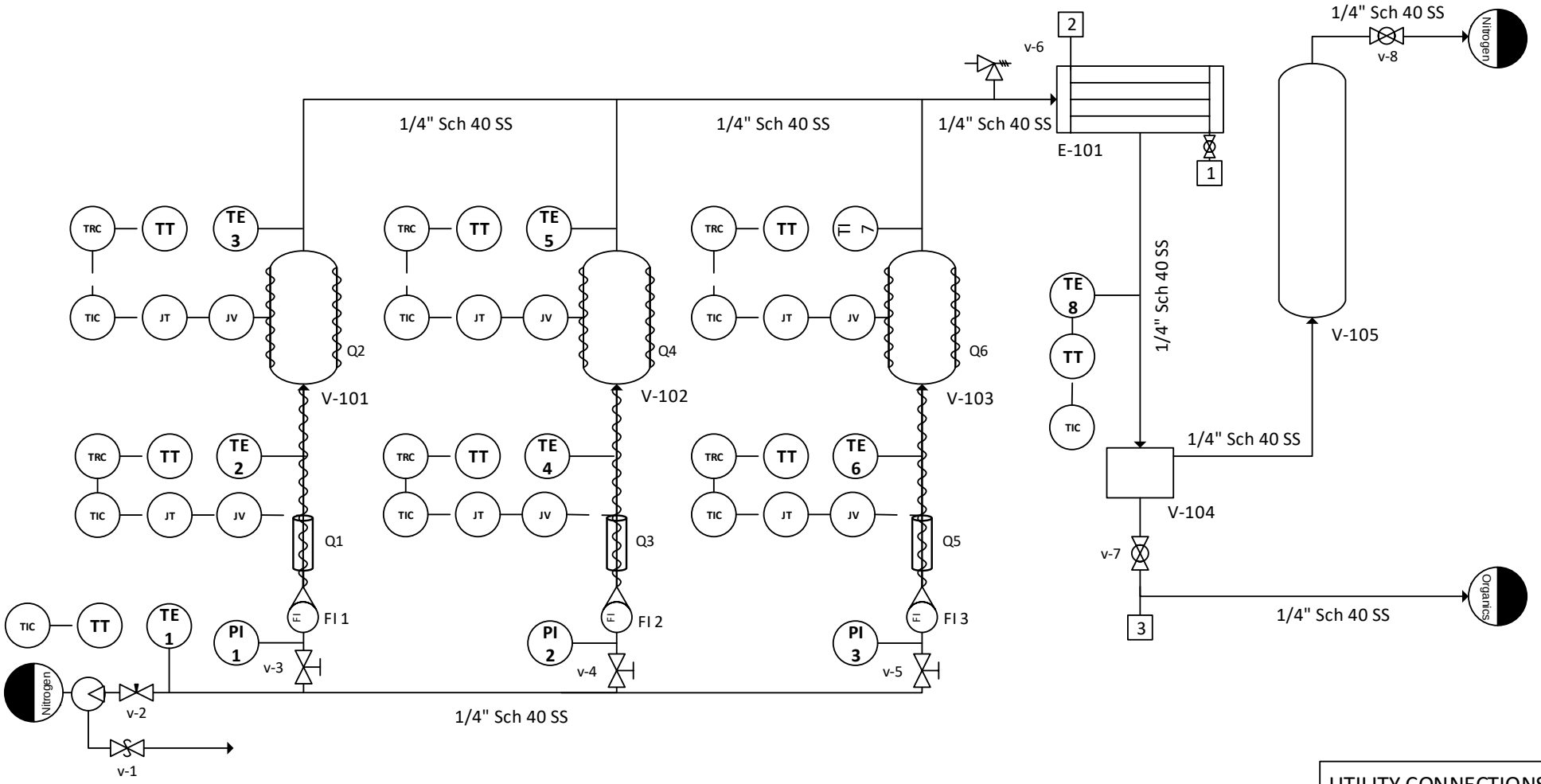

UTILITY CONNECTIONS
1. Cooling water 2. Cooling water return 3. Sample Port SS – Stainless Steel ~~~ - Electric heat tracing

Figure 3-8: Regeneration process P&ID

1. Temperature instrumentation and heating

This process contained 8 three wire Pt-100 temperature probes. Six of these probes were used for control purposes, while the other two were used to monitor the gas inlet temperature to the system and the gas outlet temperature from the condenser.

Temperature probes 1 and 8 were each connected to a DTD48484R0 temperature controllers for indication purposes only. Temperature probe 1 was connected to the line carrying the nitrogen gas from the bottle to the regeneration columns and was used to monitor the temperature of this gas. Temperature probe 8 was connected to the nitrogen gas outlet of the condenser and was used to monitor the temperature of this gas to ensure adequate cooling was taking place in the condenser.

Each column configuration consisted of a temperature probe on the inlet of the column and one inserted through the top of the column. The probe in each column was inserted at a depth of 20 mm and was used to measure the temperature of the outlet gas as it left the adsorbent bed. Temperature probes 2 through 6 represent these six column probes and were each connected to a DTB4848 VR temperature controllers. A DOP-BO32S211 HMI touch screen was used to log the temperature data of these 6 temperature probes.

Electric heat tracing was used as the energy source for the temperature regeneration technique. The heat tracing, supplied by Thermon South Africa (Pty) Ltd, was a glass yarn insulated cable with a very small winding radius. The cable had a nominal temperature rating of 450 °C and a cable length of 0,6 m, supplying 75 W, was used. Heat tracing was wrapped around the inlet tubing to the column as well as around the column itself. Solid state relays and heat sinks were used to control the electric heat tracing cables using the temperature read by the respective temperature probes.

Inlet temperature probes on the regeneration columns were used to control the heat tracing on the inlet tubing, while the outlet temperature probes were used to control the heat tracing wrapped around the columns.

The column inlet tubing, the column itself and the outlet tubing between each column and the condenser were all wrapped in 6 mm braided ceramic rope insulation. The inlet tubing and columns had insulation layers of 18 mm surrounding them, while the outlet tubing had an insulation layer of 8 mm.

2. Gas flow instrumentation

The inlet nitrogen flow to each column required controlling in order to ensure no bed fluidisation and equal flow between all three columns. The flow was manually controlled using 3 needle valves (v-

3, v-4 and v-5) and 3 variable area flowmeters (FI 1, FI 2 and FI 3). All these components were supplied by Swagelok.

3. Pressure instrumentation

During experimentation the regeneration process was open to the atmosphere and the inlet gas pressure was relatively low, 500 kPa. Pressure build-up in the system due to a blockage of some sort was however a concern. A pressure relief valve was placed on the outlet of the regeneration columns just before the stream enters the condenser.

Three pressure gauges were also placed on the inlet to each column for monitoring purposes. If these gauges showed a reading, that would be an indication of a blockage or a closed valve in the system and could then be fixed before the need for the relief valve came in.

Safety

It is always important to identify any risks or hazards associated with the operation of a piece of equipment. These hazards either need to be eliminated if possible or their risks minimized. The first step in developing the safe operation of experimental equipment is to perform a HAZOP identifying all the hazards in the system. A safe working procedure is then developed based on the risks identified. General safety requirements are then identified which need to be adhered to during all operations of the equipment.

1. HAZOP

A HAZOP study was conducted following the guidelines provided by Turton, et al. (2013). All process units, as seen in the PFD in Appendix 8.4 Figure 8-5, were considered. The full HAZOP study can be seen in Appendix 8.10.

Following the HAZOP analysis, a safe working procedure was developed and can be found in Appendix 8.11.

2. General safety

The general safety for the operation of the regeneration equipment included mandatory personal protective equipment (PPE), including:

- Closed shoes
- A lab coat
- Safety glasses

3.3 Experimental Procedures

The experimental procedures for the adsorption and regeneration experiments as well as the sample preparation procedure are explained in this subsection. For more detailed procedures, please refer to Appendix 8.12, Appendix 8.13 and Appendix 8.14 respectively.

Adsorption experimental design and procedure

A full factorial experimental design was used in the adsorption experimentation. Important variables influencing an adsorption process were identified in literature such as adsorbent type and adsorption temperature. The effects of these variables were investigated and Table 3-5 below lists the variables involved in these experiments.

Table 3-5: A list of the variables in the adsorption experiments

Controlled Variables	Independent Variables	Dependent Variables
Solution volume, 200 mL	Adsorbent type: Activated alumina F-220, Selexsorb® CD & Selexsorb® CDx	Solution concentration
Stirrer rate, 350 rpm	Adsorbate type: 1-hexanol, 1-octanol, 1-decanol	
Solvent, *n*-decane	Temperature (°C): 25, 30 & 35	
Adsorbent mass, 10 g	Initial adsorbate mass %: $0 < x_i \leq 2$	

A solution volume of 200 mL was chosen to keep the external solution phase quasi constant during sampling and ensuring only a small percentage of solution mass was removed during sampling (Daems, et al., 2007). The stirrer rate was the maximum rate possible based on the distance between stirrer plate and magnetic stirrer bar. An adsorbent mass of 10 g ensured a sufficient quantity to form an adsorbent bed in the regeneration columns while ensuring an equilibrium state would be reached during adsorption experiments and within a reasonable amount of time.

Adsorption is considered an exothermic process and generally lower temperatures are favoured. Many experimental studies investigate adsorption temperatures anywhere between 20 and 60 °C (Desta, 2013). To the author's knowledge no previous published data was found on these specific systems, therefore three adsorption temperatures towards the lower end of the range seen in literature were chosen. Corresponding to industrial relevance, the adsorption process is specifically used for purification in the petrochemical industry's downstream processes and therefore low concentration of contaminants are removed from solvents (Scholtz, 26 Oct 2016). Adsorbate initial concentrations of between 0 and 2 mass percent were therefore chosen.

The adsorption experimental procedure involved solution preparation, the experimental preparation before adsorption runs were performed, sampling during the experimental run and then obtaining the final measurements required to conclude the run.

1. Solution preparation

Solutions were prepared in 500 mL Schott bottles. They were prepared on a mass basis while ensuring at least 400 mL of solution was prepared at a time, such that two experimental runs could be performed after one solution preparation.

Due to the expensive nature of the chemicals used in these experiments and the large volumes required, solution recycling was necessary. This entailed throwing the solutions back into Schott bottles once the adsorption runs had been completed, analyzing a sample of each of these bottles and adding the required masses of solvent and adsorbate to get the solution back to its original state. This recycling technique lessened the waste produced and cost involved in this project significantly.

2. Pre-experimental run preparations

Prior to the start of each experimental run, it was required to check the water level in the bath in order to ensure the heating unit's level instrument was satisfied. The heating unit was then set to the required adsorption temperature and switched on. It was essential to ensure the bath was at the required temperature before the weighing and hanging of the adsorbent so that the time elapsed between weighing the adsorbent and submerging it into the solution was at a minimum.

Each 500 mL tall form beaker contained one adsorption system and hence was classified as an individual experimental run. The preparation of each beaker involved the weighing of the beaker with its magnetic stirrer bar before and after the addition of the solution. The beakers were then placed in the water bath to heat the solutions prior to the addition of the adsorbents to the systems. The sample vials used for each run were then weighed and the mass recorded. Finally the adsorbent was prepared by weighing the mesh basket before and after the addition of the adsorbent and hanging it on its hook above the beaker.

The adsorbents were then lowered into the beakers, the stopwatch started and the magnetic stirrer plate switched on.

3. During an experimental run

During each of the experimental runs, the beakers were sampled using a micropipette. 200 µL of each solution was sampled at specified time intervals during the course of the experimental run

resulting in 10 samples taken per experimental run. Table 3-6 below shows the sampling time intervals for the adsorption experimental runs.

Table 3-6: Details of the sampling time intervals during the adsorption experimental runs

Sample Number	1	2	3	4	5	6	7	8	9	10
Time Interval [min]	0	0	15	30	150	240	360	375	390	395

4. Experimental run conclusion procedures

After the experimental time had lapsed, the magnetic stirrer plate and heating unit were switched off and the adsorbents lifted out of the beakers. All elements then once again had to be weighed. The adsorbent containing mesh baskets, the solution containing beakers and the sample vials were all weighed and their masses recorded. The solutions were then poured back into Schott bottles and the adsorbent thrown into waste containers.

A detailed procedure of the cleaning of all the elements involved in these experiments is given in Appendix 8.15.

Regeneration experimental design and procedures

The regeneration experiments formed a cyclic experimental procedure with the adsorption experiments. Once an adsorption experiment was completed, the adsorbent was put into the regeneration column in order to remove the adsorbate and prepare the adsorbent for the next adsorption cycle.

1. Experimental design

Table 3-7 lists the variables in the regeneration experiments.

Table 3-7: A list of the regeneration experimental variables

Controlled Variables	**Independent Variables**	**Dependent Variables**
Adsorbent mass, 10 g Regeneration duration, 60 min Adsorbate, 1-hexanol Initial adsorbate mass %, 1,5 %	Adsorbent type: Activated Alumina F-220, Selexsorb® CD & Selexsorb® CDx Regeneration temperature: 180 & 205 °C	Column outlet temperature Adsorption capacity

The adsorbent mass, adsorbate type and initial adsorbate mass percentage were controlled variables chosen based on the adsorption results obtained during the adsorption equilibrium experiments. These choices are explained in section 7.1 after the presentation of the adsorption results.

A regeneration system is affected by variables such as temperature and duration of the regeneration process. In this study the regeneration temperature was varied, while the regeneration duration was kept constant. Due to time constraints the influence of both variables could not be investigated. It was decided that the regeneration temperature played more of an important role in the performance of the regeneration technique and therefore was the variable to be varied.

Based on the size of the systems investigated and on regeneration durations used in previous studies [(Lashaki, et al., 2012)and (Rauthula & Srivastava, 2011)] a regeneration duration of 1 hour was chosen. This duration did not include the time required to slowly heat the system up to the regeneration temperature. At a volumetric flowrate of 0,011 m^3/h, a 1 hour duration resulted in a large bed volume turnover (720), ensuring the purge gas had a sufficient number of opportunities to carry out desorbed components from the adsorbent bed.

As a rule of thumb, the regeneration temperature of a system is recommended to be 30 °C above the highest boiling point in a system for alumina adsorbents (Scholtz, 26 Oct 2016). In this system, the two boiling points were 157,0 °C (1-hexanol) and 174,1 °C (*n*-decane). The first regeneration temperature was therefore chosen as 205 °C.

The second regeneration temperature was chosen as 185 °C. This choice was based on trying to investigate whether a regeneration temperature closer to the boiling point of the compounds in a system could give the same or similar results, while saving energy and lessening its associated economic impacts.

2. Experimental procedure

The regeneration procedure involved initially preparing the setup by opening the regeneration columns and ensuring the outlet valve on the activated carbon trap was open. The adsorbents were then transferred from the adsorption cycle to the regeneration cycle after weighing, the columns sealed again and the nitrogen gas opened. It was essential to purge the setup of any oxygen before starting the heating process to minimize any safety risks. While purging the system, the control box was switched on and the USB drive inserted into the HMI screen to start the logging procedure. The temperature control programmes on all controllers were set to the correct regeneration temperature. The cooling water pump was then turned on and the temperature control programmes started. At the

end of the regeneration cycle, the control programmes were stopped, but the nitrogen gas was still allowed to flow through the system till the temperature probes read 50 °C. At this point the cooling water pump was switched off, the USB flash ejected from the screen and the control box switched off. The outlet valve on the activated carbon trap was closed and the system was allowed to cool down completely overnight.

The following day the regeneration columns were opened, the adsorbents removed, weighed and mass recorded and then cycled back into an adsorption cycle following the procedure described in adsorption experimental design and procedure.

Sample preparation procedure

Liquid samples were analysed using an Agilent 7890 Series gas chromatogram. The internal standard method was used and for all systems, 1-pentanol, was used as internal standard. Methanol was used as solvent. All samples were prepared as follows:

- Between 80 and 120 µL of experimental sample was added to a weighed sample vial.
- 40 µL of internal standard was then added.
- The vial is then filled with methanol, approximately 1,4 mL.

After each addition the sample vial is weighed and the mass recorded. The samples are then diluted at a ratio of 1:3 with methanol solvent.

Calibration curves were used to quantify the amounts of *n*-decane and alcohol in each sample. Calibration curves were constructed using the Agilent software by preparing 5 samples of known mass. Each sample contained a known mass of each organic chemical (*n*-decane, 1-hexanol, 1-octanol & 1-decanol) and the internal standard. Five samples of varying ratios between internal standard and organic chemicals produced calibration curves with the different response factors for each sample. These curves were then used by the Agilent programme in subsequent sample analyses using the internal standard mass inputted by the operator to calculate the mass of the n-decane and alcohol in the sample.

3.4 Repeatability and Experimental Error

Figure 3-9 represents results pertaining to repeat adsorption runs performed. The percentage alcohol removed in each system, calculated as the difference between the initial and equilibrium mass percent divided by the equilibrium mass percent, was used to determine the statistical repeatability of the adsorption runs. The 1-decanol experimental runs showed an average alcohol removal

percentage of 35,2 %, with a standard deviation of 1,25 % and a relative standard deviation (RSD) of 3,56 %. The 1-octanol experimental runs showed an average alcohol removal percentage of 57,3 %, with a standard deviation of 0,60 % and a RSD of 1,05 %. The repeatability of the adsorption experiments was therefore deemed acceptable.

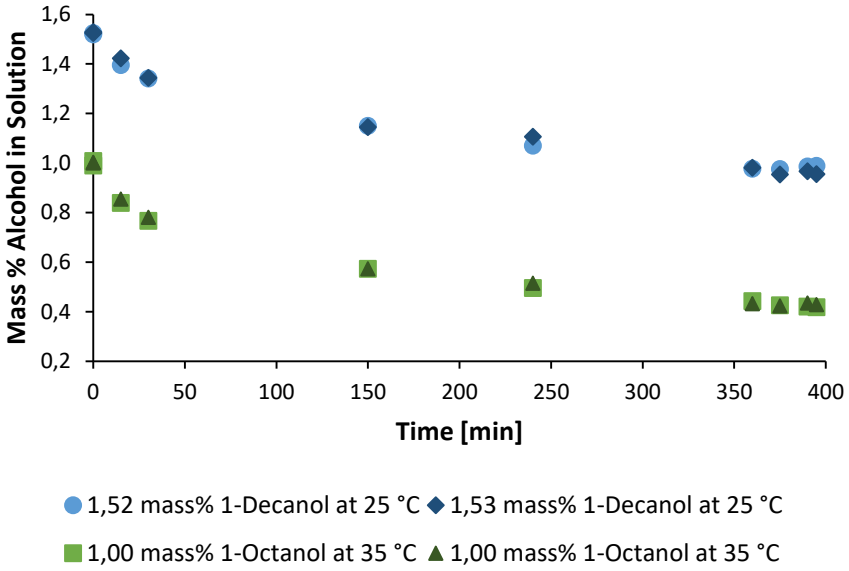

Figure 3-9: The change in alcohol mass % with time during repeated adsorption experiments for 1-decanol and 1-octanol adsorbents using the Selexsorb CDx adsorbent at adsorption temperatures of 35 and 25 C respectively

The accuracy of experimental results depends on errors in experimental procedures and analytical methods. In this work, numerous procedures were followed and where possible the errors were identified and quantified.

3.4.1. Experimental errors

In this study, numerous procedures were followed in order to complete experimental runs, using various laboratory measurement tools. The main errors identified were those associated with mass and volume measurements.

All experimental elements (adsorption solution, adsorbents, sample vials, etc.) were weighed before and after each experimental run. A calibrated two-decimal laboratory scale was used for these measurements. The error associated with these measurements was determined to be ± 0,005 g (Carlson, 2000).

All solution volumes were measured using a 250 mL graduated cylinder with 2 mL graduations. The error associated with these measurements was determined to be 0,2 mL (Carlson, 2000). Solution

samples were taken during experimental runs using a 20 - 200 µL pipette with a precision of 0,3 µL. The pipette tip wall effects were considered negligible due to pipette tip rinsing before the final sample was removed from the solution.

3.4.2. Analytical errors

The analysis of the samples taken during experimentation formed the basis of all experimental results and therefore the error involved in the preparation and analysis of these samples was the main contributor to the experimental error of this work.

A five-decimal analytical balance was used to record the mass of the sample analysed as well as the internal standard mass. Two variable pipettes (10 – 100 and 20 – 200 µL) were used to prepare samples for GC analysis. The errors associated with these pieces of equipment were assumed to be negligible in relation to the magnitude of the final measurement.

The alcohol and *n*-decane content in each sample was determined using GC calibration curves. These curves were updated every few months during experimentation to account for curve drift due to wear and tear of the GC. One set of duplicate samples were also analysed in each set of samples analysed. Samples of known mass were also analysed on several occasions throughout experimentation as an indication of drift and an average error 0,26 mg was obtained.

The measured mass of each sample was compared to the value recorded by the GC and a percentage error evaluated. The average of these percentage errors for each set of data (representing an adsorption system) formed the analytical error for that set of data. A maximum percentage error in analytical results of 3,28 % was seen.

Chapter 4: Adsorption Experimental Results

In this chapter the adsorption results are introduced and the various factors affecting an adsorption system are discussed. The factors varied in this project included the adsorption temperature, the type of adsorbate and the type of adsorbent. Each of these factors and their influence on each of the adsorption systems are discussed.

The reader is referred to Appendix 8.16, 8.17 and 8.18 for the full set of raw experimental data for each adsorption system, categorised by adsorbent type.

4.1 Adsorbent Characterisation

The three adsorbents used in this study were characterised by N_2 adsorption at 77,35 K. Figure 4-1, Figure 4-2 and Figure 4-3, show the adsorption-desorption graphs for activated alumina F-220, Selexsorb® CD and Selexsorb® CDx respectively.

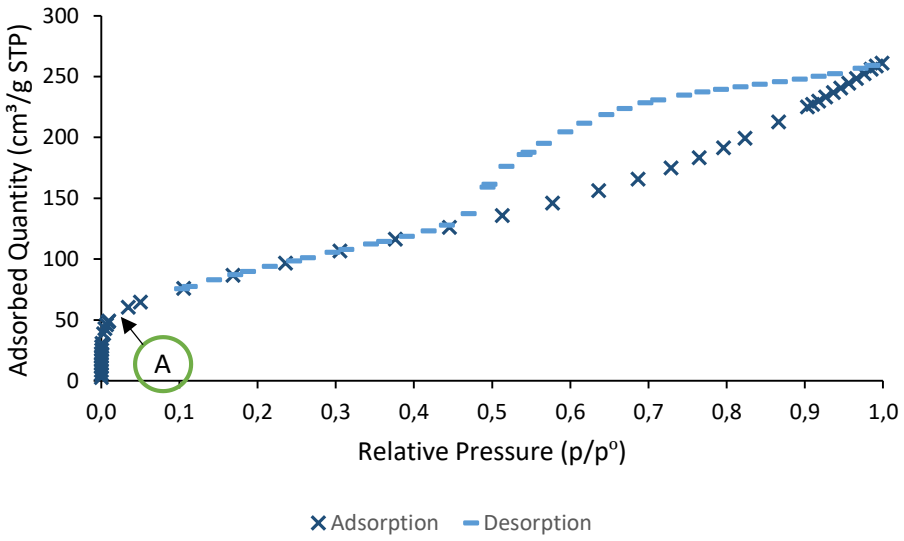

Figure 4-1: The nitrogen adsorption-desorption isotherms at 77,35 K for Activated Alumina F-220

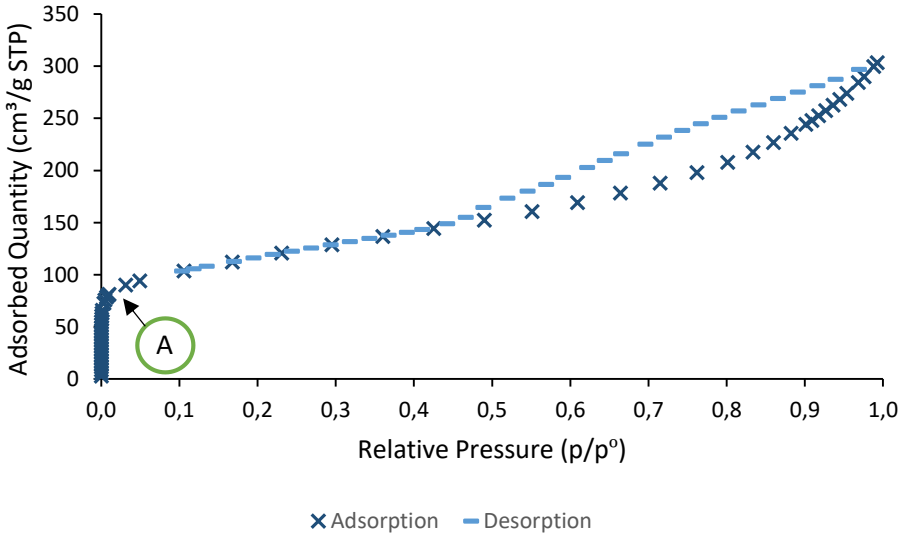

Figure 4-2: The nitrogen adsorption-desorption isotherms at 77,35 K for Selexsorb® CD

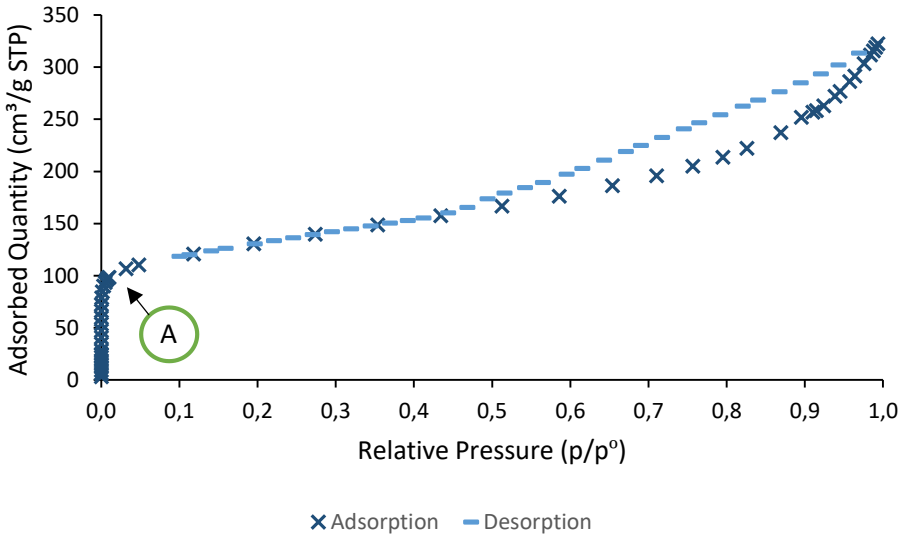

Figure 4-3: The nitrogen adsorption-desorption isotherms at 77,35 K for Selexsorb® CDx

Following the IUPAC classification (Sing, et al., 1982), the adsorption-desorption isotherm of Activated Alumina F-220 (Figure 4-1) most closely resembles a type IV isotherm with a H2 hysteresis, while that of Selexsorb CD and CDX (Figure 4-2 and Figure 4-3) resembles a type IV isotherm with a H3 hysteresis. The type IV isotherm generally represents multilayer adsorption onto mesoporous

adsorbents followed by capillary condensation (Sing, et al., 1982). The initial part of the isotherm represents monolayer adsorbate coverage on the adsorbent surface, with the start of multilayer adsorption occurring at point A on the figures (Sing, et al., 1982). The H2 hysteresis loop does not give well defined distributions of pore sizes and shapes, therefore making it difficult to interpret (Sing, et al., 1982), while the H3 hysteresis characterises adsorbents as plate-like particles with slit-shaped pores (Sing, et al., 1982).

Following these definitions, it can be said that all three adsorbents present with mesoporous structures onto which multiple layers of adsorbate molecules can be adsorbed. However, the significant increase in quantity adsorbed of N_2 for these adsorbents at very low relative pressures (the initial slope of the isotherms) suggests the adsorbents contain microporous areas too. The Density Functional Theory (DFT) was thus used to characterise the pore distributions for each adsorbent to give a better understanding of the micropore, mesopore and macropore structures of each adsorbent. The micropore, mesopore and macropore volumes for the various pore widths for each adsorbent are shown in Figure 4-4.

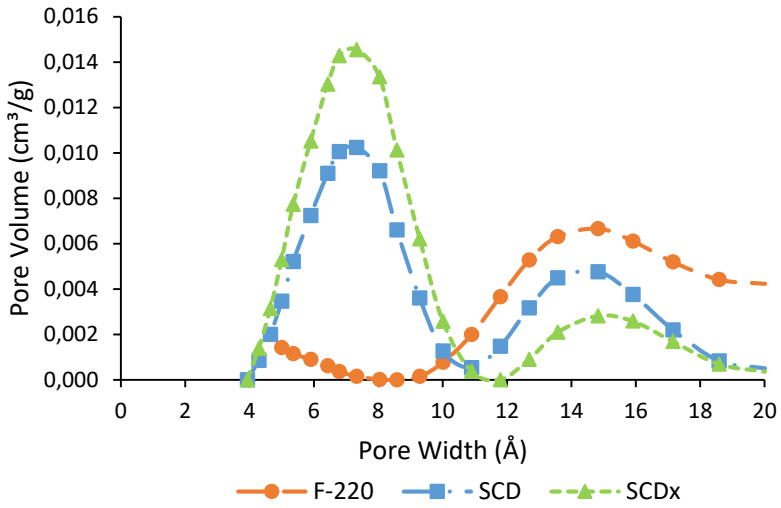

a) Micropore volumes of F-220, SCD & SCDx

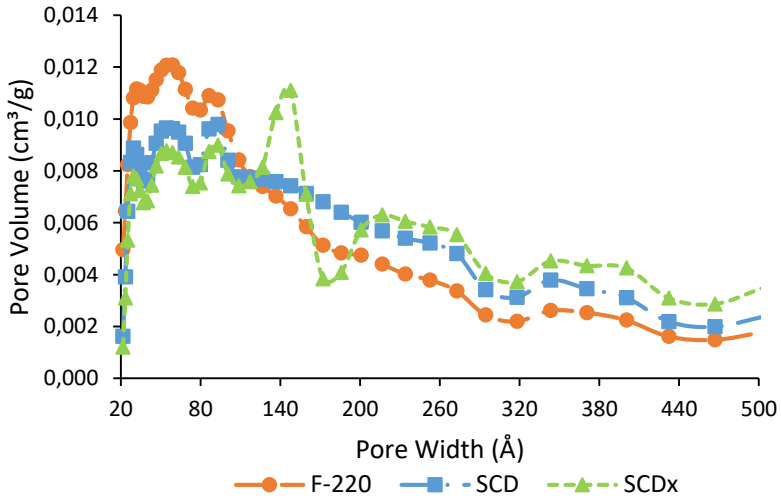

b) Mesopore volumes of F-220, SCD & SCDx

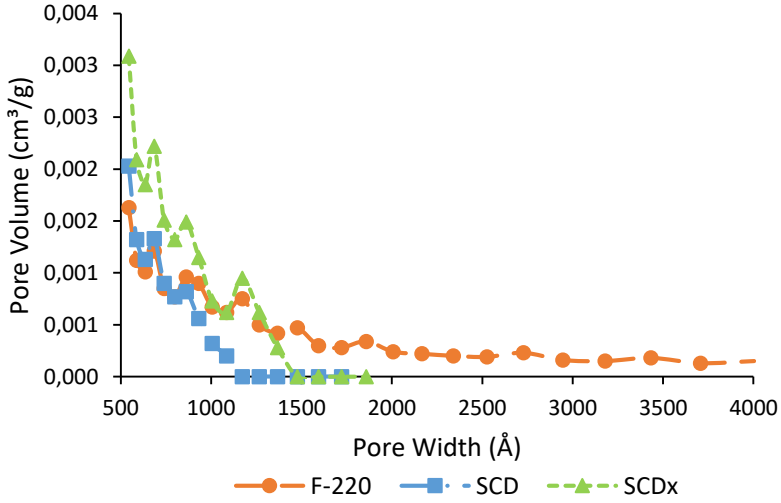

c) Macropore volumes of F-220, SCD & SCDx

Figure 4-4: The micro-, meso- and macropore volumes for Activated Alumina F-220, Selexsorb® CD and Selexsorb® CDx

When considering the micropore volumes for each adsorbent (Figure 4-4 a), the Selexsorb CDx adsorbent presents with the highest micropore volume of 0,114 cm^3/g, compared to SCD and F-220 with micropore volumes of 0,090 and 0,049 cm^3/g respectively. These micropores account for 28 % of the pores present in the SCDx adsorbent, 24 % of the pores in the SCD adsorbent and only 13 % of the pores in the F-220 adsorbent. Further characterisation of the micropores of each adsorbent using the Horvath-Kawazoe method showed the average micropore width of F-220, SCD and SCDx to be 10,88; 8,48 and 7,97 Å respectively.

All three adsorbents present with significant mesoporous volumes as is seen in Figure 4-4 b, with the F-220 adsorbent showing the highest mesoporous volume of 0,308 cm^3/g. Selexsorb® CD and CDx both have similar mesoporous volumes of 0,279 and 0,271 cm^3/g respectively. The mesopores account for 83 % of the pores in the F-220 adsorbent, 74 % of the pores in the SCD adsorbent and 67 % of the pores in the SCDx adsorbent.

The macropores in each adsorbent account for very little (less than 1 %) of each adsorbent's pore structure, however when comparing the three, the F-220 adsorbent shows the highest macropore volume of 0,015 cm^3/g.

Figure 4-5 shows the surface area make up of each adsorbent, giving the total BET surface area and the subsequent surface areas provided by the three pore structures present in each adsorbent. The BET surface areas of each adsorbent compared well to those specified by the manufacturer on the available data sheets, shown in Table 4-1. The BET surfaces areas of both the Selexsorb® adsorbents also compare well to what was found by Laredo, et al. (2016), which found that the SCD adsorbent had a BET surface area of 410 m^2/g and SCDx a BET surface area of 460 m^2/g.

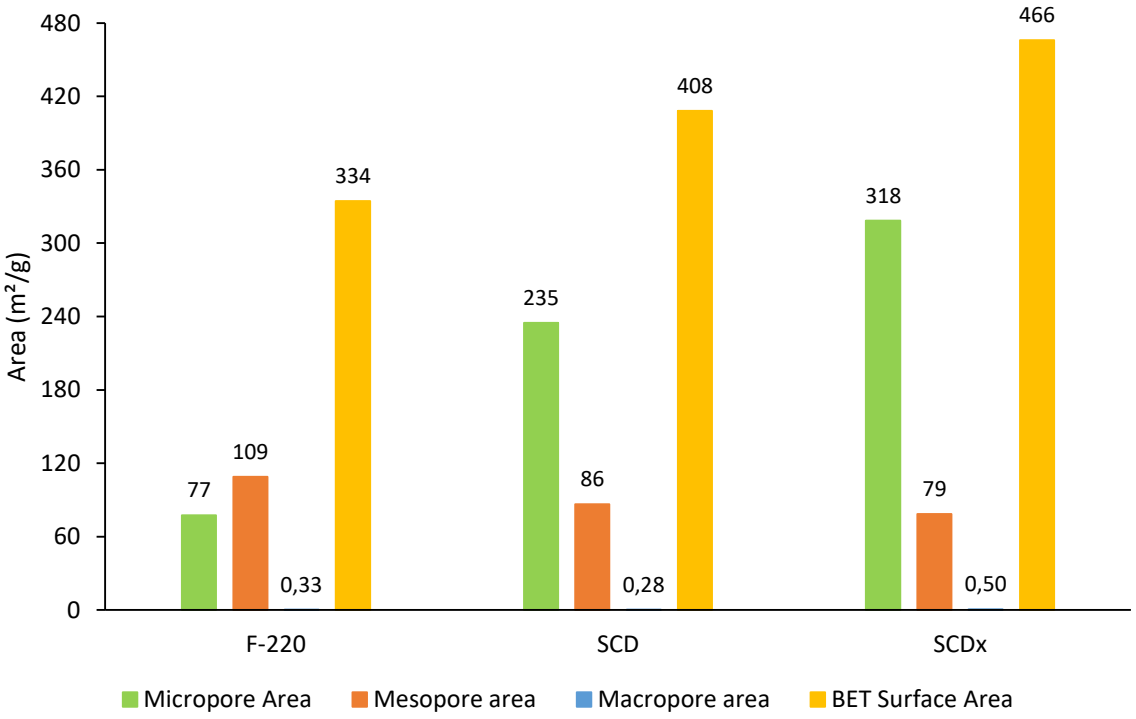

Figure 4-5: The micro-, meso- and macropore areas along with the BET surface are for adsorbents F-220, SCD and SCDx

Even though Selexsorb® CDx presents with the highest BET surface area of 466 m²/g, much of its surface area is confined in its micropores (68 %), the same is seen with the Selexsorb® CD adsorbent with 58 % of its surface area confined in micropores. In comparison, a significant portion of the Activated Alumina F-220 adsorbent's surface area lies on its external surface (44 %), with the second largest surface area confined in the mesopores (33%). This would imply that the F-220 adsorbent would be better suited for removal of larger organic molecules than the two Selexsorb adsorbents as most of its active surface area is external and easy to reach by the adsorbate molecules.

Table 4-1: Characteristic properties of adsorbents F-220, SCD and SCDx

	Activated Alumina F-220	Selexsorb® CD	Selexsorb® CDx
BET Surface Area (m²/g)	334,3	408,3	466,0
Manufacturer Surface Area (m²/g)	355,0	400,0	450,0
External Surface Area (m²/g)	147,7	86,7	68,6
Total Pore Volume (cm³/g)	0,372	0,379	0,403
Total Pore Area (m²/g)	186,6	321,6	397,4

These three adsorbents can therefore be characterised by micro and mesoporous structures showing multilayer adsorption capabilities and large surface areas. Based on these characterisations, the adsorbents appear to be viable options, with pores large enough, to remove 1-hexanol, 1-octanol and 1-decanol adsorbate molecules from *n*-decane solutions.

4.2 Alcohol Adsorption onto Activated Aluminas

This study consisted of 27 adsorption systems investigated at three initial adsorbate concentration levels. The raw adsorption data consisted of concentration values obtained over specific time intervals and measurements of variables such as solution volume and adsorbent mass. This raw data was processed in such a way that comparisons could be made between adsorbent type, adsorbate type and the effects of temperature on the various adsorption systems and so that equilibrium and kinetic modelling could be done.

4.2.1. Adsorption of alcohols from n-decane with time

Figure 4-6, Figure 4-7 and Figure 4-8show the Ci(t)/C0 versus time data for the activated alumina F-220 adsorbent for adsorbates 1-hexanol, 1-octanol and 1-decanol respectively.Figure 4-9, Figure 4-10 and Figure 4-11 show the Ci(t)/C0 versus time data for the Selexosrb® CD adsorbent for adsorbates 1-hexanol, 1-octanol and 1-decanol adsorbates respectively. Figure 4-12, Figure 4-13 and Figure 4-14 shows the same type of data for the Selexsorb® CDx adsorbent for adsorbates 1-hexanol, 1-octanol and 1-decanol.

The green markers in each of the figures represent the lowest initial adsorbate concentration for each system. In each adsorption system represented by each graph, the lowest initial adsorbate concentration presents with the highest percentage of adsorbate removed. The difference between the initial and final concentration ratios represents the percentage of adsorbate removed from the system. A larger difference is seen for the lowest initial adsorbate concentration compared to that of the middle and highest initial adsorbate concentrations for all adsorption systems.

The blue markers in each of the figures represent the highest initial adsorbate concentration for each system. In each adsorption system, the highest initial adsorbate concentration presents the lowest percentage of adsorbate removed.

The percentage adsorbate removed in each system thus decreases as the initial adsorbate concentration increases. Due to the number of adsorbent active sites available remaining constant

(mass of adsorbent was kept constant), an increase in adsorbate concentration causes an increase in competition between the molecules for these active sites. This thus causing the percentage of the adsorbate molecules removed to be less at higher initial adsorbate concentrations. Similar results were observed in a study by Kumar, et al. (2010), which investigated the effects of initial Pb2+ ion concentrations on its removal from aqueous solutions using activated carbon. The study showed that at a 100 mg/L initial Pb2+ concentration, the percentage Pb2+ removed was 90,08 %, while at 1000 mg/L it dropped to 70,35 % (Kumar, et al., 2010).

The kinetics of the adsorbate molecules for each initial adsorbate concentration is represented by the gradients of the graphs. Initially, these slopes are steep, i.e. a fast decline in adsorbate concentration is observed. However as time continues, these gradients begin to level out until a plateau is reached where the concentration ratio remains constant, within 5 % range of its value. This plateau represents the dynamic equilibrium of the system and specific examples of it can be seen in Figure 1b, Figure 5c and Figure 9a.

The steeper initial gradients are due to all active sites being vacant at the start of the adsorption process, while as molecules adsorb, the number of vacant sites decrease thereby decreasing the adsorption of the adsorbate molecules in the bulk solution. The steeper initial slopes are also due to initial adsorption taking place on the external surface of the adsorbent particles and as these sites fill up, adsorbate molecules are forced to diffuse into the porous structures of the particles (Aljebori & Alshirifi, 2012). Similar results were obtained in studies conducted by Ajebori & Alshirifi (2012) and Okoli (2014).

When comparing the initial gradients of the graphs between types of adsorbates, Figure 4-7 c to Figure 4-13 c, it can be seen that the initial slopes of 1-octanol adsorption onto activated alumina F-220 are steeper than 1-octanol adsorption onto Selexsorb® CDx. For example at the lowest initial 1-octanol concentration for both systems, a decrease of 0,41 in concentration ratio is seen for F-220 compared to the decrease of 0,28 seen for SCDx. As described in Section 4.1, the F-220 adsorbent has the largest external surface area of 147,7 m^2/g compared to that of 68, 6 m^2/g for SCDx, thus leading to faster initial adsorption as more of the active surface is readily available to adsorbate molecules without internal diffusion.

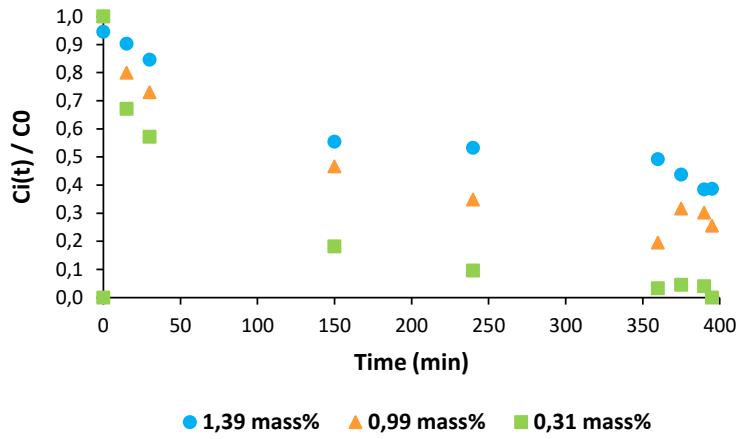

a) 1-hexanol concentration-time profiles for activated alumina F-220 at 25 °C

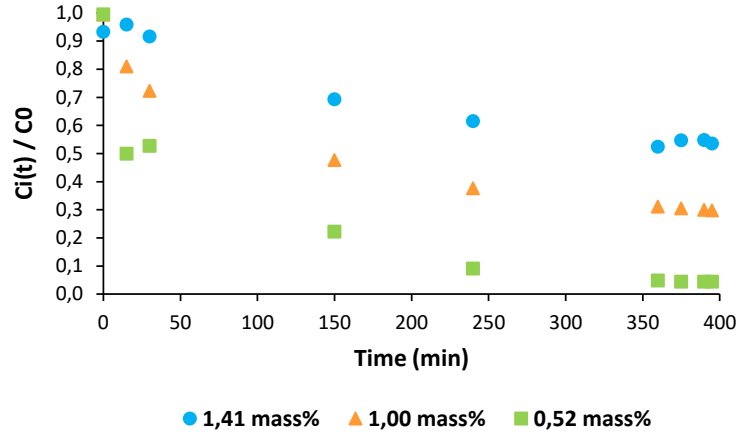

b) 1-hexanol concentration-time profiles for activated alumina F-220 at 30 °C

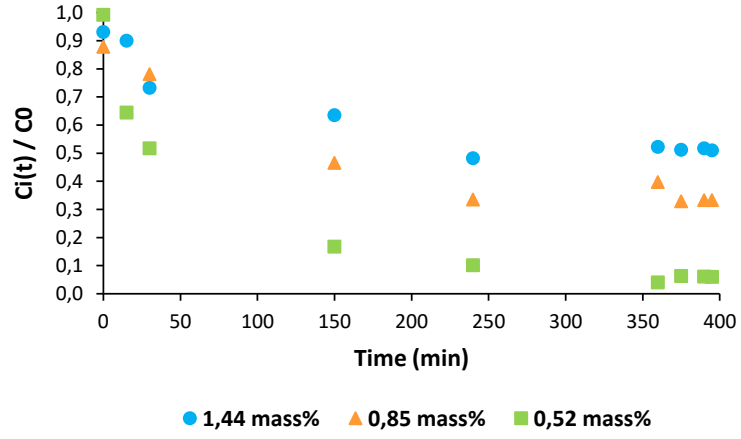

c) 1-hexanol concentration-time profiles for activated alumina F-220 at 35 °C

Figure 4-6: 1-hexanol adsorbate concentration-time profiles for three initial adsorbate concentrations of 1-hexanol in n-decane solutions adsorbed into activated alumina F-220 adsorbent at a) 25 °C, b) 30 °C and c) 35 °C

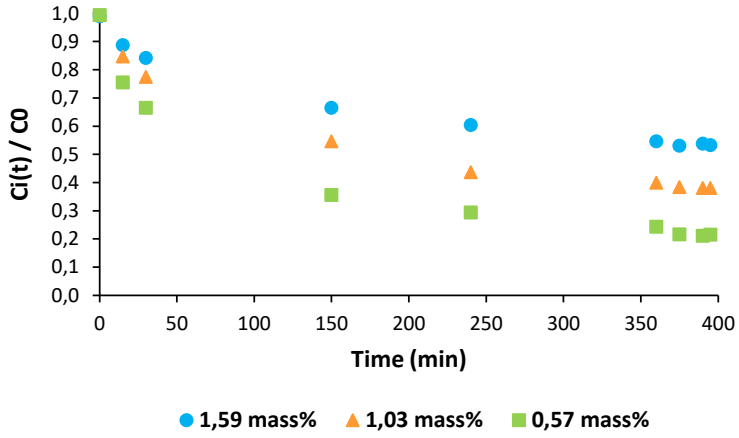

a) 1-octanol concentration-time profiles for activated alumina F-220 at 25 °C

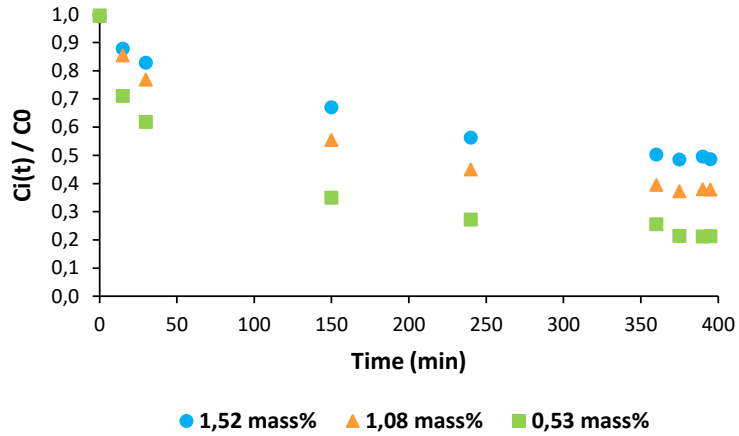

b) 1-octanol concentration-time profiles for activated alumina F-220 at 30 °C

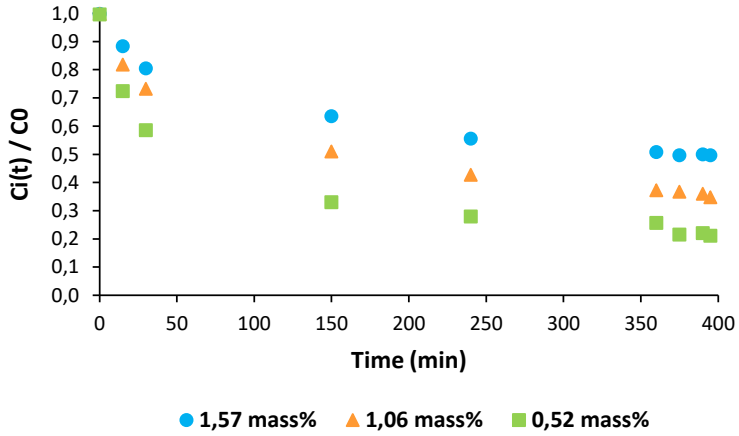

c) 1-octanol concentration-time profiles for activated alumina F-220 at 35 °C

Figure 4-7: 1-octanol adsorbate concentration-time profiles for three initial adsorbate concentrations of 1-hexanol in n-decane solutions adsorbed into activated alumina F-220 adsorbent at a) 25 °C, b) 30 °C and c) 35 °C

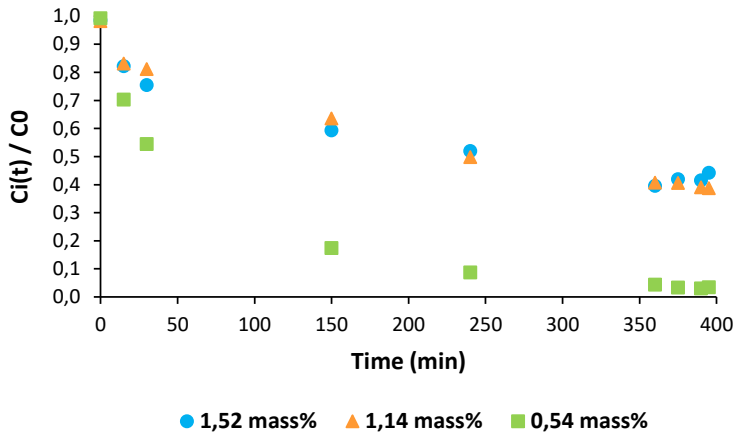

a) 1-decanol concentration-time profiles for activated alumina F-220 at 25 °C

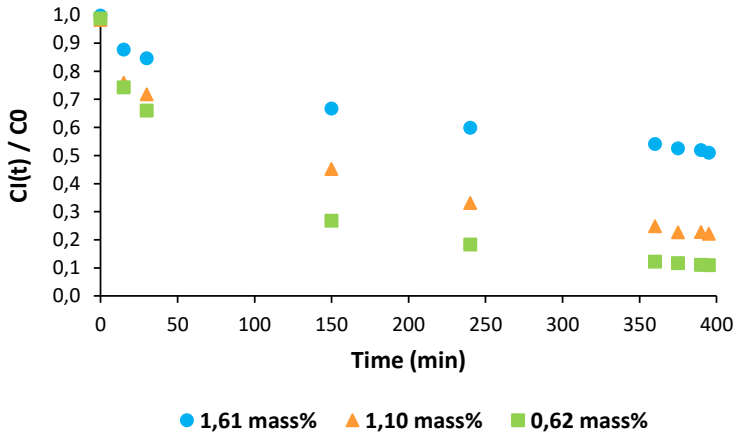

b) 1-decanol concentration-time profiles for activated alumina F-220 at 30 °C

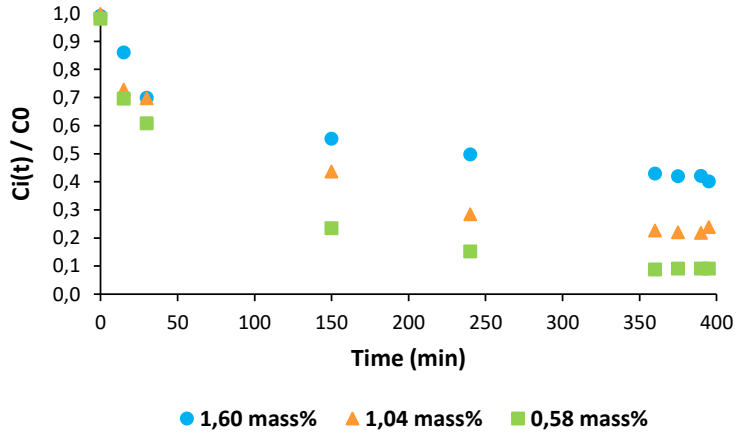

c) 1-decanol concentration-time profiles for activated alumina F-220 at 35 °C

Figure 4-8: 1-decanol adsorbate concentration-time profiles for three initial adsorbate concentrations of 1-hexanol in n-decane solutions adsorbed into activated alumina F-220 adsorbent at a) 25 °C, b) 30 °C and c) 35 °C

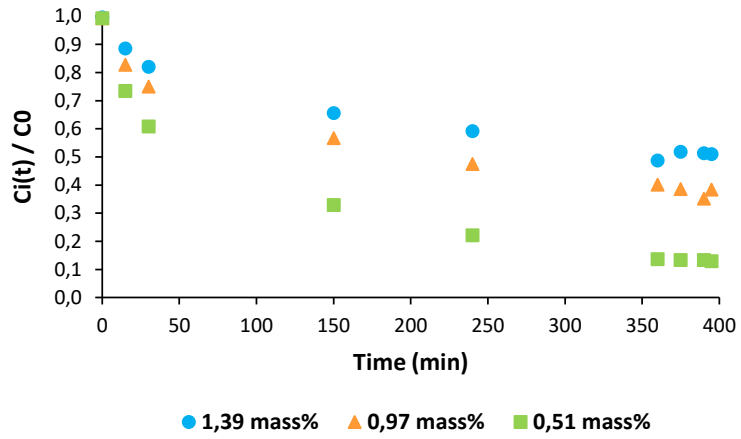

a) 1-hexanol concentration-time profiles for Selexsorb® CD at 25 °C

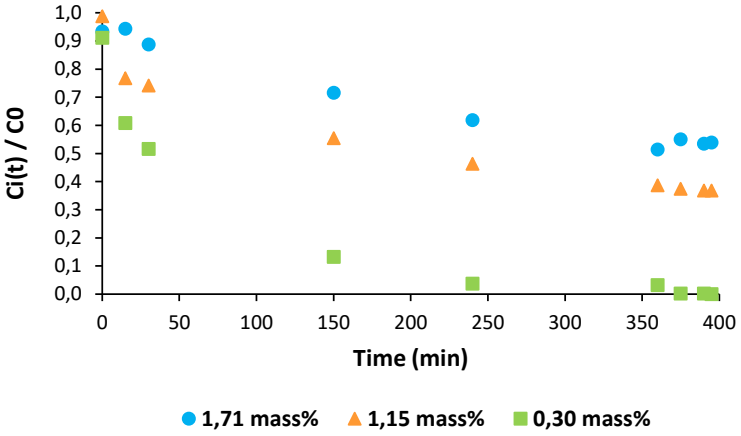

b) 1-hexanol concentration-time profiles for Selexsorb® CD at 30 °C

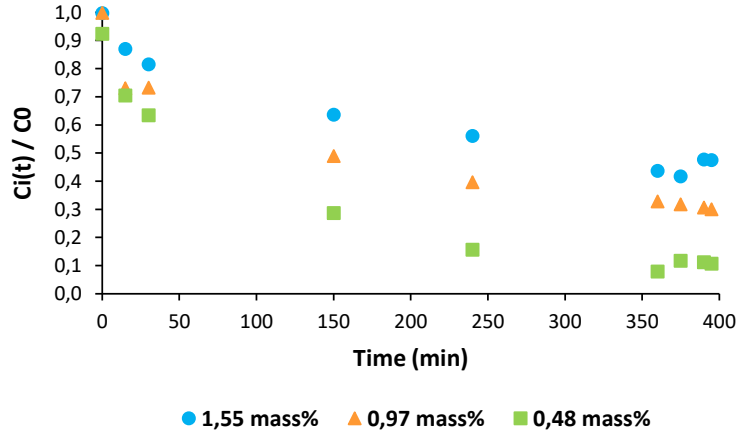

c) 1-hexanol concentration-time profiles for Selexsorb® CD at 35 °C

Figure 4-9: 1-hexanol adsorbate concentration-time profiles for three initial adsorbate concentrations of 1-hexanol in n-decane solutions adsorbed into Selexsorb® CD adsorbent at a) 25 °C, b) 30 °C and c) 35 °C

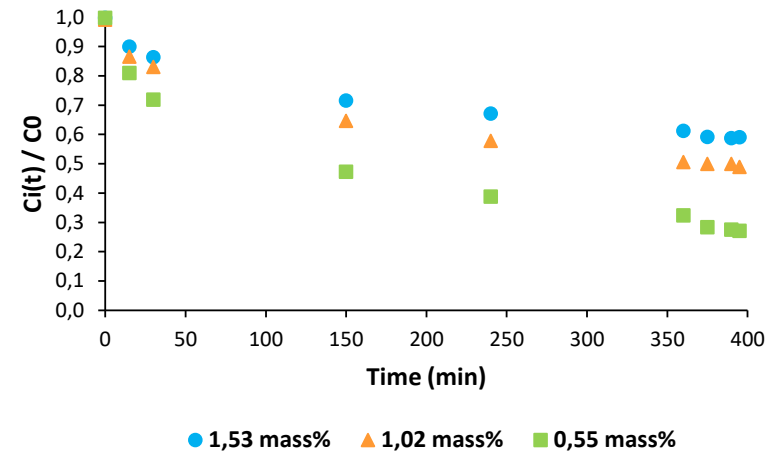

a) 1-octanol concentration-time profiles for Selexsorb® CD at 25 °C

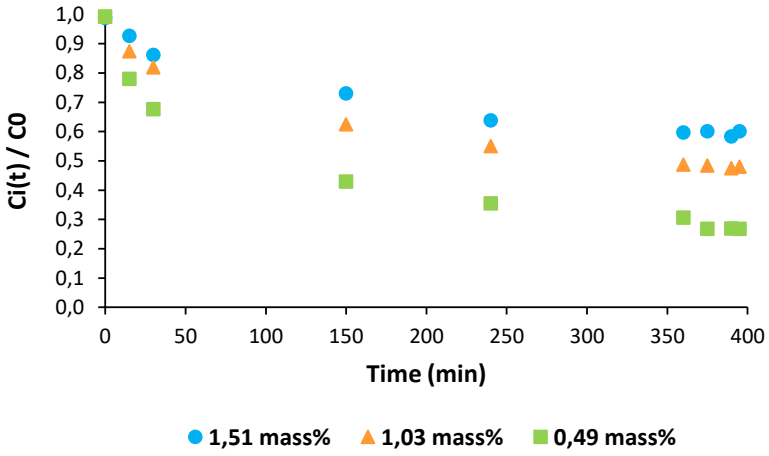

b) 1-octanol concentration-time profiles for Selexsorb® CD at 30 °C

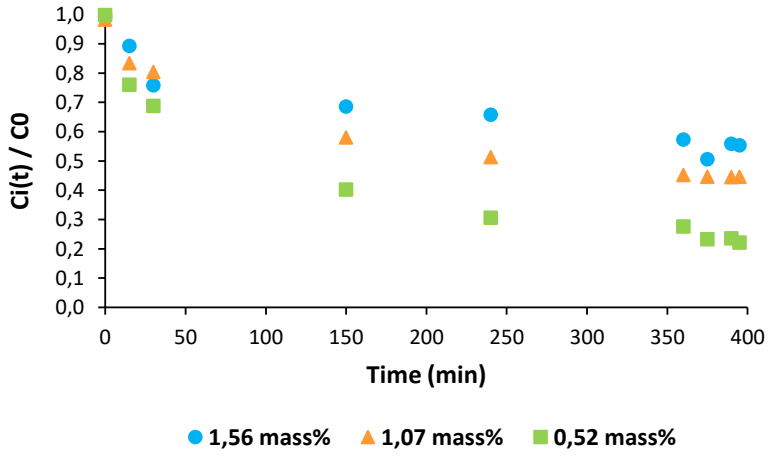

c) 1-octanol concentration-time profiles for Selexsorb® CD

Figure 4-10: 1-octanol adsorbate concentration-time profiles for three initial adsorbate concentrations of 1-hexanol in n-decane solutions adsorbed into Selexsorb® CD adsorbent at a) 25 °C, b) 30 °C and c) 35 °C

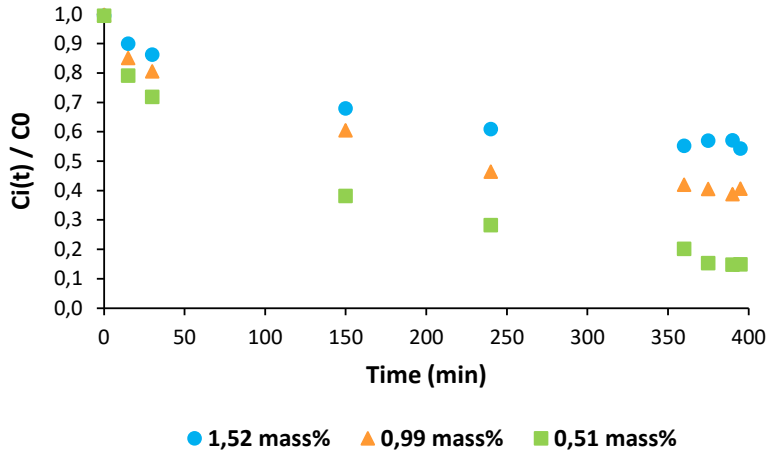

a) 1-decanol concentration-time profiles for Selexsorb® CD at 25 °C

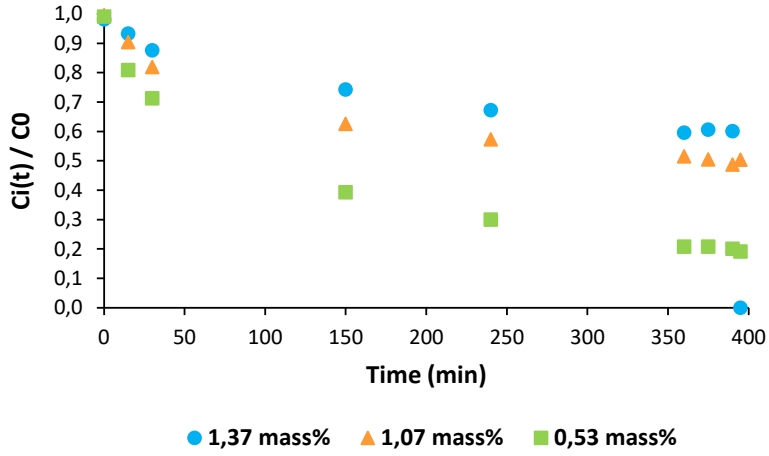

b) 1-decanol concentration-time profiles for Selexsorb® CD at 30°C

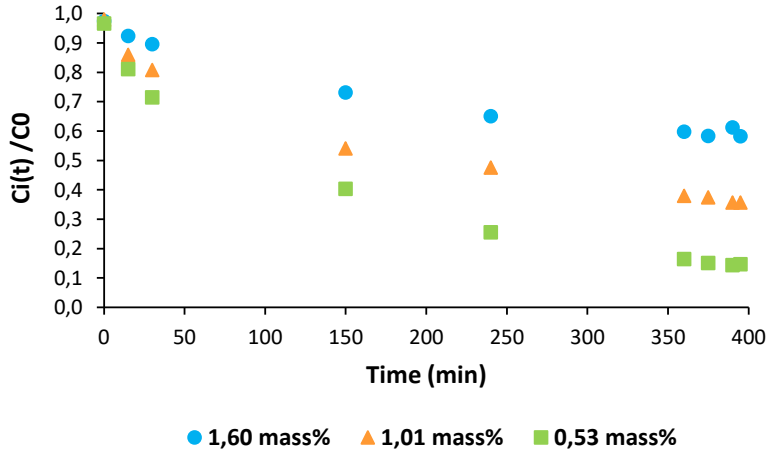

c) 1-decanol concentration-time profiles for Selexsorb®

Figure 4-11: 1-decanol adsorbate concentration-time profiles for three initial adsorbate concentrations of 1-hexanol in n-decane solutions adsorbed into Selexsorb® CD adsorbent at a) 25 °C, b) 30 °C and c) 35 °C

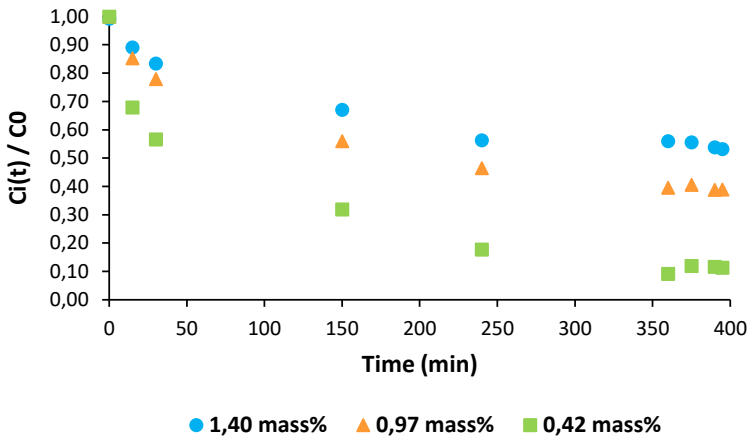

a) 1-hexanol concentration-time profiles for Selexsorb® CDx at 25 °C

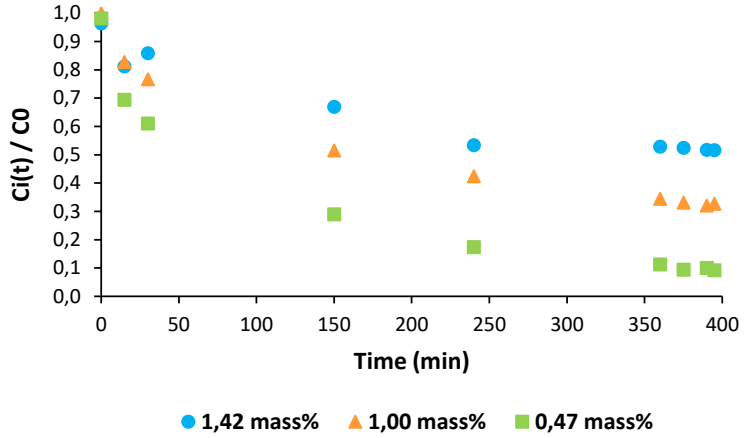

b) 1-hexanol concentration-time profiles for Selexsorb® CDx at 30 °C

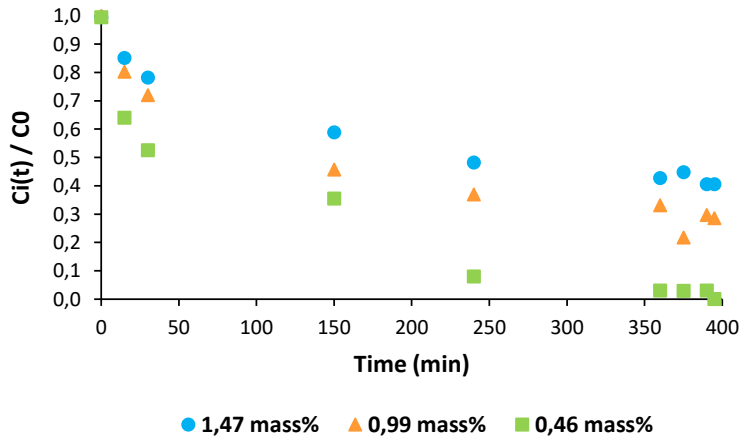

c) 1-hexanol concentration-time profiles for Selexsorb® CDx at 35 °C

Figure 4-12: 1-hexanol adsorbate concentration-time profiles for three initial adsorbate concentrations of 1-hexanol in n-decane solutions adsorbed into Selexsorb® CDx adsorbent at a) 25 °C, b) 30 °C and c) 35 °C

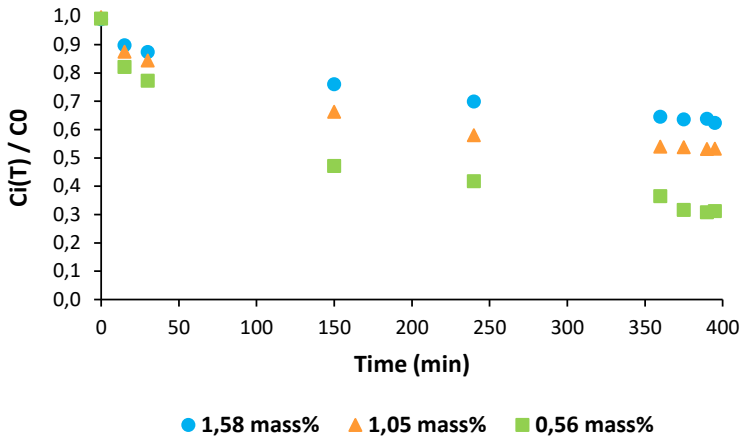

a) 1-octanol concentration-time profiles for Selexsorb® CDx at 25 °C

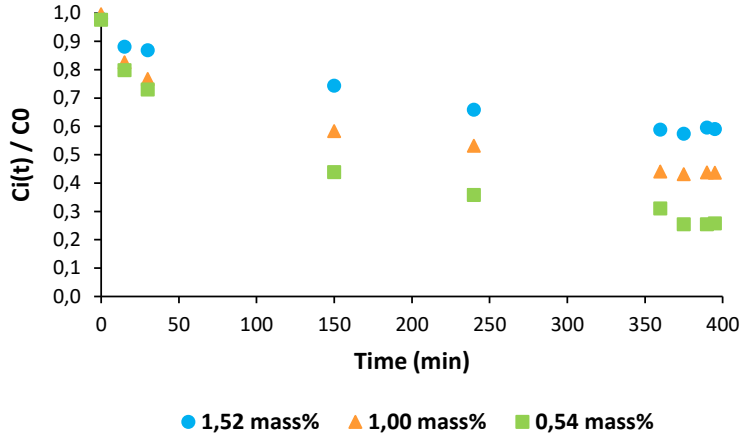

b) 1-octanol concentration-time profiles for Selexsorb® CDx at 30 °C

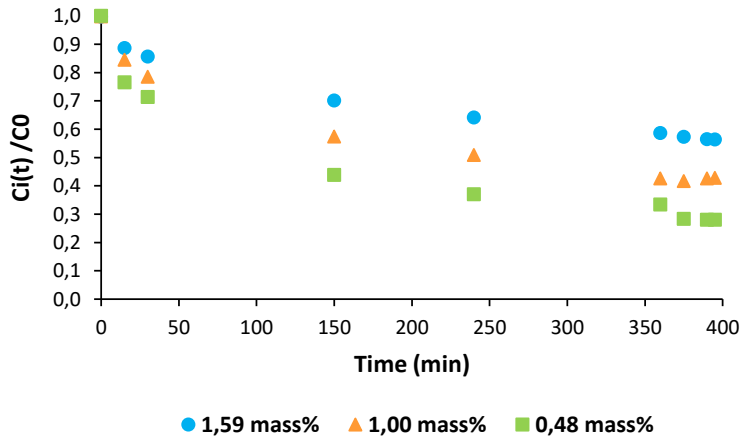

c) 1-octanol concentration-time profiles for Selexsorb® CDx at 30 °C

Figure 4-13: 1-octanol adsorbate concentration-time profiles for three initial adsorbate concentrations of 1-hexanol in n-decane solutions adsorbed into Selexsorb® CDx adsorbent at a) 25 °C, b) 30 °C and c) 35 °C

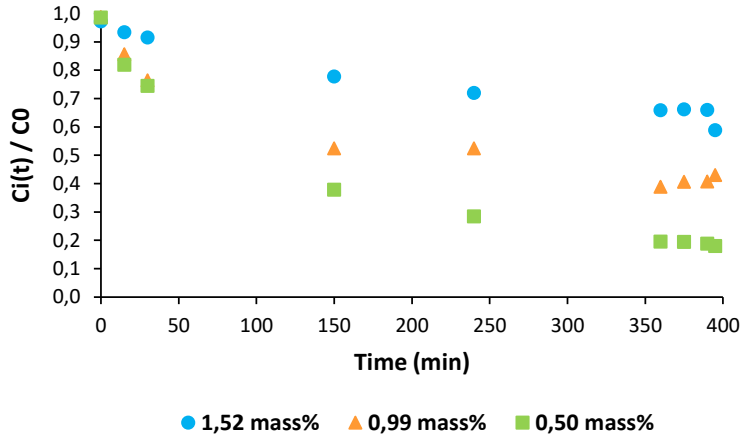

a) 1-decanol concentration-time profiles for Selexsorb® CDx at 25 °C

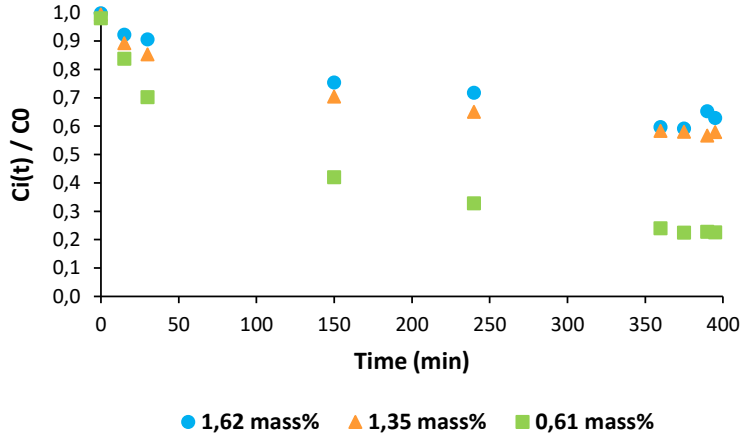

b) 1-decanol concentration-time profiles for Selexsorb® CDx at 30 °C

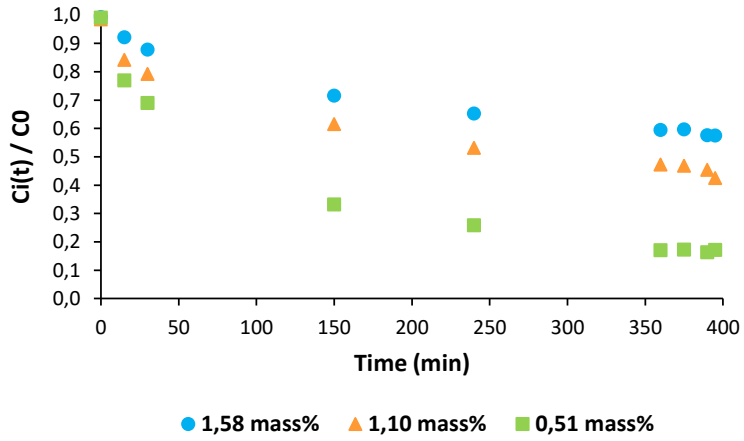

c) 1-decanol concentration-time profiles for Selexsorb® CDx at 35 °C

Figure 4-14: 1-decanol adsorbate concentration-time profiles for three initial adsorbate concentrations of 1-hexanol in n-decane solutions adsorbed into Selexsorb® CDx adsorbent at a) 25 °C, b) 30 °C and c) 35 °C

4.2.2. The influence of adsorbent type on the equilibrium adsorption of alcohols from *n*-decane

Three different adsorbents were tested in this work, activated alumina F-220, Selexsorb® CD and Selexsorb® CDx. Figure 4-15, Figure 4-16 and Figure 4-17 present the results for adsorbates 1-hexanol, 1-octanol and 1-decanol respectively.

The data presented in each figure mentioned above show that all three adsorbents were able to adsorb From a first glance at this data presented it is seen that all three adsorbents were able to adsorb an appreciable amount of each alcohol adsorbate from an n-decane solution and therefore couldan be used to remove oxygenated organics from process streams.

The general trend seen in each of these figures is an increase in adsorbent equilibrium loading as the initial concentration of alcohol in the solution increases. When an adsorption system reaches equilibrium, it does not always mean that all the adsorption sites available to the adsorbate have been occupied. Thus, at a constant temperature, an increase in adsorbate concentration in the initial solvent solution would shift the equilibrium and cause the extra adsorbate molecules to occupy the vacant sites, thereby increasing the adsorbent loading. A point will, however, be reached where all the vacant sites have been occupied and the adsorbent loading remains constant even if the adsorbate initial concentration is increased. This was seen for the 1-hexanol adsorbate at 30 °C for the two Selexsorb® adsorbents (Figure 4-15 b, red and blue markers), as well as the 1-decanol adsorbate adsorbed onto Selexsorb® CD at temperatures equal to 30 and 35 °C (Figure 4-17 b & c, red markers). An initial increase in adsorbate concentration will thus generally cause an increase in adsorbent loading, unless the adsorbent is saturated and the maximum adsorption capacity has been reached.

When comparing the data points in each graph presented in each of these figures, it's seen that the markers representing the F-220 adsorbent generally lie above those representing the two Selexsorb® adsorbents. Anomalies in this analysis are only seen in Figure 4-15 b and c, where, as the 1-hexanol concentration is increased, the Selexsorb® CD and CDx adsorbents show greater adsorbent loadings than that of the F-220 adsorbent.

Considering the adsorbent characterisations done in section 4.1, it was seen that the Activated Alumina F-220 adsorbent had the highest external surface area of 147,7 m^2/g. Almost double that of Selexsorb® CD (86,7 m^2/g) and slightly more than double that of Selexsorb® CDx (68,6 m^2/g). This indicates that a large part of the F-220's active surface area is immediately available, with little hindrance, to the adsorbate molecules for adsorption. Also, with most of both of the Selexsorb® adsorbents' surface areas being found in their microporous structures, at these equilibrium conditions

the adsorbate molecules could be lacking the drive to diffuse and adsorb onto these active sites. This would explain what is seen in Figure 4-15 b and c, for as the temperature is increased (from graph b to c) and as the initial adsorbate concentration is increased, the Selexsorb® adsorbents appear to adsorb more of the 1-hexanol adsorbate. The driving forces (temperature and adsorbate concentration) are altered giving the adsorbate molecules the energy to diffuse to smaller pore widths.

Based on these observations made and a t-test rejecting the null hypothesis within a 95 % confidence interval, the optimal adsorbent for these alcohol-alkane systems was determined to be Activated Alumina F-220 adsorbent.

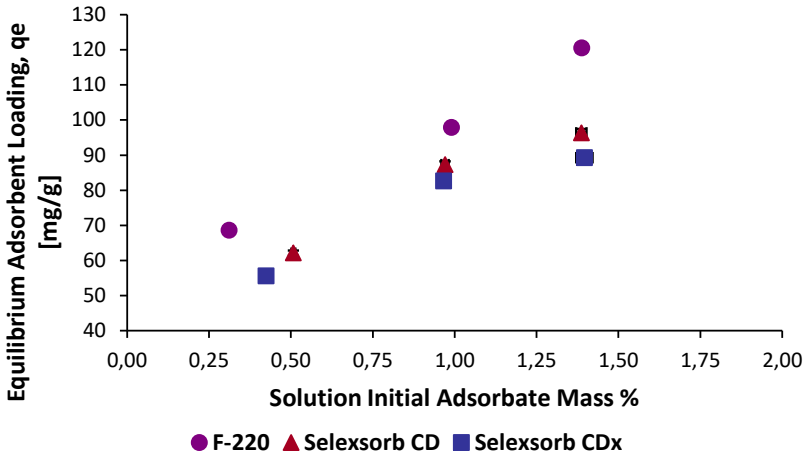

a) The adsorption of 1-hexanol at 25 °C on adsorbents F-220, SCD and SCDx

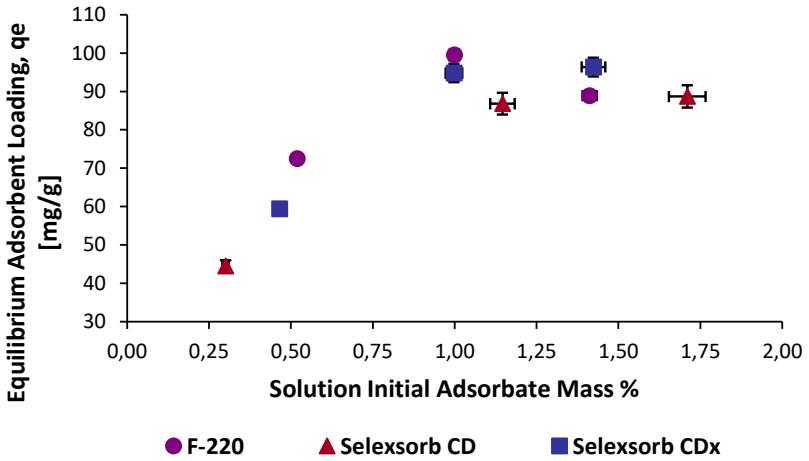

b) The adsorption of 1-hexanol at 30 °C on adsorbents F-220, SCD and SCDx

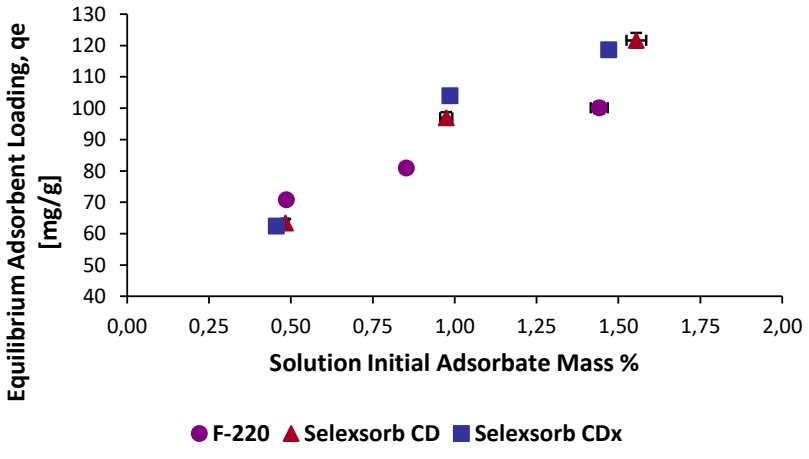

c) The adsorption of 1-hexanol at 35 °C on adsorbents F-220, SCD and SCDx

Figure 4-15: The equilibrium loadings at three initial concentration of 1-hexanol in n-decane solutions on the three adsorbents (F-220, SCD and SCDx) investigated at adsorption temperatures of a) 25 °C, b) 30 °C and c) 35 °C

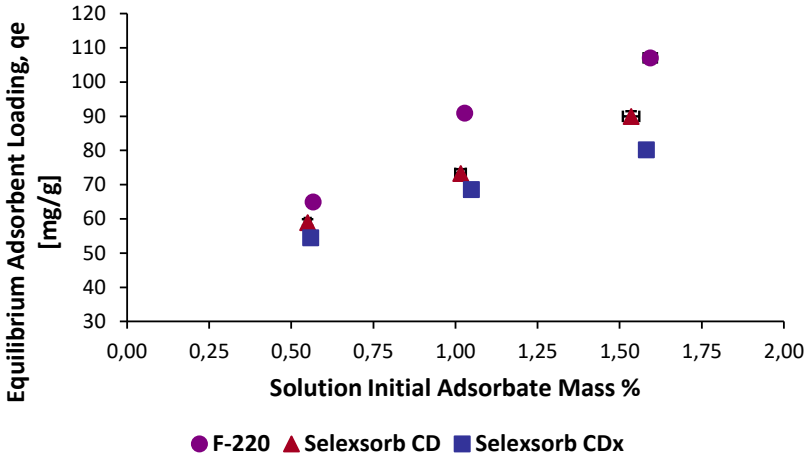

a) The adsorption of 1-octanol at 25 °C on adsorbents F-220, SCD and SCDx

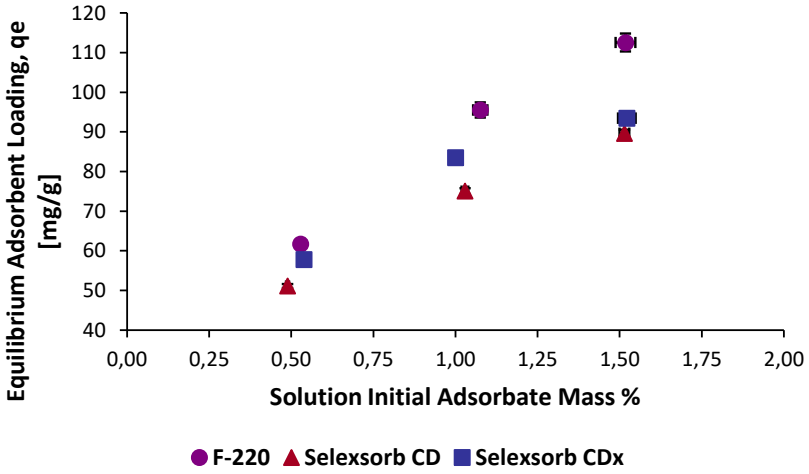

b) The adsorption of 1-octanol at 30 °C on adsorbents F-220, SCD and SCDx

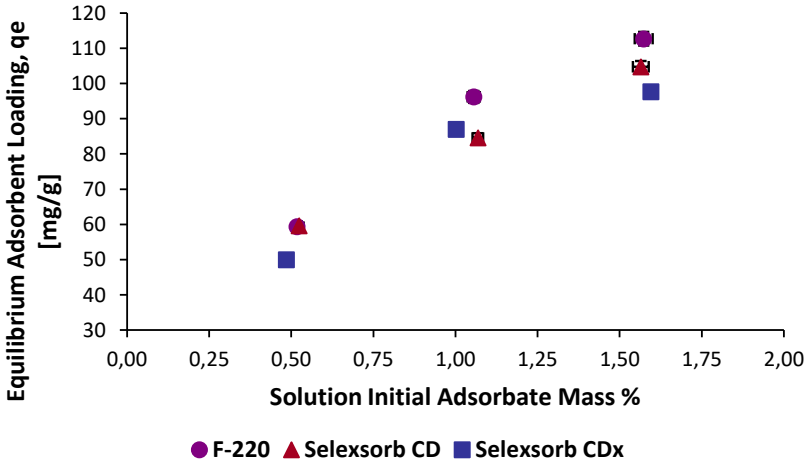

c) The adsorption of 1-octanol at 35 °C on adsorbents F-220, SCD and SCDx

Figure 4-16: The equilibrium loadings at three initial concentration of 1-octanol in n-decane solutions on the three adsorbents (F-220, SCD and SCDx) investigated at adsorption temperatures of a) 25 °C, b) 30 °C and c) 35 °C

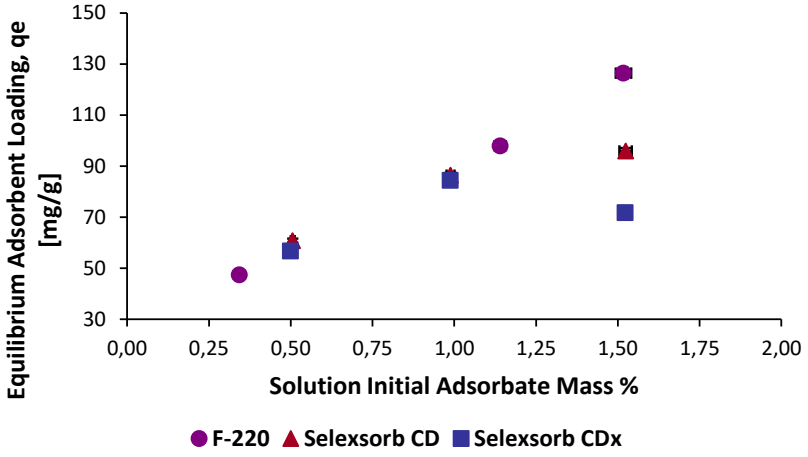

a) The adsorption of 1-decanol at 25 °C on adsorbents F-220, SCD and SCDx

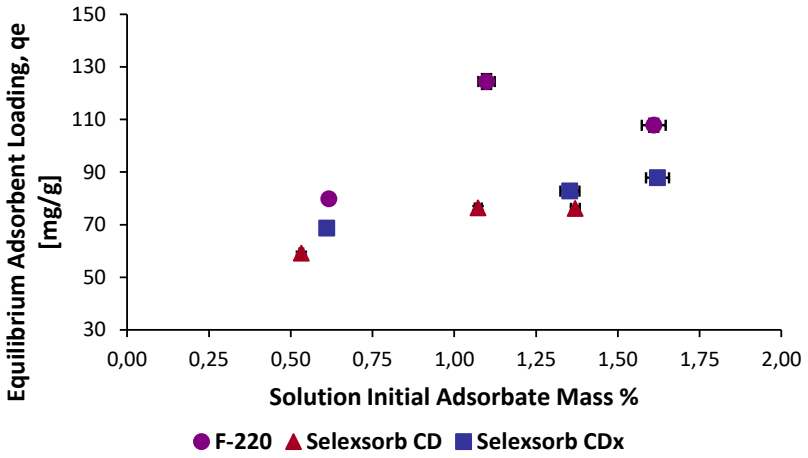

b) The adsorption of 1-decanol at 30 °C on adsorbents F-220, SCD and SCDx

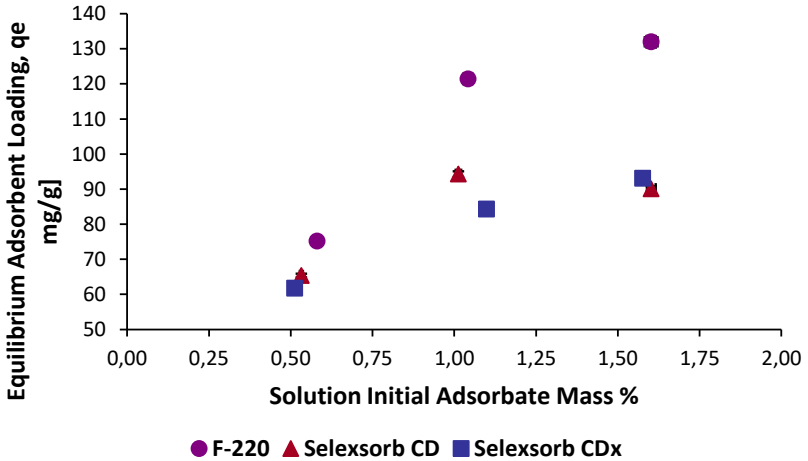

c) The adsorption of 1-decanol at 35 °C on adsorbents F-220, SCD and SCDx

Figure 4-17: The equilibrium loadings at three initial concentration of 1-decanol in n-decane solutions on the three adsorbents (F-220, SCD and SCDx) investigated at adsorption temperatures of a) 25 °C, b) 30 °C and c) 35 °C

4.2.3. The influence of temperature and adsorbate type on the equilibrium adsorption of alcohols from n-decane

Three adsorption temperatures were investigated in this work, 25 °C, 30 °C and 35 °C. Figure 4-18, Figure 4-19 and Figure 4-20 present the equilibrium loadings for each adsorbate at each temperature for activated alumina F-220, Selexsorb® CD and Selexsorb® CDx respectively.

The general trend observed from these data points in these graphs is higher adsorbent loadings at the higher temperatures of 30 and 35 ^{o}C.

Adsorption is an exothermic process and therefore lower system temperatures are preferred. However, the definition of lower adsorption temperature is relative to the adsorbent and adsorbates in the system.

For example, Mor, et al., (2007) studied the effects of temperature on the adsorption of chromium onto activated alumina and activated charcoal adsorbents. Five temperatures were studied (25, 30, 40 and 50 °C) and it was found that the activated alumina showed a maximum adsorption at a temperature of 25 °C, while the activated charcoal showed a maximum adsorption at 40 °C. In another study, Vijayakumar, et al., (2012) investigated the removal of rhodamine-B (a basic dye) using a natural adsorbent perlite. Three temperatures were investigated (30, 40 and 50 °C) and it was found that the adsorption capacity increased with an increase in temperature. Iqbal & Ashiq, (2007) investigated the adsorption of dyes onto activated charcoal at five adsorption temperatures (25, 30, 35, 40 and 45 °C). They found that the adsorption favoured the lowest adsorption temperature of 25 °C. Lastly, a study by (Knozinger & Stubner, 1978), investigated the adsorption of isobutyl alcohol onto alumina at temperatures of 70, 100 and 130 °C and found that reversible adsorption favoured the higher adsorption temperature of 130 °C. Irreverisble adsorption favoured the lowest temperature investigated, 70 °C.

All these different adsorption studies show the dependence of the best adsorption temperature on the type of adsorbent and the type of adsorbate. Generally lower adsorption temperatures are favoured, but lower is relative and dependent on the different adsorption system components.

The Selexsorb® CD and Selexsorb® CDx adsorbents both presented with significant micro- and mesoporous areas in their characterisation in section 4.1. In order for adsorbate molecules to access these areas, certain diffusion steps are required. The diffusion of a molecule requires energy and thus the need for the adsorption temperature to be at a point where sufficient energy is supplied to these molecules. When considering the graphs in Figure 4-19 and Figure 4-20, it is observed that for most of the initial adsorbate concentration data points, those representing 30 and 35 ^{o}C shower higher

adsorbent loadings. It is speculated that the reason for this is the energy required for adsorbate molecules to access the active site in these two adsorbents.

Based on these observations and a t test rejecting the null hypothesis of an optimal adsorption temperature not equal to 35 ^{o}C within a 95 % confidence interval, it was found that these adsorption systems showed better performance with an adsorption temperature of 35 ^{o}C, compared to that of 30 and 25 ^{o}C.

Comparing the adsorption of the three types of adsorbate molecules, it was observed that the 1-hexanol adsorbate molecule showed higher adsorbent loadings at various initial concentrations for each type of adsorbent. For example in Figure 4-20, the highest 1-hexanol loading is 122 mg/g, compared to the highest loading of 1-octanol, 105 mg/g, in Figure 4-20 b.

Between the three types of adsorbate molecules, 1-hexanol presents with the lowest carbon number of 6 and bond length of 11,18 Å. 1-octanol has a carbon number of 8 and a bond length of 14,26 Å, while 1-decanol has a carbon number of 10 and a bond length of 17,34 Å.

Based on all three adsorbents being mesoporous adsorbents with pore widths between 20 and 500 Å (Sing, et al., 1982), the size of these adsorbate molecules would not exclude them from being, to some extent, adsorbed. However, when considering the microporus areas of the adsorbents, the Horvath-Kawazoe method showed that the pore width for F-220, SCD and SCDx was 10,88; 8,48 and 7,97 Å respectively, thus indicating a size exclusion of the 1-octanol and 1-decanol molecules. Also, with more than 20 % of the two Selexsorb adsorbents' porous areas lying in their micropores, the average ± 10 to 20mg/g difference in loadings between the 1-hexanol adsorobent loadings and that of 1-octanol and 1-decanol seen in Figure 4-19 b&c and Figure 4-20 b&c, is not surprising.

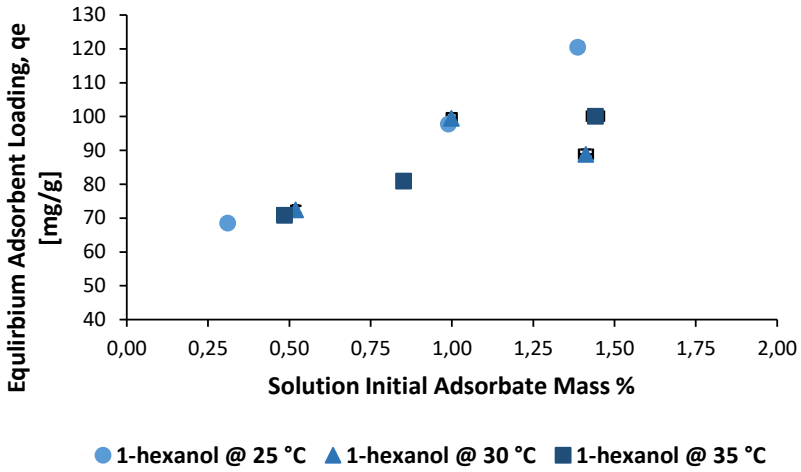

a) 1-hexanol adsorbate adsorbed onto activated alumina F-220

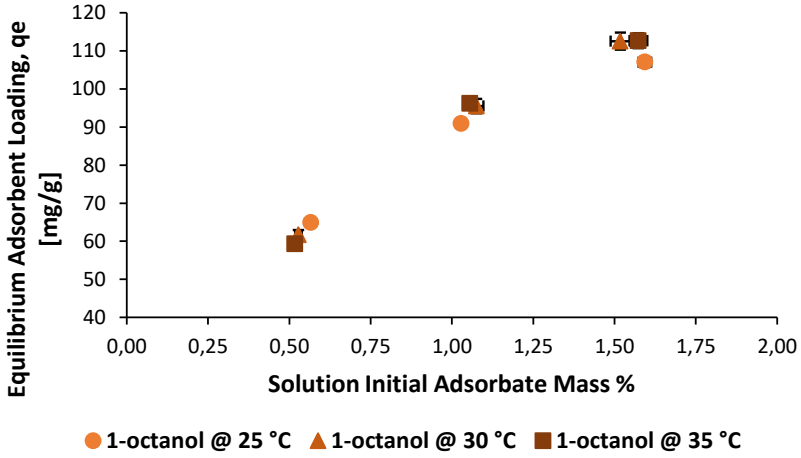

b) 1-octanol adsorbate adsorbed onto activated alumina F-220

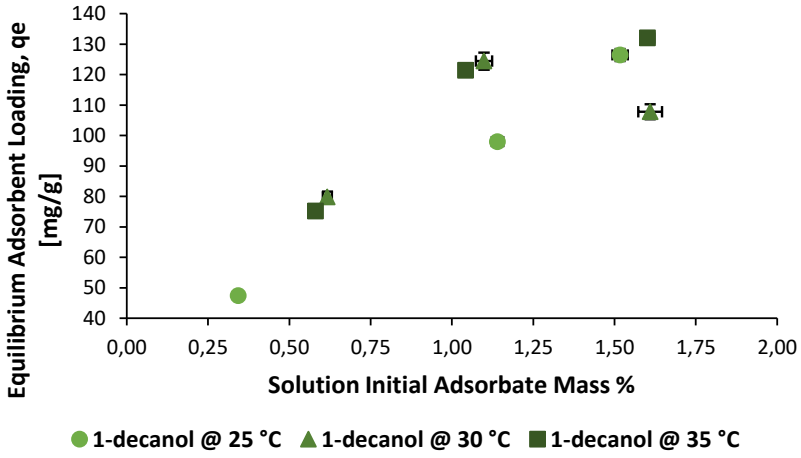

c) 1-decanol adsorbate adsorbed onto activated alumina F-220

Figure 4-18: The equilibrium loadings for adsorbates a) 1-hexanol, b) 1-octanol and c) 1-decanol adsorbed onto activated alumina F-220 at three adsorption temperatures (25, 30 and 35 °C)

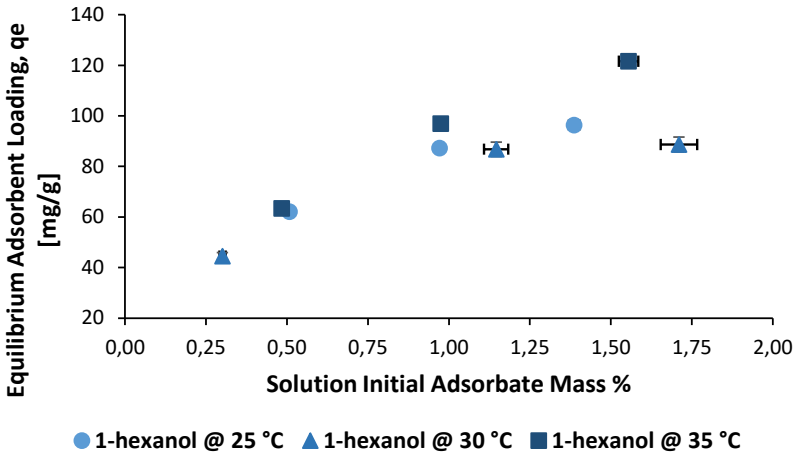

a) 1-hexanol adsorbate adsorbed onto Selexsorb CD

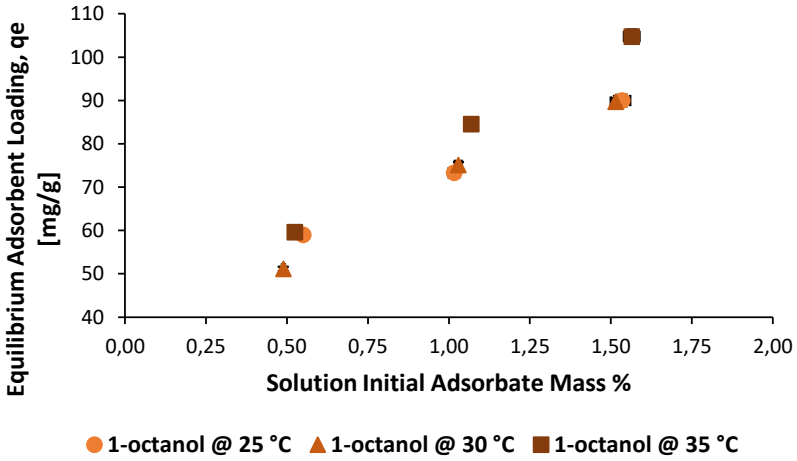

b) 1-octanol adsorbate adsorbed onto Selexsorb® CD

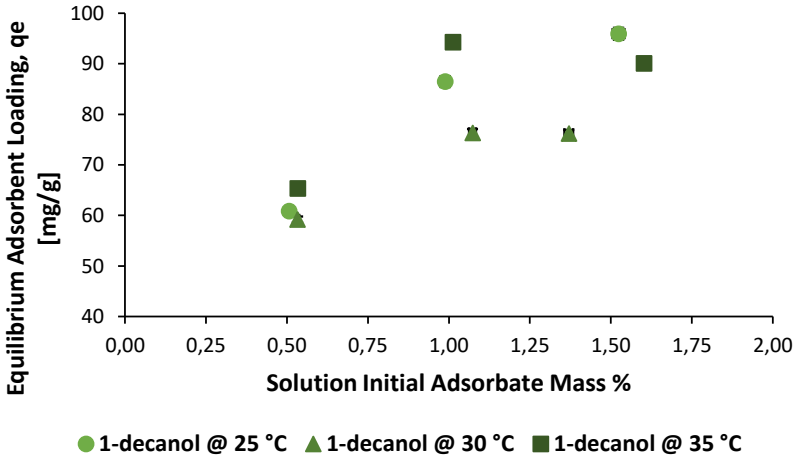

c) 1-decanol adsorbate adsorbed onto Selexsorb® CD

Figure 4-19: The equilibrium loadings for adsorbates a) 1-hexanol, b) 1-octanol and c) 1-decanol adsorbed onto Selexsorb® CD at three adsorption temperatures (25, 30 and 35 °C)

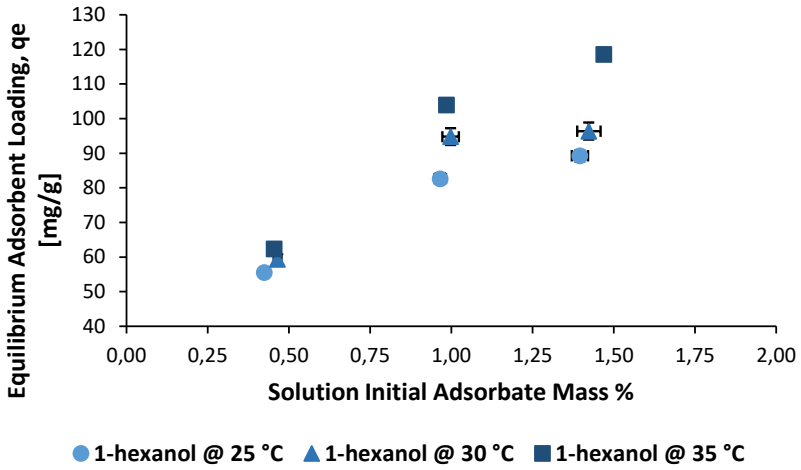

a) 1-hexanol adsorbate adsorbed onto Selexsorb® CDx

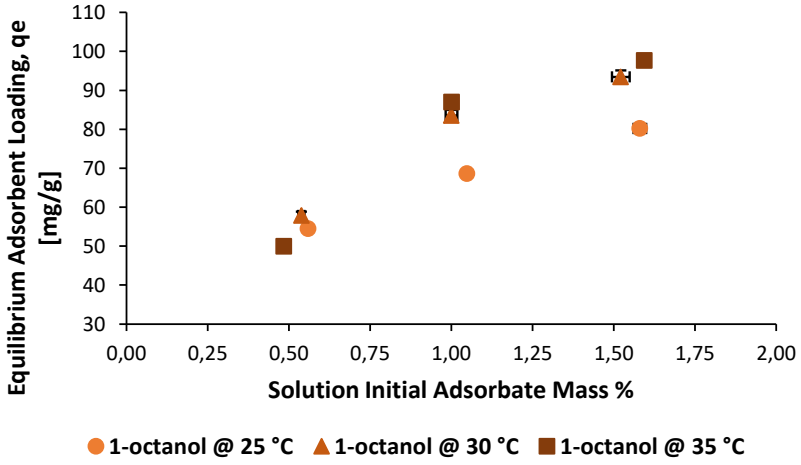

b) 1-octanol adsorbate adsorbed onto Selexsorb® CDx

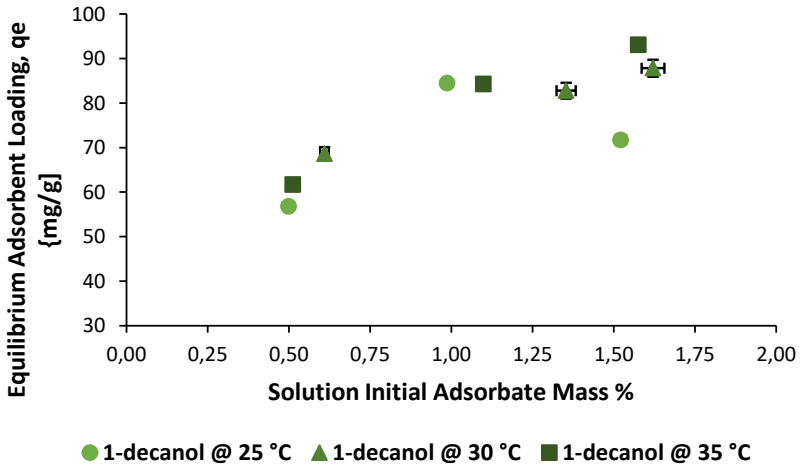

c) 1-decanol adsorbate adsorbed onto Selexsorb® CDx

Figure 4-20: The equilibrium loadings for adsorbates a) 1-hexanol, b) 1-octanol and c) 1-decanol adsorbed onto Selexsorb® CDx at three adsorption temperatures (25, 30 and 35 °C)

4.3 Adsorption Results Conclusions

This chapter presented the adsorption experimental concentration-time profiles for each adsorption system. The effects of adsorbent type, temperature and adsorbate type were discussed using the equilibrium loading values plotted against the initial concentration of alcohol in the various solutions.

It was found that the activated alumina F-220 adsorbent showed the best adsorption performance, while the most favourable adsorption temperature was found to be 35 °C. All three alcohol adsorbates tested could be removed from the *n*-decane solvent solution.

From this data, it appears that all the adsorption systems show favourable adsorption behaviour, i.e. a significant amount of alcohol adsorbate is removed from the *n*-decane solvent. However, by modelling the equilibrium data of the adsorption systems, the favourability as well as type of adsorption occurring during each adsorption process can be determined. The equilibrium modelling also provides indications on other relevant information about the adsorbent and the type of layering of the adsorbate molecules on the adsorbents surface, which may offer more insights into the behaviour of the systems under different factors.

The kinetic modelling of an adsorption system also offers more insight into the adsorption system behaviour by providing an indication of the rate-limiting step of the process. The information provided by both the equilibrium and kinetic data aids in the design fixed bed adsorption process for these systems. The modelling of the equilibrium and kinetic data is therefore presented in the next chapter.

Chapter 5: Adsorption Modelling

This chapter delves into the modelling of the adsorption systems investigated. Various models were applied in both the equilibrium and kinetic modelling and the best fit models were chosen based on a quantitative degree-of-fit determined by parameters such as the coefficient of determination and the average relative error.

5.1 Adsorption Equilibrium Modelling

An adsorption system is characterised by the type of adsorbent, the adsorbate and the adsorption temperature. The adsorption equilibrium modelling of the isotherms for all 27 adsorption systems are shown and discussed below. Firstly the isotherm models are highlighted and then the modelling approach is discussed. Next, the isotherm modelling is presented and the best model fit established.

5.1.1. Isotherm models

Three isotherm models (discussed in section 2.3.1) were applied to the equilibrium data collected namely, the Langmuir, Freundlich and Dubinin-Radushkevich models Table 5-1 highlights the three models and their respective parameters regressed in the modelling of the equilibrium data.

Table 5-1: Isotherm models applied to the adsorption equilibrium data

Model	Equation	Isotherm Parameters
Langmuir (Foo & Hameed, 2010)	$q_e = q_m K_L \frac{C_e}{1+ K_L C_e}$ [2-4]	q_m & K_L
Freundlich (Vijayakumar, et al., 2012)	$q_e = K_f C_e^{\,1/n_f}$ [2-6]	K_f & n_f
Dubinin-Radushkevich (Foo & Hameed, 2010)	$q_e = q_s \exp(-k_{ad}\varepsilon^2)$ [2-7] $\varepsilon = RT \ln\left(1 + \frac{1}{C_e}\right)$ [2-8]	q_s & k_{ad}

5.1.2. Modelling approach

A nonlinear modelling approach was conducted for both the two-parameter and three-parameter isotherm models.

In the nonlinear modelling approach, a minimisation procedure was followed. The solver add-in function in Microsoft Excel was used to determine the isotherm parameters for each adsorption system by minimising the hybrid fractional error function (HYBRID) shown below in equation [6-1].

$$HYBRID = \frac{100}{n-p}\sum_{i=1}^{n}\left[\frac{(q_{exp}-q_{calc})^2}{q_{exp}}\right] \quad [6\text{-}1]$$

The degree of fit of each model was quantitatively compared using the coefficient of determination (R^2) and the average relative error (Δq), equations [6-2] and [6-3] below (Kvalseth, 1985). Essentially, a coefficient of determination closest to 1 and a low average relative error would be an indication of the best model fit for the data.

$$R^2 = 1 - \frac{\sum(y_i-\hat{y}_i)^2}{\sum(y_i-\bar{y}_i)^2} \quad [6\text{-}2]$$

$$\Delta q = \frac{1}{n}\sum\left|\frac{q_{calc}-q_{exp}}{q_{exp}}\right| \quad [6\text{-}3]$$

Where,

y_i = the experimental value

$\hat{y}_i$ = the calculated value

$\bar{y}_i$ = the mean of the experimental values

n = number of data points

q_{calc} = the calculated value

q_{exp} = the experimental value

The Root Mean Square Error (RMSE) indicator was also used to compare the fits of each model (equation [6-4]) and it gives an indication of the absolute fit of each model to the data (Grace-Martin, 2008). A lower RMSE value is desired.

$$RMSE = \sqrt{\frac{\sum_{i=1}^{n}(q_{exp}-q_{calc})^2}{n}} \quad [6\text{-}4]$$

5.1.3. Isotherm modelling results

In this subsection, the results of the three nonlinear isotherm models fitted to the equilibrium data for all 27 adsorption systems are shown and discussed. The graphs of the models fitted to each adsorption equilibrium system can be seen in Appendix 8.19.

5.1.3.1 Modelling parameters

Table 5-2, Table 5-3 and Table 5-4 give the model parameters for each type of adsorbent and each temperature for the 1-hexanol, 1-octanol and 1-decanol adsorbates respectively. Table 5-5 provides literature model parameter values for various adsorption systems. It is seen that the model parameters in this study compare well to those presented in literature.

Table 5-2: The isotherm parameters obtained through non-linear modelling and best fit statistics for the 1-hexanol adsorbate

Models	Parameters	Activated alumina F-220			Selexsorb® CD			Selexsorb® CDx		
		25 °C	30 °C	35 °C	25 °C	30 °C	35 °C	25 °C	30 °C	35 °C
Langmuir	q_m [mg/g]	112,27	95,21	92,54	99,86	87,87	124,16	91,74	102,20	114,54
	K_L [L/mg]	0,010	0,019	0,013	0,003	0,198	0,002	0,004	0,004	0,013
	R^2	0,846	0,806	0,668	0,986	0,999	0,935	0,993	0,993	0,959
	Δq	0,065	0,044	0,0676	0,017	0,007	0,054	0,013	0,013	0,037
	RMSE	8,349	4,899	7,007	1,715	0,725	6,069	1,236	1,396	4,840
Freundlich	K_F [mg/g]	29,77	41,10	36,02	19,72	37,82	13,10	19,46	21,91	29,37
	n	6,16	9,57	8,62	5,35	9,78	3,82	5,58	5,60	5,98
	R^2	0,954	0,436	0,881	0,993	0,992	0,999	0,987	0,905	0,999
	Δq	0,040	0,081	0,0479	0,013	0,019	0,007	0,019	0,054	0,008
	RMSE	4,575	8,356	4,185	1,218	1,867	0,712	1,680	5,265	0,859
Dubinin-Radushkevich	q_s [mg/g]	108,21	93,97	89,79	92,52	87,41	109,46	86,318	96,124	110,909
	k_{ad} [mol²/J²]	0,0018	0,0012	0,0020	0,0151	0,0000	0,0140	0,0099	0,0079	0,0008
	R^2	0,811	0,844	0,592	0,948	0,998	0,843	0,971	1,000	0,938
	Δq	0,069	0,038	0,0703	0,030	0,007	0,072	0,024	0,003	0,044
	RMSE	9,236	4,387	7,766	3,315	0,809	9,465	2,479	0,355	5,935

Table 5-2 shows the isotherm parameters for the adsorption of 1-hexanol onto each adsorbent at each temperature and the grey highlighted blocks show the isotherm model that best fits each system.

For the F-220 adsorbent, the adsorption of 1-hexanol at 25 and 35 ^{o}C is best described by the Freundlich model, while at 30 ^{o}C, it is best described by the Dubinin-Radushkevich model. Both models describe systems where the adsorbent surface is heterogeneous in nature. The Freundlich model describes the multilayering of the adsorbate molecules on the adsorbent's surface, while the D-R model describes more of a pore-filling mechanism of adsorption taking place. Therefore at 30 ^{o}C, it is speculated that the 1-hexanol molecules diffuse and fill more of the pores within the adsorbent particle than at 25 and 35 ^{o}C where the molecules appear to rather form multiple layers on the adsorbent surface.

For the SCD adsorbent, once again at temperatures of 25 and 35 ^{o}C, the Freundlich model best describes each system, while at 30 ^{o}C, the Langmuir model best describes the system. The Langmuir model generally describes homogenous adsorbents with monolayering of adsorbate particles, thus indicating that at 30 ^{o}C, the 1-hexanol adsorbate molecules are generally only forming monolayers on the adsorbent particles surfaces.

For the SCDx adsorbent, at a temperature of 25 ^{o}C Langmuir fits best, at 30 ^{o}C D-R fits best and at 35 ^{o}C Freundich fits best. An increase in temperature in the 1-hexanol – SCDx systems seems to show an increase in layering and pore filling onto and within the adsorbent particles.

Table 5-3: The isotherm parameters obtained through non-linear modelling and best fit statistics for the 1-octanol adsorbate

Models	Parameters	Activated alumina F-220			Selexsorb® CD			Selexsorb® CDx		
		25 °C	30 °C	35 °C	25 °C	30 °C	35 °C	25 °C	30 °C	35 °C
Langmuir	q_m [mg/g]	117,94	130,01	133,10	94,73	99,06	114,05	85,33	104,60	120,08
	K_L [L/mg]	0,001	0,001	0,001	0,001	0,001	0,001	0,001	0,001	0,001
	R^2	0,989	0,993	1,000	0,881	0,974	0,935	0,937	1,000	0,991
	Δq	0,019	0,017	0,004	0,051	0,031	0,049	0,034	0,002	0,022
	RMSE	1,825	1,783	0,423	4,374	2,564	4,710	2,630	0,163	1,960
Freundlich	K_F [mg/g]	7,73	6,83	6,10	10,72	6,99	7,68	11,22	10,37	4,66
	n	3,26	3,06	2,94	4,17	3,44	3,35	4,53	3,96	2,84
	R^2	0,954	0,990	0,973	0,965	1,000	0,991	0,993	0,969	0,931
	Δq	0,041	0,015	0,030	0,029	0,002	0,019	0,012	0,031	0,062
	RMSE	3,721	2,097	3,667	2,373	0,186	1,779	0,908	2,643	5,360
Dubinin-Radushkevich	q_s [mg/g]	101,58	106,99	107,90	83,09	84,05	96,27	75,89	90,87	96,05
	k_{ad} [mol^2/J^2]	0,058	0,062	0,063	0,075	0,071	0,062	0,085	0,070	0,097
	R^2	0,911	0,932	0,950	0,772	0,898	0,842	0,851	0,963	0,985
	Δq	0,045	0,046	0,042	0,064	0,053	0,066	0,047	0,028	0,024
	RMSE	5,166	5,528	4,976	6,056	5,079	7,342	4,058	2,874	2,515

Table 5-3 shows the isotherm parameters for the adsorption of 1-octanol onto each adsorbent at each temperature and the grey highlighted blocks show the isotherm model that best fits each system.

The Langmuir model shows the best fit for the 1-octanol – F-220 adsorption system at all temperatures. This indicates that the 1-octanol molecules form only a monolayer on the surfaces of the adsorbent particles.

The Freundlich model shows the best fit for the 1-octanol – SCD adsorption systems at all temperatures, indicating that on this adsorbent's surfaces the 1-octanol adsorbate molecules are forming multiple layers. For the SCDx adsorbent, the 1-octanol molecules form multiple layers at a temperature of 25 ^{o}C, while at 30 and 35 ^{o}C only monolayers of the adsorbate molecules are adsorbed onto the adsorbent's surfaces.

Table 5-4: The isotherm parameters obtained through non-linear modelling and best fit statistics for the 1-decanol adsorbate

Models	Parameters	Activated alumina F-220			Selexsorb® CD			Selexsorb® CDx		
		25 °C	30 °C	35 °C	25 °C	30 °C	35 °C	25 °C	30 °C	35 °C
Langmuir	q_m [mg/g]	113,84	121,98	142,79	99,29	80,79	97,77	81,22	84,02	95,33
	K_L [L/mg]	0,009	0,004	0,003	0,003	0,004	0,004	0,004	0,005	0,003
	R^2	0,881	0,633	0,996	0,989	0,989	0,909	0,623	0,934	0,974
	Δq	0,083	0,089	0,011	0,016	0,009	0,038	0,079	0,016	0,021
	RMSE	11,277	11,156	1,477	1,579	0,828	3,838	6,948	1,555	2,134
Freundlich	K_F [mg/g]	19,08	43,38	20,51	19,10	24,84	29,25	30,09	37,79	20,03
	N	4,73	8,82	4,42	5,37	7,56	7,46	9,27	11,48	5,72
	R^2	0,927	0,356	0,897	0,986	0,945	0,727	0,388	0,890	1,000
	Δq	0,064	0,121	0,064	0,020	0,023	0,070	0,106	0,022	0,002
	RMSE	8,824	14,773	7,925	1,784	1,886	6,662	8,854	2,015	0,227
Dubinin-Radushkevich	q_s [mg/g]	110,44	116,77	128,56	91,89	76,84	92,86	78,11	81,56	89,20
	k_{ad} [mol^2/J^2]	0,001	0,016	0,012	0,02	0,02	0,02	0,02	0,03	0,02
	R^2	0,872	0,806	0,984	0,946	0,999	0,971	0,749	0,951	0,937
	Δq	0,085	0,059	0,021	0,031	0,003	0,020	0,061	0,014	0,031
	RMSE	11,709	8,102	3,124	3,434	0,260	2,183	5,670	1,339	3,304

Table 5-4 shows the isotherm parameters for the adsorption of 1-decanol onto each adsorbent at each temperature and the grey highlighted blocks show the isotherm model that best fits each system.

Again it is seen that not one model best describes each system involving the 1-decanol adsorbate molecule. More systems show pore-filling mechanisms for example the 1-decanol – F-220 adsorption system at 30 ^{o}C, the 1-decanol – SCD adsorption systems at 30 and 35 ^{o}C and the 1- decanol – SCDx adsorption systems at 25 and 30 ^{o}C, are all described better by the D-R isotherm model indicating that a pore filling mechanism is taking place.

The best fit models of all these systems investigated show how dependent each adsorption system is on every factor involved, however it is recommended that more concentrations be investigated in each of these systems to add data points to the modelling of these systems allowing for greater certainty in each of the models.

Table 5-5 below shows literature parameter values obtained for several adsorption systems. These magnitudes of these literature values compare well to the magnitude of the parameters values obtained in this work.

Table 5-5: Literature model parameter values for the isotherm models of various adsorption systems

Parameters	Chromium-Activated alumina (Mor, et al., 2007)	Chromium-Activated charcoal (Mor, et al., 2007)	Nickel-Teff straw (Desta, 2013)	Phosphate-MCM 41 (Chen, 2015)	As(III)-Activated alumina (Singh & Pant, 2004)
q_m [mg/g]	7,44	12,87	41,2	54,23	0,1803
K_L [L/mg]	0,9451	2,369	0,189	0,985	8,543
K_F [mg/g]	3,1262	0,9614	1,24	16,38	0,2249
n	0,9614	1,6162	1,10	2,094	2,222
q_s [mg/g]				42,14	0,05455
k_{ad} [mol²/kJ²]				0,028	0,0082

5.1.3.2 Modelling discussion

Isotherm models are used to evaluate and compare adsorption systems. They give an indication of maximum adsorption capacity, the type of adsorption taking place and aid in the design of adsorption systems. The three models applied to the equilibrium data collected in this study were the Langmuir, Freundlich and Dubinin-Radushkevich models. Each model gave insight into each adsorption system.

Langmuir

The K_L constant in the Langmuir isotherm is used to calculate a separation factor, R_L, given in equation [2-5], which gives an indication of the nature of each adsorption process. An R_L value between 0 and 1 is an indication of favourable adsorption (Singh & Pant, 2004).

The R_L factors for each adsorbate at each temperature for all three adsorbents are shown in Table 5-6. From the table, it is seen that for all systems the separation factor is below 1 and above 0, indicating that all the adsorption systems are favourable.

Table 5-6: The R_L values for each adsorbent, alcohol and temperature investigated

Adsorbate	**1-Hexanol**			**1-Octanol**			**1-Decanol**		
T (°C)	**25**	**30**	**35**	**25**	**30**	**35**	**25**	**30**	**35**
Activated alumina F-220	0,935	0,894	0,920	0,990	0,992	0,993	0,940	0,968	0,977
Selexsorb® CD	0,978	0,486	0,983	0,990	0,992	0,991	0,979	0,975	0,973
Selexsorb® CDx	0,973	0,971	0,921	0,990	0,991	0,994	0,974	0,963	0,979

Adsorption capacity, q_m, is an indication of maximum adsorption capacity for a specific adsorption system. When comparing the maximum adsorption capacity of the various systems in Table 5-2, Table 5-3 and Table 5-4, it is seen that the activated alumina F-220 generally has the maximum adsorption capacity compared to that of Selexsorb® CD and Selexsorb® CDx, with it showing capacities of 103,8 and 130,0 mg/g compared to that of 99,3 and 99,0 mg/g for SCD and 81,2 and 104,6 mg/g for SCD. This is in agreement with the comparisons made in section 4.3.1, confirming that the activated alumina F-220 is the best adsorbent to use in the removal of 1-alcohols from an *n*-decane solvent.

The Langmuir parameters also seem to generally show increases as temperature is increased for each adsorbate-adsorbent system. This in indicative of these systems preferring the slightly higher

adsorption temperatures investigated in this study as adsorption increases (represented by the higher parameter values) with an increase in temperature. This is in agreement with the findings of section 4.3.2.

Freundlich

The constant, n_f, in the Freundlich isotherm is a measure of adsorption intensity giving an indication of the type of adsorption occurring. An n_f value less than 1 is an indication of a chemisorption process occurring, while an n_f value greater than 1 indicates a physisorption process occurring (Desta, 2013).

Table 5-7 below gives the adsorption intensity values for each adsorption system. It is seen that all these values are above 1, indicating that all these adsorbates are physically adsorbed to their respective adsorbents at all the temperatures investigated.

Table 5-7: Adsorption intensity, n_f, values for each adsorption system investigated

Adsorbate	**1-Hexanol**			**1-Octanol**			**1-Decanol**		
T (°C)	**25**	**30**	**35**	**25**	**30**	**35**	**25**	**30**	**35**
Activated alumina F-220	6,16	9,57	8,62	3,26	3,06	2,94	4,73	8,82	4,42
Selexsorb® CD	5,35	9,79	3,82	4,17	3,44	3,35	5,37	7,56	7,46
Selexsorb® CDx	5,58	5,60	5,98	4,53	3,96	2,84	9,27	11,48	5,72

The Freundlich parameters, K_f and n_f are also influenced by temperature, in most systems showing increases in value as temperature is increased, except for systems with 1-octanol as adsorbate. As n_f is a measure of adsorption intensity the increase in its value is indicative of each adsorption system showing increases in their adsorbate-adsorbent interactions as temperature increases.

Dubinin-Radushkevich

The mean free energy is calculated using equation [2-9] and the k_{ad} parameter obtained from the Dubinin-Radushkevich model fits. Table 5-8 gives the mean free energy values for each equilibrium adsorption system modelled.

A mean free energy of less than 8 kJ/mol is indicative of a physisorption adsorption process. For all the systems investigated in this study, the mean free energy was well below 8 kJ/mol, indicating that

in all these systems, physical bonds are formed between adsorbent and adsorbate. This is in agreement with the results of the adsorption intensity given by the Freundlich equation.

Table 5-8: The mean free energy, E, values for each adsorption system in kJ/mol

Adsorbate	1-Hexanol			1-Octanol			1-Decanol		
T (°C)	**25**	**30**	**35**	**25**	**30**	**35**	**25**	**30**	**35**
Activated alumina F-220	0,017	0,021	0,016	0,003	0,003	0,003	0,001	0,001	0,001
Selexsorb® CD	0,006	0,383	0,006	0,003	0,003	0,003	0,001	0,001	0,001
Selexsorb® CDx	0,007	0,008	0,025	0,002	0,003	0,002	0,001	0,001	0,001

The Dubinin-Radushkevich parameters, q_m and k_{ad}, also generally show increases as temperature is increased. This again just confirms what has been seen throughout the modelling of the adsorption equilibrium data as well as the comparisons made in chapter 4 with regards to these systems showing better adsorption at slightly higher adsorption temperatures.

5.1.4. Isotherm modelling conclusions

The equilibrium data of all adsorption systems investigated was modelled using three commonly used isotherm models. These models provide information about the adsorption capacity and type of adsorption taking place for each adsorption system. The modelling results confirmed the deductions made in chapter 4 regarding the best performing adsorbent (F-220) and the adsorption performance increasing with an increase in temperature. The best fit model for each system also gave an indication of the adsorption mechanisms taking place in each system.

5.2 Adsorption Kinetic Modelling

This section presents the adsorption kinetic modelling of all 81 kinetic adsorption systems. First, an overview of the kinetic models is given. The activated alumina F-220 kinetic results are presented, followed by the parameters obtained for each kinetic adsorption system and eacah model. Lastly, the results are discussed.

5.2.1. Kinetic models and the modelling approach

Three kinetic models were applied to the kinetic data collected in this project. Weber-Morris is a diffusional kinetic model giving an indication of whether or not intra-particle diffusion is the sole rate-limiting step. Pseudo-first-order and Pseudo-second-order are two adsorption reaction models which assume that the adsorption step is the rate-limiting step in the adsorption process. These models are described in sections 2.4.1 and 2.4.2. Table 5-9 below gives the kinetic models and their parameters.

Table 5-9: Adsorption kinetic models applied to the kinetic data

Model	Equation	Parameters
Weber-Morris (Tan & Hameed, 2017)	$q_t = k_{int} t^{1/2} + B$ [2-15]	K_{int} & B
Pseudo-First-Order (Tan & Hameed, 2017)	$q = q_e(1 - e^{-k_1 t})$ [2-16]	q_e & k_1
Pseudo-Second-Order (Tan & Hameed, 2017)	$q = \frac{k_2 {q_e}^2 t}{1 + k_2 q_e t}$ [2-17]	q_e, & k_2

A non-linear modelling approach was undertaken for all four models using a minimisation procedure. The solver add-in function in Microsoft Excel was used to determine the kinetic model parameters for each adsorption system by minimising the hybrid fractional error function (HYBRID).

Equilibrium adsorbent loading, q_e, values used in the kinetic models were treated as parameters in the modelling of each system and then compared to the experimental q_e values.

The statistics that were used in the isotherm modelling were also used for the kinetic modelling to determine the degree of fit of each model. Those included the coefficient of determination (R^2), the average relative error (Δq) and the RMSE indicator. The % error between the model equilibrium capacity, q_e, prediction and the experimental value was also used to determine the best fitting model.

5.2.2. Kinetic modelling results

The reader is referred to Appendix 8.20, 8.21 and 8.22 for the graphs of the modelling results of the three adsorbents investigated.

Table 5-10, Table 5-11 and Table 5-12 give the kinetic parameters for adsorption systems with activated alumina F-220 as adsorbent and adsorbates 1-hexanol, 1-octanol and 1-decanol respectively.

Table 5-10: Kinetic model parameters for 1-hexanol adsorbed onto activated alumina F-220 at all three adsorption temperatures

Models	Parameters	25 °C			30 °C			35 °C		
		1-hexanol								
		1,39	0,99	0,31	1,41	1,00	0,52	1,44	0,85	0,52
Weber-Morris	k_{int} [mg/(g·min^{½})]	6,01	5,58	3,28	4,24	4,94	2,63	5,61	4,10	3,21
	B [mg/g]	0,00	7,14	12,32	0,00	10,13	25,12	5,94	6,53	17,01
	R^2	0,930	0,999	0,959	0,918	0,984	0,965	0,838	0,726	0,949
	Δq	0,107	0,009	0,056	0,376	0,055	0,057	0,190	0,729	0,069
	RMSE	9,348	0,737	3,754	9,562	3,558	2,854	12,538	21,033	4,114
Pseudo-1st-Order	k_1 [1/min]	0,013	0,018	0,024	0,005	0,021	0,037	0,020	0,014	0,029
	q_e [mg/g]	103,39	96,11	64,60	108,45	88,66	65,47	95,17	76,67	67,78
	R^2	0,996	0,893	0,964	0,999	0,947	0,775	0,883	0,848	0,967
	Δqe[%]	14,22	1,78	5,82	21,99	10,89	9,65	4,97	5,30	4,31
	Δq	0,042	0,122	0,080	0,023	0,081	0,148	0,155	0,522	0,064
	RMSE	2,227	10,539	3,552	1,271	6,417	7,238	10,629	15,646	3,318
Pseudo-2nd-Order	k_2 [g/(mg·min)]	8,55E-05	1,43E-04	3,52E-04	2,21E-05	1,93E-04	6,87E-04	1,66E-04	1,42E-04	4,28E-04
	q_e [mg/g]	133,01	118,25	74,86	164,78	106,29	71,69	115,59	95,18	76,83
	R^2	0,988	0,948	0,991	0,999	0,985	0,873	0,905	0,827	0,995
	Δqe[%]	10,35	20,84	9,14	85,36	6,83	1,07	15,42	17,57	8,47
	Δq	0,044	0,092	0,044	0,023	0,046	0,112	0,151	0,561	0,029
	RMSE	3,823	7,315	1,722	1,083	3,389	5,436	9,578	16,704	1,322

Table 5-10 shows the kinetic parameter results for 1-hexanol adsorbed onto activated alumina F-220 with the grey highlighted blocks representing the model that best fits each system at a particular temperature and initial 1-hexanol concentration. At temperatures of 25 and 30 ºC, the Weber-Morris model appears to fit the data best, while at 35 ºC, the Pseudo-1st-Order model fits best.

The Weber-Morris model best describes systems in which diffusion of molecules is the rate-limiting step (Tan & Hameed, 2017). When the B parameter in the model is equal to zero, the kinetics of the adsorption process is purely limited by the intra-particle diffusion of the adsorbent molecules, while if the parameter is not equal to zero, the kinetics is limited by more diffusion steps than just intra-particle diffusion (Tan & Hameed, 2017). At the highest concentration for both systems at 25 and 30 ºC, the process appears to be solely controlled by intra-particle diffusion, while for the other two lower concentrations in these systems, other diffusion steps also slow down the kinetics of the adsorption process. At a higher alcohol concentration, the gradient difference between the solution and the adsorbent particle is a greater driving force, than at lower concentrations, which pushes the adsorbate molecules to the adsorbent surface aiding in faster diffusion of the molecules to the adsorbent's surface. However, the diffusion of the molecules then to the pores of the adsorbent could be slow due to pathways being small or blocked, thus leading to intra-particle diffusion slowing the process down. The concentration gradient at lower concentrations is not as much of a driving force, which slows down the diffusion of the molecules to the active surface sites of the adsorbent particles.

The Pseudo-1st-Order model describes systems which are adsorption reaction limited, implying that the physical reaction of the molecule to the adsorbent active site is slowing down the rate of adsorption (Tan & Hameed, 2017). At a temperature of 35 ºC, it is speculated that the temperature aids in energising the diffusion rates of the adsorbate molecules to the active sites making these rates faster compared to the physical reaction step occurring between the adsorbate molecule and the adsorbent surface.

Table 5-11: Kinetic model parameters for 1-octanol adsorbed onto activated alumina F-220 at all three adsorption temperatures

Models	Parameters	25 °C			30 °C			35 °C		
		1-octanol								
		1,59	1,03	0,57	1,52	1,08	0,53	1,57	1,06	0,52
Weber-Morris	k_{int} [mg/(g·min^{½})]	5,42	4,69	3,03	5,60	4,87	2,58	5,79	4,67	2,50
	B [mg/g]	6,01	6,06	10,21	5,93	5,74	14,65	7,08	12,09	14,43
	R^2	0,990	0,978	0,955	0,995	0,983	0,943	0,980	0,978	0,913
	Δq	0,035	0,060	0,066	0,029	0,065	0,070	0,076	0,063	0,099
	RMSE	3,001	3,943	3,648	2,290	3,529	3,489	4,537	3,895	4,166
Pseudo-1st-Order	k_1 [1/min]	0,017	0,018	0,024	0,017	0,018	0,030	0,019	0,022	0,031
	q_e [mg/g]	93,81	81,78	58,50	96,07	84,03	55,42	99,80	86,02	54,07
	R^2	0,951	0,957	0,972	0,910	0,950	0,962	0,950	0,950	0,985
	Δqe[%]	12,39	10,08	9,92	14,65	12,06	10,17	11,44	10,59	8,89
	Δq	0,091	0,082	0,069	0,115	0,075	0,074	0,070	0,074	0,038
	RMSE	6,795	5,487	2,876	9,680	6,136	2,856	7,237	5,861	1,741
Pseudo-2nd-Order	k_2 [g/(mg·min)]	1,42E-04	1,74E-04	3,69E-04	1,36E-04	1,69E-04	5,44E-04	1,46E-04	2,23E-04	5,78E-04
	q_e [mg/g]	115,32	99,77	68,14	118,60	102,81	62,57	121,84	101,86	60,88
	R^2	0,985	0,987	0,995	0,958	0,985	0,992	0,986	0,988	1,000
	Δqe[%]	7,70	9,70	4,93	5,37	7,61	1,43	8,13	5,87	2,58
	Δq	0,059	0,050	0,034	0,084	0,041	0,036	0,037	0,038	0,004
	RMSE	3,755	2,983	1,191	6,600	3,340	1,338	3,880	2,924	0,203

Table 5-11 shows the kinetic parameter results for 1-octanol adsorbed onto activated alumina F-220 with the grey highlighted blocks representing the model that best fits each system at a particular temperature and initial 1-octanol concentration. At each temperature, the two higher initial 1-octanol concentrations are best described by the Weber-Morris model, while at the lowest concentration, the Pseudo-2nd-Order model best describes these systems.

The 6 systems best described by the Weber-Morris model all show B values of greater than zero, implying that intra-particle diffusion is not the sole rate-controlling step. At the lowest 1-octanol concentrations, the adsorption reaction step is the rate-controlling step. This could be due to less 1-octanol molecules present at the lowest concentration, meaning less diffusion competition making the diffusion of the molecules faster compared to the actual adsorption of each molecule to an active site on the adsorbent's surface.

Table 5-12: Kinetic model parameters for 1-decanol adsorbed onto activated alumina F-220 at all three adsorption temperatures

Models	Parameters	25 °C			30 °C			35 °C		
		1-decanol								
		1,52	1,14	0,34	1,61	1,10	0,62	1,60	1,04	0,58
Weber-Morris	k_{int} [mg/(g·min^{½})]	5,78	4,60	2,30	5,28	5,74	4,07	6,47	5,57	3,62
	B [mg/g]	18,18	7,43	7,66	6,97	15,72	8,60	15,15	19,23	12,46
	R^2	0,993	0,989	0,939	0,994	0,994	0,960	0,918	0,988	0,962
	Δq	0,036	0,054	0,094	0,029	0,028	0,057	0,133	0,036	0,052
	RMSE	2,829	2,849	3,199	2,429	2,479	4,629	10,054	3,558	4,001
Pseudo-1st-Order	k_1 [1/min]	0,025	0,017	0,024	0,017	0,021	0,020	0,024	0,023	0,024
	q_e [mg/g]	106,77	80,89	44,37	92,60	106,44	74,34	116,59	106,55	70,18
	R^2	0,841	0,844	0,981	0,938	0,903	0,974	0,935	0,880	0,963
	Δqe[%]	15,56	17,43	6,38	14,10	14,45	6,85	11,67	12,26	6,64
	Δq	0,117	0,168	0,046	0,113	0,130	0,079	0,094	0,146	0,083
	RMSE	13,381	10,772	1,764	7,537	10,261	3,684	8,947	11,137	3,964
Pseudo-2nd-Order	k_2 [g/(mg·min)]	2,02E-04	1,72E-04	4,97E-04	1,46E-04	1,74E-04	2,25E-04	1,74E-04	1,96E-04	3,07E-04
	q_e [mg/g]	125,98	99,13	51,61	113,52	126,49	88,84	137,91	125,07	81,76
	R^2	0,915	0,910	0,999	0,976	0,957	0,994	0,964	0,941	0,991
	Δqe[%]	0,37	1,19	8,92	5,30	1,67	11,31	4,49	2,99	8,76
	Δq	0,086	0,140	0,010	0,083	0,096	0,046	0,088	0,111	0,048
	RMSE	9,771	8,200	0,324	4,687	6,839	1,803	6,673	7,824	1,995

Table 5-12 shows the kinetic parameter results for 1-decanol adsorbed onto activated alumina F-220 with the grey highlighted blocks representing the model that best fits each system at a particular temperature and initial 1-decanol concentration. Every system, besides for the highest 1-decanol concentration at 35 ºC system, is best described by the Weber-Morris model, thus indicating that diffusion is the rate-limiting step in these systems.

The B value in every systems is also not equal to zero, indicating that intra-particle diffusion is not the sole rate-limiting step and that the diffusion of the particles to the adsorbent is also slow and influencing the overall rate of each process. The reason for the high concentration 1-decanol – F-220 at 35 ºC system being better described by the Pseudo-2nd-Order model is unknown, however it indicates that within this system, the rate of the adsorption process is governed by the physical adsorption reaction step.

Table 5-13, Table 5-14 and Table 5-15 give the kinetic parameters for adsorption systems with Selexsorb® CD as adsorbent and adsorbates 1-hexanol, 1-octanol and 1-decanol respectively.

Table 5-13: Kinetic model parameters for 1-hexanol adsorbed onto Selexsorb® CD at all three adsorption temperatures

Models	Parameters	25 °C			30 °C			35 °C		
		1-hexanol								
		1,39	0,97	0,51	1,71	1,15	0,30	1,55	0,97	0,48
Weber-Morris	k_{int} [mg/(g·min^{½})]	5,10	3,95	2,92	4,47	3,59	1,98	6,07	4,10	3,18
	B [mg/g]	4,79	10,38	9,71	0,00	17,31	10,75	5,96	19,28	9,27
	R^2	0,962	0,993	0,979	0,968	0,998	0,929	0,996	0,985	0,984
	Δq	0,043	0,043	0,062	0,174	0,018	0,061	0,024	0,053	0,036
	RMSE	2,018	1,920	2,353	5,601	0,934	2,930	2,089	2,846	2,251
Pseudo-1st-Order	k_1 [1/min]	0,017	0,023	0,025	0,007	0,028	0,028	0,017	0,026	0,022
	q_e [mg/g]	86,11	72,10	55,44	95,11	72,62	42,04	102,99	83,39	59,68
	R^2	0,950	0,911	0,939	0,975	0,848	0,959	0,884	0,856	0,934
	Δqe[%]	10,65	17,41	10,75	7,25	16,35	5,52	15,33	13,94	5,84
	Δq	0,103	0,093	0,074	0,111	0,140	0,080	0,122	0,152	0,109
	RMSE	8,991	6,675	4,054	4,885	8,082	2,214	12,027	8,962	4,649
Pseudo-2nd-Order	k_2 [g/(mg·min)]	1,54E-04	2,69E-04	4,00E-04	4,39E-05	3,68E-04	6,86E-04	1,25E-04	3,01E-04	3,25E-04
	q_e [mg/g]	106,60	85,61	64,79	131,03	83,43	47,62	127,79	95,94	70,45
	R^2	0,977	0,965	0,982	0,984	0,922	0,985	0,940	0,923	0,976
	Δqe[%]	10,61	1,93	4,30	47,76	3,90	7,02	5,06	0,99	11,14
	Δq	0,070	0,056	0,036	0,072	0,103	0,050	0,091	0,118	0,075
	RMSE	6,100	4,170	2,192	3,932	5,769	1,340	8,616	6,554	2,785

Table 5-13 shows the kinetic parameter results for 1-hexanol adsorbed onto Selexsorb® CD with the grey highlighted blocks representing the model that best fits each system at a particular temperature and initial 1-hexanol concentration. Once again it is observed that all the systems are described best be the Weber-Morris model, with only one exception being the lowest 1-hexanol concentration – SCD at 25 ºC system.

Once again all these systems are diffusion rate limited, with only one system indicating intra-particle diffusion as the sole rate-limiting step (1-hexanol at 1,71 mass% at 30 ºC).

Table 5-14: Kinetic model parameters for 1-octanol adsorbed onto Selexsorb® CD at all three adsorption temperatures

Models	Parameters	25 °C			30 °C			35 °C		
		1-octanol								
		1,53	1,02	0,06	1,51	1,03	0,49	1,56	1,07	0,52
Weber-Morris	k_{int} [mg/(g·min^{½})]	4,28	3,61	2,76	4,86	3,85	2,31	4,36	4,14	2,74
	B [mg/g]	6,27	5,66	6,37	0,00	4,20	8,12	13,71	8,86	9,08
	R^2	0,993	0,997	0,978	0,987	0,991	0,963	0,880	0,986	0,963
	Δq	0,028	0,018	0,062	0,077	0,038	0,075	0,139	0,041	0,056
	RMSE	2,035	1,192	2,274	3,209	2,055	2,513	8,332	2,774	2,998
Pseudo-1st-Order	k_1 [1/min]	0,018	0,018	0,021	0,013	0,017	0,025	0,028	0,019	0,023
	q_e [mg/g]	74,99	63,55	50,19	81,29	66,41	44,69	80,71	75,35	52,73
	R^2	0,937	0,924	0,954	0,948	0,949	0,963	0,861	0,938	0,958
	Δqe[%]	16,67	13,33	31,55	9,36	11,54	12,56	22,95	10,88	11,52
	Δq	0,102	0,117	0,072	0,099	0,089	0,063	0,130	0,116	0,089
	RMSE	6,110	5,692	3,335	6,365	4,912	2,513	8,963	5,873	3,183
Pseudo-2nd-Order	k_2 [g/(mg·min)]	1,94E-04	2,29E-04	3,61E-04	1,18E-04	2,01E-04	5,08E-04	3,01E-04	2,16E-04	4,00E-04
	q_e [mg/g]	91,43	77,46	59,77	103,52	81,66	51,96	94,18	90,49	61,60
	R^2	0,977	0,969	0,989	0,977	0,984	0,994	0,898	0,976	0,988
	Δqe[%]	1,60	5,63	18,49	15,44	8,76	1,66	10,09	7,02	3,36
	Δq	0,070	0,086	0,037	0,059	0,056	0,026	0,127	0,084	0,054
	RMSE	3,672	3,645	1,616	4,229	2,731	1,028	7,683	3,660	1,678

Table 5-14 shows the kinetic parameter results for 1-octanol adsorbed onto Selexsorb® CD with the grey highlighted blocks representing the model that best fits each system at a particular temperature and initial 1-octanol concentration. All systems, with 2 exceptions, are best described by the Weber-Morris model.

The lowest 1-octanol concentrations at both temperatures of 30 and 35 ºC, show the best fit model to be the Pseudo-2nd-Order model, indicating that the rate of the adsorption process is limited by the physical adsorption reaction step. It is also interesting to note, that once again at 30 ºC and the highest 1-octanol concentration, the B value in the Weber-Morris model is equal to zero indicating that that system's rate is solely influenced by intra-particle diffusion.

Table 5-15: Kinetic model parameters for 1-decanol adsorbed onto Selexsorb® CD at all three adsorption temperatures

Models	Parameters	25 °C			30 °C			35 °C		
		1-decanol								
		1,52	0,99	0,51	1,37	1,07	0,53	1,60	1,01	0,53
Weber-Morris	k_{int} [mg/(g·min^{½})]	5,41	4,33	3,00	4,03	4,08	3,11	4,79	4,94	3,43
	B [mg/g]	1,50	4,48	3,88	0,00	1,25	3,33	0,00	2,02	2,14
	R^2	0,992	0,987	0,981	0,996	0,970	0,982	0,993	0,988	0,991
	Δq	0,029	0,028	0,042	0,061	0,095	0,056	0,060	0,034	0,045
	RMSE	2,703	2,805	2,349	1,542	3,921	2,376	2,489	3,043	1,864
Pseudo-1st-Order	k_1 [1/min]	0,014	0,016	0,017	0,012	0,016	0,017	0,011	0,015	0,016
	q_e [mg/g]	91,64	74,98	52,58	69,38	67,79	53,71	85,73	83,67	58,15
	R^2	0,961	0,921	0,964	0,940	0,975	0,965	0,972	0,962	0,952
	Δqe[%]	4,50	13,27	13,59	8,93	11,20	9,25	4,83	11,23	11,03
	Δq	0,094	0,125	0,089	0,115	0,053	0,072	0,095	0,096	0,083
	RMSE	6,043	7,015	3,232	5,874	3,570	3,291	4,899	5,456	4,254
Pseudo-2nd-Order	k_2 [g/(mg·min)]	1,12E-04	1,68E-04	2,63E-04	1,20E-04	1,73E-04	2,53E-04	8,38E-05	1,29E-04	2,04E-04
	q_e [mg/g]	115,62	92,57	64,25	89,63	84,73	65,91	111,99	105,15	72,41
	R^2	0,987	0,962	0,991	0,971	0,995	0,992	0,988	0,988	0,984
	Δqe[%]	20,49	7,08	5,59	17,65	10,99	11,36	24,32	11,56	10,79
	Δq	0,066	0,097	0,057	0,069	0,035	0,039	0,076	0,067	0,052
	RMSE	3,468	4,898	1,643	4,089	1,522	1,517	3,237	3,129	2,432

Table 5-15 shows the kinetic parameter results for 1-decanol adsorbed onto Selexsorb® CD with the grey highlighted blocks representing the model that best fits each system at a particular temperature and initial 1-decanol concentration. All systems are best described by the Weber-Morris model indicating that all systems are diffusion rate-controlled. The B values are all greater than zero, except for the highest concentrations of 1-decanol at temperatures of 30 and 35 ºC. At these temperature and concentrations, the B value is equal to zero meaning that these systems are solely intra-particle diffusion rate controlled.

Table 5-16, Table 5-17 and Table 5-18 give the kinetic parameters for adsorption systems with Selexsorb® CDx as adsorbent and adsorbates 1-hexanol, 1-octanol and 1-decanol respectively.

Table 5-16: Kinetic model parameters for 1-hexanol adsorbed onto Selexsorb® CDx at all three adsorption temperatures

Models	Parameters	25 °C			30 °C			35 °C		
		1-hexanol								
		1,40	0,97	0,42	1,42	1,00	0,47	1,47	0,99	0,46
Weber-Morris	k_{int} [mg/(g·min^{½})]	4,72	4,30	2,48	4,66	4,71	2,71	6,02	4,72	2,93
	B [mg/g]	5,16	5,16	12,05	10,96	6,88	10,53	9,71	11,71	14,23
	R^2	0,962	0,990	0,989	0,926	0,991	0,978	0,989	0,966	0,888
	Δq	0,070	0,048	0,040	0,140	0,030	0,043	0,046	0,066	0,089
	RMSE	5,218	2,415	1,453	7,505	2,515	2,279	3,503	4,891	5,171
Pseudo-1st-Order	k_1 [1/min]	0,017	0,018	0,029	0,016	0,018	0,025	0,019	0,021	0,026
	q_e [mg/g]	81,86	74,25	50,30	87,84	82,64	53,30	105,73	87,19	61,99
	R^2	0,950	0,945	0,894	0,819	0,944	0,937	0,931	0,965	0,667
	Δqe[%]	8,30	10,18	9,55	8,87	12,82	10,23	10,85	16,12	0,73
	Δq	0,087	0,082	0,100	0,212	0,098	0,099	0,094	0,075	0,150
	RMSE	6,026	5,680	4,603	11,726	6,307	3,854	8,967	4,962	8,899
Pseudo-2nd-Order	k_2 [g/(mg·min)]	1,65E-04	1,88E-04	5,58E-04	1,62E-04	1,75E-04	4,37E-04	1,45E-04	2,12E-04	4,26E-04
	q_e [mg/g]	100,29	90,97	57,61	105,94	100,72	61,79	128,31	103,36	70,27
	R^2	0,977	0,983	0,955	0,867	0,982	0,980	0,975	0,993	0,772
	Δqe[%]	12,36	10,04	3,60	9,92	6,25	4,07	8,19	0,56	12,52
	Δq	0,055	0,049	0,062	0,194	0,066	0,062	0,060	0,040	0,121
	RMSE	4,100	3,179	2,983	10,040	3,615	2,186	5,412	2,199	7,369

Table 5-16 shows the kinetic parameter results for 1-hexanol adsorbed onto Selexsorb® CDx with the grey highlighted blocks representing the model that best fits each system at a particular temperature and initial 1-hexanol concentration. Most of the systems presented above show that the Weber-Morris model best describes their adsorption kinetics, while three of the systems are best described by the Pseudo-2nd-Order model.

The B parameters for the systems best described by the Weber-Morris model are all greater than zero, therefore indicating that intra-particle diffusion is not the sole rate-limiting step. The three systems best described by the Pseudo-2nd-Order model show that their rate is controlled more by the physical adsorption reaction step.

Table 5-17: Kinetic model parameters for 1-octanol adsorbed onto Selexsorb® CDx at all three adsorption temperatures

Models	Parameters	25 °C			30 °C			35 °C		
		1-octanol								
		1,58	1,05	0,56	1,52	1,00	0,54	1,59	1,00	0,48
Weber-Morris	k_{int} [mg/(g·min^{½})]	3,74	3,52	2,64	4,35	3,76	2,73	4,67	4,27	2,19
	B [mg/g]	7,78	4,69	4,24	7,79	12,45	5,94	7,76	7,95	8,36
	R^2	0,999	0,988	0,959	0,991	0,993	0,968	0,995	0,991	0,961
	Δq	0,011	0,036	0,058	0,051	0,034	0,052	0,021	0,036	0,053
	RMSE	0,531	2,212	3,029	2,398	1,778	2,772	1,849	2,237	2,474
Pseudo-1st-Order	k_1 [1/min]	0,020	0,017	0,018	0,018	0,024	0,020	0,018	0,020	0,024
	q_e [mg/g]	66,75	61,90	47,37	76,96	71,08	49,85	82,71	76,01	43,30
	R^2	0,882	0,942	0,976	0,840	0,905	0,968	0,971	0,936	0,955
	Δqe[%]	16,79	9,78	13,07	17,66	14,89	13,83	2,96	12,62	13,33
	Δq	0,133	0,115	0,087	0,166	0,104	0,083	0,083	0,095	0,095
	RMSE	7,424	4,845	2,308	10,307	6,601	2,778	7,157	6,140	2,642
Pseudo-2nd-Order	k_2 [g/(mg·min)]	2,45E-04	2,19E-04	3,11E-04	1,89E-04	3,06E-04	3,41E-04	1,80E-04	2,13E-04	5,21E-04
	q_e [mg/g]	80,61	75,79	57,34	93,99	83,32	59,52	100,54	91,70	50,18
	R^2	0,943	0,977	0,992	0,908	0,960	0,993	0,928	0,978	0,985
	Δqe[%]	0,49	10,47	5,24	0,57	0,23	2,91	15,30	5,42	0,44
	Δq	0,099	0,086	0,056	0,137	0,071	0,050	0,114	0,062	0,060
	RMSE	5,157	3,043	1,324	7,800	4,298	1,328	4,500	3,600	1,513

Table 5-17 shows the kinetic parameter results for 1-octanol adsorbed onto Selexsorb® CDx with the grey highlighted blocks representing the model that best fits each system at a particular temperature and initial 1-octanol concentration. The same trends that were seen for 1-octanol – F-220 adsorption systems are seen here for the 1-octanol – SCD adsorption systems.

The lowest 1-octanol concentration at each temperature are all best described by the Pseudo-2nd-Order model indicating that these systems are rate-controlled by the adsorption reaction step, while all the other systems at the higher 1-octanol concentrations are diffusion rate limited. The B values for all of these systems are not equal to zero showing once again that intra-particle diffusion is not the sole rate-limiting step.

Table 5-18: Kinetic model parameters for 1-decanol adsorbed onto Selexsorb® CDx at all three adsorption temperatures

Models	Parameters	25 °C			30 °C			35 °C		
		1-decanol								
		1,52	0,99	0,50	1,62	1,35	0,61	1,58	1,10	0,51
Weber-Morris	k_{int} [mg/(g·min^{½})]	3,75	4,32	3,12	4,55	4,03	3,64	4,95	3,96	3,16
	B [mg/g]	0,00	6,43	1,09	0,00	5,94	2,72	0,00	10,18	5,68
	R^2	0,996	0,959	0,978	0,978	0,997	0,972	0,994	0,994	0,972
	Δq	0,047	0,091	0,047	0,069	0,023	0,092	0,041	0,027	0,046
	RMSE	1,454	4,950	2,612	4,229	1,276	3,353	2,172	1,685	2,983
Pseudo-1st-Order	k_1 [1/min]	0,010	0,020	0,015	0,010	0,018	0,017	0,013	0,022	0,019
	q_e [mg/g]	67,07	75,22	52,90	80,47	70,28	61,51	84,05	72,57	56,61
	R^2	0,960	0,932	0,979	0,904	0,923	0,966	0,967	0,914	0,967
	Δqe[%]	6,53	10,97	6,87	8,382	15,106	10,404	9,72	13,93	8,28
	Δq	0,113	0,071	0,079	0,154	0,106	0,057	0,085	0,110	0,085
	RMSE	4,562	6,400	2,579	8,727	6,363	3,739	5,182	6,606	3,231
Pseudo-2nd-Order	k_2 [g/(mg·min)]	1,07E-04	2,09E-04	2,03E-04	9,18E-05	2,08E-04	2,15E-04	1,06E-04	2,56E-04	2,78E-04
	q_e [mg/g]	87,48	91,17	66,44	104,47	85,77	75,89	107,78	86,37	68,21
	R^2	0,980	0,964	0,996	0,935	0,969	0,992	0,990	0,966	0,992
	Δqe[%]	21,91	7,91	16,97	18,953	3,597	10,545	15,78	2,43	10,52
	Δq	0,094	0,044	0,049	0,133	0,074	0,037	0,046	0,074	0,052
	RMSE	3,222	4,636	1,162	7,198	4,013	1,762	2,862	4,144	1,595

Table 5-18 shows the kinetic parameter results for 1-decanol adsorbed onto Selexsorb® CDx with the grey highlighted blocks representing the model that best fits each system at a particular temperature and initial 1-decanol concentration. These systems show varying behaviour between diffusion rate limited and adsorption reaction rate limited as the initial 1-decanol concentration changes at the three adsorption temperatures.

The highest 1-decanol concentration at each temperature is best described by the Weber-Morris model and all show B values of zero, indicating that these systems are all solely intra-particle rate limited.

Most of the kinetic adsorption systems investigated appear to be diffusion rate limited, while a few show that the adsorption reaction controls their rate. Some general trends seen in the kinetic parameters include the increase of the k value with an increase in adsorbate concentration as well as with an increase in temperature. Both these factors influence the diffusion of a molecule. An increase in concentration, increases the concentration gradient between the bulk solution and the adsorbent's surface, thus increasing the rate of the diffusion of the molecules resulting in a higher k value. Diffusion is also faster at a higher temperature because at higher temperatures molecules have more energy to move thereby increasing the rate of diffusion and consequently resulting in a higher rate constant (k value).

The 1-hexanol rate constants also seem to generally be higher than the 1-octanol and 1-decanol rate constants, indicating that the rate of 1-hexanol adsorption is faster than 1-octanol and 1-decanol allowing more to be adsorbed before equilibrium is reached.

5.2.3. Kinetic modelling results discussion and conclusions

Kinetic modelling is required to give indications of the rate limiting steps involved in an adsorption process. The adsorption reaction step, where the adsorbate molecules bonds with the surface of the adsorbent or the diffusion step, where the molecule is travelling to the adsorption site, can be the rate limiting step.

The Weber-Morris model provides a good indication of whether the adsorption process is intra-particle diffusion rate-limited or if more than one step is controlling the rate. The B parameter in the Weber-Morris model will be equal to zero if the rate of the adsorption process is solely controlled by intra-particle diffusion (Ozacar, et al., 2008). If B does not equal zero, it is an indication of that diffusion of the adsorbate molecules through the boundary layer is also slow enough to be rate-controlling (Ozacar, et al., 2008), or that the adsorption of the adsorbate molecules onto the external adsorbent surface is slow (Ghorai & Pant, 2005).

From the kinetic parameters for all the adsorption systems, it is seen that most of the B values are not equal to zero, therefore giving the impression that the diffusion of the particles into the pores of the adsorbent surface is not the only diffusion step controlling the process. This was found to be the case for most of the systems best described by the Weber-Morris model..

The kinetic models best describing each kinetic adsorption system have thus given an indication of which step in the movement of adsorbate molecule from the bulk solution to the adsorbent surface and subsequent reaction with the active site controls the rate of the entire process.. Most of the systems appeared to be diffusion rate limited, while a few showed that the physically adsorption reaction of their adsorbate molecules to the adsorbent's active sites controls the rate of their adsorption process.

5.3 Adsorption Modelling conclusions

This chapter looked at the equilibrium and kinetic modelling of the various systems investigated in this work to compare the various adsorption systems investigated and obtain a better understanding of the adsorption mechanisms taking place.

The isotherm modelling revealed that all the adsorption systems display favourable adsorption behaviour, significant adsorbent loading values were obtained under all conditions, and that the adsorbate-adsorbent bonding was of a physical nature, i.e. physisorption. The mean free energy analysis, confirmed the adsorption intensity parameter indications from the Freundlich isotherm model, giving energies of less than 8 kJ/mol indicating a physical bond between adsorbent and adsorbate.

Maximum adsorption capacities confirmed the findings in chapter 4 concluding that the activated alumina F-220 adsorbent performed the best compared to Selexsorb® CD and Selexsorb® CDx adsorbents. Adsorption capacities also generally increased with an increase in temperature confirming that these adsorption systems show improved performance at slightly higher adsorption temperatures.

The kinetic modelling of the adsorption systems revealed most systems were diffusion rate-limited, while only a few were limited by the rate of the physical adsorption reaction step.

Chapter 6: Regeneration Results

This chapter introduces the adsorption-regeneration cycle results for the systems investigated. First the choice of adsorption system is discussed. The preliminary results, which were used to establish the regeneration procedure and to get an idea of how the systems would perform, are then discussed. Lastly, the results for the 6 adsorption-regeneration systems investigated are presented and discussed.

The focus of the adsorption-regeneration cycle experiments was to investigate the effects of the regeneration process on the adsorbents and test the validity of the equipment designed and developed for future regeneration studies. One cycle consisted of two batch experiments, adsorption and regeneration, and several cycles were performed to evaluate the ability of the regeneration technique in restoring each adsorbent's capacity.

6.1 Adsorption System

The adsorption system chosen was based on the initial adsorption experiments performed and considering the boiling points of the adsorbates. When considering temperature, type of adsorbate and initial adsorbate concentration, the adsorption system showing the greatest adsorbate loading was considered for further experimentation.

Figure 6-1, Figure 6-2 and Figure 6-3 give the adsorbent loadings for activated alumina F-220, Selexsorb® CD and Selexsorb® CDx respectively. When considering the Selexsorb® CD and Selexsorb® CDx adsorbent loadings (Figure 6-2 and Figure 6-3), it is seen that the higher loadings are between 1,40 and 1,60 solution initial alcohol mass percent and that the 1-hexanol adsorbate (blue markers) shows the higher loadings at an adsorption temperature of 35 °C (triangle markers). However, when considering the adsorbent loadings for activated alumina F-220, it is seen that the 1-decanol adsorbate (green markers) gives higher loadings than 1-hexanol and 1-octanol, at a temperature of 35 °C.

From the adsorbent loadings, it was clear that 35 °C was a good choice for adsorption temperature and that a solution initial alcohol mass percentage between 1,40 and 1,60 should be chosen. The choice of adsorbate was then between 1-hexanol and 1-decanol. When considering the boiling points of these two adsorbates, 1-hexanol with a boiling point of 157 °C and 1-decanol of 230 °C, it was decided that 1-hexanol would be the adsorbate of choice. The lower boiling point component was chosen in order to keep regeneration temperatures close to 200 °C as this was a new experimental setup being tested with new procedures.

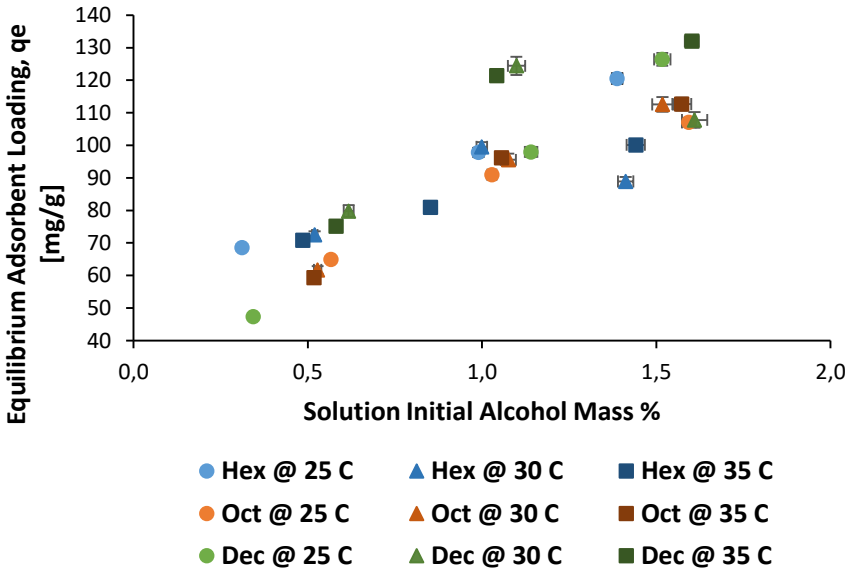

Figure 6-1: The activated alumina F-220 equilibrium adsorbent loading for each adsorbate (1-hexanol, 1-octanol & 1-decanol) at each adsorption temperature investigated (25, 30 & 35 °C)

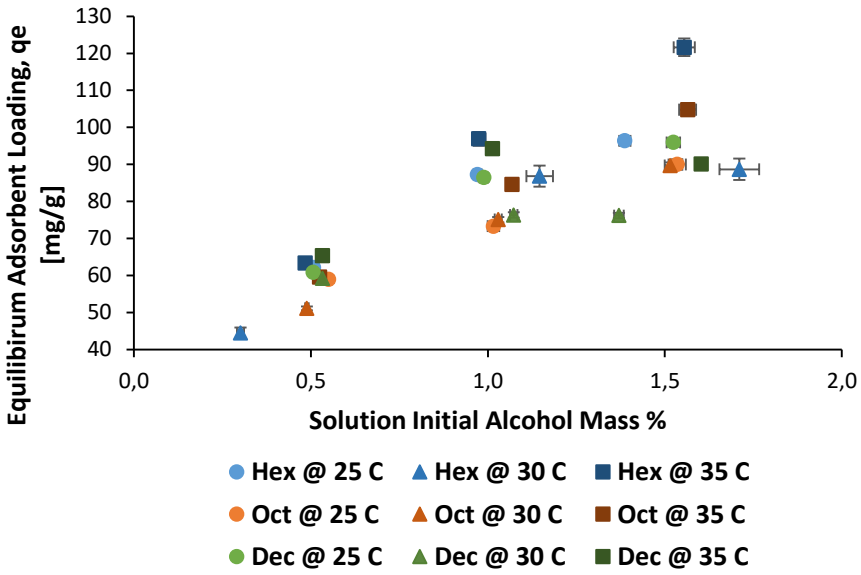

Figure 6-2: The Selexsorb® CD equilibrium adsorbent loading for each adsorbate (1-hexanol, 1-octanol & 1-decanol) at each adsorption temperature investigated (25, 30 & 35 °C)

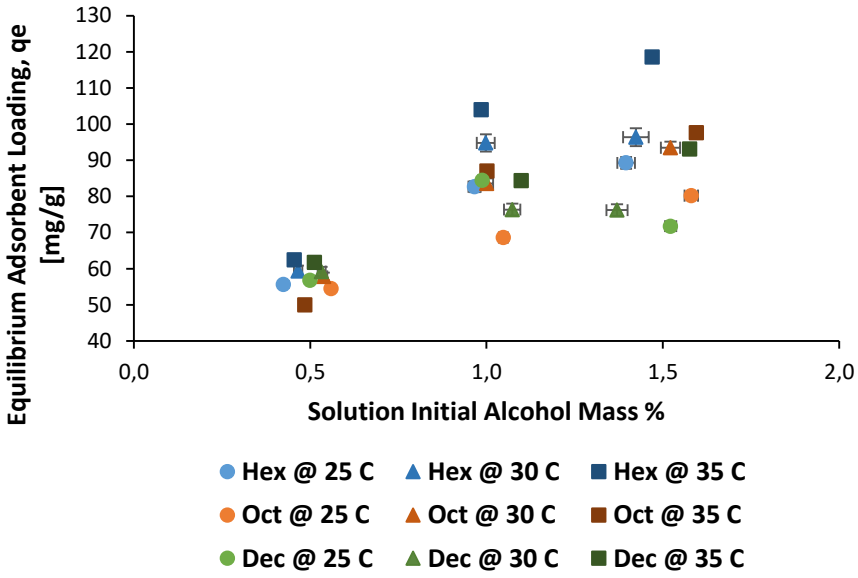

Figure 6-3: The Selexsorb® CDx equilibrium adsorbent loading for each adsorbate (1-hexanol, 1-octanol & 1-decanol) at each adsorption temperature investigated (25, 30 & 35 °C)

The final adsorption system chosen was therefore 1-hexanol as adsorbate at an initial mass percentage of 1,50 and at an adsorption temperature of 35 °C.

6.2 Regeneration System

Two of the most important variables in these regeneration experiments were regeneration temperature and duration. As discussed in Section 3.3, the regeneration duration was chosen as a constant variable with a time of 60 min, while two regeneration temperatures were investigated (185 and 205 °C).

6.3 Preliminary Adsorption-Regeneration Experimental Results

The preliminary experiments consisted of 4 adsorption and 3 regeneration cycles, beginning and ending with an adsorption cycle. Three experiments could be run simultaneously, therefore a run for each adsorbent type was conducted. The adsorption cycles were left to run overnight. Due to the lengthy regeneration period required, the regeneration equipment not being able to be left on and alone overnight and the physical sampling required during the adsorption cycle, both could not be conducted consecutively on the same day.

The purpose of the preliminary experiments was to establish the regeneration experimental procedure, as this was a new experimental setup with new procedures. It was also required to get an

idea on how many adsorption-regeneration cycles were needed to see a decrease in adsorption capacity. Based on the size of the systems tested, a concern was that many cycles would be required before a decrease in adsorption capacity would be seen.

The effects of the regeneration cycle on each adsorbent were quantified by comparing the total percentage alcohol removed the solution (removal efficiency) and equilibrium adsorbent loading after each adsorption cycle.

Figure 6-4 shows the removal efficiency results for the preliminary runs performed.

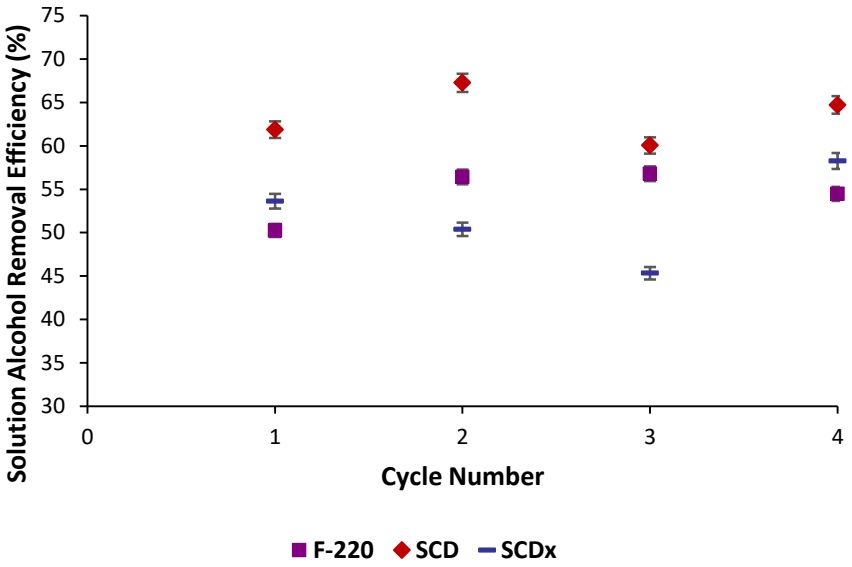

Figure 6-4: The percentage of total alcohol removed from the adsorption solution for each adsorbent type (F-220, SCD and SCDx) after adsorption cycles 1, 2, 3 and 4

For adsorbents F-220 and SCD an initial increase is seen in alcohol removal efficiency after adsorption cycle 2. These increases were attributed to contaminants that may have been on the adsorbents prior to the first adsorption cycle because the adsorbents were used in the condition they were received in. Experimentation started with an adsorption cycle, therefore after the first regeneration cycle, these two adsorbents were 'cleaner' and removed more adsorbate.

The initial decrease seen in the alcohol removal efficiency for adsorbent SCDx and subsequent decrease for adsorbent SCD is an expected outcome. Temperature can damage the surface of an adsorbent and its adsorption sites, as well as not efficiently desorb and remove the adsorbates thereby causing less adsorption to take place in the subsequent adsorption cycles.

The increase in alcohol removal efficiency for the SCD adsorbent after adsorption cycle 4 is explained using Figure 6-5 and Figure 6-6. Due to initial experimental difficulties with the adsorbent

mesh baskets used in the adsorption experiments, some adsorbent was lost while taking the mesh basket out of the regeneration column. The adsorbent fell into the column or out into the fume hood. The adsorbent mass therefore decreased as shown below in Figure 6-6, while however causing an increase in the equilibrium adsorbent loading. This is due to the inverse relationship between adsorbent loading (q) and adsorbent mass (W) as can be seen in equation [7-1].

$$q = \frac{(C_i - C_e) * V}{W} \qquad [7\text{-}1]$$

During an adsorption process, if all parameters remain constant besides for the adsorbent mass, the system will still behave the same, i.e. adsorb more or less the same amount. However due to the lower adsorbent mass, the adsorbent loading will be more.

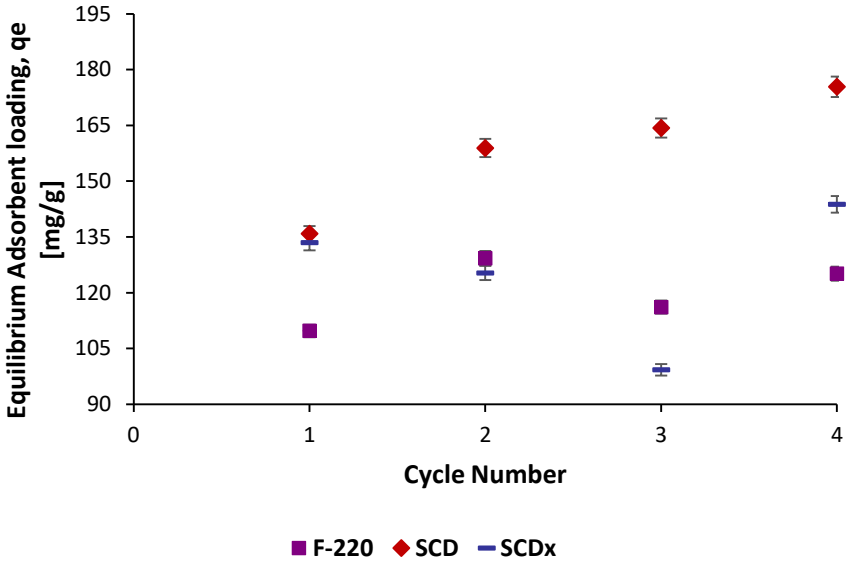

Figure 6-5: The equilibrium adsorbent loadings after each adsorption cycle for adsorbents F-220, SCD and SCDx

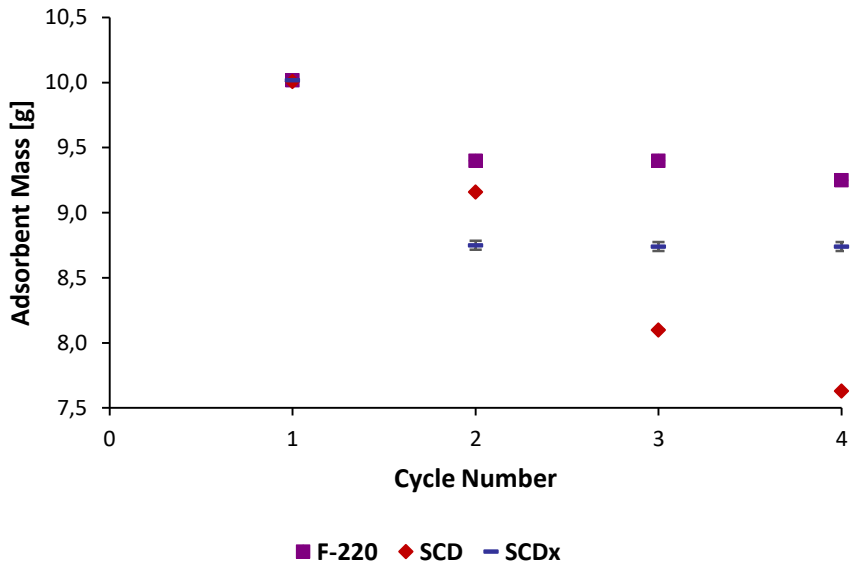

Figure 6-6: The mass of adsorbent before each adsorption cycle for adsorbents F-220, SCD and SCDx

Based on the results obtained during the preliminary experiments and the experimental difficulties experienced, it was decided that the adsorption-regeneration cycles would start with a regeneration cycle and led to the design and construction of the column inserts.

This was expected to eliminate the initial increase seen in the alcohol removal efficiency and the loss of adsorbent mass during experimentation. It was also noted that four cycles would not be enough to show a decrease in adsorption capacity and therefore eight cycles would be performed for the subsequent regeneration tests.

6.4 Adsorption-Regeneration Experimental Results

The adsorption results for each adsorbent regenerated at temperatures of 185 °C and 205 °C are presented and discussed in this section. The reader is referred to Appendix 8.21 for the raw experimental data for the adsorption-regeneration experiments.

6.4.1. 185 °C regeneration temperature results

The three adsorbents, Selexsorb® CDx, Selexsorb® CD and activated alumina F-220, were subjected to 8 adsorption-regeneration cycles excluding the initial regeneration cycle.

Figure 6-7, Figure 6-8 and Figure 6-9 show the alcohol removal efficiencies, the adsorbent loadings and the adsorbent mass changes for each adsorbent over the 8 adsorption regeneration cycles respectively.

The data in Figure 6-7 shows the alcohol removal efficiency of each adsorbent after the previous cycle's regeneration process. For all three adsorbents it is seen that for the first four cycles the alcohol adsorption efficiency remains relatively constant, within a 5% range of the average percentage alcohol removed for each adsorbent.

Adsorbents SCD and SCDx then show significant decreases in efficiency after adsorption cycle 5 and a similar efficiency after cycle 6, followed by decreases in efficiencies after cycles 7 and 8. The F-220 adsorbent exhibits slightly different behaviour with a significant decrease only being shown after cycle 6's adsorption run, while then also showing a decrease in percentage alcohol removed from solution thereafter.

In industry, generally a 10 % decline in adsorption capacity is seen after 1 regeneration cycle (Scholtz, 26 Oct 2016). However, based on the massive system size difference between industrial processes and these investigated here, it was expected that only after several adsorption-regeneration cycles, would a decline in capacity be seen. Based on the experimental quantities used in these experiments, initial stabile and efficient adsorption-regeneration systems are seen, after which a slow decline in adsorption efficiency is seen with every regeneration cycle performed. On average an overall 24 % decrease in adsorption capacity is seen for adsorbents Selexsorb® CD and CDx, while an 18 % decrease is seen for adsorbent activated alumina F-220.

It is speculated that the decrease in adsorbent capacity is a result of the adsorbent's active sites being damaged due to repeated exposure to high temperatures. This reasoning could not be confirmed in this work and in future studies scanning electron microscope imaging should be performed before adsorption-regeneration cycles are conducted and again once a decline in capacity is seen. This should give a visual indication as to whether the surface of the adsorbent changes in any way.

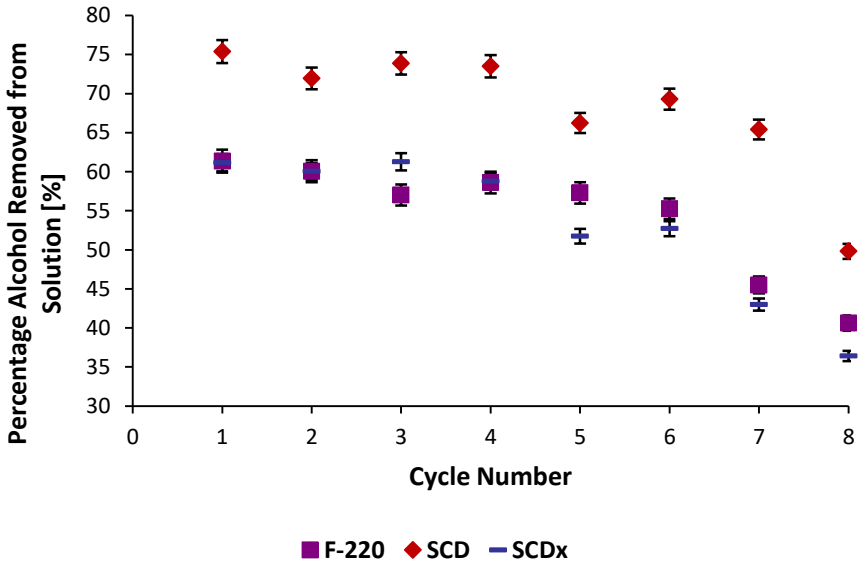

Figure 6-7: The percentage of total alcohol removed from the adsorption solution for each adsorbent type (F-220, SCD and SCDx) after each adsorption cycle in the 185 °C regeneration runs

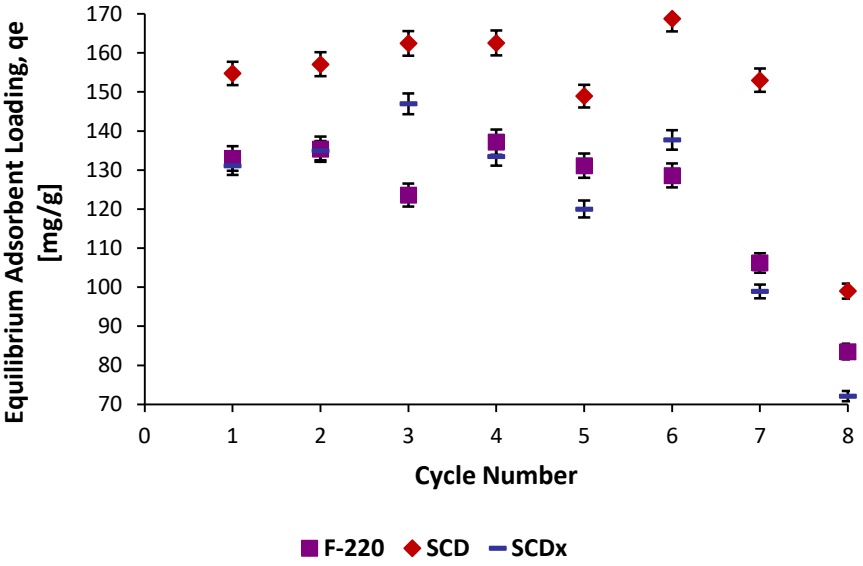

Figure 6-8: The equilibrium adsorbent loading for adsorbents F-220, SCD and SCDx after each adsorption cycle for the 185 °C regeneration runs

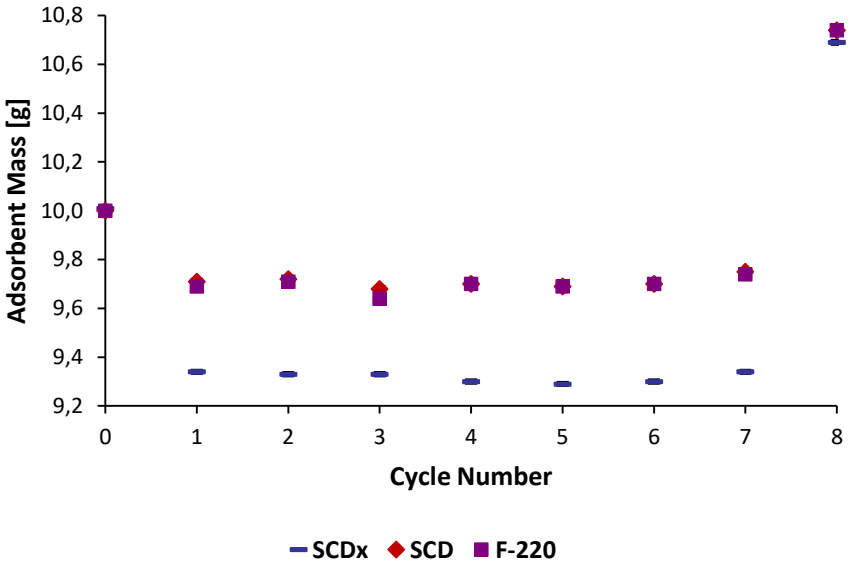

Figure 6-9: The mass of adsorbent before each adsorption cycle for adsorbents F-220, SCD and SCDx for the 185 C regeneration runs

The initial decrease in adsorbent mass seen in Figure 6-9 is due to the initial regeneration cycle in essence cleaning the adsorbents. The adsorbent masses then stay relatively constant across the next 7 cycles. The increase in adsorbent mass before adsorption 8 was due to unforeseen circumstances that led to a time delay between cycles 7 and 8. The adsorbents were kept in the column inserts in a closed container, however in this time the adsorbents may have adsorbed molecules from its surrounding environment.

The temperature profiles for the 8 cycles are shown below in Figure 6-10, Figure 6-11 and Figure 6-12 for adsorbents activated alumina F-220, Selexsorb® CD and Selexsorb® CDx respectively. In industry, the outlet temperature in the regeneration process is one of the most important variables monitored as it gives an indication of what components are desorbing (Scholtz, 26 Oct 2016). The temperature-time profiles generated during these regeneration cycles were expected to show temperature plateaus. The plateaus represent the vapourising of compounds within the adsorbent bed. In more complex systems, the outlet temperature profiles will give an indication of what components are desorbing and when in a regeneration process. The outlet temperature profile not reaching the 185 °C regeneration temperature in some cases in the figures, can be interpreted as the organic adsorbates desorbing and vapourising.

In order to obtain clearer temperature plateaus, it is recommended that in future studies the size of the adsorption bed and hence the physical mass of adsorbate molecules present be increased. Due to the systems in this work being quite small (10 g of adsorbent with on average 4 g of adsorbed mass), the desorbing of the adsorbate molecules was not always noticeable on the temperature profiles.

These temperature profiles will also be very useful when more complex adsorption systems (binary and ternary systems) are investigated, giving an indication of when which adsorbate is desorbing and whether there are any other components present in the system that were not known before.

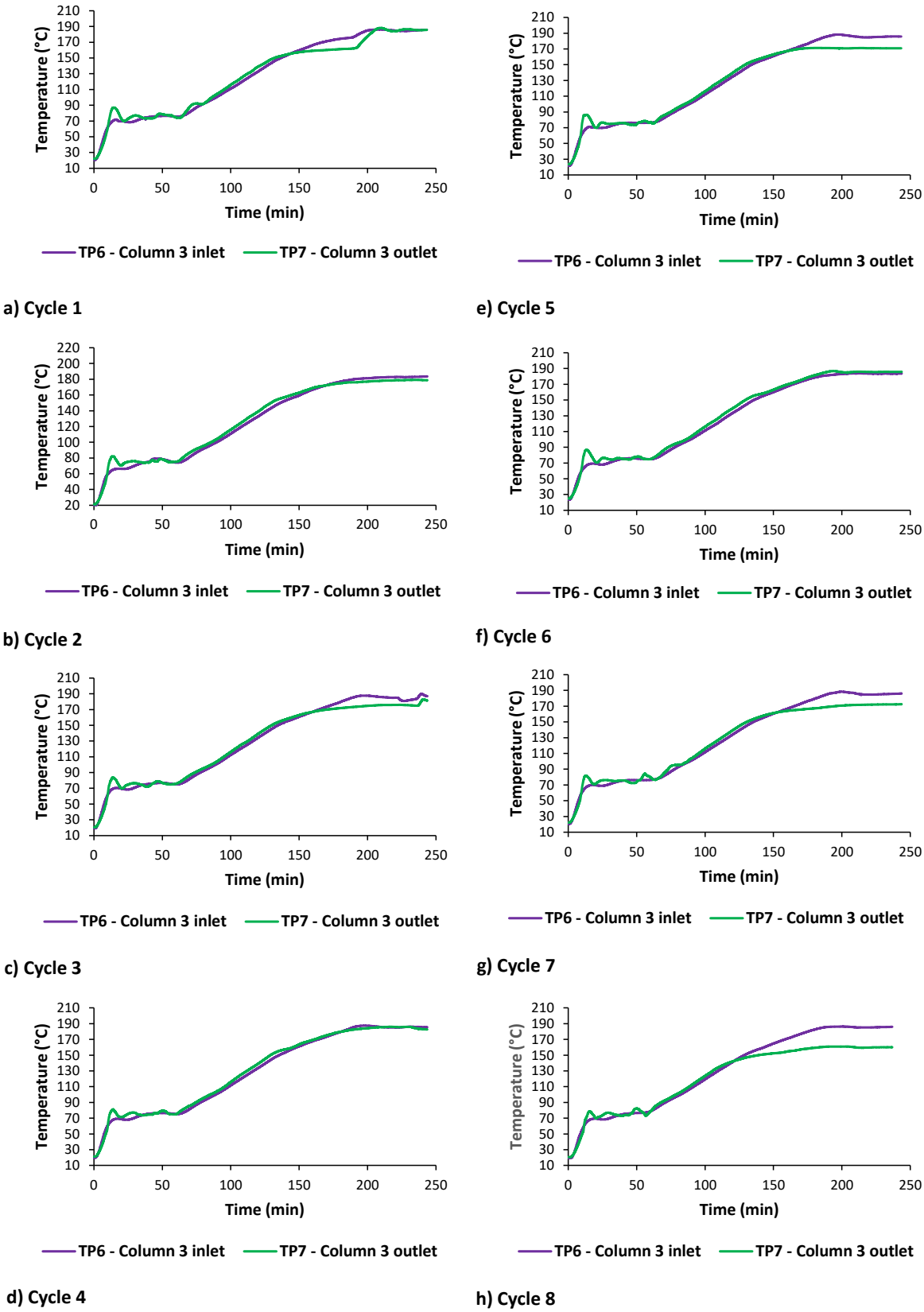

Figure 6-10: Activated alumina F-220 adsorbent temperature profiles for all 8 regeneration cycles at a regeneration temperature of 185 °C

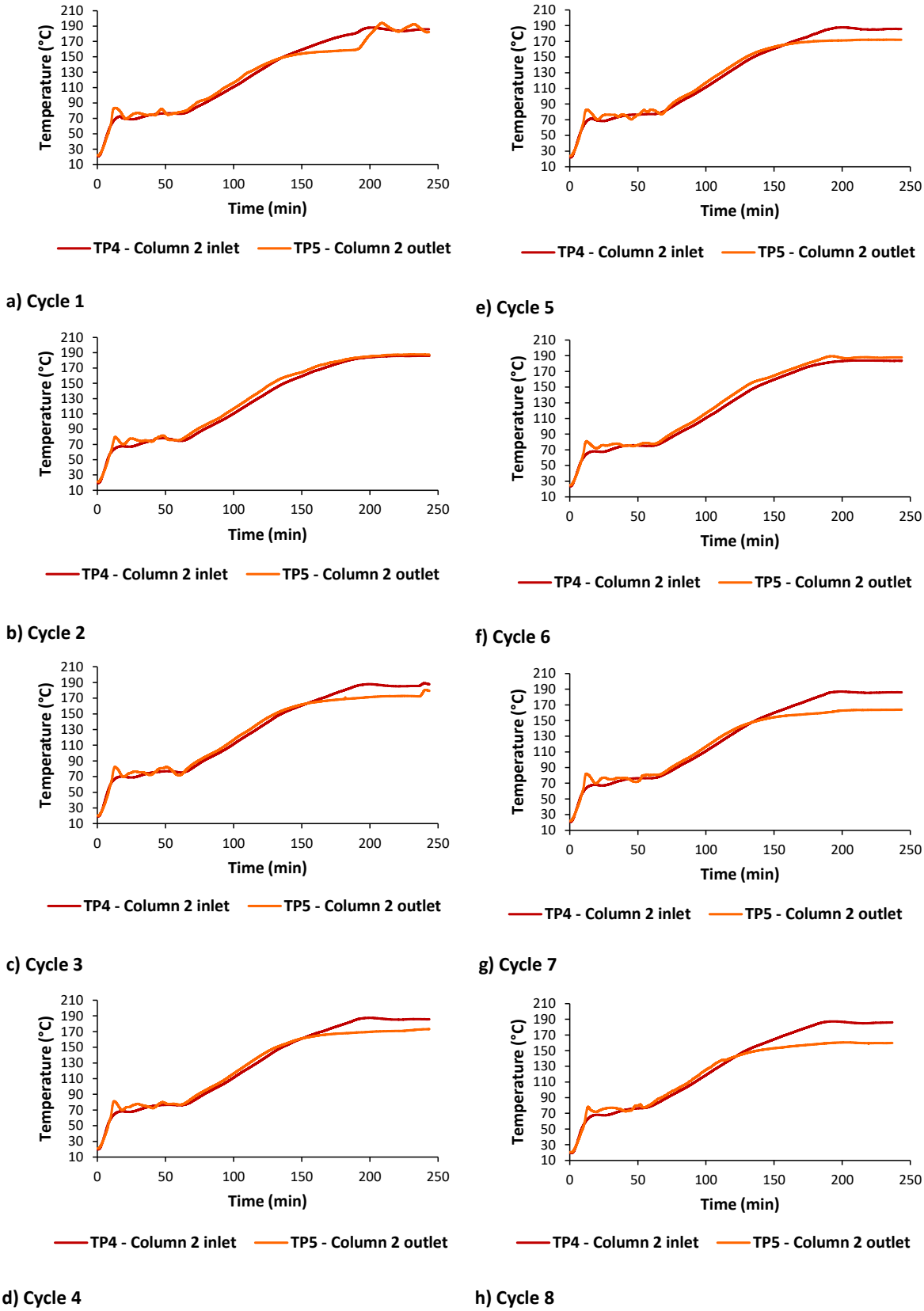

Figure 6-11: Selexsorb® CD adsorbent temperature profiles for all 8 regeneration cycles at a regeneration temperature of 185 °C

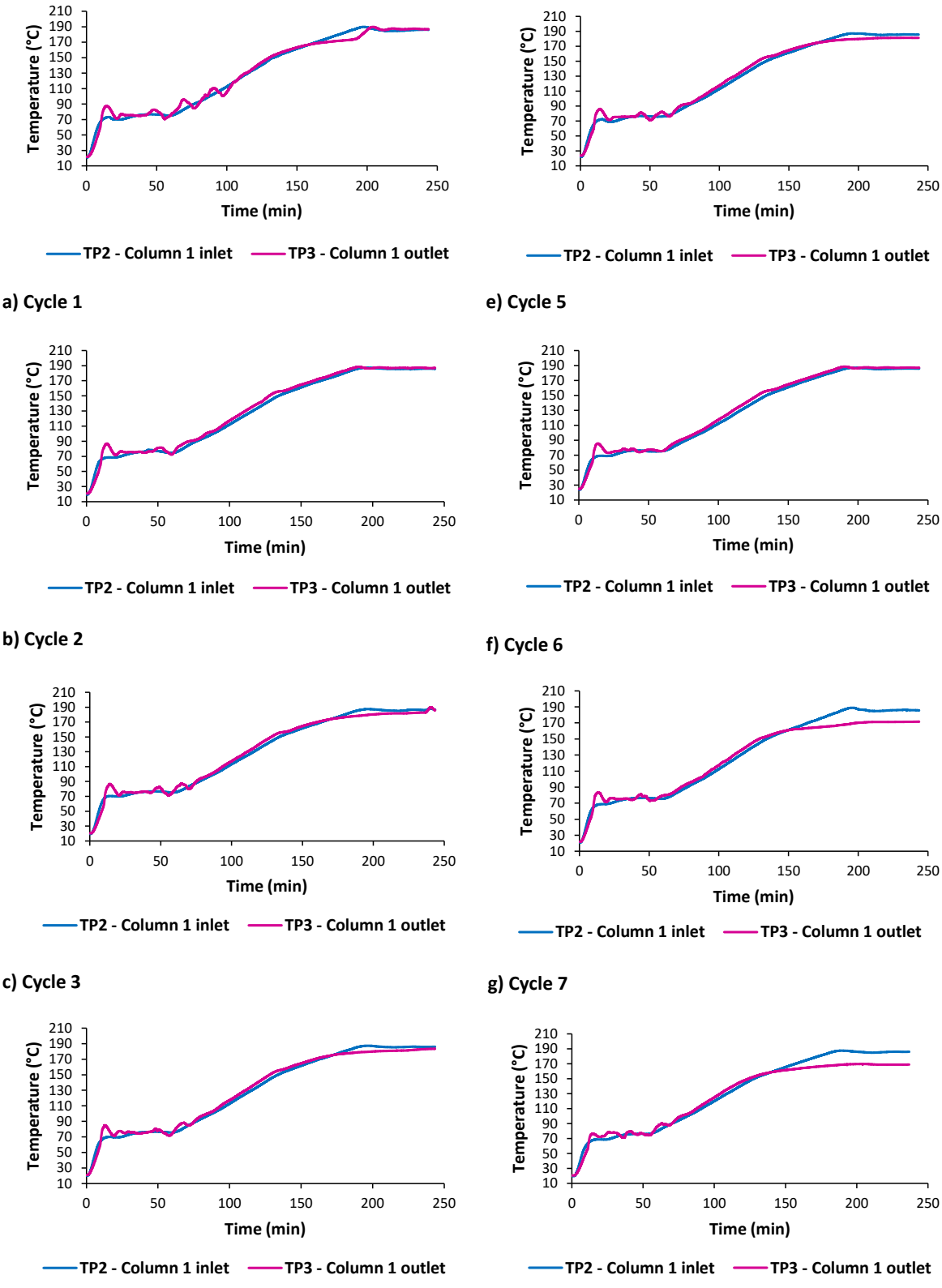

Figure 6-12: Selexsorb® CDx adsorbent temperature profiles for all 8 regeneration cycles at a regeneration temperature of 185 °C

6.4.2. 205 °C regeneration temperature results

Figure 6-13, Figure 6-14 and Figure 6-15 show the alcohol removal efficiency, the equilibrium adsorbent loading and the adsorbent mass for each cycle respectively.

The percentage of alcohol removed from solution data in Figure 6-13, shows a bit more scatter than was seen in the data at 185 °C. Adsorbent SCD and F-220 show the same general trend, with significant decreases only occurring at cycle 7. The SCDx adsorbent, however, shows unusual behaviour with significant initial increases in removal efficiency in cycles 2 and 3 and then slowly decreasing from there. These same trends can be seen in the equilibrium adsorbent loadings in Figure 6-14.

Overall the SCD adsorbent shows a decrease in removal efficiency of 13,5 %, while SCDx and F-220 show a decrease of 12,3 %.

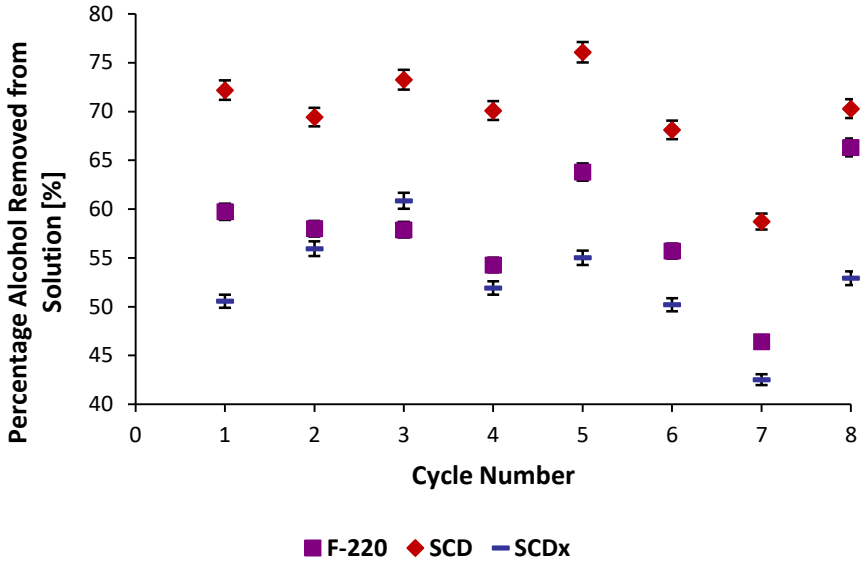

Figure 6-13: The percentage of total alcohol removed from the adsorption solution for each adsorbent type (F-220, SCD and SCDx) after each adsorption cycle in the 205 °C regeneration runs

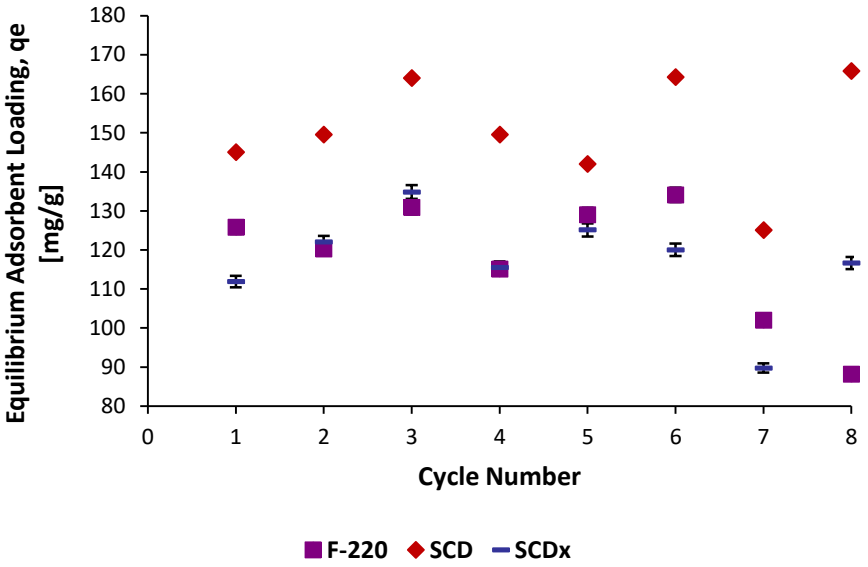

Figure 6-14: The equilibrium adsorbent loading for adsorbents F-220, SCD and SCDx after each adsorption cycle for the 205 °C regeneration runs

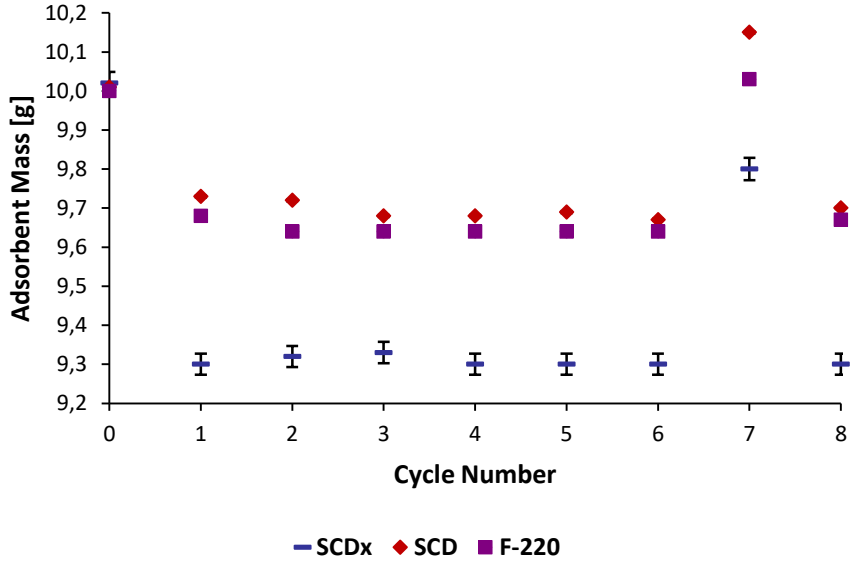

Figure 6-15: The mass of adsorbent before each adsorption cycle for adsorbents F-220, SCD and SCDx for the 205 C regeneration runs

The initial decrease in adsorbent mass seen in Figure 6-15 above is again due to the initial regeneration cycle cleaning the adsorbents. The adsorbent masses then stay relatively constant across the next 6 cycles. The increase in adsorbent mass before adsorption 7 was due to unforeseen circumstances that led to a time delay between cycles 6 and 7. Again the adsorbents were kept in the column inserts in a closed container and in this time the adsorbents may have adsorbed molecules from its surrounding environment.

Figure 6-16, Figure 6-18 and Figure 6-17 show the temperature profiles for adsorbents F-220, SCD and SCDx respectively for each of their 7 cycles. It is noted that the temperature data for cycle 8 was unfortunately corrupted due to an unexpected power failure during the regeneration cycle.

Once again in some cycles, for some of the adsorbents, plateaus are seen in the column outlet temperatures. These are also related to the desorbing and vapourising of the adsorbate molecules.

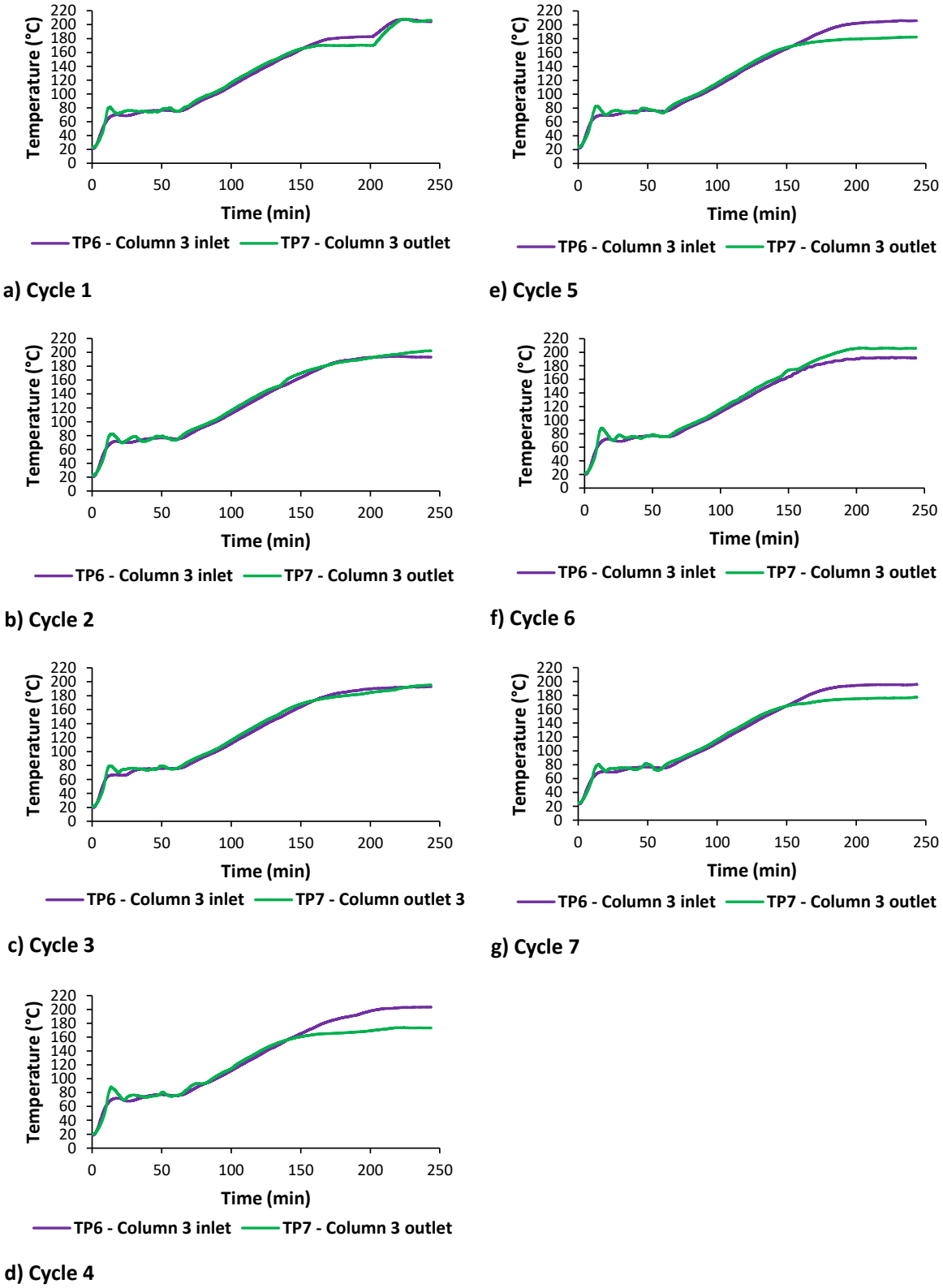

Figure 6-16: Activated alumina F-220 adsorbent temperature profiles for all 8 regeneration cycles at a regeneration temperature of 205 °C

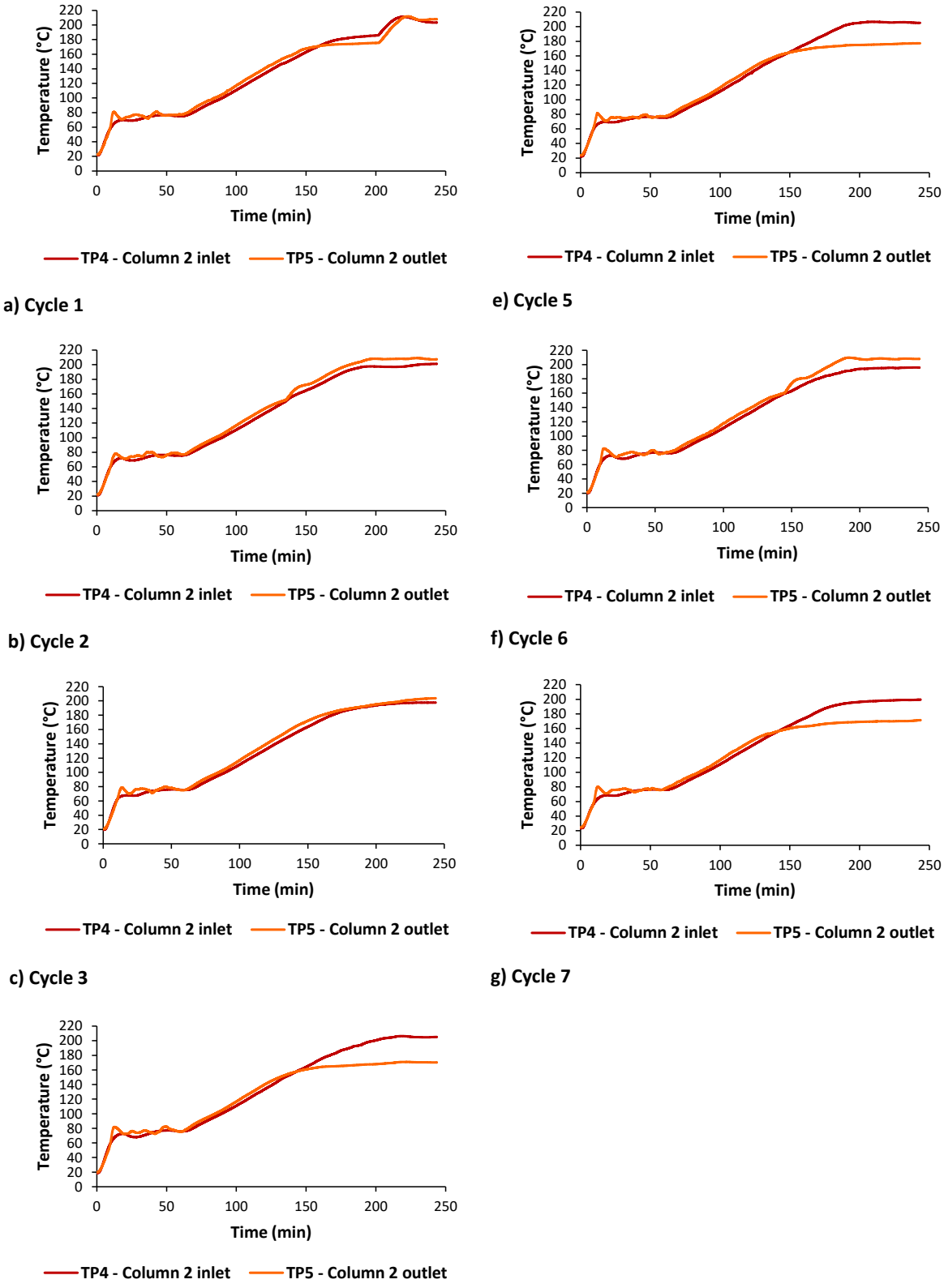

Figure 6-17: Selexsorb® CD adsorbent temperature profiles for all 8 regeneration cycles at a regeneration temperature of 205 °C

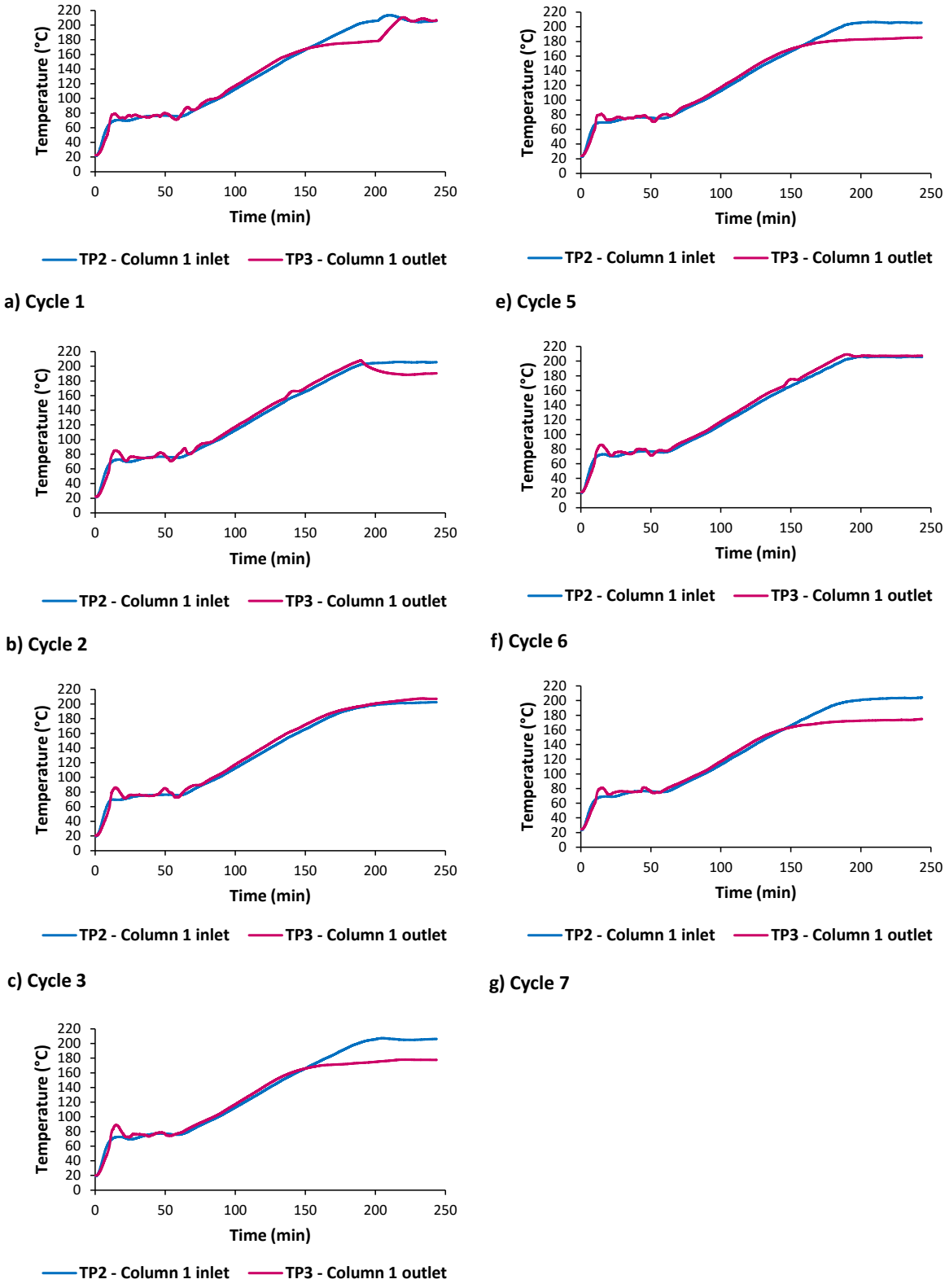

Figure 6-18: Selexsorb® CD adsorbent temperature profiles for all 8 regeneration cycles at a regeneration temperature of 205 °C

6.5 Regeneration Comparisons and Conclusions

The activated alumina F-220 adsorbent shows the lowest decline in alcohol removal efficiency at a regeneration temperature of 185 °C and 205 °C. The Selexsorb® CD adsorbent shows the highest decline in removal efficiency at both regeneration temperature, but it also has the highest initial removal efficiency, still making it outperform the other two adsorbents. The Selexsorb® CDx adsorbents shows the poorest performance overall, even though initially it shows increases in alcohol removal efficiency, overall it still under performs.

The regeneration process at 185 °C results in higher declines in alcohol removal efficiencies for all three adsorbents (between 18 and 24 %). While at 205 °C, the regeneration process over 8 cycles only results in an overall efficiency decrease of between 12 and 13 %. It is therefore speculated that at 185 °C not all the adsorbate molecules are being removed from the adsorbents.

All three adsorbents seem to be thermally stable at both regeneration temperatures and both regeneration processes performed well. The regeneration equipment developed was able to successfully regenerate three activated alumina adsorbents loaded with the 1-hexanol adsorbate and produce outlet temperature profiles which in future work, and in more complex systems, could give a better indication of when what adsorbate is desorbing.

Scanning electron microscopy imaging of the adsorbents is also recommended to be performed in future work to give a visual indication of whether each adsorbent's surface is altered by the application of several heat cycles. This should aid in explaining and verifying the decline in adsorption capacity seen over time.

Chapter 7: Conclusions and Recommendations

7.1 Conclusions

The overarching aim of this project was to investigate the adsorption of alcohol solutes (1-hexanol, 1-octanol and 1-decanol) from an alkane solvent (*n*-decane) using three industrially used adsorbents (activated alumina F-220, Selexsorb® CD and Selexsorb® CDx) and to test the regeneration effects on these adsorbents. This was achieved through completing the following objectives.

1. Design and develop batch adsorption and regeneration experimental setups

A heated water bath design was used for the batch adsorption experimental setup. The bath included a specifically designed lid that allowed the continuous sampling of solutions during all adsorption runs and held mesh baskets, containing the adsorbents, in place submerging the adsorbents in the solutions without the need for further filtration and processing after an adsorption cycle.

A column temperature regeneration process was designed and developed. The setup included three regeneration columns which used inlet and outlet Pt-100 temperature probes to control the electric heat tracing around the inlet tubing and columns. Nitrogen purge gas was used to carry the desorbed materials out of the adsorbent beds and a condenser was subsequently used to cool the gas and condense the organics. A liquid and activated carbon trap followed the condenser to clean the nitrogen gas before it was expelled to the environment.

2. Adsorbent characterisation

The three alumina based adsorbents (Activated Alumina F-220, Selexsorb® CD and Selexsorb® CDx) used in this study were characterised using Nitrogen adsorption-desorption tests at 77,35 K. The adsorption-desorption isotherms for each adsorbent showed type IV isotherm behaviour with F-220 showing an H2 hysteresis and SCD and SCDx a H3 hysteresis according to the IUPAC isotherm classification (Sing, et al., 1982). Based on further pore analysis using the DFT model, it was found that the two Selexsorb® adsorbents had higher microporous volumes compared to that of F-220. SCDx presented with the largest BET surface area and F-220 had the largest external surface area. The BET surface areas of each adsorbent compared well with those specified by BASF.

Each adsorbent was classified as a mesoporous adsorbent and therefore was deemed a viable adsorbent in the application of removing the 1-hexanol, 1-octanol and 1-decanol alcohols from the *n*-decane solutions investigated.

3. The effect of type of adsorbent, temperature and type of adsorbate on the adsorption process

Adsorption tests were performed using the three alumina based adsorbents characterised, three types of alcohol adsorbates with carbon numbers of 6, 8 and 10 and at three adsorption temperatures (25, 30 and 35 °C).

The three adsorbents tested were activated alumina F-220, Selexsorb® CD and Selexsorb® CDx. The two Selexsorb® adsorbents formed part of a BASF range of adsorbents modified to enhance their organic molecule adsorption capabilities and were tested against a fairly generic activated alumina adsorbent. All three adsorbents were able to remove the adsorbate molecules from the *n*-decane solvent to some extent, at all the adsorption temperatures investigated. However, the activated alumina F-220 adsorbent appeared to offer the best adsorption performance with regards to these systems, showing higher equilibrium adsorbent loadings than that of the two Selexsorb® adsorbents. These results were attributed to the larger external surface area seen in the F-220 adsorbent's characterisation compared to that of adsorbents SCD and SCDx. With the F-220 adsorbent offering adsorbate molecules more easily accessible (less energy intensive diffusion mechanisms required) active sites, it is not surprising that the F-220 adsorbent was able to adsorb more of each adsorbate at the temperatures investigated in this work.

The effect of temperature was investigated and it was found that these adsorption systems preferred the slightly higher adsorption temperatures. Adsorption is generally considered an exothermic process therefore favouring lower system temperatures. However, the quantification of 'lower' was found to be relative to each specific adsorption system, with numerous examples given from literature where some systems showed greater adsorption at 25 ^{o}C and others at 70 ^{o}C (Mor, et al., 2007), (Vijayakumar, et al., 2012), (Iqbal & Ashiq, 2007) and (Knozinger & Stubner, 1978). With the adsorbents presenting with significant porous areas, the energy supplied to these systems by slightly higher system temperatures, aided in the diffusion of the molecules to the meso- and micropores. These systems were therefore found to give better adsorption performance at the higher adsorption temperature of 35 ^{o}C.

Three alcohol adsorbates were used in this study (1-hexanol, 1-octanol and 1-decanol). All three adsorbates showed an affinity for each adsorbent with significant adsorbent loading values (ranging

between 50 and 140 mg/g) being seen at all three temperatures. Generally, the 1-hexanol adsorbate showed the greater adsorbent loadings overall. All three adsorbents also presented with microporous areas having an average pore width of 10,88 Å, 8,48 Å and 7,97 Å for adsorbent F-220, SCD and SCDx respectively. The size of each alcohol was found to be 11,18 Å, 14,26 Å and 17,34 Å for 1-hexanol, 1-octanol and 1-decanol respectively. It was apparent, when comparing the adsorbate molecule size and the average micropore size of each adsorbent, that each type of adsorbate would be hindered from most of the microporous areas present in these adsorbents due to their size.

4. Equilibrium and kinetic modelling of adsorption data

The equilibrium modelling involved applying 3 models to the 27 adsorption equilibrium systems investigated in this project. From the modelling data of the Langmuir and Freundlich models, all the adsorption systems were found to show favourable adsorption behaviour and were indicative of physisorption processes occurring. The mean free energy, calculated from the Dubinin-Radushkevich model constant, confirmed the Freundlich model findings, with $E < 8$ kJ/mol for all adsorption systems. The maximum adsorption capacity trends of each adsorbate across the three types of adsorbents confirmed what was seen in the adsorption results comparisons made, showing that the activated alumina F-220 adsorbent provided better adsorption results than the other two adsorbents.

The best fit model for each adsorption system provids insight into the mechanism involved in each system ranging from a monolayer or multilayer mechanism to a pore-filling mechanism. It is however recommended that more initial alcohol concentrations be investigated for each adsorption system in order to add data points to the isotherm being modelled, thus reducing the uncertainty in the modelling.

The kinetic modelling involved applying 3 models to the 81 kinetic adsorption systems investigated in this project. These models gave indications of the rate-controlling steps within each adsorption process. Based on the parameters of each model, no individual step in the movement of adsorbate molecule from bulk solution to adsorption site was solely responsible for controlling the adsorption rate, but rather a combination of these diffusion and adsorption reaction steps controlled the rate of each adsorption process investigated.

Most of the kinetic adsorption systems were diffusion rate controlled, while a few showed that the physical adsorption reaction step controlled the rate of their adsorption process. Generally the rate constants obtained showed increases with increases in temperature and concentration. Based on an increase in concentration causing an increase in gradient between the bulk solution and the adsorbent surface, the increase in rate constants was explained by the larger gradient forcing molecules to

diffuse faster between the bulk solution and the adsorbent surface. An increase in temperature causes molecules to become more energetic allowing them to diffuse faster, thus increasing the rate constant obtained in the modelling of the systems.

5. Cyclic adsorption-regeneration tests

The regeneration process was tested on 3 adsorption systems each using a different adsorbent. The adsorption process involved removing 1-hexanol from *n*-decane adsorbed at a temperature of 35°C for adsorbents activated alumina F-220, Selexsorb® CD and Selexsorb® CDx. Each adsorbent was then regenerated at a temperature of 185 or 205 °C. For each adsorption-regeneration system 8 cycles were performed.

All three adsorbents showed thermal stability and the activated alumina F-220 adsorbent showed the lowest decrease in alcohol removal efficiency for both regeneration temperatures. The regeneration results showed the effectiveness of the equipment developed in restoring the adsorbent's capacity after several adsorption cycles. Each adsorbent's capacity was restored for at least four adsorption-regeneration cycles.

The regeneration process occurring at 185 °C showed higher removal efficiencies for each adsorbent overall, but a greater decline in these efficiencies was seen over the 8 cycles. The 205 °C regeneration process showed slightly lower alcohol removal efficiencies, however the overall decrease in each adsorbent's removal efficiency was less than at 185 °C. Reasons for the decline in adsorbent capacity over cycles and the difference in capacity decline at the two regeneration temperatures could not be cemented based on these results alone. It is therefore recommended that in future studies, scanning electron microscopic imaging of the adsorbents be done so give an indication of whether the adsorbent surface is in any way being altered by the periods of intense heat supplied during regeneration.

7.2 Future Work Recommendations

Based on the results found in this project, the following recommendations for future work are made:

1. It would be beneficial to study the adsorption systems in a larger initial alcohol mass percent range ($0 < x < 5$, %)in order to cement the adsorption isotherm predictions for each system.

2. Building upon this research, slightly higher adsorption temperatures should be investigated, namely 40 and 60 ^{o}C, in order to find the optimum adsorption temperature.

3. Binary adsorption systems should be investigated to determine the interactions between adsorbate molecules and how it affects the adsorption of each, i.e. 1-hexanol – 1-octanol in *n*-decane, 1-hexanol – 1-decanol in *n*-decane, 1-octanol – 1-decanol in *n*-decane.

4. More adsorption-regeneration cycle experiments should be investigated to perfect the method and the number of cycles performed should be increased (12 cycles). Building upon that, factors such as regeneration duration (30 min and 120 min) and purge gas flowrate can also be investigated to test its influence on the regeneration process. Do scanning electron microscopic imaging of adsorbents tested before and after several adsorption-regeneration cycles.

References

Ayawei, N., Ebelegi, A. N. & Wankasi, D., 2017. Modelling and Interpretation of Adsorption Isotherms. *Hindawi Journal of Chemistry,* pp. 1-11.

BASF, 2009. *F-220, Activated Alumina for Liquid and Gas Drying: data sheet.* s.l.:s.n.

BASF, 2009. *Selexsorb CD, Smooth spherical adsorbent for the removal of polar compounds: data sheet.* s.l.:s.n.

BASF, 2009. *Selexsorb CDx, Alumina-based spherical adsorbent for the removal of polar compounds: data sheet.* s.l.:s.n.

Basmadjian, D., 1997. *The Little Adsorption Book: A practical guide for engineers and scientists.* Florida: CRC Press.

Beheera, S. K., Kim, J.-H., Guo, X. & Park, H.-S., 2008. Adsorption equilibrium and kinetics of polyvinyl alcohol from aqueous solution on powdered activated carbon. *Journal of Hazardous Materials,* Volume 153, pp. 1207 - 1214.

Cai, S. & Sohlberg, K., 2003. Adsorption of alcohols on gamma-alumina (1 1 0 C). *Journal of Molecular Catalysis A: Chemical,* Volume 193, pp. 157 - 164.

Carlson, G. A., 2000. *Experimental Error and Uncertainty.* University of Rochester: Department of Electrical and Computer Science.

Cavalcante Jr., C. L., 2000. Industrial adsorption separation processes: Fundamentals, modeling and applications. *Latin American Applied Research,* Volume 30, pp. 357-364.

Chen, X., 2015. Modeling of Experimental Adsorption Isotherm Data. *Information,* Volume 6, pp. 14-22.

Chiou, C. T., 2002. Fundamentals of the Adsorption Theory. In: *Partition and Adsorption of Organic Contaminants in Environmental Systems.* s.l.:John Wiley and Sons, Inc., pp. 39-52.

Daems, I. et al., 2007. Molecular Cage Nestling in the Liquid-Phase Adsorption of n-Alkanes in 5A Zeolites. *The Journal of Physical Chemistry C,* Volume 111, pp. 2191-2197.

Desta, M. B., 2013. Batch Sorption Experiments: Langmuir and Freundlich Isotherm Studies for the Adsorption of Textile Metal Ions onto Teff Straw Agricultural Waste. *Hindawi Journal of Thermodynamics,* pp. 1-6.

Diaz, E., Ordonez, S., Vega, A. & Coca, J., 2004. Adsorption characterisation of different volatile organic compounds over alumina, zeolites and activated carbon using inverse gas chromatography. *Journal of Chromatography A,* Volume 1049, pp. 139 - 146.

Ezeh, K. et al., 2017. Utilising the Sorption Capacity of Local Nigerian Sawdust for Attenuation of Heavy Metals from Solution:Isotherm, Kinetic, and Thermodynamic Investigations. *The Pacific Journal of Science and Technology,* 18(1), pp. 251-264.

Foo, K. & Hameed, B., 2010. Insights into the modeling of adsorption isotherm systems. *Chemical Engineering Journal,* Volume 156, pp. 2-10.

Ghorai, S. & Pant, K. K., 2005. Equlibrium, kinetics and breakthrough studies for adsorption of flouride on activated alumina. *Separation and Purification Technology,* Volume 42, pp. 265-271.

Grace-Martin, K., 2008. *Assessing the Fit of Regression Models.* [Online]
Available at: https://www.theanalysisfactor.com/assessing-the-fit-of-regression-models/
[Accessed August 2018].

Green, D. W. & Perry, R. H., 2008. *Perry's Chemical Engineers' Handbook.* 8th ed. New York: McGraw-Hill.

Iqbal, M. J. & Ashiq, M. N., 2007. Adsorption of dyes from aqueous solutions on activated charcoal. *Jounral of Hazardous Materials,* Volume 139, pp. 57-66.

Knozinger, H. & Stubner, B., 1978. Adsorption of alcohols on alumina. 1. Gravimetric and infrared spectroscopic investigation. *The Journal of Physical Chemistry,* 82(13), pp. 1526-1532.

Kvalseth, T. O., 1985. Cautionary Note About R^2. *The American Statistician,* 39(4), pp. 279-285.

Laredo, G. C. et al., 2016. Comparison of the metal–organic framework MIL-101 (Cr) versus four commercial adsorbents for nitrogen compounds removal in diesel feedstocks. *Fuel,* Volume 180, pp. 284 - 291.

Largitte, L. & Pasquier, R., 2016. A review of the kinetics adsorption models and their application to the adsorption of lead by an activated carbon. *Chemical Engineering Research and Design,* Volume 109, pp. 495-504.

Lashaki, M. J. et al., 2012. Effect of Adsorption and Regeneration Temperature on Irreversible Adsorption of Organic Vapors on Beaded Activated Carbon. *Environmental Science and Technology,* Volume 46, pp. 4083-4090.

Mahramanlioglu, M., Kizilcikli, I. & Bicer, I. O., 2002. Adsorption of flouride from aqueous solution by acid treated spent bleaching earth. *Journal of Flourine Chemistry,* Volume 115, pp. 41-47.

Marczewski, A. W., 2002. *Adsorption.org.* [Online]
Available at: http://adsorption.org/awm/ads/Het-src.htm
[Accessed June 2018].

Martin, R. J. & No, W. J., 1987. The repeated exhaustion and chemical regeneration of activated carbon. *Water Research Journal,* 21(8), pp. 961 - 965.

Moreno-Castilla, C., 2004. Adsorption of organic molecules from aqueous solutions on carbon materials. *Carbon,* Volume 42, pp. 83 - 94.

Mor, S., Ravindra, K. & Bishnoi, N. R., 2007. Adsorption of chromium from aqueous solution by activated alumina and activated charcoal. *Bioresource Technology,* Volume 98, pp. 954-957.

Muzic, M., Sertic-Bionda, K. & Adzamic, T., 2012. Evaluation of commercial adsorbents and their application for desulfurization of model fuel. *Clean Technologies Evnironmental Policy,* Volume 14, pp. 283 - 290.

National Research Council, 1998. *Separation Technologies for Industries of the Future.* Washington, DC: The National Academies Press.

Oguz, E. & Keskinler, B., 2005. Determination of adsorption capacity and thermodynamic parameters of the PAC used for bomaplex red CR-L dye removal. *Colloids and Surfaces A,* Volume 268, pp. 124-130.

Ozacar, M., Sengil, I. A. & Turkmenler, H., 2008. Equilibrium and kinetic data, and adsorption mechanism for adsorption of lead onto valonia tannin resin. *Chemical Engineering Journal,* Volume 143, pp. 32-42.

Ozkaya, B., 2006. Adsorption and desorption of phenol on activated carbon and a comparison of isotherm models. *Journal of Hazardous Materias,* Volume 129, pp. 158-163.

Pak, S.-H. & Jeon, Y.-W., 2016. Effect of vacuum regeneration of activated carbon on volatile organic compound adsorption. *Environmental Engineering Research,* 22(2), pp. 169 - 174.

Polaert, I., Estel, L., Huyghe, R. & Thomas, M., 2010. Adsorbents regeneration under microwave irradiation for dehydration and volatile organic compounds gas treatment. *Chemical Engineering Journal,* Volume 162, pp. 941 - 948.

QIU, H. et al., 2009. Critical review in adsorption kinetic models. *Journal of Zhejiang University Science A,* 10(5), pp. 716-724.

Qureshi, N., Hughes, S., Maddox, I. S. & Cotta, M. A., 2005. Energy-efficient recovery of butanol from model solutions. *Bioprocess and Biosystems Engineering,* Volume 27, pp. 215 - 222.

Ramaswamy, S., Huang, H.-J. & Ramarao, B. V., 2013. *Separation and Purification Technologies in Biorefineries.* 1st ed. United Kingdom: John Wiley and Sons, Ltd.

Rauthula, M. S. & Srivastava, V. C., 2011. Studies on adsorption/desorption of nitrobenzene and humic acid onto/from activated carbon. *Chemical Engineering Journal,* Volume 168, pp. 35-43.

Rockmann, R. & Kalies, G., 2007. Liquid adsorption of n-octane/octanol/ethanol on SBA-16 silica. *Journal of Colloid and Interface Science,* Volume 315, pp. 1 - 7.

Ruthven, D. M., 1984. *Principles of Adsorption and Adsorption Processes.* New York: John Wiley & Sons, Inc..

Saha, P. & Chowdhury, S., 2011. Insight Into Adsorption Thermodynamics. In: P. M. Tadashi, ed. *Thermodynamics.* Croatia: InTech, pp. 349 - 364.

Scholtz, J., 26 Oct 2016. *Personal Communication.* s.l.:s.n.

Seader, J. D., Henley, E. J. & Roper, D. K., 2011. *Separation Process Principles: chemical and biochemical operations.* 3rd ed. New Jersey: John Wiley & Sons, Inc..

Serbezov, A., Moore, J. D. & Wu, Y., 2011. Adsorption equilibrium of water vapour on Selexsorb-CDX commercial activated alumina adsorbent. *Journal of Chemical and Engineering Data,* Volume 56, pp. 1762-1769.

Simonin, J.-P., 2016. On the comparison of pseudo-first order and pseudo-second order rate laws in the modeling of adsorption kinetics. *Chemical Engineering Journal,* Volume 300, pp. 254-263.

Singh, T. S. & Pant, K. K., 2004. Equilibrium, kinetics and thermodynamic studies for adsorption of AS(III) on activated alumina. *Separation and Purification Technology,* Volume 36, pp. 139-147.

Sing, K. S. et al., 1982. Reporting physisorption data for gas/solid systems. *International Union of Pure and Applied Chemistry,* 54(11), pp. 2201-2218.

Suzuki, M., 1990. *Adsorption Engineering.* Tokyo: Kodansha Ltd..

Tan, K. & Hameed, B., 2017. Insight into the adsorption kinetics models for the removal of contaminants from aqueous solutions. *Journal of the Taiwan Institute of Chemical Engineers,* Volume 74, pp. 25-48.

Tosun, I., 2012. Ammonium Removal from Aqueous Solutions by Clinoptilolite: Determination of Isotherm and Thermodynamic Parameters and Comparison of Kinetics by the Double Exponential Model and Conventional Kinetic Models. *Internation Journal of Environmental Research and Public Health,* Volume 9, pp. 970-984.

Turton, R. et al., 2013. *Analysis, Synthesis, and Design of Chemical Processes.* 4th ed. New Jersey: Pearson Education.

Vijayakumar, G., Tamilarasan, R. & Dharmendirakumar, M., 2012. Adsorption, Kinetic, Equilibrium and Thermodynamic studies on the removal of basic dye Rhodamine-B from aqueous solution by the use of natural adsorbent perlite. *Journal of Materials and Environmental Science,* 3(1), pp. 157-170.

Yang, R. T., 2003. *Adsorbents: Fundamentals and Applications.* New Jersey: John Wiley & Sons, Inc..

Chapter 8: Appendices

8.1 Water Bath Lid and Hold Plate Drawings

Figure 8-1 and Figure 8-2 show the water bath and hold plate drawings for the adsorption experimental setup.

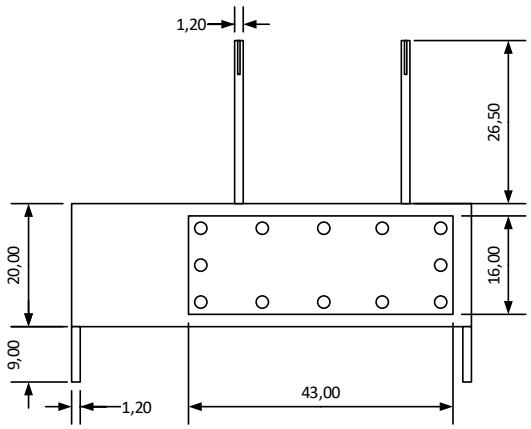

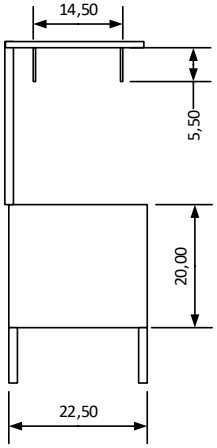

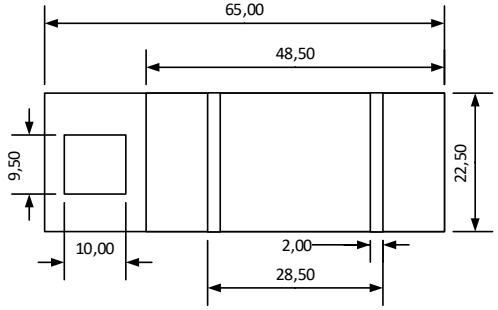

Figure 8-1: Adsorption water bath detailed drawing

PARTS LIST		
Qty	Dimensions	Description
1	430 x 160 mm	Plastic window in the wall of the water bath
12	6 mm nuts and bolts	6 mm nuts and bolts used to fasten the window to the water bath
4	12 x 9 mm SS rods	Stainless Steel rods used as support legs for the water bath
2	12 x 265 mm SS rods	Stainless Steel rods used as supports to hold the bath lid
2	225 x 20 x 2,5 mm SS plate	Stainless Steel plates with hooks holding the water bath lid
Scale 10:1 Units mm	Title: Adsorption Water Bath	Rev no. 001

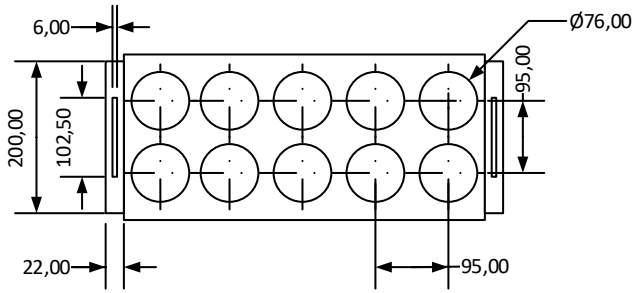

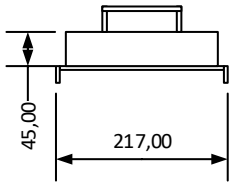

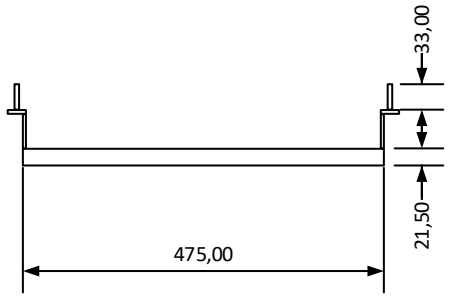

PARTS LIST		
Qty	Dimensions	Description
2	108 x 6 mm SS rod	Stainless steel rods used as handles to lift water bath hold lid

Scale 10:1 Units mm	Title: Water Bath Hold Plate	Rev no. 001

Figure 8-2: Water bath hold plate detailed drawing

8.2 Mesh Basket Drawing

Figure 8-3 gives the detailed drawing for the adsorbent mesh basket.

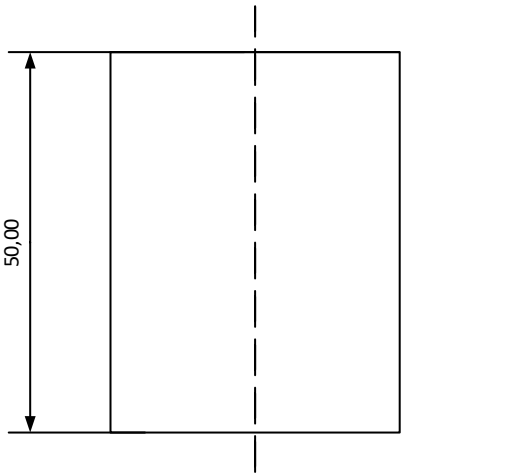

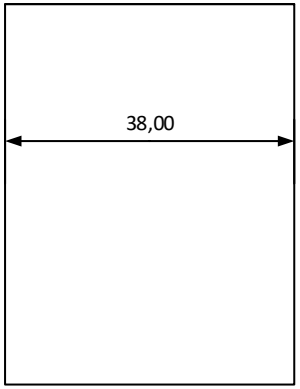

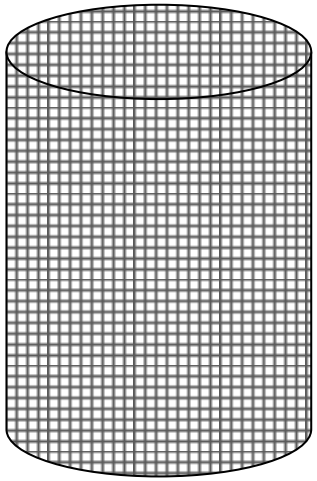

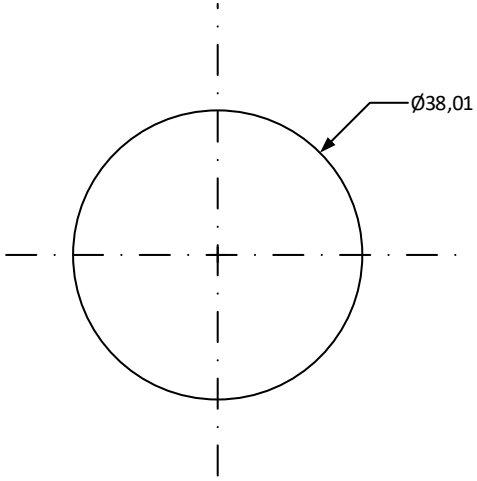

PARTS LIST		
Qty	Dimensions	Description
20 x single mesh basket unit	38 x 50 mm SS 2 mm mesh	2 mm rectangular stainless steel mesh pieces shaped into baskets

Scale 1:1 Units mm	Title: Adsorbent Mesh Basket	Rev no. 001

Figure 8-3: Adsorbent mesh basket drawing

8.3 Water Bath Lid

Figure 8-4 gives the detailed drawing for the water bath lid.

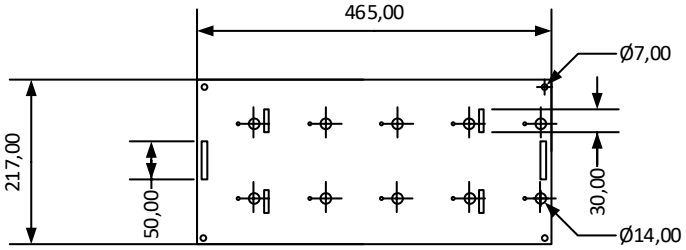

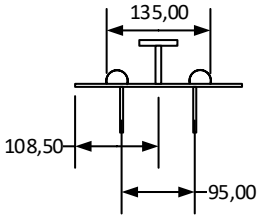

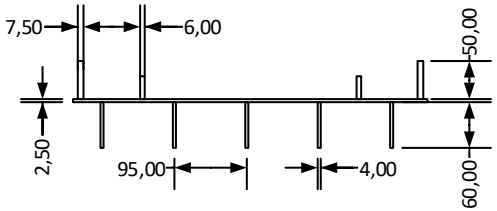

Figure 8-4: Water bath lid drawing

PARTS LIST		
Qty	Dimensions	Description
10	60 x 4 mm SS hooks	Hooks to hold the mesh basket in the centre of the beaker
4	6 mm SS loops	Loops to hook onto lid stand connect to water bath
2	50 x 7,5 mm SS rods	Rods to act as handles to lift and lower lid
2	50 x 7,5 mm SS rods	Rods as base for handles

Scale 10:1 Units mm	Title: Water Bath Lid	Rev no. 001

8.4 Process Flow Diagram (PFD)

The detailed PFD for the regeneration process experimental setup is shown below in Figure 8-5.

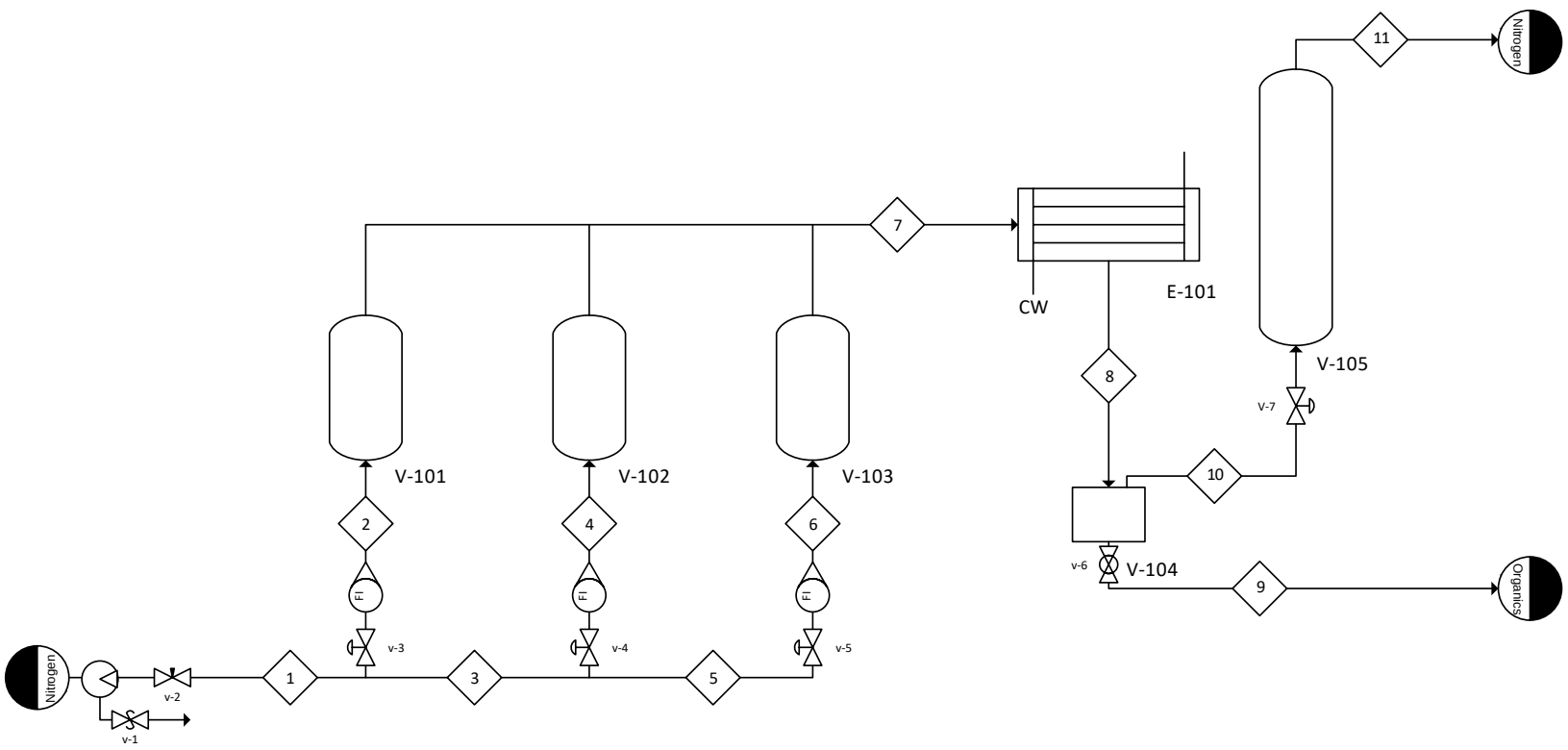

Figure 8-5: Regeneration setup process flow diagram

8.5 Regeneration columns and their parts

The equipment specification sheet is given below, a detailed drawing of the regeneration column is shown in Figure 8-6 and a drawing of the column inserts can be seen in Figure 8-7.

Regeneration Columns					
Equipment label	V-101		V-102	V-103	
Maximum Diameter	38,00	mm	Maximum Height	120,00	mm
Process Data					
Gas flow direction	Enters through the bottom of the column and flows out the top				
Operating temperature			205 / 180	°C	
Operating pressure			2,00	bar(abs)	
Gas mass flowrate			0.021	kg/h	
Calculated pressure drop			0,07	kPa	
Adsorbent bed height			20,00	mm	
Adsorbent particle size			3,20	mm	
Adsorbent bulk density			665 - 785	kg/m³	
Construction and Materials					
Column material			Stainless steel		
Column outer diameter			38,01	mm	
Column thickness			1,50	mm	
Column height			35,01	mm	
Top					
Flange material			Stainless steel		
Flange diameter			80,00	mm	
Flange thickness			8,00	mm	
Number of bolts			6		
Gasket material			Graphite		
Gasket thickness			3,00	mm	
Bottom					
Distributor type			¼” Dixon rings		
Distributor material			Stainless steel		
Maximum operating temperature			450	°C	
Maximum operating pressure			8	bar(abs)	

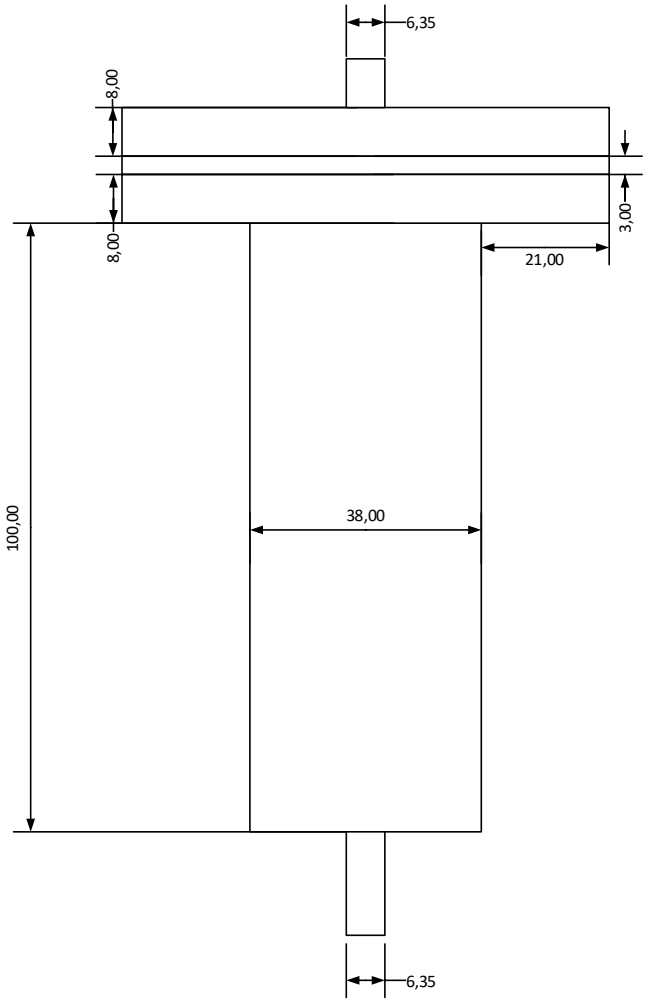

Top Flange:
80 mm OD
8 mm thickness
6 x 6 mm bolts on a PCD of 60 mm
Centre ¼" tube fitting (Outlet tube)
Off centre ¼" tube fitting (Temperature probe)

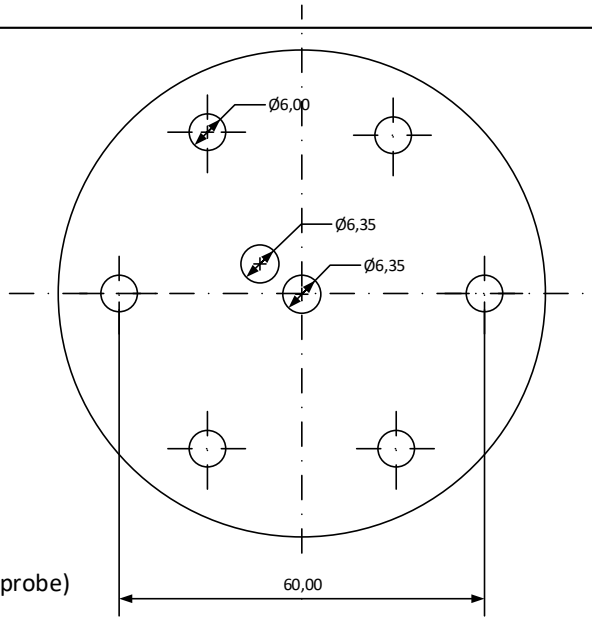

Bottom Flange:
80 mm OD
8 mm thickness
6 x 6 mm bolts on a PCD of 60 mm
35 mm centre hole

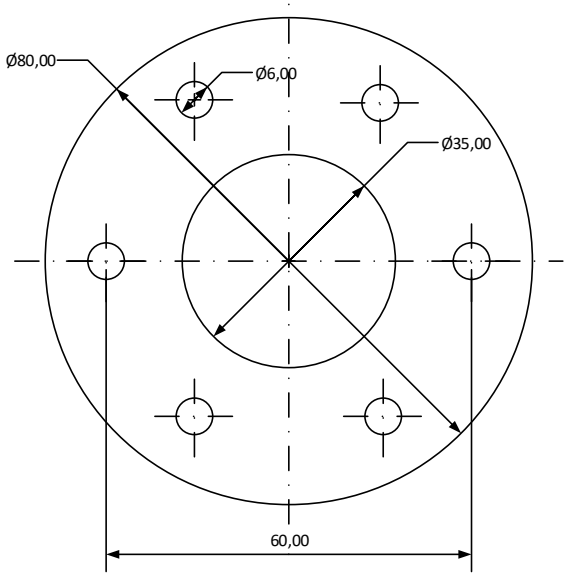

Figure 8-6: Regeneration column detailed drawing

Scale 1:1 Units mm	Title: Regeneration Column	Rev no. 001

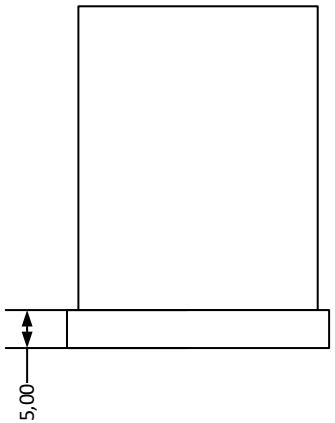

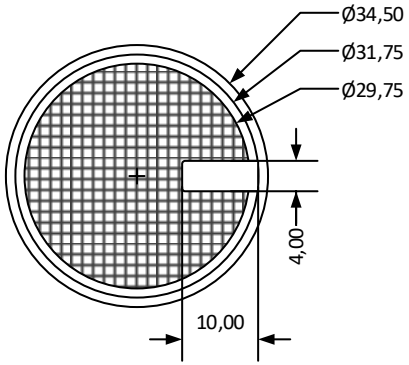

Figure 8-7: Column inserts detailed drawing

PARTS LIST		
Qty	Dimensions	Description
3	33 x 60 mm	Stainless steel tubing to hold the adsorbent within the column
3	2,50 mm SS mesh	Stainless steel mesh to act as a hold plate in the column insert
3	34,50 x 5 mm	Manufactured stainless steel rings to hold mesh plate

Scale 1:1 Units mm	Title: Column Insert for Adsorbent	Rev no. 001

8.6 Condenser Specifications and Drawing

The equipment specification sheet for the condenser in the regeneration process system is shown below and a detailed drawing is given in Figure 8-8.

Condenser					
Equipment label	E-101				
Maximum Diameter	130,00	mm	Maximum Height	335,00	mm
Process Data					
Counter flow condenser					
	Shell side		Tube side		
	In	Out	In	Out	
Process fluid	Water		Nitrogen gas carrying organic vapours		
[kg/h]					
Total fluid flow	0,55	0,55			
Total liquid flow	0,55	0,55	0		
Total vapour flow	0	0			
[°C]					
Inlet temperature	18	18	205	20	
[bar(abs)]					
Operating pressure	1,00		6,00		
Pressure drop [kPa]	negligible		4,88		
Number of passes	1		1		
Heat duty [kJ/h]	43,33				
Construction and Materials					
Tube					
Material	Copper				
Length	1 000,00		mm		
Outer diameter	6,35		mm		
Thickness	0,90		mm		
Spiral inner diameter	80,00		mm		
Shell					
Material	Stainless steel				
Length	295,00		mm		
Outer diameter	130,00		mm		
Thickness	2,50		mm		

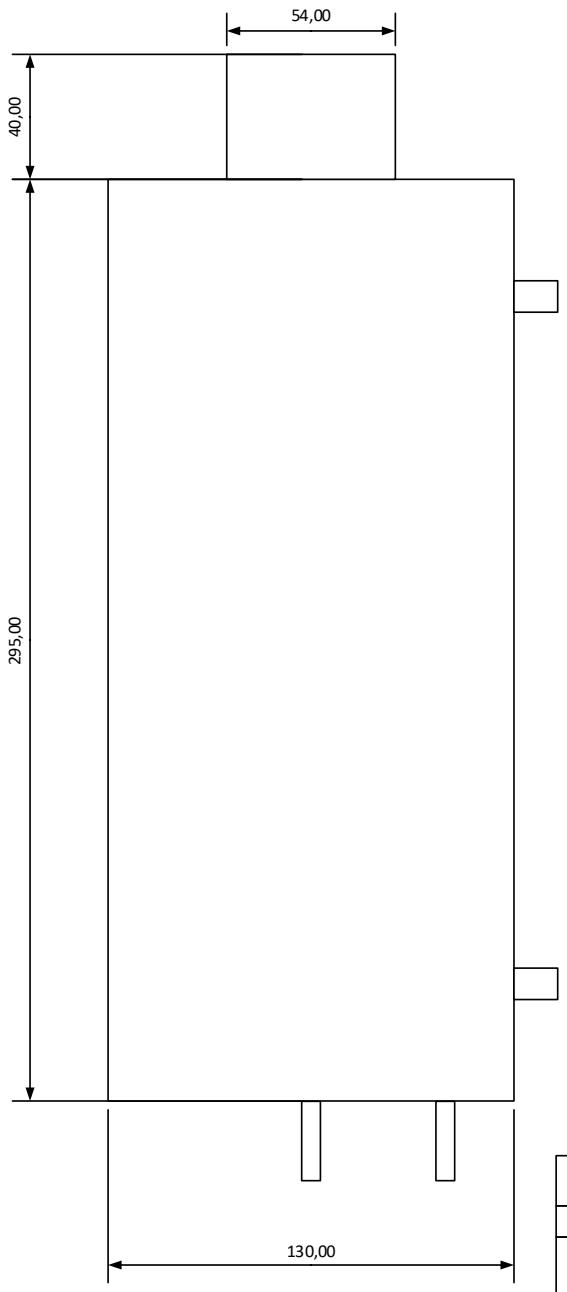

PARTS LIST		
Qty	Dimensions	Description
2	6,35 mm	2 ¼" outlets
2	8 mm	Cooling water inlet and outlet
1	40 x 54 mm	Water refill opening at the top of the condenser
1	6,35 x 1 000 mm	Spiral copper tubing carrying the nitrogen gas
Scale 2:1 Units mm	Title: Condenser	Rev no. 001

Figure 8-8: Condenser detailed drawing

8.7 Organics Trap Specifications and Drawing

The equipment specification sheet for the organics trap is shown below and the detailed drawing can be seen in Figure 8-9.

Organics Trap					
Equipment label	V-104				
Maximum Length	70,00	mm	Maximum Height	360,00	mm
Process Data					
Gas flow direction	Enters through the top of the trap, through the water and then out through the top corner				
Operating temperature			20,00	°C	
Operating pressure			5,950	bar(abs)	
Gas mass flowrate			0,062	kg/h	
Calculated pressure drop				kPa	
Liquid			Water		
Liquid volume			175,00	mL	
Liquid height			30,00	mm	
Construction and Materials					
Trap material			Stainless steel 316		
Trap length			100,00	mm	
Trap bredth			100,00	mm	
Trap height			55,00	mm	
Top					
Flange material			Perspex		
Flange dimensions			132,00 x 132,00	mm	
Flange thickness			11,50	mm	
Number of bolts			8		
Gasket material			Rubber		
Gasket thickness			1,00	mm	
Bottom					
Flange material			Stainless Steel 316		
Flange dimensions			132,00 x 132,00	mm	
Flange thickness			5,00	mm	

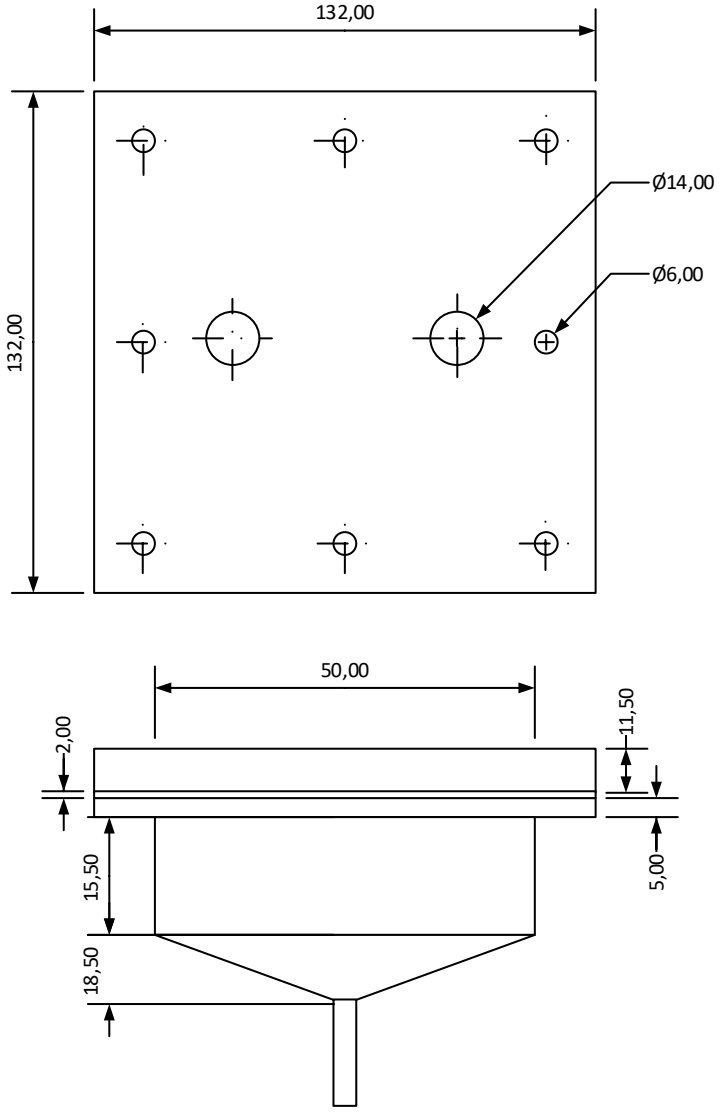

PARTS LIST		
Qty	Dimensions	Description
1	132 x 132 x 11,5 mm	Perspex top flange
1	132 x 132 x 5 mm	Stainless steel flange
1	132 x 132 x 2 mm	Rubber gasket
8	6 mm	Nuts and bolts

Scale 2:1 Units mm	Title: Organics Trap	Rev no. 001

Figure 8-9: Organics trap detailed drawing

8.8 Activated Carbon Trap Specifications and Drawing

The equipment specification sheet for the activated carbon trap is shown below and the detailed drawing is shown in Figure 8-10.

Activated Carbon Trap					
Equipment label	V-10				
Maximum Diameter	70,00	mm	Maximum Height	360,00	mm
Process Data					
Gas flow direction	Enters through the bottom of the column and flows out the top				
Operating temperature			20,00	°C	
Operating pressure			5,90	bar(abs)	
Gas mass flowrate			0,062	kg/h	
Calculated pressure drop			0,285	kPa	
Activated carbon bed height			292	mm	
Activated carbon particle size			1,7	mm	
Activated carbon bulk density			520	kg/m³	
Construction and Materials					
Column material			Stainless steel 316		
Column outer diameter			70,00	mm	
Column thickness			2,12	mm	
Column height			292	mm	
Flange material			Stainless steel 316		
Flange diameter			110,00	mm	
Flange thickness			5,00	mm	
Number of bolts			6		
Gasket material			Rubber		
Gasket thickness			1,00	mm	

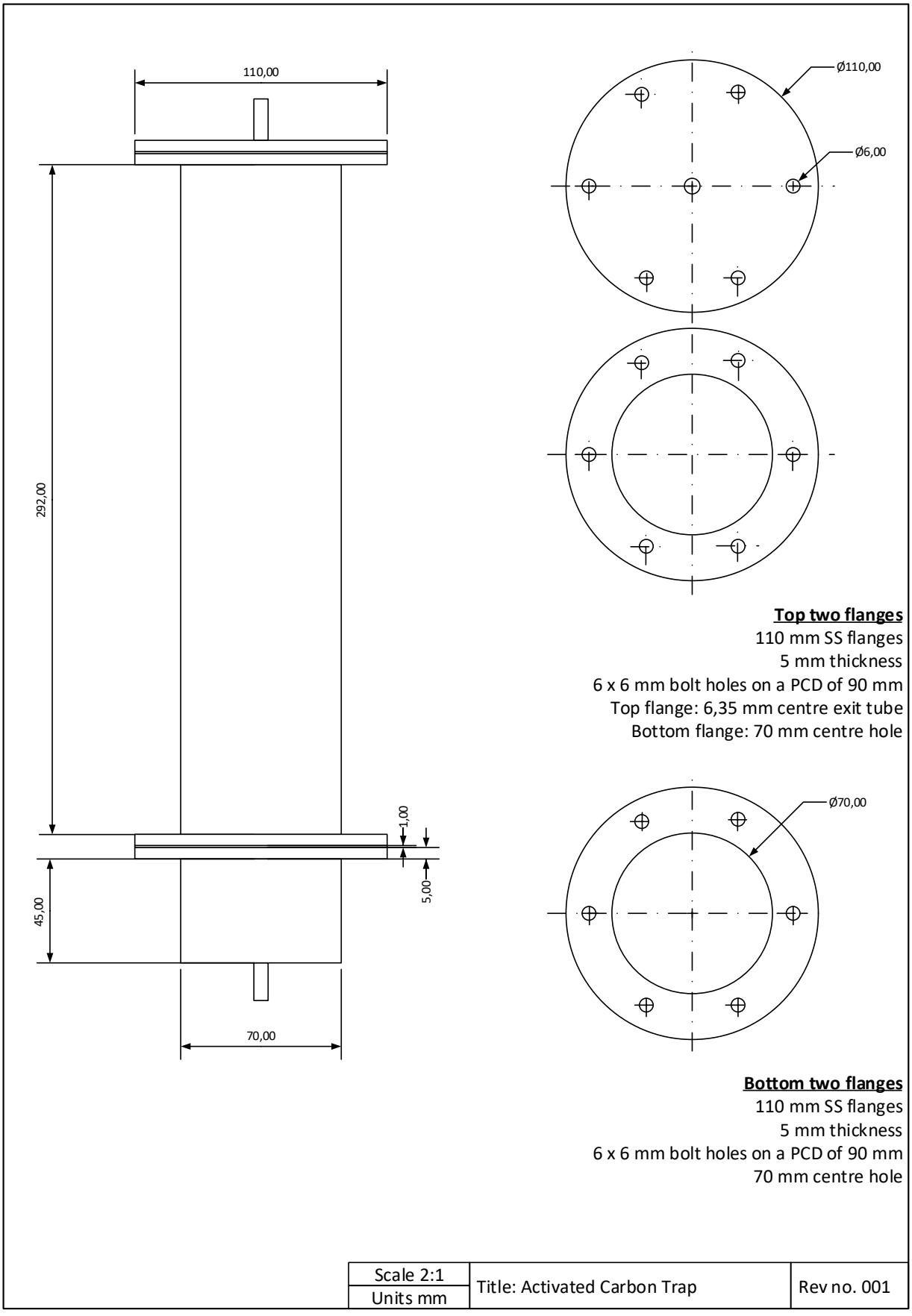

Figure 8-10: Activated carbon trap drawing

8.9 Regeneration System Control Design Form

The control design form for the regeneration system is given below.

Control Objectives

1. Safety
   a) Maximum temperature in the system may not exceed 450 °C
   b) No gas should escape from the regeneration columns during an experimental run
   c) System pressure should not exceed 2 bar during an experimental run
2. Environmental protection
   a) No organic material is to be released into the atmosphere with the nitrogen gas
   b) The nitrogen gas is to be cooled as much as possible before being released to the atmosphere
3. Equipment protection
   a) Process maximum design temperature is not to be exceeded
   b) Process maximum design pressure is not to be exceeded
4. Smooth operation and production rate
   a) None
5. Product quality
   a) None
6. Profit
   a) None
7. Monitoring and diagnosis
   a) Sensors and displays are needed to monitor the temperature and pressure of the system in order to maintain proper process operation
   b) Temperature sensors, display and control is extremely important and needs to be recorded as it forms part of the experimental variables

Measurements

Variable	Type of Sensor	Sensor range & nominal value	Special Information
P1	Dial pressure gauge	0 – 100 kPa	
P2	Dial pressure gauge	0 – 100 kPa	
P3	Dial pressure gauge	0 – 100 kPa	
F1	Variable area flowmeter	0,22 – 2,2 ft^3/h	

F2	Variable area flowmeter	0,22 – 2,2 ft³/h
F3	Variable area flowmeter	0,22 – 2,2 ft³/h
T1	PT100	
T2	PT100	
T3	PT100	
T4	PT100	
T5	PT100	
T6	PT100	
T7	PT100	
T8	PT100	

Manipulated Variables

I.D.	Description	Highest rating
Q1	Heat transferred to V-101 inlet nitrogen tube	75 W, 450 °C
Q2	Heat transferred to unit V-101	75 W, 450 °C
Q3	Heat transferred to V-102 inlet nitrogen tube	75 W, 450 °C
Q4	Heat transferred to unit V-102	75 W, 450 °C
Q5	Heat transferred to V-103 inlet nitrogen tube	75 W, 450 °C
Q6	Heat transferred to unit V-103	75 W, 450 °C

Constraints

Variable	Limit values	Measured/Inferred	Hard/soft	Penalty
Nitrogen inlet temperature	High – 350 °C	Measured	Hard	Equipment damage, personal injury
Nitrogen outlet temperature	High – 310 °C	Measured	Hard	Equipment damage, personal injury
System pressure	High	Measured	Hard	Equipment damage, personal injury

Additional Considerations

None.

8.10 HAZOP Documentation

Table 8-1, Table 8-2 and Table 8-3 below give the HAZOP analysis for each process unit in the regeneration process.

Table 8-1: HAZOP analysis for regeneration process units V-101, V-102 and V-103:

Process Units: V-101, V-102, V103				
Intention: Adsorbent regeneration				
Guide Words	**Deviation**	**Cause**	**Consequence**	**Action**
None, no	Nitrogen gas flow in column inlet streams	Any valves closed on the inlet streams	Tubing will heat up possibly causing some deformation to inlet tubing	Always make sure all valves are open and that gas is flowing before switching on electrical heat tracing and temperature control
More of	Temperature in column inlet streams	Heat tracing malfunction	System running at a higher temperature, adsorbent cracking	Temperature control needs to be in place, high temperature alarms, temperatures need to be monitored
More of	Nitrogen gas in column inlet streams	Gas bottle regulator malfunction, control valve (v-3, v-4, v-5) malfunction	Possible fluidisation in adsorbent beds, decrease in heat transfer in adsorbent beds – decreasing regeneration efficiency	Gas flow meters and pressure gauges on the inlet column streams need to be monitored
More than	Heat losses	No insulation, extreme temperature difference between system and ambient air	Decrease in energy efficiency – higher costs Operator safety – exposed hot surfaces	Columns, inlet and outlet tubing needs to be insulated

Table 8-2: HAZOP analysis for regeneration process unit E-101

Process Units: E-101				
Intention: Condensation of organic compounds in vapour				
Guide Words	**Deviation**	**Cause**	**Consequence**	**Action**
None, no	Cooling water	Blockage in pipe, cooling water bath empty	Very hot gas flowing through organics and activated carbon traps causing damage to equipment and hot gases being released to the atmosphere	Switch off electrical heat tracing, keep nitrogen gas flowing, fix cooling water problem
More of	Cooling water inlet temperature	Water bath cooling insufficient	Condenser outlet vapour stream temperature too high, organics not condensing	Vapour outlet stream temperature to be monitored as well as the cooling water bath temperature. Ice can be added to condenser.
More of	Vapour inlet temperature	Inadequate temperature control on regeneration columns	Not enough cooling occurring in condenser causing a higher vapour temperature on the outlet which affects downstream units	Increase cooling water flow, add ice to the condenser, fix heating problem on the regeneration columns
Less of	Cooling water flow	Blockage in pipe, cooling water bath pump not working properly	Condenser outlet vapour stream temperature too high, organics not condensing	Vapour outlet stream must be monitored, problem must be found and fixed, top up condenser with cold water till problem is solved

Table 8-3: HAZOP analysis for regeneration process units V-104 and V-105

Process Units: V-104, V-105				
Intention: Trap organic compounds before nitrogen is released into atmosphere				
Guide Words	**Deviation**	**Cause**	**Consequence**	**Action**
None, no				
More of	Temperature on inlet gas stream	Inadequate cooling in condenser	Higher temperatures in traps could lead to equipment damage, higher temperature gas released to atmosphere	Solve cooling problem, possibly shut down equipment
Other than	Gas flow through organics trap outlet valve, v-6	Valve v-6 left open	Gas released where it shouldn't be and before any last remaining organics has been removed	Close valve v-6
Other than	Activated carbon trap lid closed	Operator mistake	Pressure build-up in the system	Immediately remove the lid so that gas can be released to the atmosphere

8.11 Safe Working Procedure for the Regeneration Process

SAFE WORK PROCEDURE (SWP) FOR

The regeneration of activated alumina adsorbents used to remove 1-hexanol from n-decane using a specifically designed regeneration experimental setup at pressures below 2 bar and well controlled high temperatures.

OVERVIEW OF THE TASK:

a) Scope

Temperature regeneration experiments will be performed at temperatures between 180 and 210 °C using nitrogen as the carrier gas for durations of between 3 and 8 hours. The regeneration of 3 activated alumina adsorbents, Selexsorb® CDx, Selexsorb® CD and F-220, will be done once an adsorption cycle has been completed removing 1-hexanol from *n*-decane.

The experiments will be performed in a specifically designed bench scale regeneration experimental setup in a fume hood.

The experimental work will be performed in lab C225 in the Process Engineering Building at Stellenbosch University.

b) Authorisation

This procedure is to be carried out by Jomaré Groenewald in lab C225 under the supervision of Prof. Burger and Prof. Schwarz. A thorough understanding of the risks and hazards involved with the equipment is required before the person undertaking this task may begin.

c) Hazards

- Harmful and flammable chemicals
- High temperatures
- Electrical heating

d) Personal Protective Equipment (PPE) [minimum PPE required to be worn by all personnel working on task]

Closed shoes, lab coat, safety glasses, nitrile gloves

e) Emergency Response/First aid requirements

CO2 fire extinguisher

Eyewash bottle

UNDERTAKING THE TASK:

f) Step-by-step Procedure

- Preparation/Precautions:
- Preparing Equipment

1. Close all valves besides for the three inlet tube needle valves (v-3, v-4 and v-5)
2. Fill the chiller bath with water
3. Fill the condenser with water [E-101]
4. Fill the activated carbon trap [V-105] with activated carbon
5. Pour 175 mL of water in the organics trap [V-104]
6. Remove the support rod from the bottom of the flow meters
7. Unscrew the regeneration columns and place them on the hold beams
8. Check all gas bottle connections for any irregularities

- Experimental Procedure:

1. Switch on pump and open condenser water inlet valve (v-9)
2. Switch on the chiller bath
3. Weigh adsorbent filled mesh baskets and record the mass of each one
4. Place the adsorbent filled mesh baskets in the regeneration columns
5. Reconnect the regeneration columns to their lids and ensure all nuts and bolts are fastened tightly
6. Place support rod back into place beneath the flow meters

7. Open the gas bottles and allow cold nitrogen to flush the system and remove oxygen for 15 minutes
8. Switch on the extraction fan
9. Record the inlet flow measurements to the columns on the flow meter readings
10. Switch on the control box
11. Put the USB drive into the HMI screen which starts the logging procedure
12. Choose the temperature program for the 3 inlet temperature controllers based on the regeneration temperature and duration being tested and start heating
13. Ensure all logging is occurring correctly
14. Monitor and record the condenser outlet temperature regularly
15. Test for gas leaks at the lids of the regeneration column before the inlet temperature of each column reaches 50 °C
16. Allow the system to run for the required regeneration duration
17. Stop the temperature control program on the 3 temperature controllers at the end of the experimental run
18. Switch off the electric heat tracing
19. Stop the logging procedure by pressing the stop button on the screen
20. Continue to allow nitrogen gas to run through the system till the temperatures on the outlet of the regeneration columns read 80 °C
21. Switch off the condenser cooling water pump
22. Close the nitrogen gas bottle
23. Allow the entire system to cool further overnight
24. Unscrew the regeneration columns and let them rest on the hold beams
25. Remove the mesh baskets from the columns
26. Weigh and record the mass of each adsorbent filled mesh basket

g) Clean-up Procedures (including any waste disposal)

Cleaning experimental setup:

1. Open valve, v-6, and empty contents into glass vial

2. Close valve, v-6.

8.12 Detailed Adsorption Experimental Procedure

A step-by-step procedure for the adsorption experiments performed is given below.

8.12.1. Preparation procedure

1. Fill water bath with water
2. Label sample vials for each beaker
3. Switch on multi plug
4. Switch on immersion heater and set to experimental temperature
5. Switch on magnetic stirrer plate
6. Record ambient temperature

8.12.2. Experimental procedure

1. Weigh all sample vials (10 sample vials) for each beaker and record the mass
2. Place one magnetic stirrer bar in each 500 mL glass beaker
3. Weigh glass beaker 1, record the mass and zero the scale
4. Measure 200 mL of solution 1 using a graduated cylinder
5. Pour 200 mL of solution 1 into beaker 1 and record the mass
6. Remove beaker 1 from the scale, zero the scale and record the total mass of beaker 1 and solution 1
7. Place beaker 1 in the heated water bath
8. Repeat steps 3 to 7 for the remaining beakers and solutions
9. Take two samples from each beaker in sample vials x1 and x2 (where x refers to the beaker number)
10. Weigh mesh basket 1 (including lid) and record the mass
11. Weigh out the required amount of adsorbent for mesh basket 1 and record the mass
12. Pour the weighed adsorbent into mesh basket 1, weigh the basket again and record the mass

13. Hang mesh basket 1 on the lid hook above beaker 1
14. Repeat steps 9 to 12 for the remaining mesh baskets
15. Remove the bath lid from the hooks and submerge the mesh baskets in the solutions their respective solutions
16. Start the experimental run time
17. Set the magnetic stirrer plate to the required stirring rate (slowly increase the stirring rate starting from zero in order to ensure all magnetic stirrer bars are moving)
18. Fasten the lid in all four corners using the wing nuts
19. Take 0,2 mL samples of the solution in each beaker at the required sample intervals using a pipette (sample vials x3 to x9)
20. Record the ambient temperature and bath temperature throughout the experimental run
21. After the last sample, at the end of the experimental run, turn off the immersion heater
22. Unfasten the lid and lift and hang it on the lid hooks
23. Allow the fluid to drip off the mesh baskets (Be careful not to spill any liquid on the beaker hold plate or in the water)
24. Turn the magnetic stirrer plate back to zero
25. Remove mesh basket 1, weigh it and record the mass
26. Throw adsorbent into waste container and put the mesh basket in soapy water
27. Repeat steps 24 and 25 for all mesh baskets
28. Allow each beaker's contents to be mixed for several seconds before removing them from the water bath
29. Take a final sample of each beaker's contents in sample vial x10
30. Remove the beakers from the water bath and place them on paper towel to allow the water to run off
31. Dry, weigh and record the mass of each beaker
32. Pour the contents of each beakers into the appropriate labelled solution Schott bottle
33. Weigh the sample vials of each beaker again and record the mass

34. Switch off the magnetic stirrer plate

35. Switch of the multi plug

8.13 Detailed Regeneration Experimental Procedure

A step-by-step procedure for the regeneration experiments performed is given below.

8.13.1. Preparation procedure

1. Check the connections to the gas bottle and ensure outlet valve is open
2. Untighten the bolts of the 3 regeneration columns and remove them
3. Remove the support rod underneath the flowmeters
4. Allow the regeneration columns to sit on the support bars beneath them
5. Open the outlet valve on the activated carbon trap
6. Ensure all other valves are closed, besides for the 3 regeneration column inlet valves (needles valves set to a specific openness to achieve the required flowrate)

8.13.2. Experimental procedure

1. Weigh the adsorbent filled mesh basket and record the mass
2. Weigh the column insert, record the mass and zero the scale
3. Pour the adsorbent into the column insert, ensuring no adsorbent is left in the mesh basket
4. Weigh the column insert containing the adsorbent and record the mass
5. Zero the scale and record the mass of the column insert and adsorbent
6. Place the column insert into the regeneration column
7. Repeat steps 1 through 6 for the other two mesh baskets
8. Push the regeneration columns back into position below their respective top flanges
9. Place the support rod back in underneath the flowmeters
10. Fasten the bolts onto the nuts at the top of the regeneration columns
11. Ensure all bolts are tightly fastened
12. Open the nitrogen gas bottle and ensure there is flow through each column
13. Switch on the extraction fan in the fume hood
14. Switch on the control box

15. Set the regeneration temperature on the 6 controllers' programmes
16. Insert the USB drive into the portal on the back of the HMI screen
17. Switch on the electric trace heating
18. Start the temperature control programme on each controller
19. Switch on the cooling water pump and open the inlet water valve
20. Switch on the chiller bath
21. Record the gas inlet temperature to the system a few times throughout the experimental run
22. Record the condenser outlet temperature a few times throughout the experimental run
23. On completion of the experiment, stop the controller programmes on all 6 controllers
24. Switch of the electric trace heating
25. Allow the nitrogen gas to flow through the system till the regeneration outlet column temperature read a temperature of 50 °C
26. Close the nitrogen gas bottle
27. Eject the USB drive on the HMI screen and then remove it
28. Close the cooling water inlet valve and switch off the water pump
29. Switch off the chiller bath
30. Switch off the extraction fan
31. Close the activated carbon trap outlet valve
32. Switch off the control box
33. Allow the system to completely cool down overnight
34. Loosen the bolts of the regeneration columns, the following day
35. Remove the support rod beneath the flowmeters
36. Rest the regeneration columns on the support bars
37. Remove the column inserts with adsorbent

38. Weigh the column insert with adsorbent and record the mass
39. Weigh the mesh basket and zero the scale
40. Pour the adsorbent into the mesh basket ensuring no adsorbent is left in the column insert
41. Weigh the adsorbent in the mesh basket and record the mass
42. Zero the scale
43. Weigh the mesh basket and adsorbent and record the mass
44. Repeat steps 38 through 43 for the other two column inserts
45. Move to the adsorption cycle

8.14 Detailed Sample Preparation Procedure

A step-by-step procedure for the preparation of samples for GC analysis is given below. Ten samples were taken per experimental run and samples were labelled x1 to x10, where x corresponded to the beaker the samples were taken from. This was done to ensure no sample mix ups occurred as more than one experimental run was performed at a time.

For the runs with initial adsorbate concentrations in the range of between 1 and 2 mass %, the following sample, internal standard and solvent amounts were used in sample preparation.

- 90 µL of experimental sample
- 40 µL of internal standard
- 1,4 mL of solvent
- All samples were diluted

For the runs with initial adsorbate concentrations in the range of between 0 and 1 mass %, the following sample, internal standard and solvent volumes were used in sample preparation.

- 120 µL sample
- 40 µL internal standard
- 1,4 mL of solvent
- Only samples 1 to 4 were diluted

8.14.1. Preparation procedure

1. Label 22 sample vials
    a. Label 11 sample vials from x1S to x10S, with 2 sample vials bring A and B of one specific sample (e.g. x1S, x2S, x3AS, x3BS, x4S, x5S, x6S, x7S, x8S, x9S, x10S)
    b. Label the last eleven sample vials from x1D to x10D, remembering the 2 A and B sample vials (e.g. x1D, x2D, x3AD, x3BD, x4D, x5D, x6D, x7D, x8D, x9D, x10D)
2. Weigh sample x1S on the 5 decimal analytical balance and record the mass
3. Remove the sample vial and wait for the scale to stabilise at zero
4. Place sample x2S on the balance

5. Pipette the required experimental sample volume from sample x1 into sample vial x1S
6. Record the mass of sample vial x2S
7. Remove the sample vial and wait for the scale to stabilise at zero
8. Place sample x3AS on the balance
9. Pipette the required experimental sample volume from sample x2 into sample vial x2S
10. Record the mass of sample vial x3AS
11. Remove the sample vial and wait for the scale to stabilise at zero
12. Place sample x3BS on the balance
13. Pipette the required experimental sample volume from sample x3 into sample vial x3AS
14. Record the mass of sample vial x3BS
15. Remove the sample vial and wait for the scale to stabilise at zero
16. Place sample x4S on the balance
17. Pipette the required experimental sample volume from sample x3 into sample vial x3BS
18. Record the mass of sample vial x4S
19. Remove the sample vial and wait for the scale to stabilise at zero
20. Place sample x5S on the balance
21. Pipette the required experimental sample volume from sample x4 into sample vial x4S
22. Record the mass of sample vial x5S
23. Remove the sample vial and wait for the scale to stabilise at zero
24. Place sample x6S on the balance
25. Pipette the required experimental sample volume from sample x5 into sample vial x5S
26. Record the mass of sample vial x6S
27. Remove the sample vial and wait for the scale to stabilise at zero
28. Place sample x7S on the balance
29. Pipette the required experimental sample volume from sample x6 into sample vial x6S

30. Record the mass of sample vial x7S
31. Remove the sample vial and wait for the scale to stabilise at zero
32. Place sample x8S on the balance
33. Pipette the required experimental sample volume from sample x7 into sample vial x7S
34. Record the mass of sample vial x8S
35. Remove the sample vial and wait for the scale to stabilise at zero
36. Place sample x9S on the balance
37. Pipette the required experimental sample volume from sample x8 into sample vial x8S
38. Record the mass of sample vial x9S
39. Remove the sample vial and wait for the scale to stabilise at zero
40. Place sample x10S on the balance
41. Pipette the required experimental sample volume from sample x9 into sample vial x9S
42. Record the mass of sample vial x10S
43. Remove the sample vial and wait for the scale to stabilise at zero
44. Place sample x1S on the balance
45. Pipette the required experimental sample volume from sample x10 into sample vial x10S
46. Record the mass of sample vial x1S and its contents
47. Remove the sample vial and wait for the scale to stabilise at zero
48. Place sample x2S on the balance
49. Pipette the required internal standard volume into sample vial x1S
50. Record the mass of sample vial x2S and its contents
51. Repeat the entire process for all 11 sample vials, pipetting the required internal standard volume into each vial
52. Repeat the entire process again for all 11 sample vials, pipetting the required solvent volume into each vial

53. Vortex each sample for a couple of seconds

8.14.2. Dilution procedure

1. Pipette 450 µL of sample x1S into sample vial x1D
2. Repeat step 1 for the other 10 samples
3. Fill sample vials x1D through x10D with solvent (roughly 2 x 650 µL)
4. Vortex each diluted sample for a couple of seconds

8.15 Detailed Cleaning procedure

All glassware, sample vials, mesh baskets and magnetic stirrer bars were cleaned following the same procedure. This step-by-step procedure is listed below.

8.15.1. Cleaning procedure

1. Wash all experimental components in soapy water
2. Rinse all the components with tap water
3. Wash all the components in acetone
4. Rinse all the components with reverse osmosis water
5. Place all the components on laboratory paper towel and allow them to dry

The adsorption experimental equipment was cleaned by wiping down its various surfaces with acetone.

8.16 Activated Alumina F-220 Raw Experimental Data

Table 8-4, Table 8-5 and Table 8-6 below give the gas chromatography results for 1-hexanol adsorbate at the 3 system temperatures investigated.

Table 8-4: Gas chromatography data for the 1-hexanol, activated alumina F-220 at 25 °C adsorption system

	A		**B**		**C**	
	n-decane	1-hexanol	*n*-decane	1-hexanol	*n*-decane	1-hexanol
Time (min)	**Mass (mg)**					
0	65,3715	0,8731	63,8384	0,6384	71,6513	0,3586
0	65,8726	0,9741	63,8773	0,6381	72,0386	0,0891
15	66,1086	0,8341	63,1865	0,5100	70,8358	0,2407
30	66,2330	0,7811	63,4445	0,4658	71,3738	0,2050
150	63,4922	0,5113	63,5783	0,2979	71,9909	0,0652
240	66,2042	0,4919	63,6320	0,2220	72,0452	0,0344
360	65,3567	0,4546	62,5177	0,1248	72,0994	0,0119
375	65,4706	0,4040	64,3314	0,2015	81,8353	0,0179
390	63,3374	0,3550	63,6345	0,1926	81,5483	0,0158
395	61,4417	0,3568	59,4788	0,1631	81,5554	0,0000

Table 8-5: Gas chromatography data for the 1-hexanol, activated alumina F-220 at 30 °C adsorption system

	A		**B**		**C**	
	n-decane	1-hexanol	*n*-decane	1-hexanol	*n*-decane	1-hexanol
Time (min)	**Mass (mg)**					
0	62,8032	0,8273	63,5571	0,6462	87,4381	0,4577
0	61,1388	0,9463	63,8266	0,6393	87,0351	0,4536
15	62,9211	0,8506	64,4582	0,5209	82,6707	0,2278
30	63,5801	0,8133	63,6933	0,4652	87,1229	0,2404
150	63,5723	0,6152	64,1017	0,3064	81,9930	0,1014
240	63,0732	0,5460	64,1072	0,2420	87,5651	0,0417
360	63,3846	0,4651	64,1031	0,2004	86,2628	0,0221
375	62,3983	0,4856	64,1803	0,1963	83,2626	0,0205
390	63,1839	0,4863	64,2230	0,1928	85,4581	0,0203
395	62,2828	0,4757	63,7652	0,1915	85,0802	0,0203

Table 8-6: Gas chromatography data for the 1-hexanol, activated alumina F-220 at 35 °C adsorption system

	A		B		C	
	n-decane	1-hexanol	*n*-decane	1-hexanol	*n*-decane	1-hexanol
Time (min)	**Mass (mg)**					
0	63,7467	0,9923	63,1282	0,6116	86,7530	0,4507
0	63,1771	0,8645	63,7268	0,4785	87,6057	0,4577
15	62,7821	0,8350	63,7480	0,6164	88,7440	0,2926
30	62,2251	0,6796	64,9790	0,4257	90,4207	0,2350
150	63,5522	0,5898	64,1260	0,2539	86,7720	0,0759
240	64,0378	0,4470	64,3499	0,1828	89,8261	0,0460
360	63,6950	0,4850	64,0712	0,2167	88,0574	0,0232
375	62,6775	0,4750	63,3451	0,1794	102,9334	0,0361
390	63,6897	0,4805	64,6572	0,1814	98,9697	0,0348
395	63,7127	0,4739	64,1402	0,1813	102,3305	0,0339

Table 8-7, Table 8-8 and Table 8-9 below give the gas chromatography results for 1-octanol adsorbate at the 3 system temperatures investigated.

Table 8-7: Gas chromatography data for the 1-octanol, activated alumina F-220 at 25 °C adsorption system

	A		B		C	
	n-decane	1-octanol	*n*-decane	1-octanol	*n*-decane	1-octanol
Time (min)	**Mass (mg)**					
0	63,3390	1,0214	63,5605	0,6588	87,8094	0,4995
0	64,1413	1,0427	64,1521	0,6676	86,5227	0,4931
15	63,4157	0,9158	64,6681	0,5617	88,5336	0,3745
30	63,2951	0,8688	64,1458	0,5133	86,3643	0,3301
150	63,7832	0,6855	64,0364	0,3619	88,8642	0,1762
240	63,3939	0,6231	64,2080	0,2890	89,2867	0,1458
360	63,7702	0,5630	64,5919	0,2643	89,9158	0,1204
375	63,0871	0,5469	64,2362	0,2540	103,8329	0,1342
390	63,3980	0,5545	64,7138	0,2522	101,9397	0,1304
395	62,9725	0,5498	64,6561	0,2522	104,4045	0,1330

Table 8-8: Gas chromatography data for the 1-octanol, activated alumina F-220 at 30 °C adsorption system

	A		B		C	
	n-decane	1-octanol	*n*-decane	1-octanol	*n*-decane	1-octanol
Time (min)	**Mass (mg)**					
0	65,1085	0,9890	63,8707	0,6936	88,6137	0,4728
0	64,1127	1,0026	63,1138	0,6871	88,8582	0,4693
15	65,2137	0,8745	63,6681	0,5899	86,4083	0,3348
30	66,5199	0,8256	62,9263	0,5304	87,9894	0,2913
150	67,0952	0,6676	63,5427	0,3830	89,8849	0,1648
240	67,6122	0,5602	64,0302	0,3109	90,3362	0,1285
360	67,2832	0,5010	63,2166	0,2729	89,6430	0,1205
375	66,6173	0,4831	63,2337	0,2575	99,8004	0,1263
390	67,3381	0,4934	63,5883	0,2624	99,3544	0,1250
395	65,0971	0,4843	63,3049	0,2617	99,3390	0,1256

Table 8-9: Gas chromatography data for the 1-octanol, activated alumina F-220 at 35 °C adsorption system

	A		B		C	
	n-decane	1-octanol	*n*-decane	1-octanol	*n*-decane	1-octanol
Time (min)	**Mass (mg)**					
0	63,0501	1,0066	63,6789	0,6841	87,7840	0,4589
0	63,1192	1,0100	64,3320	0,6815	87,9843	0,4549
15	63,4266	0,8909	63,8488	0,5585	88,7408	0,3308
30	62,6885	0,8111	62,9227	0,4997	82,3783	0,2675
150	63,4535	0,6406	64,6572	0,3484	85,2879	0,1505
240	62,9907	0,5602	63,9461	0,2920	89,0318	0,1275
360	63,6106	0,5120	64,2705	0,2542	86,3723	0,1170
375	63,3962	0,5000	63,3824	0,2505	94,1404	0,1229
390	63,4385	0,5034	62,9521	0,2458	103,4603	0,1255
395	63,9941	0,5001	60,7621	0,2375	101,2120	0,1204

Table 8-10, Table 8-11 and Table 8-12 below give the gas chromatography results for 1-decanol adsorbate at the 3 system temperatures investigated.

Table 8-10: Gas chromatography data for the 1-decanol, activated alumina F-220 at 25 °C adsorption system

	A		B		C	
	n-Decane	1-Decanol	*n*-Decane	1-Decanol	*n*-Decane	1-Decanol
Time (min)	**Mass (mg)**					
0	63,2371	0,9956	63,3269	0,7216	64,1457	0,2224
0	64,1396	0,9665	64,0274	0,7475	64,0463	0,2193
15	61,9423	0,8057	63,7494	0,6108	64,2558	0,1552
30	64,2638	0,7397	63,3700	0,5958	64,2148	0,1203
150	65,0797	0,5821	63,2318	0,4667	65,1227	0,0384
240	64,2195	0,5101	63,4023	0,3658	65,2037	0,0192
360	61,8988	0,3879	63,0731	0,2984	87,0442	0,0095
375	63,3226	0,4113	63,7909	0,2978	87,9488	0,0099
390	64,3501	0,4071	62,9753	0,2869	85,9110	0,0087
395	65,3983	0,4332	63,8858	0,2841	86,1561	0,0102

Table 8-11: Gas chromatography for the 1-decanol, activated alumina F-220 at 30 °C adsorption system

	A		B		C	
	n-Decane	1-Decanol	*n*-Decane	1-Decanol	*n*-Decane	1-Decanol
Time (min)	**Mass (mg)**					
0	62,2892	1,0219	64,2397	0,7139	86,9621	0,5350
0	62,8072	1,0249	66,5790	0,7394	87,5164	0,5484
15	63,0383	0,8981	63,2958	0,5521	86,3756	0,4023
30	62,7384	0,8663	66,3982	0,5220	87,3217	0,3578
150	63,1555	0,6835	67,4571	0,3288	88,6520	0,1452
240	62,9853	0,6129	65,5293	0,2408	89,8131	0,0991
360	63,3467	0,5543	66,0605	0,1806	89,9143	0,0663
375	63,0537	0,5376	60,5738	0,1462	101,7156	0,0795
390	62,9629	0,5321	57,4516	0,1472	97,0639	0,0752
395	63,1772	0,5219	60,4598	0,1428	100,3373	0,0746

Table 8-12: Gas chromatography data for the 1-decanol, activated alumina F-220 at 35 °C adsorption system

	A		B		C	
	n-Decane	1-Decanol	*n*-Decane	1-Decanol	*n*-Decane	1-Decanol
Time (min)	**Mass (mg)**					
0	69,7884	1,1305	66,2664	0,7016	70,4315	0,4216
0	70,3790	1,1515	66,7552	0,6988	71,1474	0,4055
15	68,9033	0,9815	63,0732	0,5101	69,2353	0,2880
30	59,5396	0,7983	66,5776	0,4880	69,4630	0,2516
150	70,8147	0,6312	67,3052	0,3055	71,5226	0,0969
240	72,3800	0,5671	62,8371	0,1991	71,7954	0,0627
360	71,5836	0,4898	64,9302	0,1584	71,0531	0,0365
375	85,7878	0,5745	66,1038	0,1546	86,2423	0,0452
390	87,1488	0,5769	64,3120	0,1529	89,0095	0,0452
395	83,1305	0,5496	67,5219	0,1676	89,4122	0,0452

8.17 Selexsorb® CD Raw Experimental Data

Table 8-13, Table 8-14 and Table 8-15 below give the gas chromatography results for 1-hexanol adsorbate at the 3 system temperatures investigated.

Table 8-13: Gas chromatography data for the 1-hexanol, Selexsorb® CD at 25 °C adsorption system

	A		B		C	
	n-decane	1-hexanol	*n*-decane	1-hexanol	*n*-decane	1-hexanol
Time (min)	**Mass (mg)**					
0	63,8933	0,8999	63,7677	0,6283	70,7578	0,3612
0	63,6996	0,8942	63,5308	0,6194	69,9907	0,3567
15	63,6541	0,7944	63,5752	0,5164	70,7332	0,2638
30	63,0519	0,7361	63,2071	0,4682	70,1637	0,2184
150	63,5998	0,5882	63,8222	0,3539	71,5995	0,1183
240	63,9460	0,5310	63,1934	0,2963	72,1937	0,0797
360	64,0237	0,4378	63,7207	0,2506	71,9683	0,0493
375	63,6311	0,4654	63,6090	0,2411	79,3801	0,0529
390	63,4133	0,4604	63,0615	0,2195	81,0440	0,0527
395	63,5704	0,4574	63,7831	0,2393	79,1364	0,0510

Table 8-14: Gas chromatography data for the 1-hexanol, Selexsorb® CD at 30 °C adsorption system

	A		B		C	
	n-decane	1-hexanol	*n*-decane	1-hexanol	*n*-decane	1-hexanol
Time (min)	**Mass (mg)**					
0	49,7659	0,9296	54,7414	0,6296	89,6822	0,2923
0	50,4605	0,8138	52,5714	0,6142	88,1634	0,2445
15	49,4325	0,8224	48,0972	0,4774	81,1134	0,1631
30	50,3059	0,7734	56,1575	0,4611	87,7581	0,1385
150	50,5725	0,6239	54,2578	0,3445	89,0327	0,0355
240	49,7809	0,5392	54,5124	0,2885	88,5047	0,0101
360	52,1552	0,4477	51,6406	0,2407	86,6423	0,0000
375	52,5218	0,4795	52,7697	0,2330	102,6729	0,0008
390	50,6653	0,4657	51,5390	0,2287	101,6800	0,0000
395	49,2241	0,4698	53,6803	0,2290	96,2947	0,0000

Table 8-15: Gas chromatography data for the 1-hexanol, Selexsorb® CD at 35 °C adsorption system

	A		B		C	
	n-decane	1-hexanol	*n*-decane	1-hexanol	*n*-decane	1-hexanol
Time (min)	**Mass (mg)**					
0	62,2936	0,9946	64,4043	0,6345	87,2963	0,3962
0	63,2471	0,9876	64,2554	0,6314	88,5623	0,4622
15	63,5195	0,8612	60,8848	0,4620	87,5418	0,3020
30	63,5796	0,8078	63,4525	0,4630	90,4864	0,2719
150	63,4141	0,6300	64,2288	0,3095	90,2432	0,1227
240	64,5102	0,5549	63,7863	0,2504	90,4358	0,0669
360	64,0717	0,4317	64,0338	0,2073	83,6518	0,0419
375	64,1736	0,4130	64,2256	0,2004	103,3187	0,0624
390	63,8055	0,4723	63,7428	0,1934	101,1316	0,0598
395	63,4731	0,4704	63,2348	0,1897	96,5019	0,0569

Table 8-16, Table 8-17 and Table 8-18 below give the gas chromatography results for 1-octanol adsorbate at the 3 system temperatures investigated.

Table 8-16: Gas chromatography data for the 1-octanol, Selexsorb® CD at 25 °C adsorption system

	A		B		C	
	n-decane	1-octanol	*n*-decane	1-octanol	*n*-decane	1-octanol
Time (min)	**Mass (mg)**					
0	63,6309	0,9900	64,9151	0,6663	88,8566	0,4919
0	63,1339	0,9859	63,9276	0,6556	88,7378	0,4900
15	63,5203	0,8883	64,3532	0,5722	87,6248	0,3974
30	63,3771	0,8524	63,6828	0,5488	88,7815	0,3528
150	63,0157	0,7064	64,3800	0,4269	90,2022	0,2316
240	63,8141	0,6628	64,6777	0,3821	89,7064	0,1902
360	63,0023	0,6043	64,6878	0,3338	88,1112	0,1586
375	63,0141	0,5843	63,7444	0,3300	100,8239	0,1735
390	61,9651	0,5800	64,7928	0,3300	98,6545	0,1685
395	62,9855	0,5832	63,4753	0,3229	97,9314	0,1662

Table 8-17: Gas chromatography data for the 1-octanol, Selexsorb® CD at 30 °C adsorption system

	A		B		C	
	n-decane	1-octanol	*n*-decane	1-octanol	*n*-decane	1-octanol
Time (min)	**Mass (mg)**					
0	64,7763	1,0017	62,6500	0,6461	85,8098	0,4236
0	64,0196	0,9790	62,6407	0,6569	85,6596	0,4183
15	66,1753	0,9177	63,3785	0,5695	86,3169	0,3286
30	65,1383	0,8541	63,7374	0,5342	84,9055	0,2850
150	65,0209	0,7235	63,8921	0,4071	88,9235	0,1810
240	65,4063	0,6323	63,4490	0,3590	89,7047	0,1497
360	65,0287	0,5914	63,8828	0,3179	88,2594	0,1292
375	67,3877	0,5955	63,5293	0,3159	103,0089	0,1317
390	65,0521	0,5781	63,3216	0,3093	103,6619	0,1321
395	63,9966	0,5951	63,2825	0,3132	102,6761	0,1318

Table 8-18: Gas chromatography data for the 1-octanol, Selexsorb® CD at 35 °C adsorption system

	A		B		C	
	n-decane	1-octanol	*n*-decane	1-octanol	*n*-decane	1-octanol
Time (min)	**Mass (mg)**					
0	63,9665	1,0168	62,9718	0,6738	89,0780	0,4672
0	63,3114	1,0060	63,9782	0,6972	88,6767	0,4692
15	63,2855	0,9032	62,3572	0,5719	86,1234	0,3562
30	57,1224	0,7673	63,4087	0,5513	88,4588	0,3222
150	63,9335	0,6941	63,4112	0,3979	90,6836	0,1884
240	63,5848	0,6655	62,9667	0,3518	81,7227	0,1435
360	63,0236	0,5797	63,0429	0,3097	86,9077	0,1295
375	56,6638	0,5113	64,0920	0,3060	105,7214	0,1365
390	63,3350	0,5650	63,8664	0,3047	105,2813	0,1383
395	63,3050	0,5600	63,8461	0,3058	98,0301	0,1294

Table 8-19, Table 8-20 and Table 8-21 below give the gas chromatography results for 1-decanol adsorbate at the 3 system temperatures investigated.

Table 8-19: Gas chromatography data for the 1-decanol, Selexsorb® CD at 25 °C adsorption system

	A		B		C	
	n-decane	1-decanol	*n*-decane	1-decanol	*n*-decane	1-decanol
Time (min)	**Mass (mg)**					
0	65,2365	1,0056	65,3254	0,6479	63,8751	0,3245
0	65,3217	1,0147	64,2371	0,6454	63,2133	0,3219
15	64,9670	0,9098	65,3106	0,5506	63,0014	0,2557
30	65,2522	0,8719	64,3509	0,5211	62,5476	0,2324
150	62,9493	0,6872	65,7337	0,3917	63,9695	0,1236
240	64,6083	0,6157	61,6385	0,3008	63,5944	0,0914
360	64,3393	0,5589	65,2765	0,2716	63,7148	0,0652
375	65,0315	0,5765	63,5229	0,2624	63,6585	0,0607
390	65,1282	0,5768	65,5254	0,2513	64,2607	0,0587
395	64,3798	0,5491	65,6091	0,2632	58,5025	0,0591

Table 8-20: Gas chromatography data for the 1-decanol, Selexsorb® CD at 30 °C adsorption system

	A		B		C	
	n-decane	1-decanol	*n*-decane	1-decanol	*n*-decane	1-decanol
Time (min)	**Mass (mg)**					
0	61,3274	0,8497	62,5943	0,6864	63,1300	0,3393
0	63,2835	0,8813	63,3831	0,6799	62,4015	0,3327
15	63,2099	0,8073	62,5821	0,6172	62,7939	0,2718
30	62,0667	0,7583	62,8564	0,5597	62,3106	0,2392
150	63,3212	0,6429	58,4841	0,4275	63,9017	0,1321
240	63,1266	0,5813	63,2501	0,3912	63,7304	0,1008
360	63,5615	0,5152	63,2585	0,3518	62,8960	0,0698
375	63,0324	0,5243	63,2203	0,3444	80,6910	0,0851
390	63,0003	0,5198	63,0500	0,3328	81,4119	0,0825
395			62,1520	0,3438	80,8574	0,0784

Table 8-21: Gas chromatography data for the 1-decanol, Selexsorb® CD at 35 °C adsorption system

	A		B		C	
	n-decane	1-decanol	*n*-decane	1-decanol	*n*-decane	1-decanol
Time (min)	**Mass (mg)**					
0	61,3330	0,9842	64,7142	0,6561	64,6617	0,3336
0	62,7591	1,0368	66,2377	0,6834	64,3142	0,3571
15	62,5383	0,9335	66,2944	0,5761	64,9716	0,2800
30	63,0039	0,9053	66,1409	0,5413	63,3678	0,2467
150	62,6078	0,7385	66,3790	0,3620	63,0723	0,1394
240	62,2489	0,6578	65,6397	0,3188	63,5979	0,0882
360	61,9726	0,6047	64,9086	0,2540	64,9289	0,0567
375	62,6978	0,5901	65,7186	0,2506	64,5860	0,0521
390	63,3445	0,6193	64,7608	0,2390	64,1527	0,0498
395	60,2652	0,5882	63,9751	0,2389	62,6925	0,0508

8.18 Selexsorb® CDx Raw Experimental Data

Table 8-22, Table 8-23 and Table 8-24 below give the gas chromatography results for 1-hexanol adsorbate at the 3 system temperatures investigated.

Table 8-22: Gas chromatography data for the 1-hexanol, Selexsorb® CDx at 25 °C adsorption system

	A		B		C	
	n-decane	1-hexanol	*n*-decane	1-hexanol	*n*-decane	1-hexanol
Time (min)	**Mass (mg)**					
0	63,4158	0,9013	63,4174	0,6186	88,8143	0.3798
0	62,8391	0,8859	63,2388	0,6173	89,1863	0.3791
15	63,5255	0,7953	63,8828	0,5263	88,9563	0.2572
30	63,2340	0,7444	62,8905	0,4809	89,7931	0.2145
150	63,2289	0,5989	63,5315	0,3458	89,6377	0.1206
240	63,6282	0,5021	63,6572	0,2867	90,2264	0.0670
360	63,2058	0,4996	62,5907	0,2442	84,1098	0.0345
375	63,4866	0,4956	63,5660	0,2503	96,0203	0.0563
390	62,6020	0,4803	63,6078	0,2394	105,5043	0.0548
395	63,2347	0,4749	62,9109	0,2400	103,5180	0.0533

Table 8-23: Gas chromatography data for the 1-hexanol, Selexsorb® CDx at 30 °C adsorption system

	A		B		C	
	n-decane	1-hexanol	*n*-decane	1-hexanol	*n*-decane	1-hexanol
Time (min)	**Mass (mg)**					
0	69,8961	0,9731	70,0073	0,7072	85,4307	0,4027
0	69,9328	1,0463	70,1112	0,7054	83,7920	0,3884
15	70,4084	0,8197	70,2049	0,5843	83,2881	0,2745
30	70,5818	0,8670	69,7696	0,5415	84,9171	0,2414
150	69,9847	0,6762	69,7278	0,3636	86,5509	0,1147
240	64,0860	0,5388	70,2297	0,2998	77,1646	0,0686
360	69,1278	0,5339	70,2710	0,2432	76,6381	0,0445
375	70,3294	0,5299	69,6452	0,2342	86,5515	0,0373
390	69,7494	0,5227	69,7110	0,2268	77,5019	0,0398
395	70,0969	0,5211	70,4770	0,2310	77,0236	0,0364

Table 8-24: Gas chromatography data for the 1-hexanol, Selexsorb® CDx at 35 °C adsorption system

	A		B		C	
	n-decane	1-hexanol	*n*-decane	1-hexanol	*n*-decane	1-hexanol
Time (min)	**Mass (mg)**					
0	62,4687	0,9412	63,5123	0,6313	63,9448	0,2915
0	63,0193	0,9308	63,4218	0,6321	62,9314	0,2885
15	63,0855	0,7959	63,8129	0,5068	63,6649	0,1856
30	62,9116	0,7314	63,7945	0,4545	64,3311	0,1523
150	63,9145	0,5502	63,8912	0,2886	64,0195	0,0000
240	62,4078	0,4510	64,6560	0,2327	64,6800	0,0230
360	63,0757	0,3998	64,4419	0,2086	81,7142	0,0105
375	66,8712	0,4191	64,5556	0,1366	80,6981	0,0100
390	63,2488	0,3791	64,0994	0,1875	82,2324	0,0106
395	63,3618	0,3786	63,2365	0,1800	39,3444	0,0000

Table 8-25, Table 8-26 and Table 8-27 below give the gas chromatography results for 1-octanol adsorbate at the 3 system temperatures investigated.

Table 8-25: Gas chromatography data for the 1-octanol, Selexsorb® CDx at 25 °C adsorption system

	A		B		C	
	n-decane	1-octanol	*n*-decane	1-octanol	*n*-decane	1-octanol
Time (min)	**Mass (mg)**					
0	62,0546	0,9886	62,8279	0,6648	63,8484	0,3605
0	62,2787	1,0084	63,1477	0,6692	63,4158	0,3550
15	61,4841	0,8966	62,7926	0,5836	63,7939	0,2940
30	62,3601	0,8728	62,5371	0,5629	63,6868	0,2766
150	62,8083	0,7589	62,9855	0,4426	64,2484	0,1688
240	63,1528	0,6979	62,7142	0,3869	64,9373	0,1497
360	62,6694	0,6447	62,8150	0,3600	63,9390	0,1307
375	62,5445	0,6357	62,6534	0,3592	80,9315	0,1385
390	62,8320	0,6372	63,7416	0,3550	81,1181	0,1349
395	62,7061	0,6225	62,4184	0,3552	81,6042	0,1364

Table 8-26: Gas chromatography data for the 1-octanol, Selexsorb® CDx at 30 °C adsorption system

	A		B		C	
	n-decane	1-octanol	*n*-decane	1-octanol	*n*-decane	1-octanol
Time (min)	**Mass (mg)**					
0	64,0451	0,9945	66,6216	0,6674	83,2645	0,4549
0	67,2991	1,0351	64,9209	0,6618	88,8905	0,4771
15	65,0915	0,8934	63,4224	0,5487	88,4519	0,3718
30	67,2801	0,8811	63,3252	0,5100	87,3947	0,3402
150	67,6511	0,7546	61,5234	0,3876	87,4239	0,2043
240	65,1715	0,6679	64,5988	0,3527	88,2422	0,1668
360	64,8678	0,5965	63,4954	0,2926	86,4417	0,1445
375	63,9841	0,5823	62,2341	0,2866	102,8310	0,1478
390	66,7692	0,6037	64,2059	0,2902	102,0081	0,1479
395	66,2194	0,5989	63,6314	0,2899	103,1016	0,1496

Table 8-27: Gas chromatography data for the 1-octanol, Selexsorb® CDx at 35 °C adsorption system

	A		B		C	
	n-decane	1-octanol	*n*-decane	1-octanol	*n*-decane	1-octanol
Time (min)	**Mass (mg)**					
0	63,0510	1,0203	66,3389	0,6720	64,4467	0,3139
0	63,2310	1,0264	66,8199	0,6752	64,4656	0,3141
15	64,1143	0,9066	66,0974	0,5693	63,7471	0,2403
30	63,5799	0,8761	67,1390	0,5286	64,0116	0,2241
150	64,0817	0,7174	67,0539	0,3864	64,9041	0,1378
240	63,4842	0,6568	66,2950	0,3425	64,7003	0,1163
360	63,7602	0,6006	66,1398	0,2872	64,3831	0,1050
375	63,6191	0,5866	66,0786	0,2806	81,4375	0,1089
390	63,8147	0,5777	65,8040	0,2869	82,1811	0,1074
395	63,1257	0,5766	67,0709	0,2886	81,2121	0,1078

Table 8-28, Table 8-29 and Table 8-30 below give the gas chromatography results for 1-decanol adsorbate at the 3 system temperatures investigated.

Table 8-28: Gas chromatography data for the 1-decanol, Selexsorb® CDx at 25 °C adsorption system

	A		B		C	
	n-decane	1-decanol	*n*-decane	1-decanol	*n*-decane	1-decanol
Time (min)	**Mass (mg)**					
0	63,2809	0,9798	65,0707	0,6509	62,8952	0,3120
0	60,0803	0,9268	63,8856	0,6352	63,3399	0,3211
15	62,8763	0,8900	64,6157	0,5503	63,8183	0,2592
30	64,1282	0,8720	62,9693	0,4915	63,1311	0,2357
150	63,7101	0,7408	61,0965	0,3373	64,5970	0,1198
240	63,3926	0,6858	65,5384	0,3372	64,4958	0,0898
360	63,5923	0,6276	62,9657	0,2497	63,4276	0,0618
375	63,9974	0,6307	64,1733	0,2613	78,9011	0,0750
390	63,1249	0,6287	65,4735	0,2622	78,6554	0,0727
395	56,1739	0,5610	64,7840	0,2762	79,3386	0,0697

Table 8-29: Gas chromatography data for the 1-decanol, Selexsorb® CDx at 30 °C adsorption system

	A		B		C	
	n-decane	1-decanol	*n*-decane	1-decanol	*n*-decane	1-decanol
Time (min)	**Mass (mg)**					
0	62,9557	1,0380	63,7599	0,8802	86,6508	0,5223
0	63,2851	1,0426	63,7535	0,8695	87,0266	0,5434
15	63,2222	0,9589	63,7068	0,7808	88,4376	0,4459
30	66,0620	0,9419	63,8310	0,7460	81,6920	0,3741
150	65,6053	0,7838	63,4226	0,6157	89,4907	0,2235
240	66,0551	0,7466	63,6217	0,5686	89,9487	0,1745
360	62,0578	0,6205	63,6048	0,5103	86,6020	0,1275
375	62,8926	0,6145	63,7100	0,5076	101,1839	0,1493
390	67,8016	0,6780	62,3768	0,4954	99,6407	0,1511
395	64,5863	0,6535	62,9296	0,5065	99,3704	0,1502

Table 8-30: Gas chromatography data for the 1-decanol, Selexsorb® CDx at 35 °C adsorption system

	A		B		C	
	n-decane	1-decanol	*n*-decane	1-decanol	*n*-decane	1-decanol
Time (min)	**Mass (mg)**					
0	62,7162	1,0067	63,3490	0,6961	72,5583	0,3751
0	63,9024	1,0210	63,8716	0,7174	71,9651	0,3687
15	63,6587	0,9351	63,3578	0,5952	71,7199	0,2865
30	64,6789	0,8908	64,2406	0,5603	72,1362	0,2568
150	64,4648	0,7262	62,7961	0,4350	72,4372	0,1235
240	64,2461	0,6619	63,6492	0,3761	75,8227	0,0964
360	63,7852	0,6036	63,5966	0,3343	72,8063	0,0635
375	64,3340	0,6054	63,9461	0,3314	89,6297	0,0772
390	62,9859	0,5844	64,0498	0,3210	87,8436	0,0731
395	63,6353	0,5838	63,6388	0,3010	90,2463	0,0769

8.19 Isotherm Modelling Graphs

Figure 8-11, Figure 8-12 and Figure 8-13 show the isotherm modelling results for 1-hexanol, 1-octanol and 1-decanol adsorbed onto activated alumina F220 respectively.

Figure 8-14, Figure 8-15 and Figure 8-16 show the isotherm modelling results for 1-hexanol, 1-octanol and 1-decanol adsorbed onto Selexsorb® CD respectively.

Figure 8-17, Figure 8-18 and Figure 8-19 show the isotherm modelling results for 1-hexanol, 1-octanol and 1-decanol adsorbed onto Selexsorb® CDx respectively.

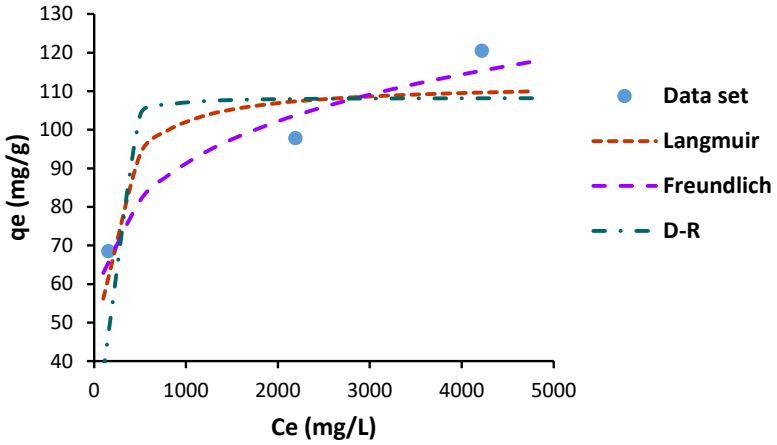

(a) Two-parameter isotherm modelling at 25 °C

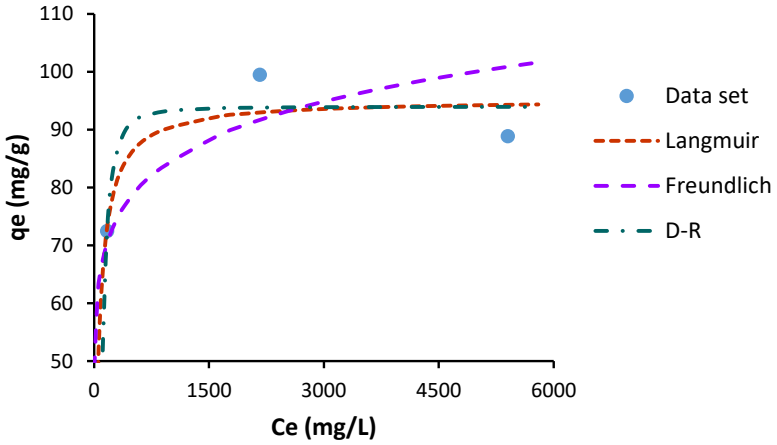

(b) Two-parameter isotherm modelling at 30 °C

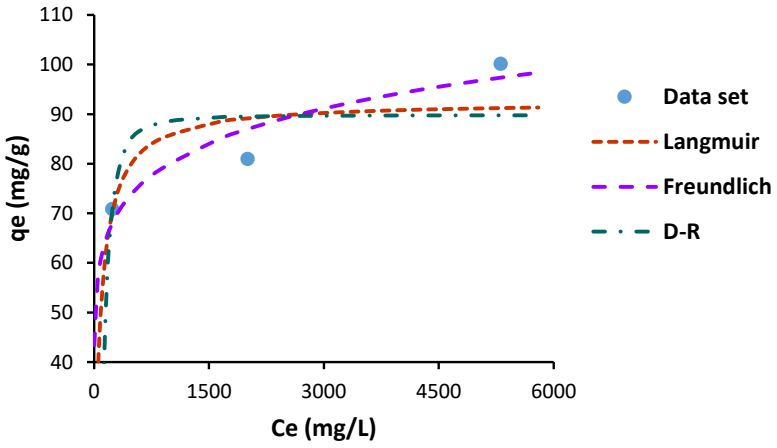

(c) Two-parameter isotherm modelling at 35 °C

Figure 8-11: The isotherm modelling results for 1-hexanol adsorbate adsorbed onto activated alumina F-220 at adsorption temperatures of a) 25, b) 30 and c) 35 °C

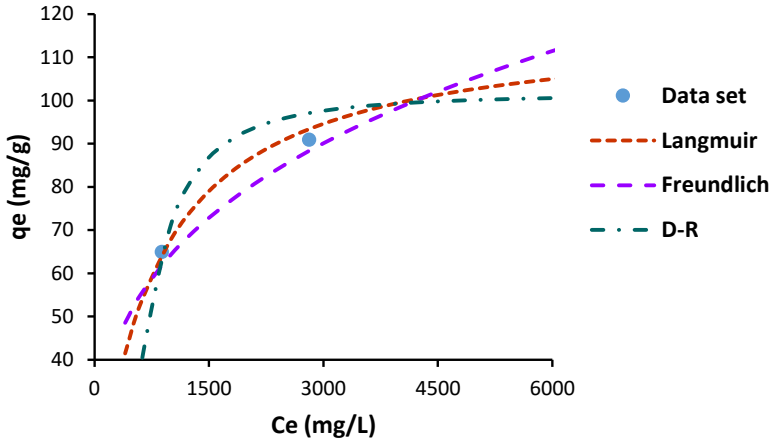

(a) Two-parameter isotherm modelling at 25 °C

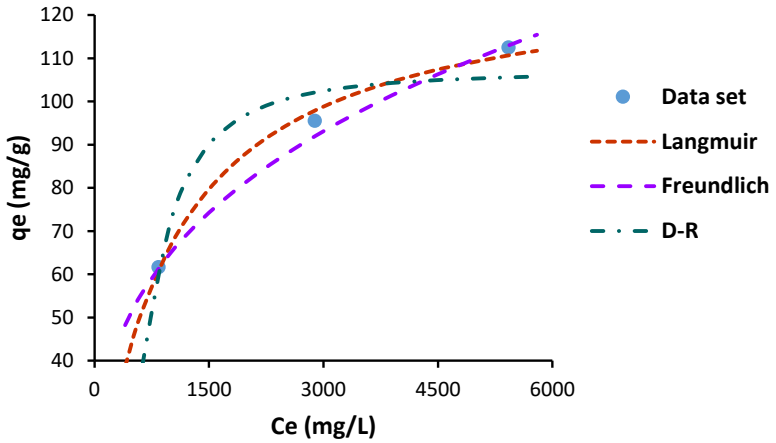

(b) Two-parameter isotherm modelling at 30 °C

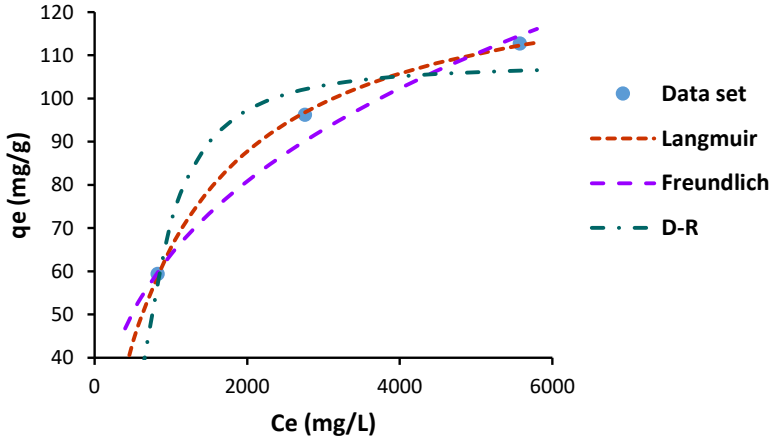

(c) Two-parameter isotherm modelling at 35 °C

Figure 8-12: The isotherm modelling results for 1-octanol adsorbate adsorbed onto activated alumina F-220 at adsorption temperatures of a) 25, b) 30 and c) 35 °C

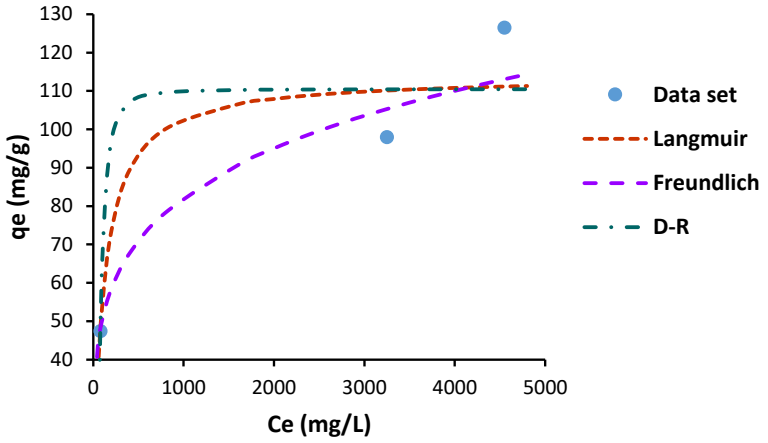

(a) Two-parameter isotherm modelling at 25 °C

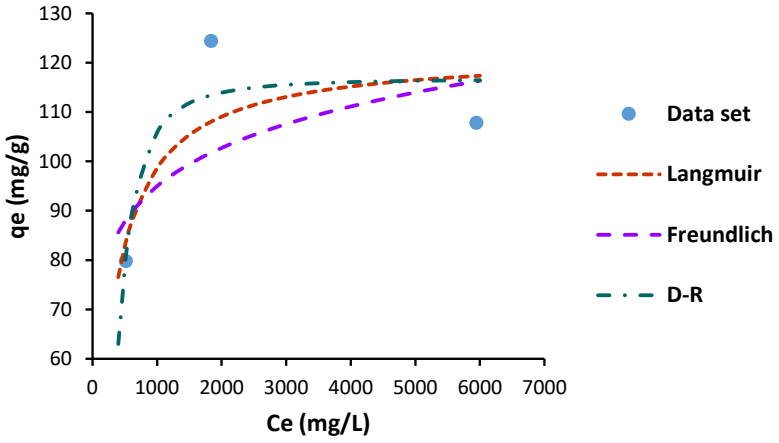

(b) Two-parameter isotherm modelling at 30 °C

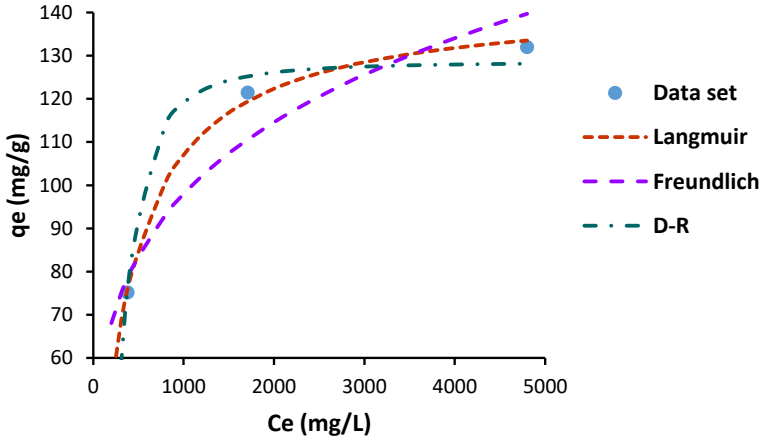

(c) Two-parameter isotherm modelling at 35 °C

Figure 8-13: The isotherm modelling results for 1-decanol adsorbate adsorbed onto activated alumina F-220 at adsorption temperatures of a) 25, b) 30 and c) 35 °C

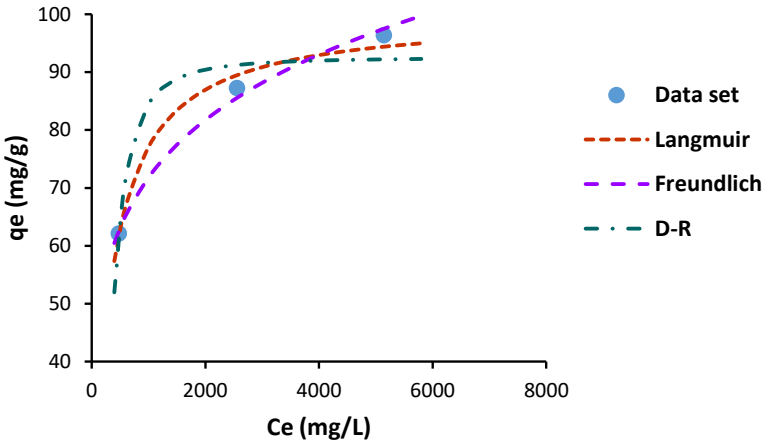

(a) Two-parameter isotherm modelling at 25 °C

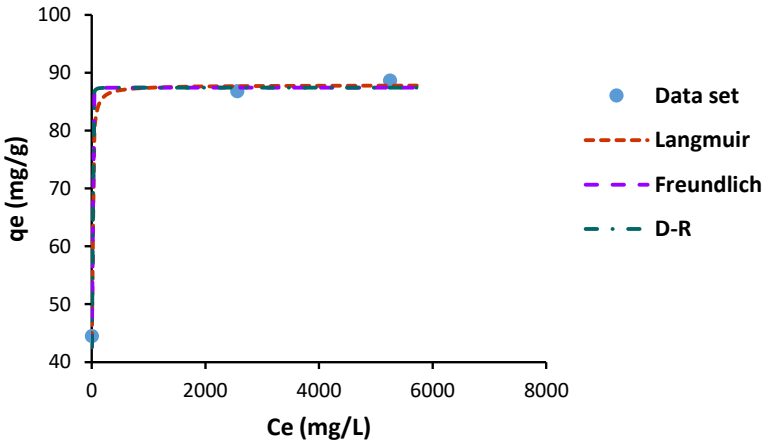

(b) Two-parameter isotherm modelling at 30 °C

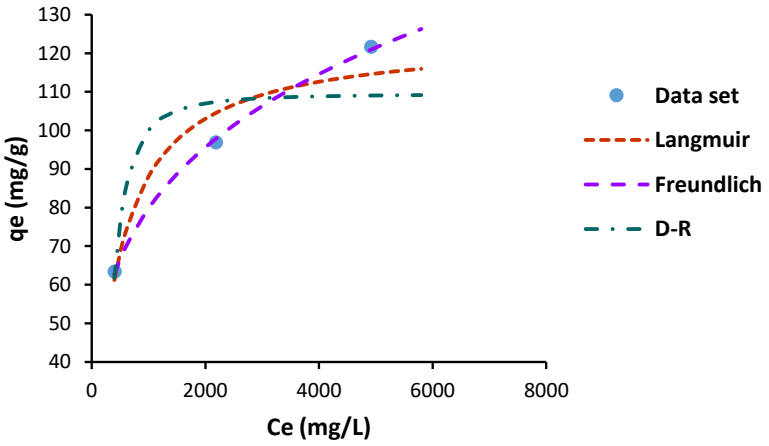

(c) Two-parameter isotherm modelling at 35 °C

Figure 8-14: The isotherm modelling results for 1-hexanol adsorbate adsorbed onto Selexsorb® CD at adsorption temperatures of a) 25, b) 30 and c) 35 °

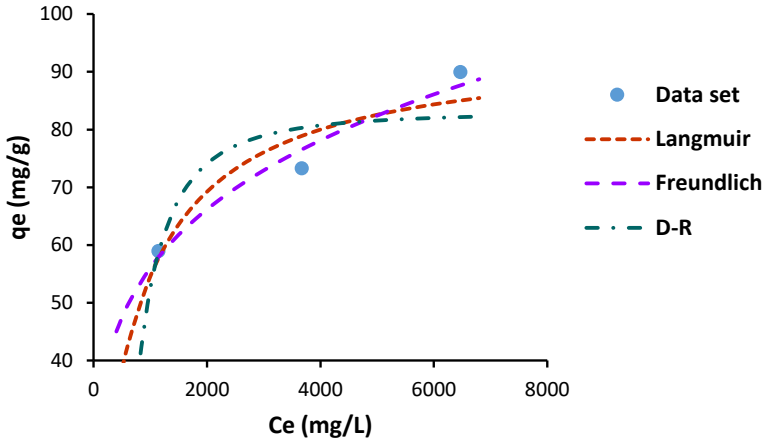

(a) Two-parameter isotherm modelling at 25 °C

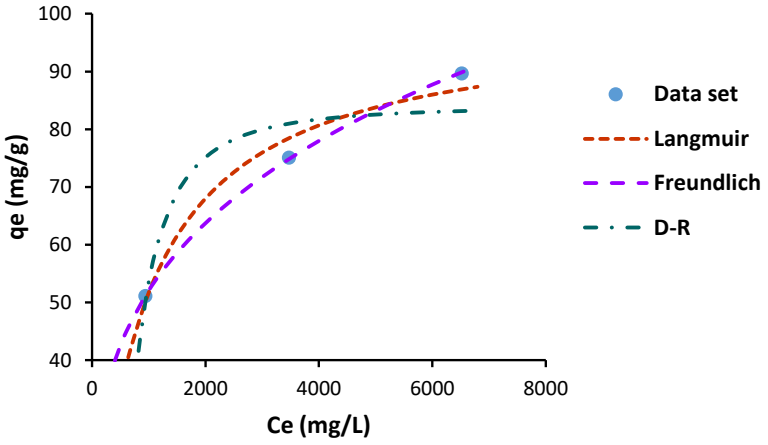

(b) Two-parameter isotherm modelling at 30 °C

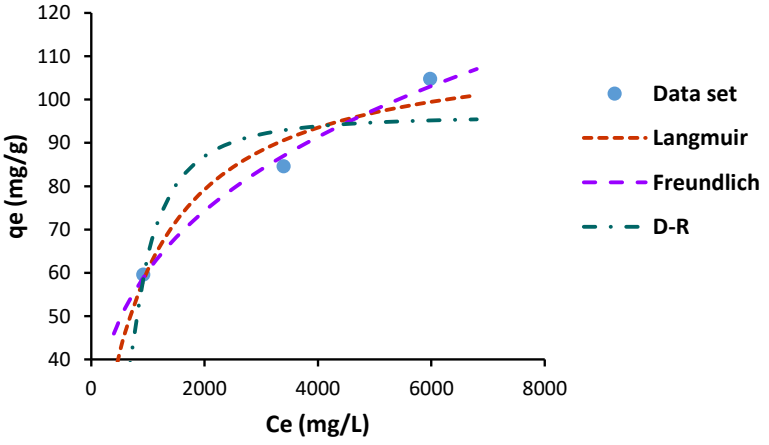

(c) Two-parameter isotherm modelling at 35 °C

Figure 8-15: The isotherm modelling results for 1-octanol adsorbate adsorbed onto Selexsorb® CD at adsorption temperatures of a) 25, b) 30 and c) 35 °C

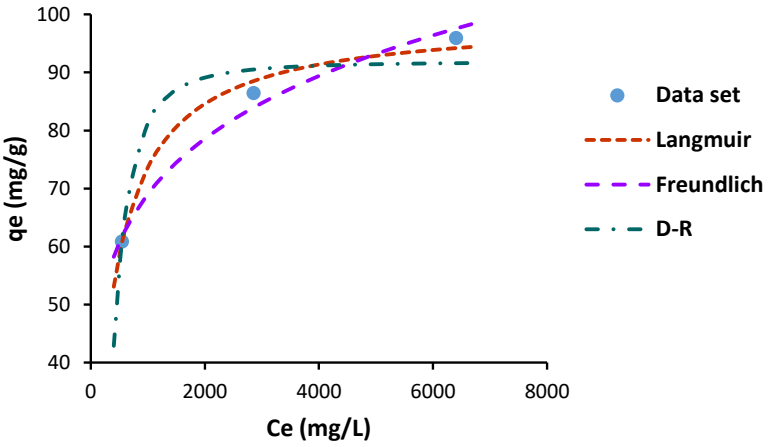

(a) Two-parameter isotherm modelling at 25 °C

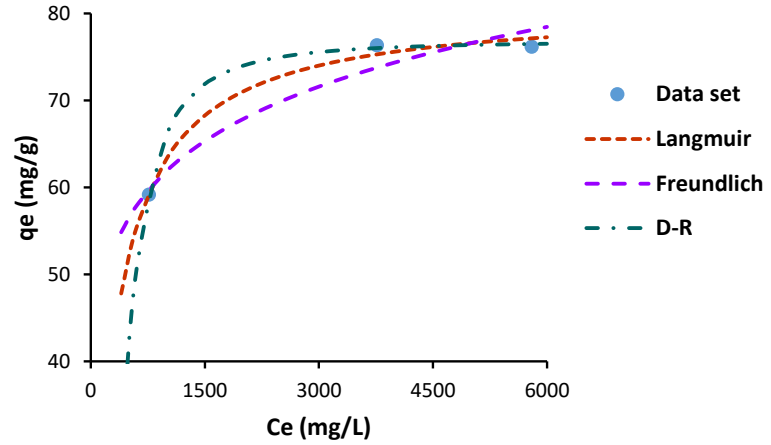

(b) Two-parameter isotherm modelling at 30 °C

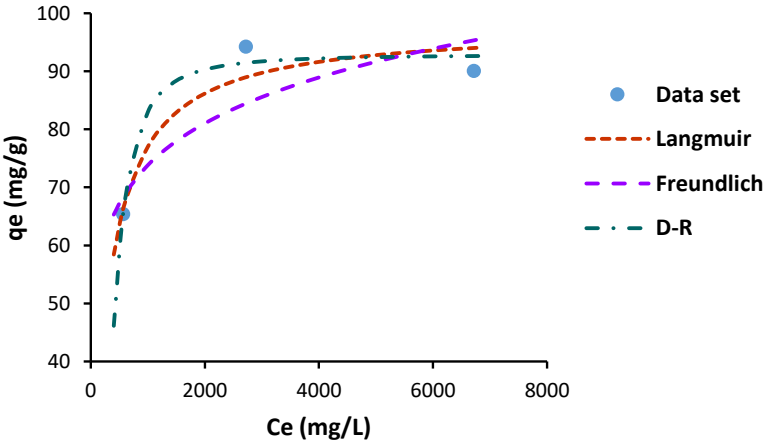

(c) Two-parameter isotherm modelling at 35 °C

Figure 8-16: The isotherm modelling results for 1-decanol adsorbate adsorbed onto Selexsorb® CD at adsorption temperatures of a) 25, b) 30 and c) 35 °C

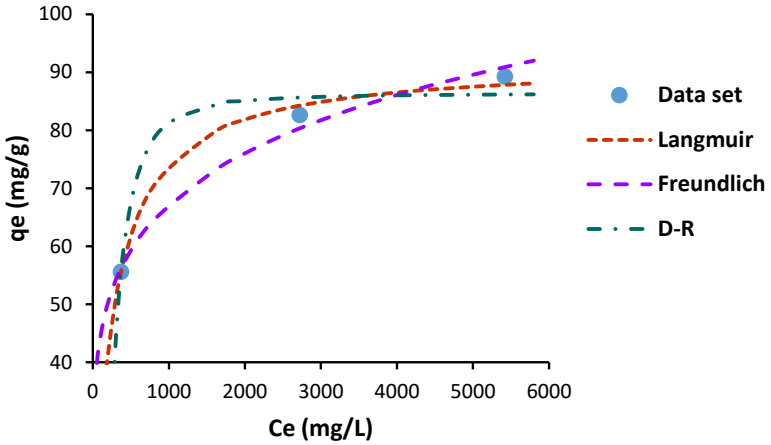

(a) Two-parameter isotherm modelling at 25 °C

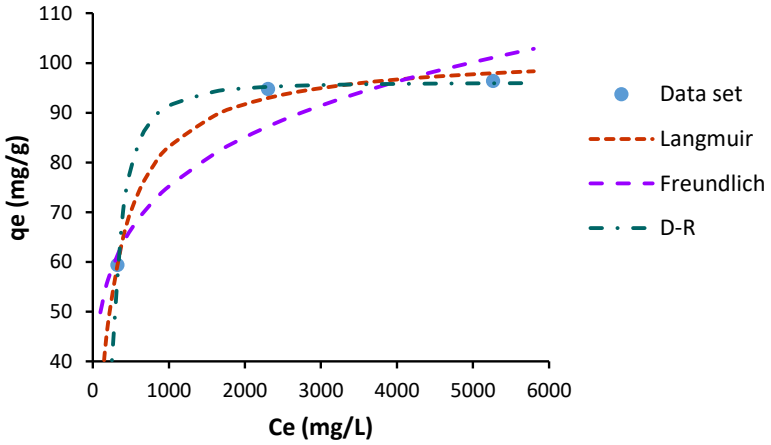

(b) Two-parameter isotherm modelling at 30 °C

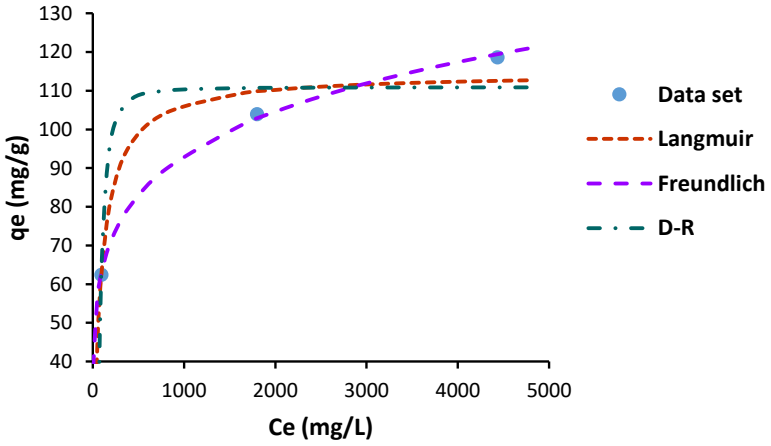

(c) Two-parameter isotherm modelling at 35 °C

Figure 8-17: The isotherm modelling results for 1-hexanol adsorbate adsorbed onto Selexsorb® CDx at adsorption temperatures of a) 25, b) 30 and c) 35 °C

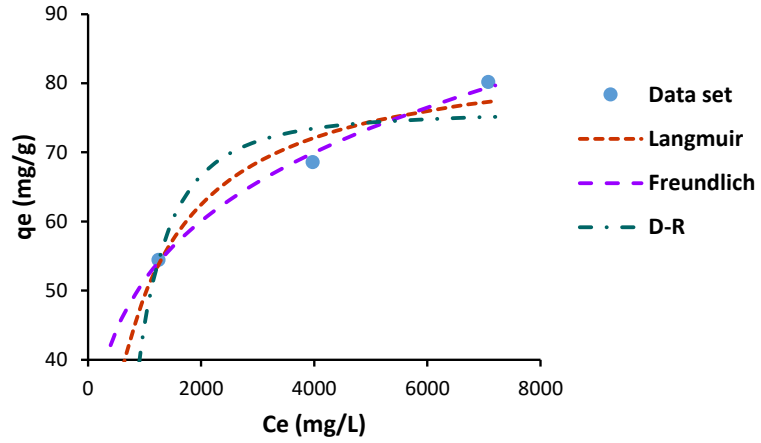

(a) Two-parameter isotherm modelling at 25 °C

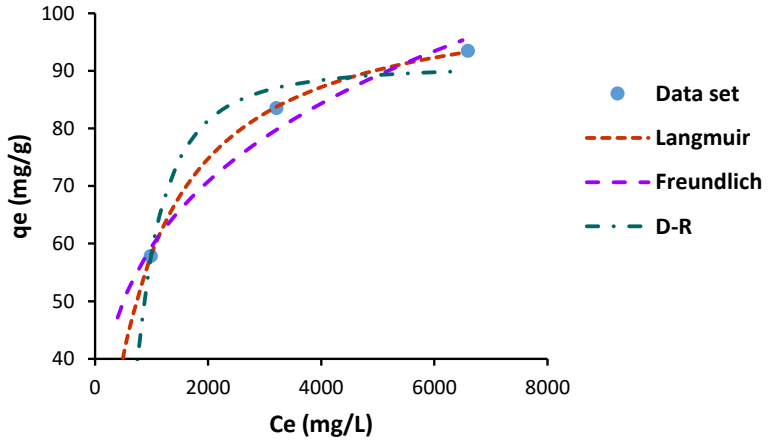

(b) Two-parameter isotherm modelling at 30 °C

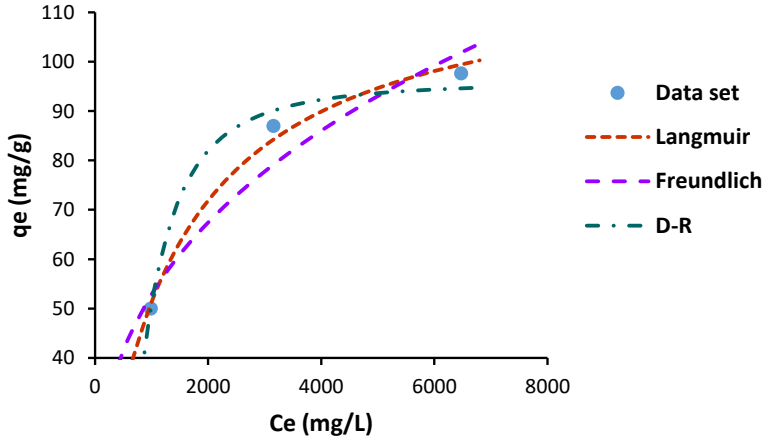

(c) Two-parameter isotherm modelling at 35 °C

Figure 8-18: The isotherm modelling results for 1-octanol adsorbate adsorbed onto Selexsorb® CDx at adsorption temperatures of a) 25, b) 30 and c) 35 °C

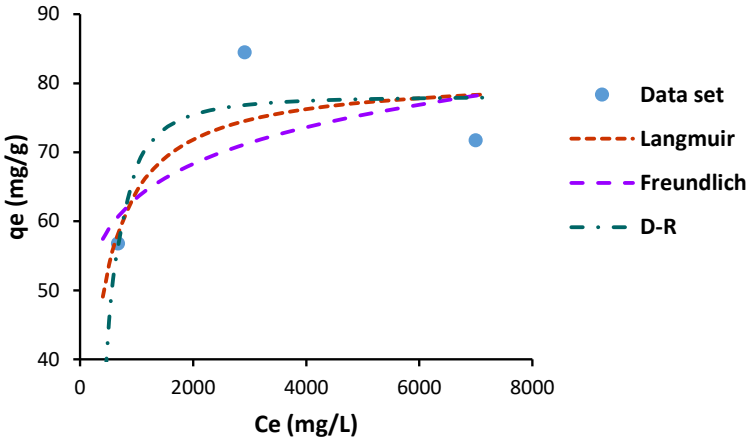

(a) Two-parameter isotherm modelling at 25 °C

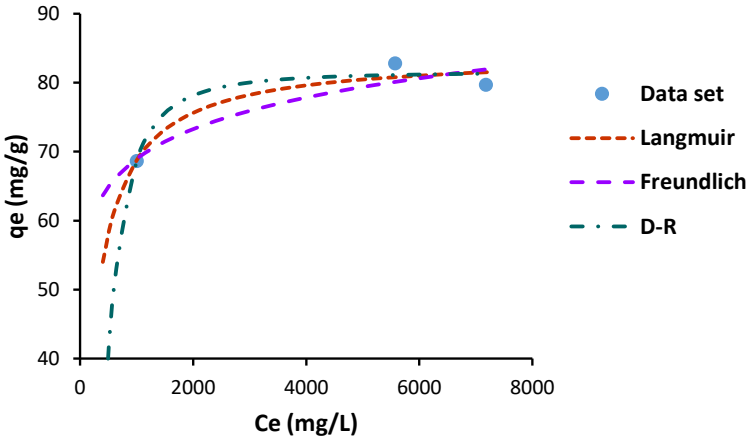

(b) Two-parameter isotherm modelling at 30 °C

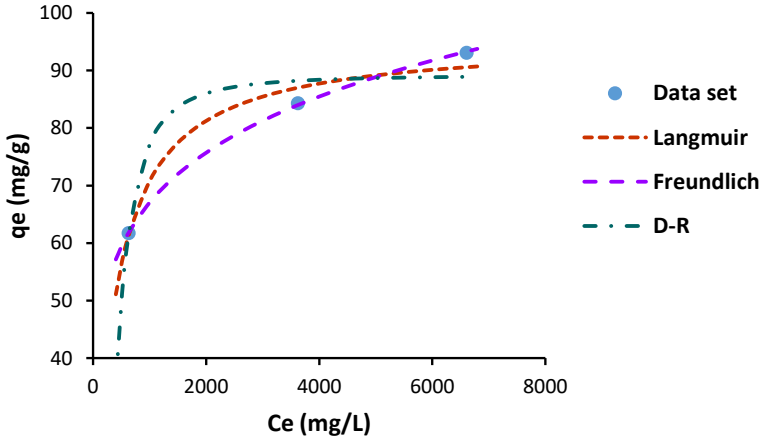

(c) Two-parameter isotherm modelling at 35 °C

Figure 8-19: The isotherm modelling results for 1-decanol adsorbate adsorbed onto Selexsorb® CDx at adsorption temperatures of a) 25, b) 30 and c) 35 °

8.20 Activated Alumina F-220 Kinetic Modelling Graphs

Figure 8-20, Figure 8-21 and Figure 8-22give the kinetic modelling results for 1-hexanol adsorbed onto activated alumina F-220 at temperatures of 25, 30 and 35 °C respectively.

Figure 8-23, Figure 8-24 and Figure 8-25 give the kinetic modelling results for 1-octanol adsorbed onto activated alumina F-220 at temperatures of 25, 30 and 35 °C respectively.

Figure 8-25, Figure 8-26 and Figure 8-27 give the kinetic modelling results for 1-decanol adsorbed onto activated alumina F-220 at temperatures of 25, 30 and 35 °C respectively.

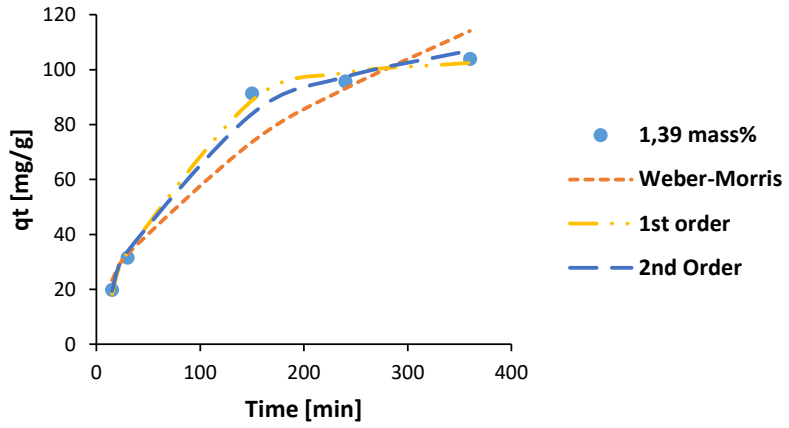

a) 1-hexanol kinetic model fits at 25 °C and 1,39 initial mass% of alcohol in solution

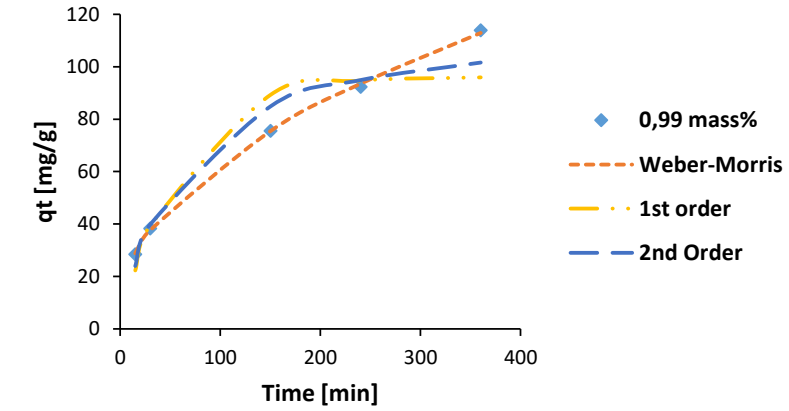

b) 1-hexanol kinetic model fits at 25 °C and 0,99 initial mass% of alcohol in solution

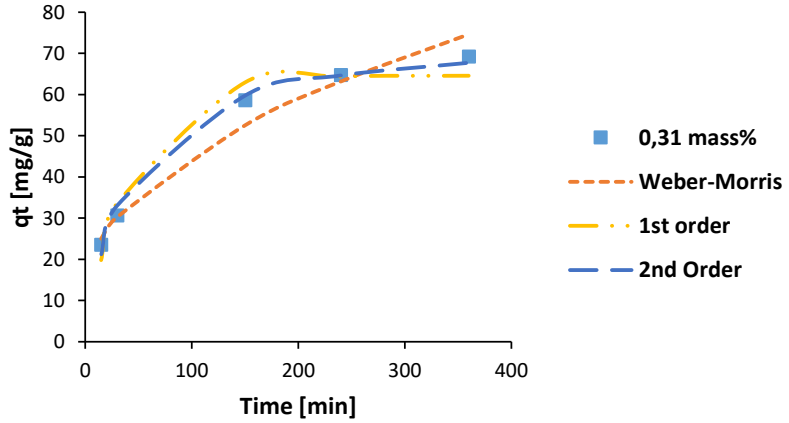

c) 1-hexanol kinetic model fits at 25 °C and 0,31 initial mass% of alcohol in solution

Figure 8-20: The kinetic modelling results for 1-hexanol at solution initial alcohol mass percentages of a) 1,39, b) 0,99 and c) 0,31 adsorbed onto activated alumina F-220 at a temperature of 25 °C.

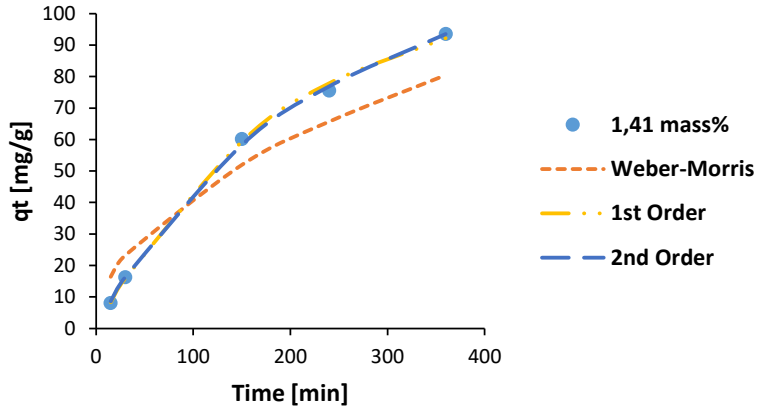

a) 1-hexanol kinetic model fits at 30 °C and 1,41 initial mass% of alcohol in solution

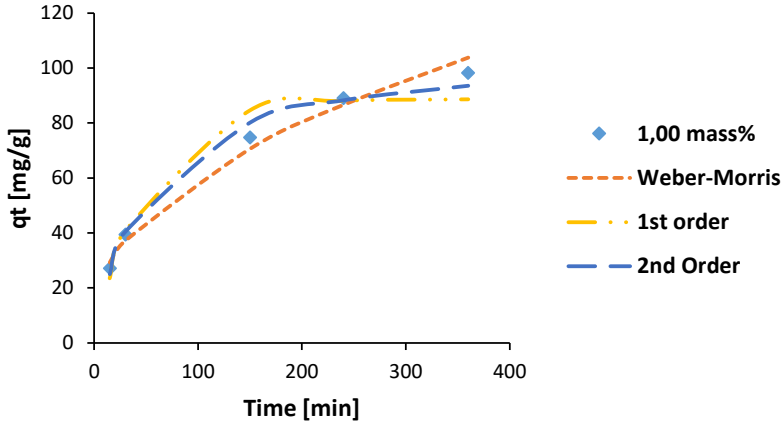

b) 1-hexanol kinetic model fits at 30 °C and 1,00 initial mass% of alcohol in solution

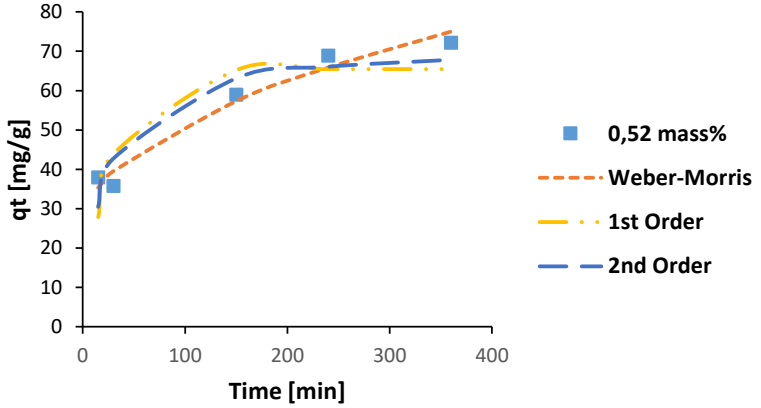

c) 1-hexanol kinetic model fits at 30 °C and 0,52 initial mass% of alcohol in solution

Figure 8-21: The kinetic modelling results for 1-hexanol at solution initial alcohol mass percentages of a) 1,41, b) 1,00 and c) 0,52 adsorbed onto activated alumina F-220 at a temperature of 30 °C.

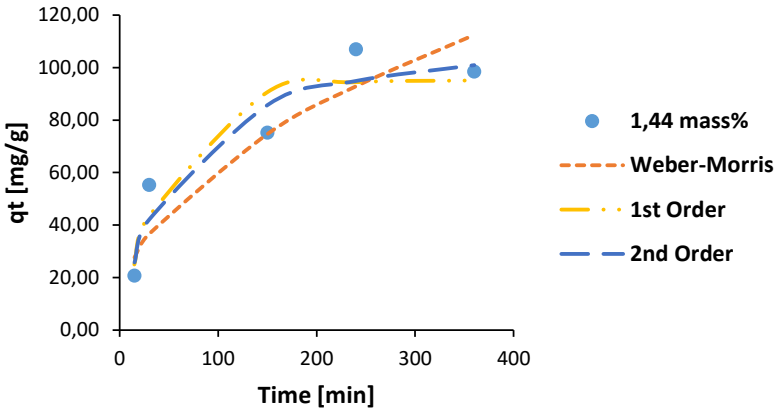

a) 1-hexanol kinetic model fits at 35 °C and 1,44 initial mass% of alcohol in solution

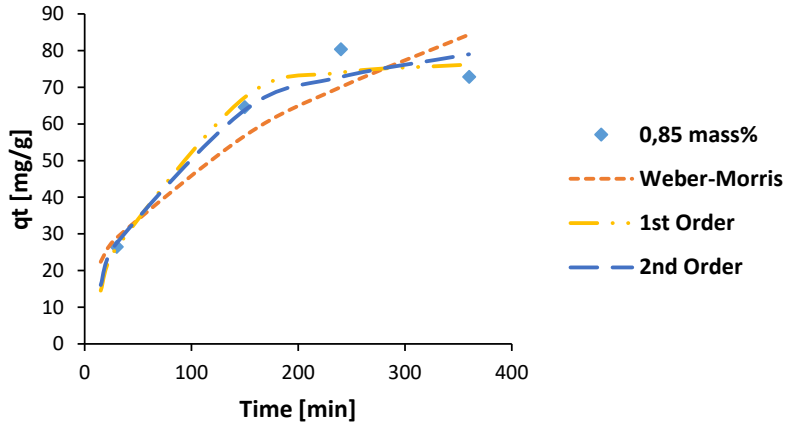

b) 1-hexanol kinetic model fits at 35 °C and 0,85 initial mass% of alcohol in solution

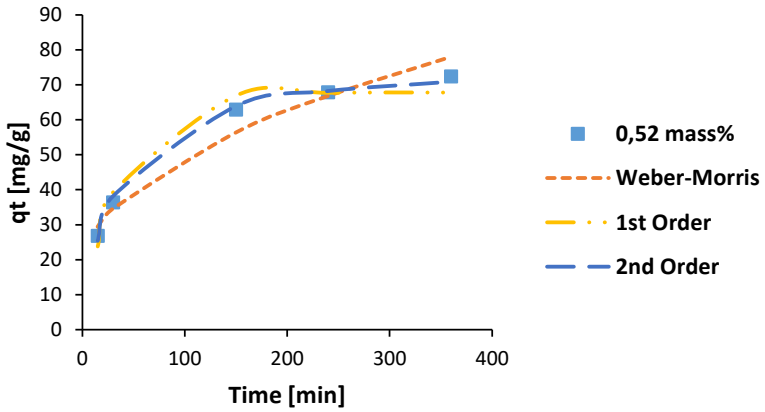

c) 1-hexanol kinetic model fits at 35 °C and 0,52 initial mass% of alcohol in solution

Figure 8-22: The kinetic modelling results for 1-hexanol at solution initial alcohol mass percentages of a) 1,44, b) 0,85 and c) 0,52 adsorbed onto activated alumina F-220 at a temperature of 35 °C.

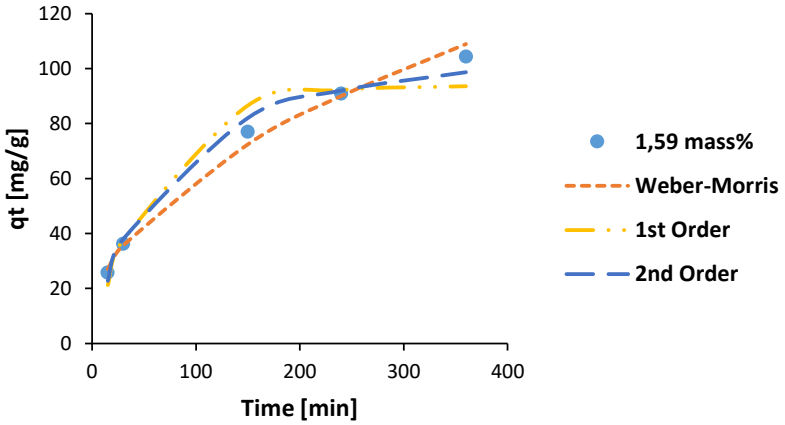

a) 1-octanol kinetic model fits at 25 °C and 1,59 initial mass% of alcohol in solution

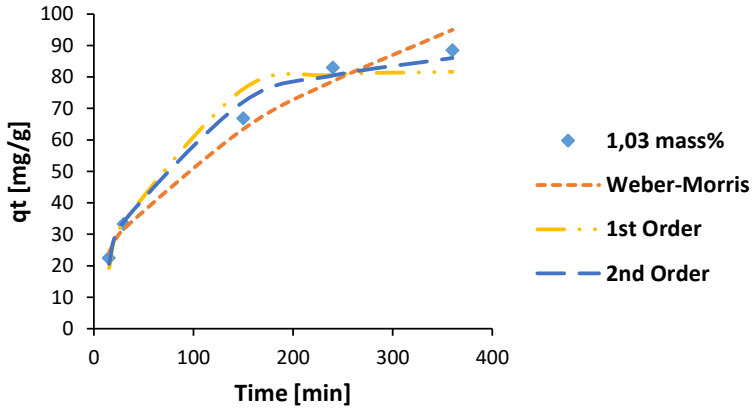

b) 1-octanol kinetic model fits at 25 °C and 1,03 initial mass% of alcohol in solution

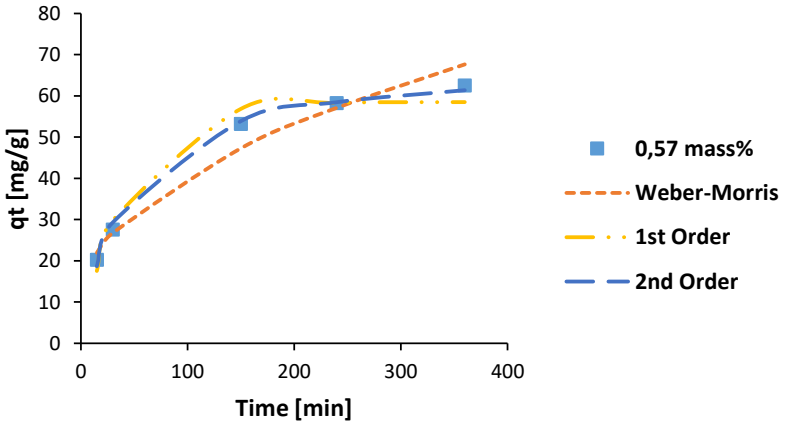

c) 1-octanol kinetic model fits at 25 °C and 0,57 initial mass% of alcohol in solution

Figure 8-23: The kinetic modelling results for 1-octanol at solution initial alcohol mass percentages of a) 1,59, b) 1,03 and c) 0,57 adsorbed onto activated alumina F-220 at a temperature of 25 °C

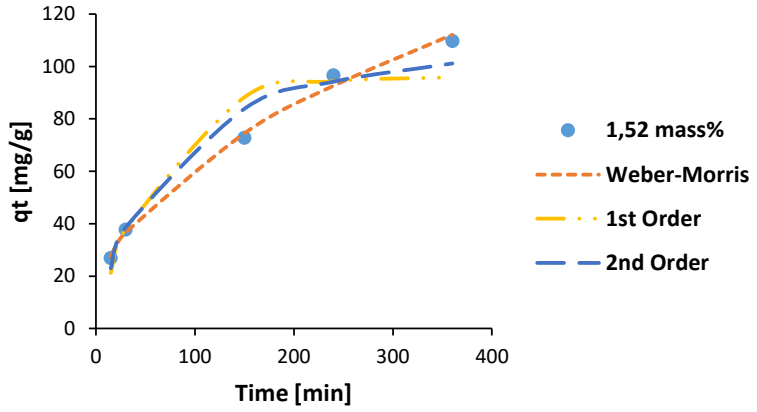

a) 1-octanol kinetic model fits at 30 °C and 1,52 initial mass% of alcohol in solution

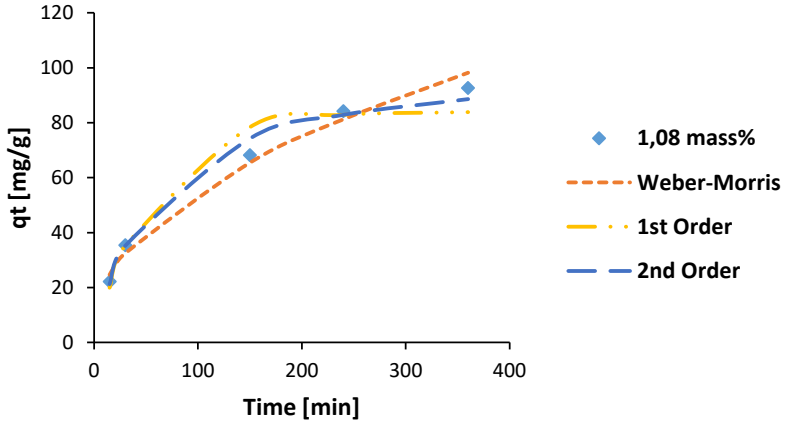

b) 1-octanol kinetic model fits at 30 °C and 1,08 initial mass% of alcohol in solution

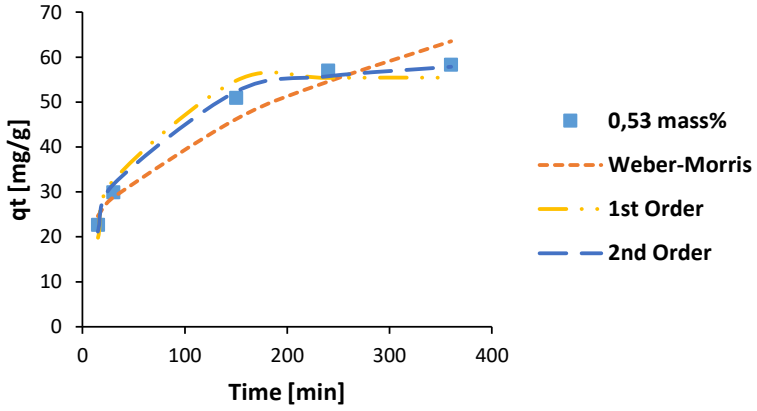

c) 1-octanol kinetic model fits at 30 °C and 0,53 initial mass% of alcohol in solution

Figure 8-24: The kinetic modelling results for 1-octanol at solution initial alcohol mass percentages of a) 1,52, b) 1,08 and c) 0,53 adsorbed onto activated alumina F-220 at a temperature of 30 °C

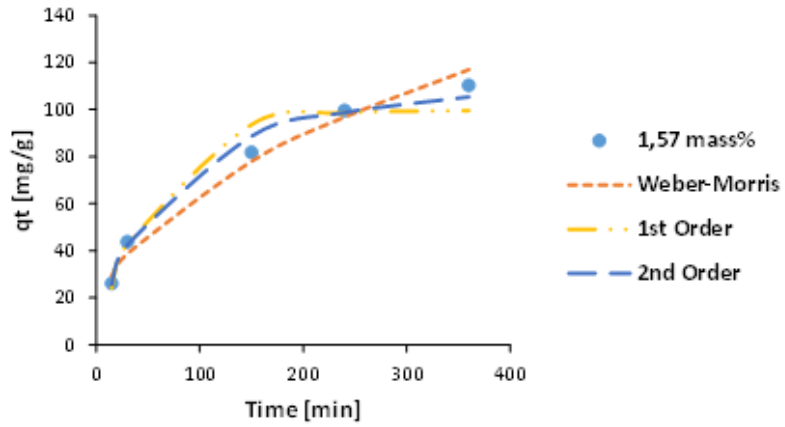

a) 1-octanol kinetic model fits at 35 °C and 1,57 initial mass% of alcohol in solution

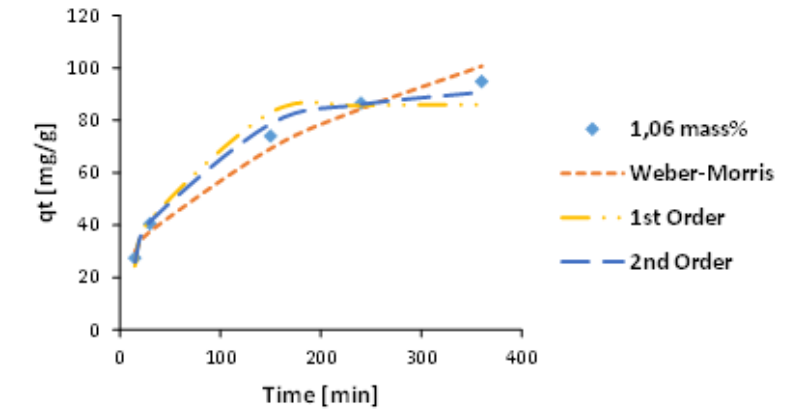

b) 1-octanol kinetic model fits at 35 °C and 1,06 initial mass% of alcohol in solution

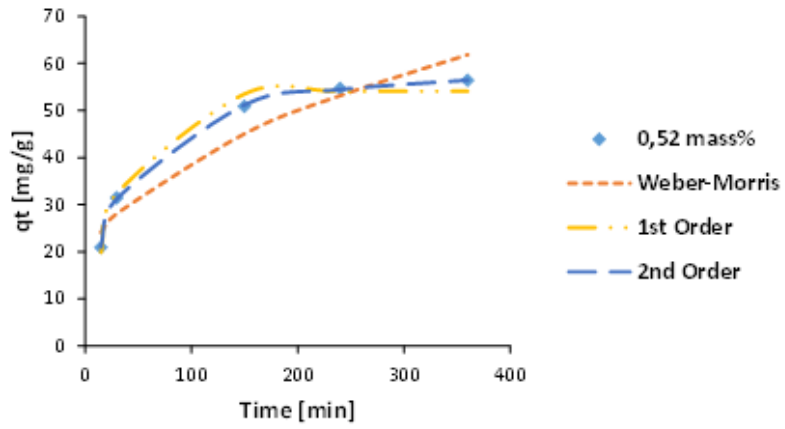

c) 1-octanol kinetic model fits at 35 °C and 0,52 initial mass% of alcohol in solution

Figure 8-25: The kinetic modelling results for 1-octanol at solution initial alcohol mass percentages of a) 1,57, b) 1,06 and c) 0,52 adsorbed onto activated alumina F-220 at a temperature of 35 °C

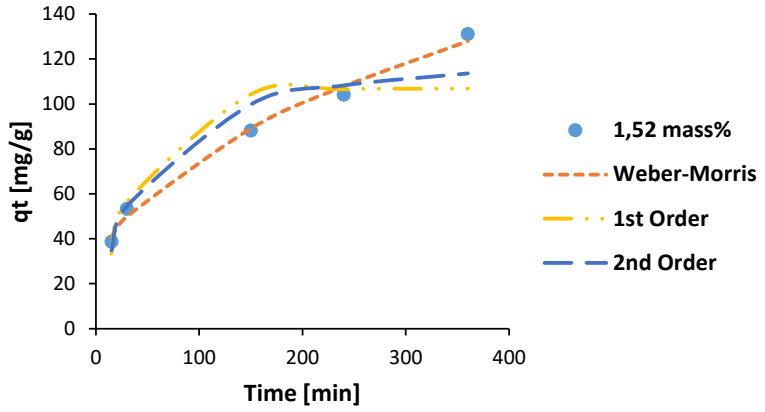

a) 1-decanol kinetic model fits at 25 °C and 1,52 initial mass% of alcohol in solution

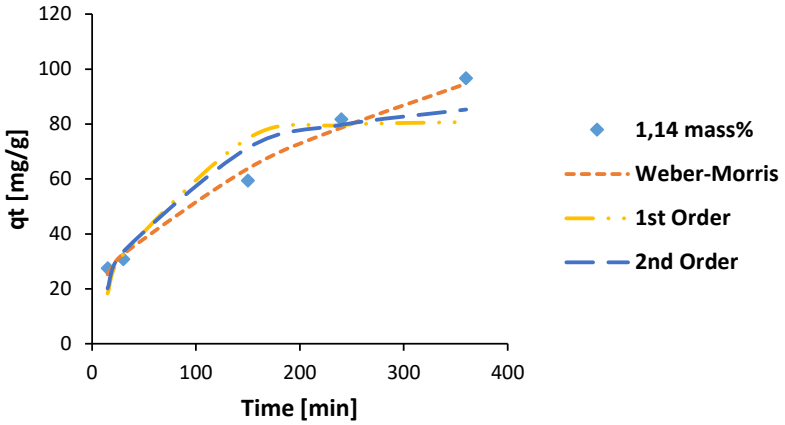

b) 1-decanol kinetic model fits at 25 °C and 1,14 initial mass% of alcohol in solution

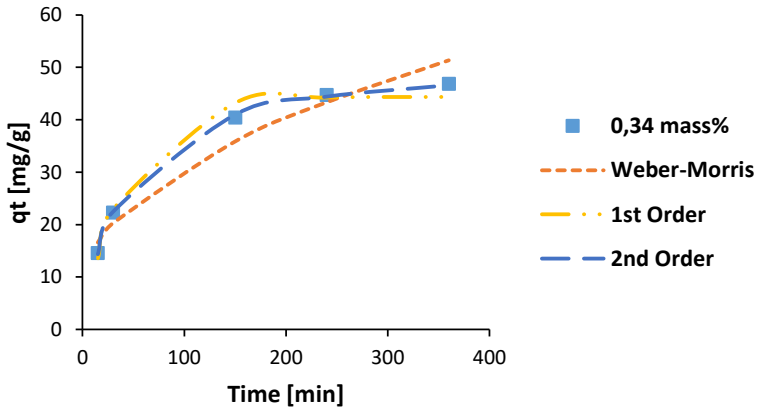

c) 1-decanol kinetic model fits at 25 °C and 0,34 initial mass% of alcohol in solution

Figure 8-26: The kinetic modelling results for 1-decanol at solution initial alcohol mass percentages of a) 1,52, b) 1,14 and c) 0,34 adsorbed onto activated alumina F-220 at a temperature of 25 °C

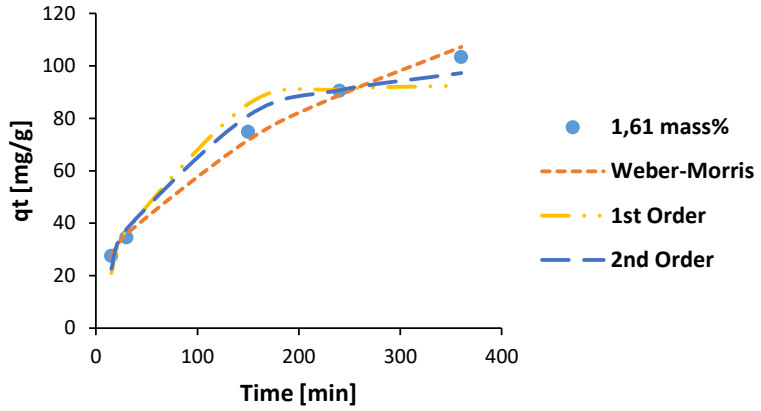

a) 1-decanol kinetic model fits at 30 °C and 1,61 initial mass% of alcohol in solution

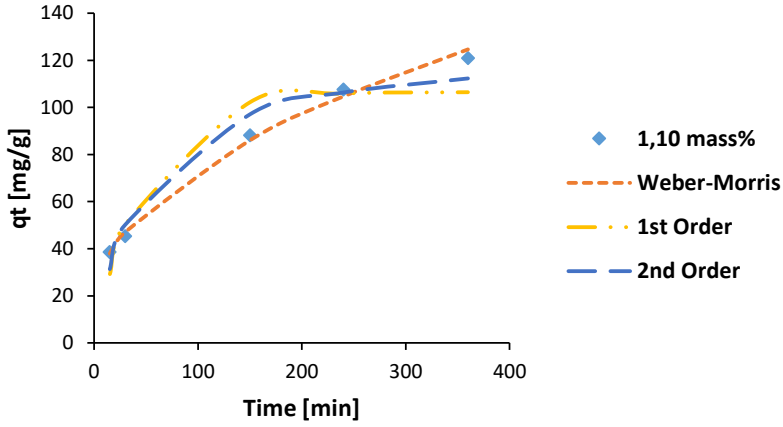

b) 1-decanol kinetic model fits at 30 °C and 1,10 initial mass% of alcohol in solution

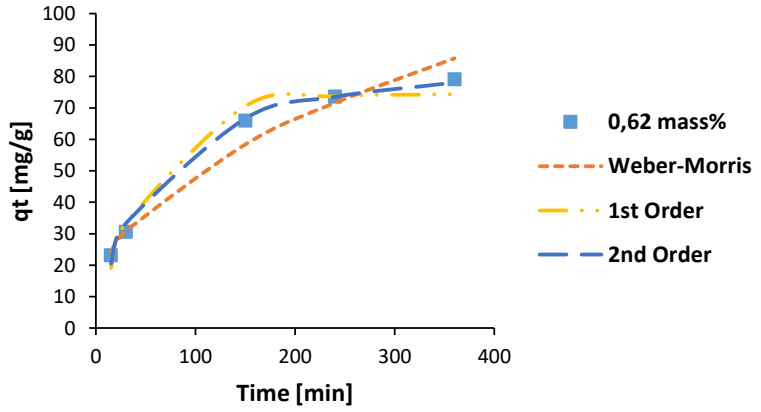

c) 1-decanol kinetic model fits at 30 °C and 0,62 initial mass% of alcohol in solution

Figure 8-27: The kinetic modelling results for 1-decanol at solution initial alcohol mass percentages of a) 1,61, b) 1,10 and c) 0,62 adsorbed onto activated alumina F-220 at a temperature of 30 °C

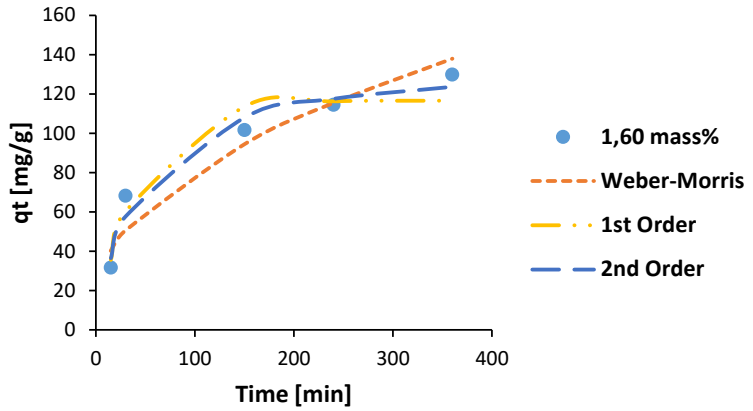

a) 1-decanol kinetic model fits at 35 °C and 1,60 initial mass% of alcohol in solution

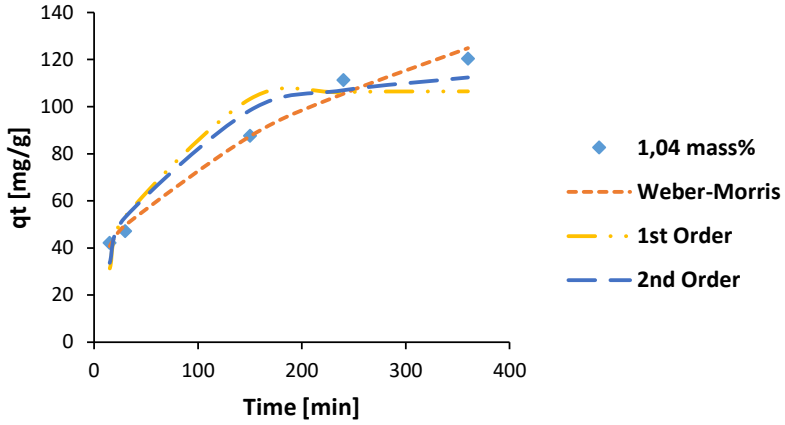

b) 1-decanol kinetic model fits at 35 °C and 1,04 initial mass% of alcohol in solution

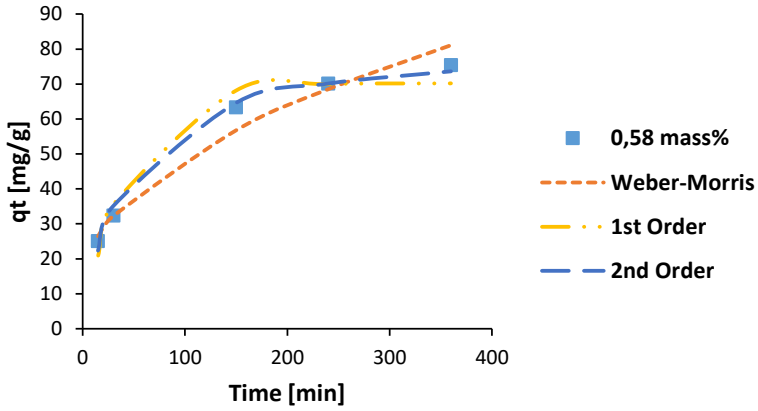

c) 1-decanol kinetic model fits at 35 °C and 0,58 initial mass% of alcohol in solution

Figure 8-28: The kinetic modelling results for 1-decanol at solution initial alcohol mass percentages of a) 1,60, b) 1,04 and c) 0,58 adsorbed onto activated alumina F-220 at a temperature of 35 °C

8.21 Selexsorb® CD Kinetic Modelling Graphs

Figure 8-29, Figure 8-30 and Figure 8-31 give the kinetic modelling results for 1-hexanol adsorbed onto Selexsorb® CD at temperatures of 25, 30 and 35 °C respectively.

Figure 8-32, Figure 8-33 and Figure 8-34 give the kinetic modelling results for 1-octanol adsorbed onto Selexsorb® CD at temperatures of 25, 30 and 35 °C respectively.

Figure 8-35, Figure 8-36 and Figure 8-37 give the kinetic modelling results for 1-decanol adsorbed onto Selexsorb® CD at temperatures of 25, 30 and 35 °C respectively.

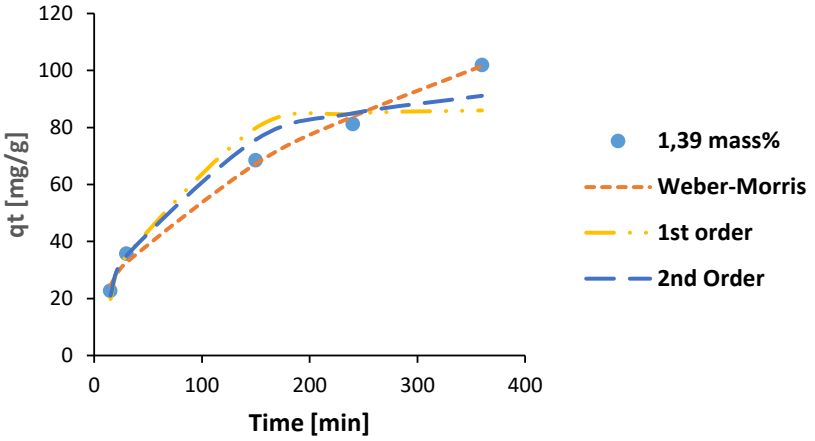

a) 1-hexanol kinetic model fits at 25 °C and 1,39 initial mass% of alcohol in solution

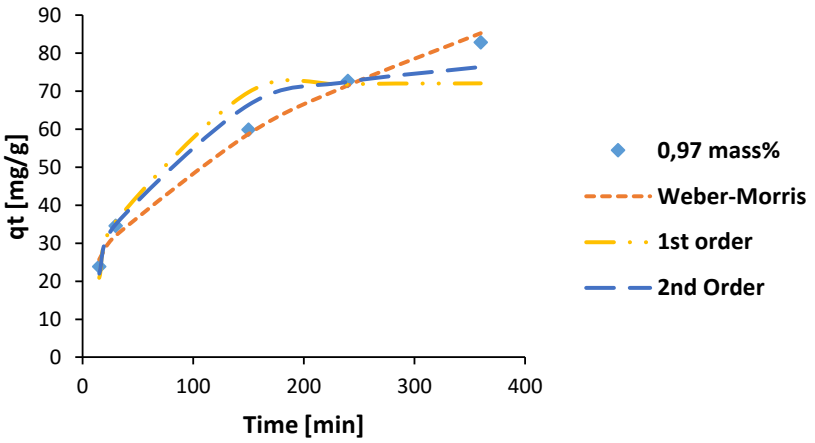

b) 1-hexanol kinetic model fits at 25 °C and 0,97 initial mass% of alcohol in solution

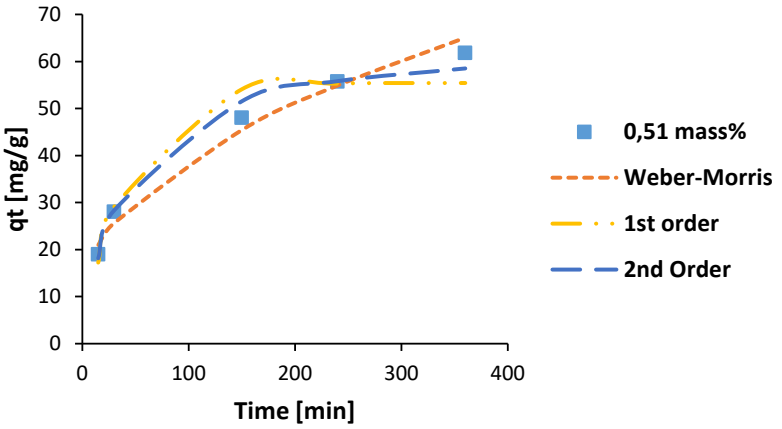

c) 1-hexanol kinetic model fits at 25 °C and 0,51 initial mass% of alcohol in solution

Figure 8-29: The kinetic modelling results for 1-hexanol at solution initial alcohol mass percentages of a) 1,39, b) 0,97 and c) 0,51 adsorbed onto Selexsorb® CD at a temperature of 25 °C.

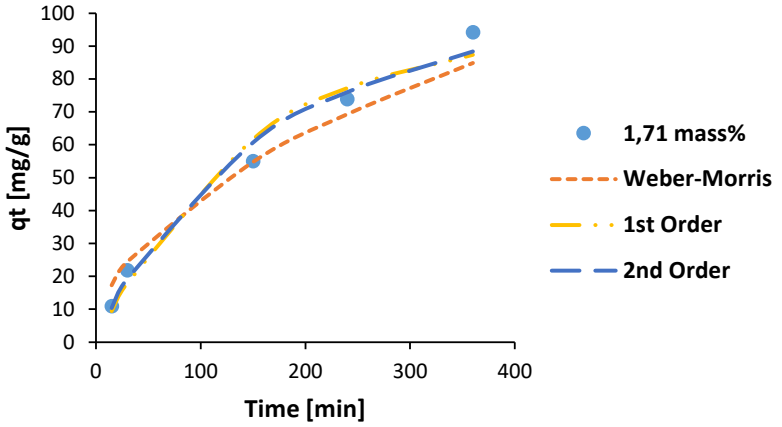

a) 1-hexanol kinetic model fits at 30 °C and 1,71 initial mass% of alcohol in solution

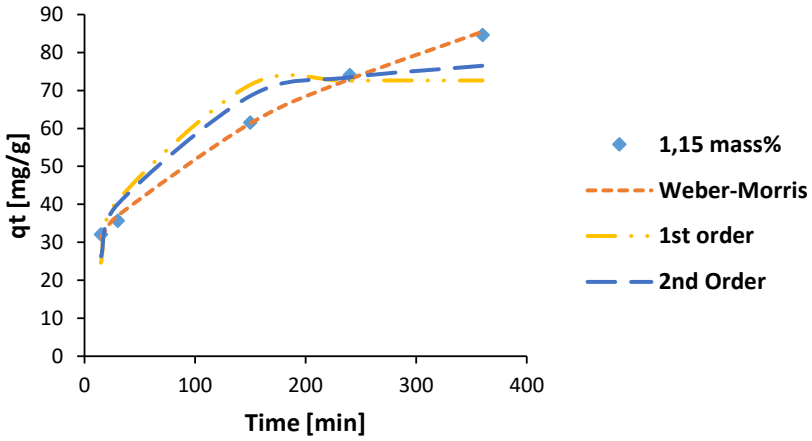

b) 1-hexanol kinetic model fits at 30 °C and 1,15 initial mass% of alcohol in solution

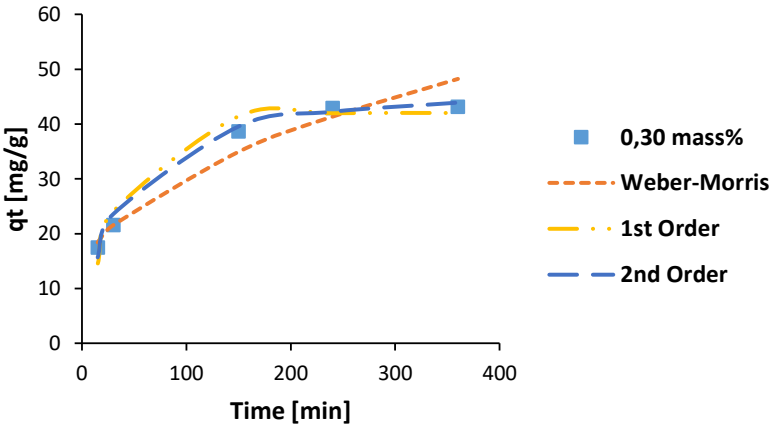

c) 1-hexanol kinetic model fits at 30 °C and 0,30 initial mass% of alcohol in solution

Figure 8-30: The kinetic modelling results for 1-hexanol at solution initial alcohol mass percentages of a) 1,71, b) 1,15 and c) 0,30 adsorbed onto Selexsorb® CD at a temperature of 30 °C.

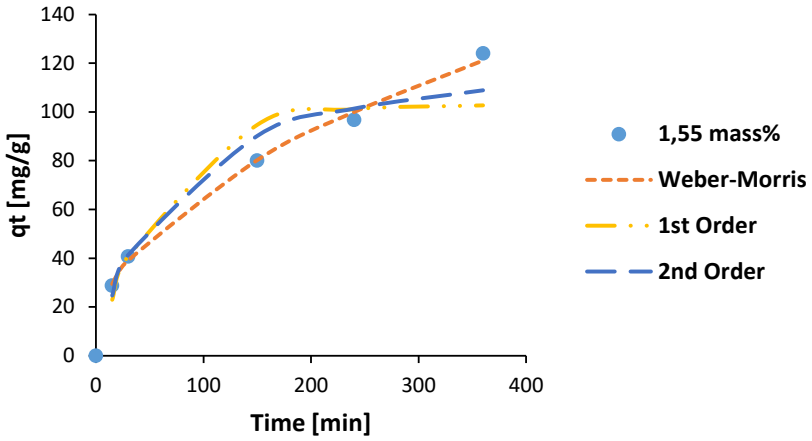

a) 1-hexanol kinetic model fits at 35 °C and 1,55 initial mass% of alcohol in solution

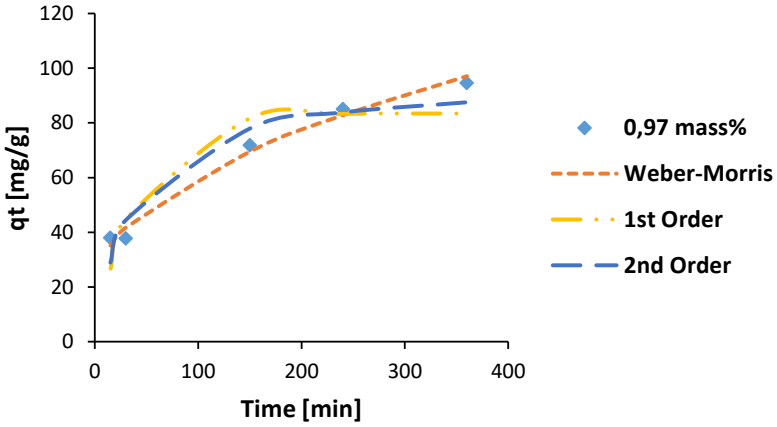

b) 1-hexanol kinetic model fits at 35 °C and 0,97 initial mass% of alcohol in solution

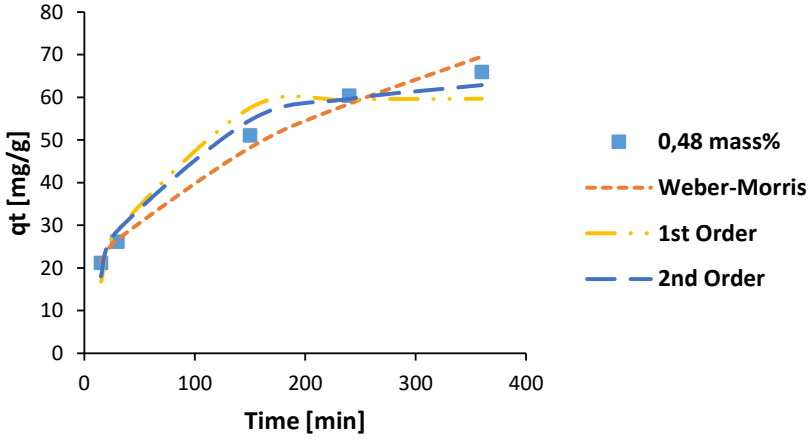

c) 1-hexanol kinetic model fits at 35 °C and 0,48 initial mass% of alcohol in solution

Figure 8-31: The kinetic modelling results for 1-hexanol at solution initial alcohol mass percentages of a) 1,55, b) 0,97 and c) 0,48 adsorbed onto Selexsorb® CD at a temperature of 35 °C.

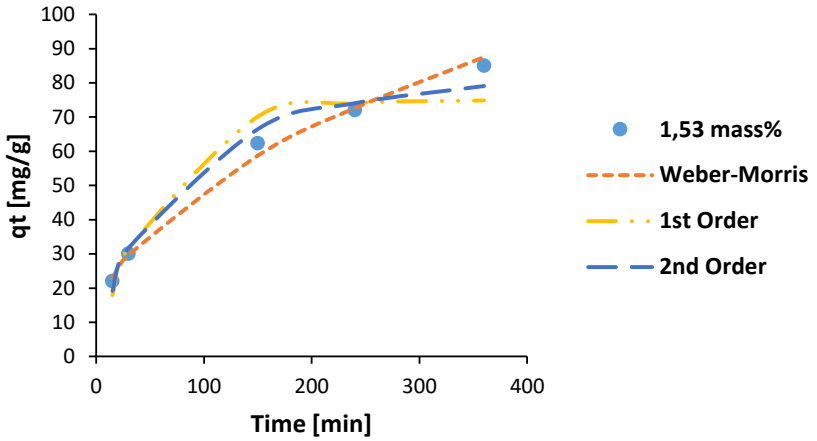

a) 1-octanol kinetic model fits at 25 °C and 1,53 initial mass% of alcohol in solution

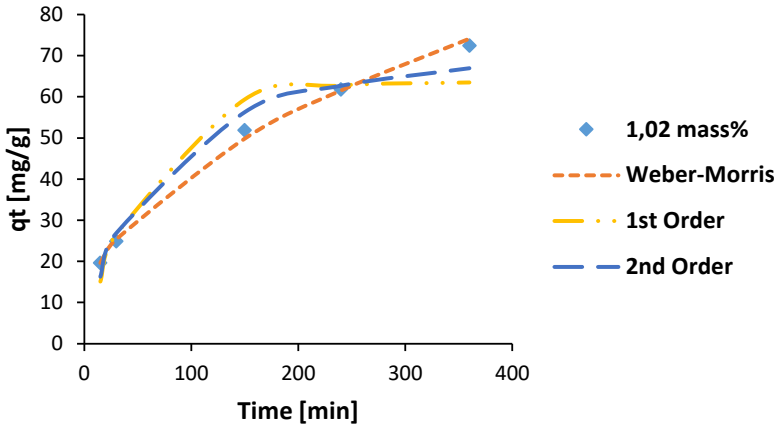

b) 1-octanol kinetic model fits at 25 °C and 1,02 initial mass% of alcohol in solution

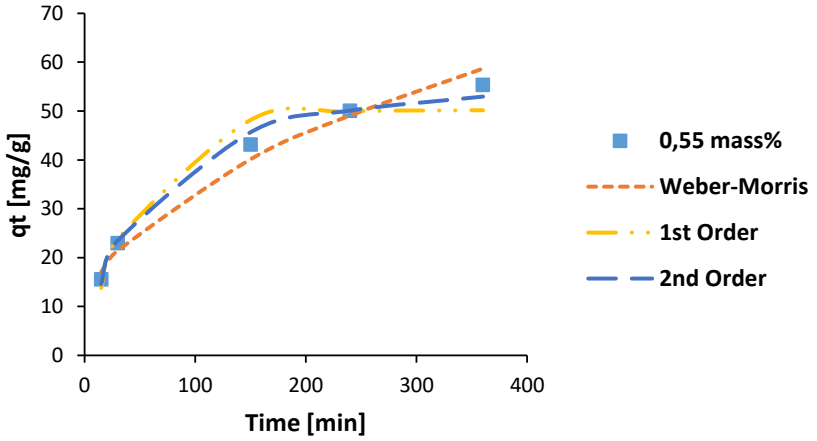

c) 1-octanol kinetic model fits at 25 °C and 0,55 initial mass% of alcohol in solution

Figure 8-32: The kinetic modelling results for 1-octanol at solution initial alcohol mass percentages of a) 1,53, b) 1,02 and c) 0,55 adsorbed onto Selexsorb® CD at a temperature of 25 °C.

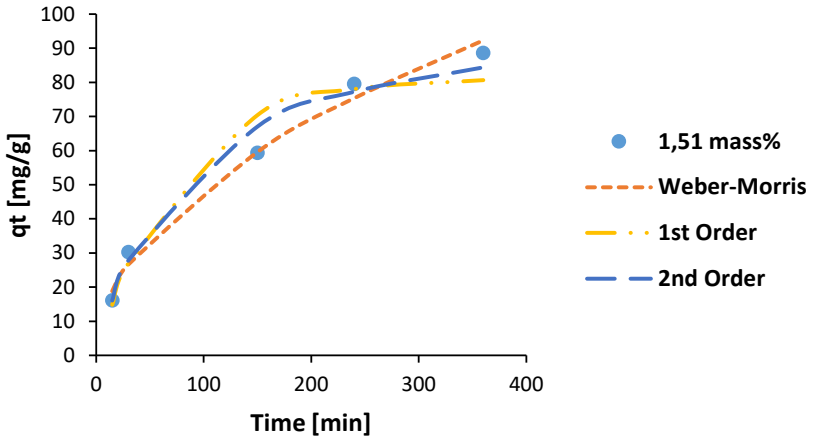

a) 1-octanol kinetic model fits at 30 °C and 1,51 initial mass% of alcohol in solution

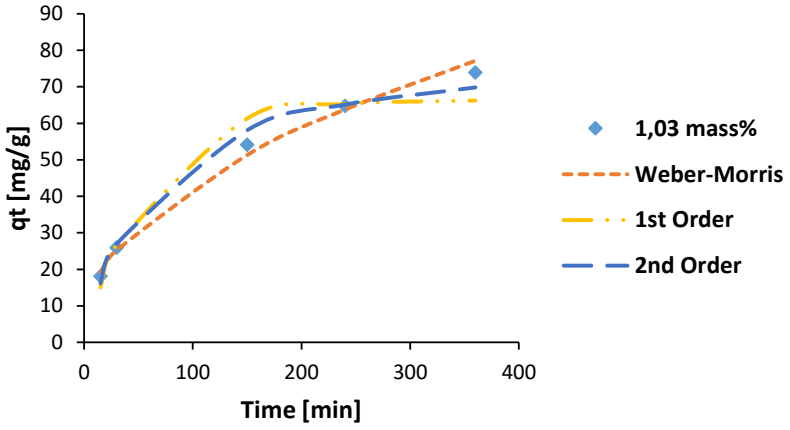

b) 1-octanol kinetic model fits at 30 °C and 1,03 initial mass% of alcohol in solution

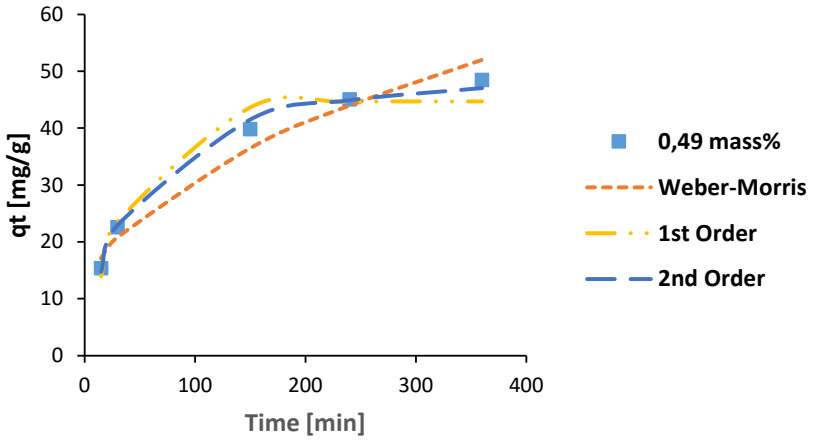

c) 1-octanol kinetic model fits at 30 °C and 0,49 initial mass% of alcohol in solution

Figure 8-33: The kinetic modelling results for 1-octanol at solution initial alcohol mass percentages of a) 1,51, b) 1,03 and c) 0,49 adsorbed onto Selexsorb® CD at a temperature of 30 °C.

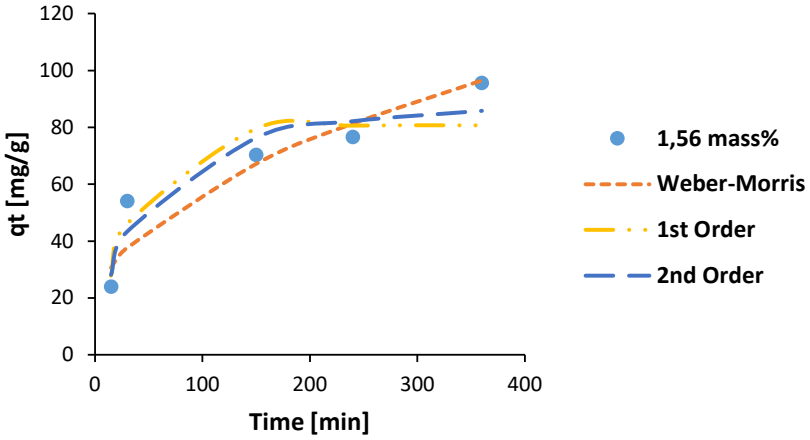

a) 1-octanol kinetic model fits at 35°C and 1,56 initial mass% of alcohol in solution

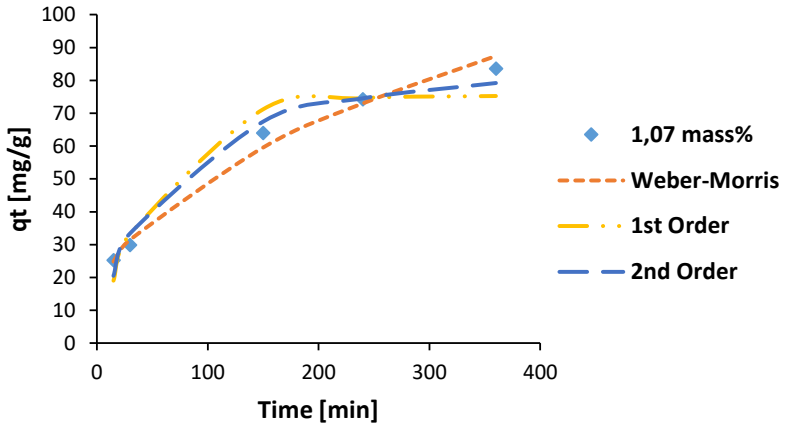

b) 1-octanol kinetic model fits at 35 °C and 1,07 initial mass% of alcohol in solution

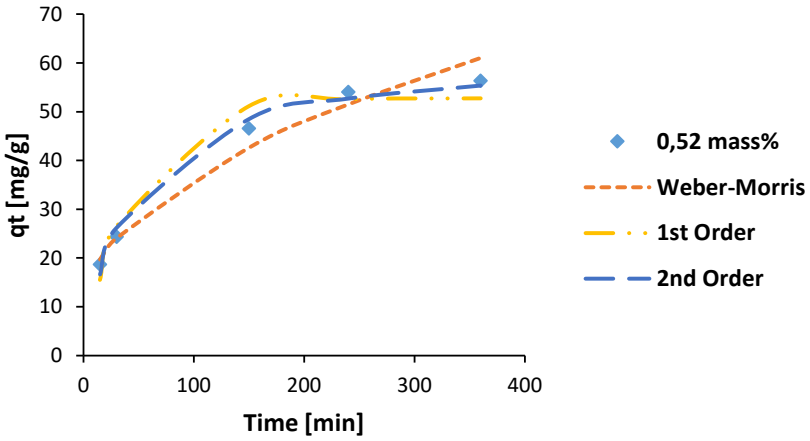

c) 1-octanol kinetic model fits at 35 °C and 0,52 initial mass% of alcohol in solution

Figure 8-34: The kinetic modelling results for 1-octanol at solution initial alcohol mass percentages of a) 1,56, b) 1,07 and c) 0,52 adsorbed onto Selexsorb® CD at a temperature of 35 °C.

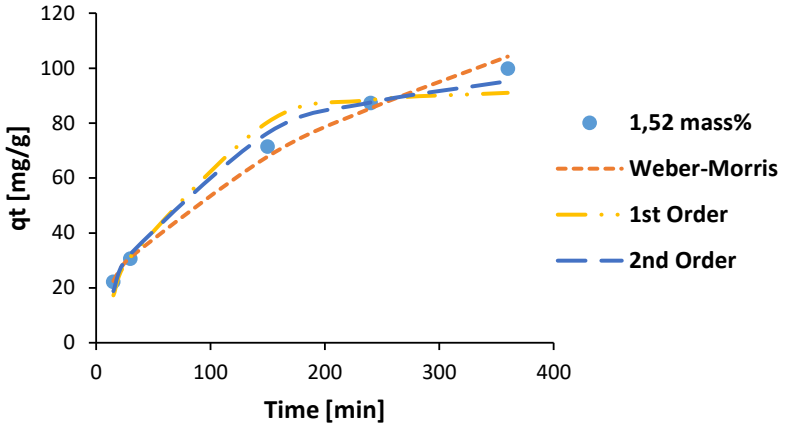

a) 1-decanol kinetic model fits at 25 °C and 1,52 initial mass% of alcohol in solution

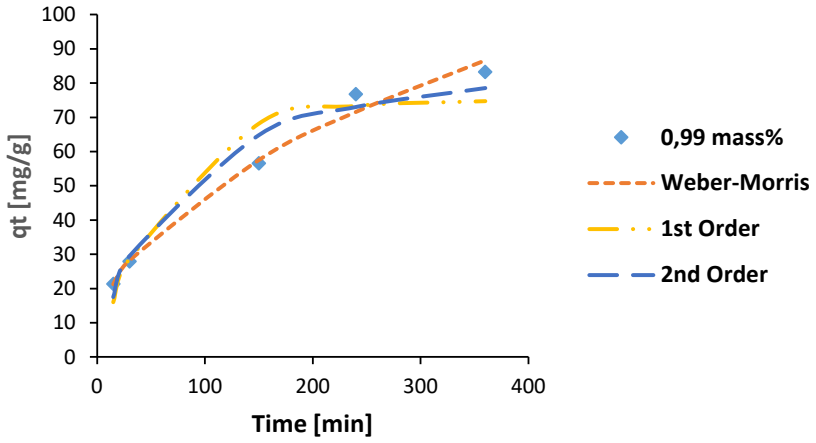

b) 1-decanol kinetic model fits at 25 °C and 0,99 initial mass% of alcohol in solution

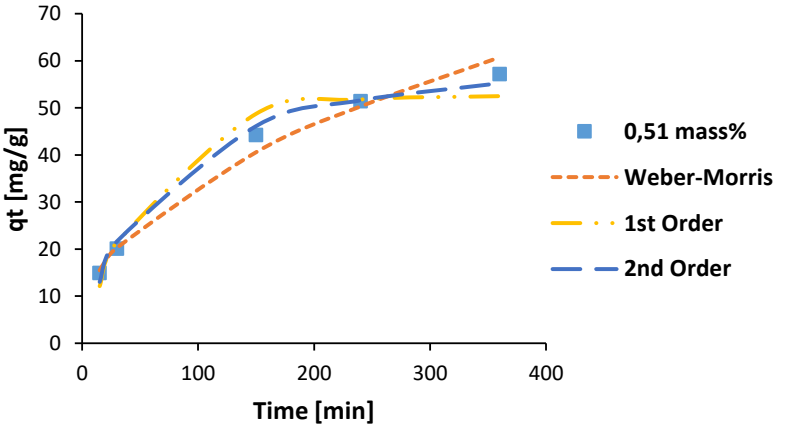

c) 1-decanol kinetic model fits at 25 °C and 0,51 initial mass% of alcohol in solution

Figure 8-35: The kinetic modelling results for 1-decanol at solution initial alcohol mass percentages of a) 1,52, b) 0,99 and c) 0,51 adsorbed onto Selexsorb® CD at a temperature of 25 °C.

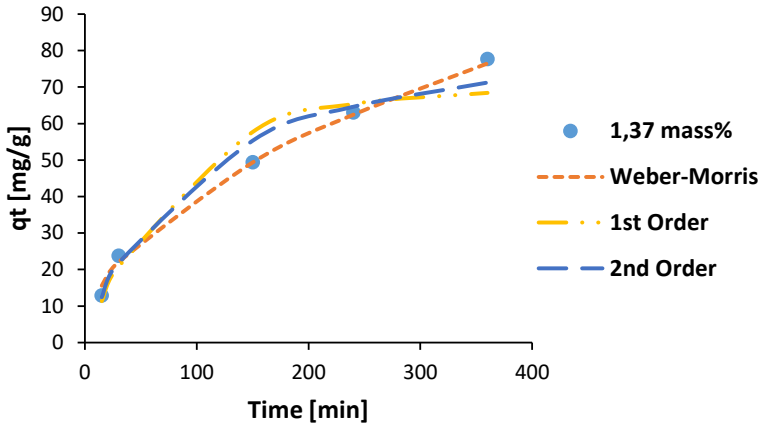

a) 1-decanol kinetic model fits at 30 °C and 1,37 initial mass% of alcohol in solution

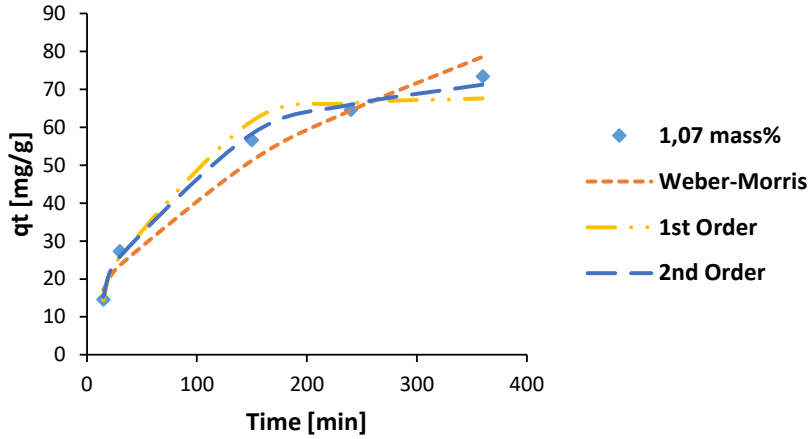

b) 1-decanol kinetic model fits at 30 °C and 1,07 initial mass% of alcohol in solution

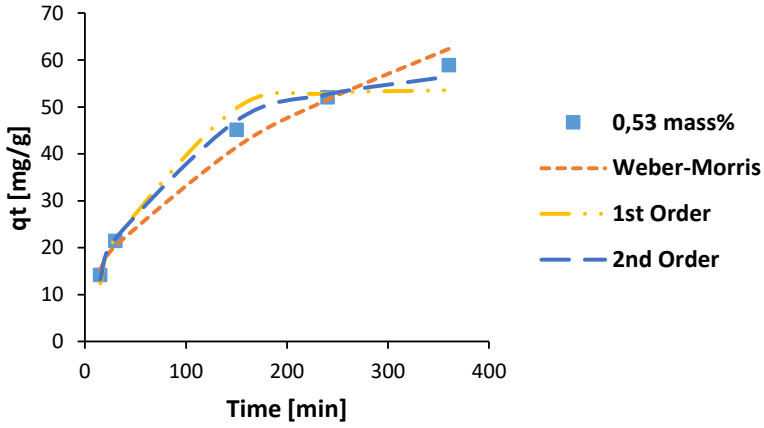

c) 1-decanol kinetic model fits at 30 °C and 0,53 initial mass% of alcohol in solution

Figure 8-36: The kinetic modelling results for 1-decanol at solution initial alcohol mass percentages of a) 1,37, b) 1,07 and c) 0,53 adsorbed onto Selexsorb® CD at a temperature of 30 °C.

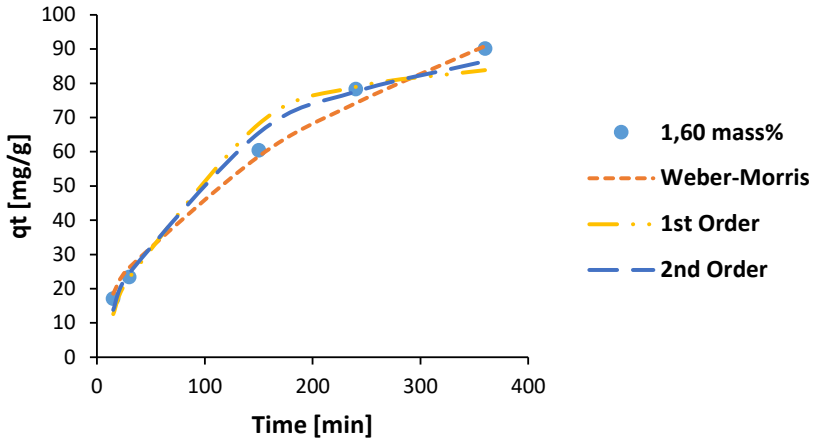

a) 1-decanol kinetic model fits at 35 °C and 1,60 initial mass% of alcohol in solution

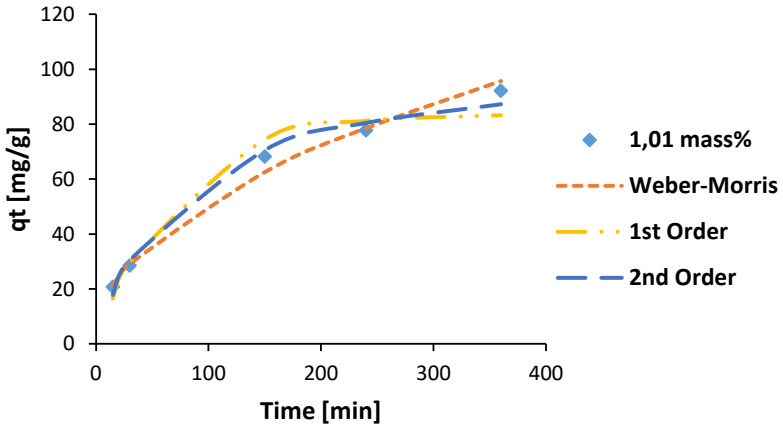

b) 1-decanol kinetic model fits at 35 °C and 1,01 initial mass% of alcohol in solution

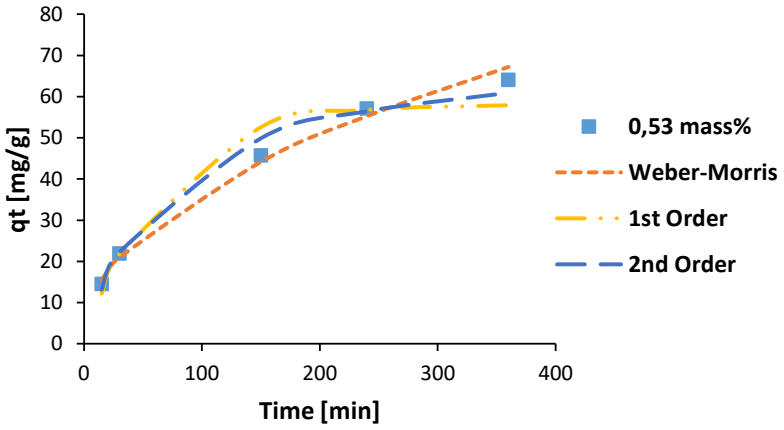

c) 1-decanol kinetic model fits at 35 °C and 0,53 initial mass% of alcohol in solution

Figure 8-37: The kinetic modelling results for 1-decanol at solution initial alcohol mass percentages of a) 1,60, b) 1,01 and c) 0,53 adsorbed onto Selexsorb® CD at a temperature of 35 °C.

8.22 Selexsorb® CDx Kinetic Modelling graphs

Figure 8-38, Figure 8-39 and Figure 8-40 give the kinetic modelling results for 1-hexanol adsorbed onto Selexsorb® CDx at temperatures of 25, 30 and 35 °C respectively.

Figure 8-41, Figure 8-42 and Figure 8-43 give the kinetic modelling results for 1-hexanol adsorbed onto Selexsorb® CDx at temperatures of 25, 30 and 35 °C respectively.

Figure 8-44, Figure 8-45 and Figure 8-46 give the kinetic modelling results for 1-hexanol adsorbed onto Selexsorb® CDx at temperatures of 25, 30 and 35 °C respectively.

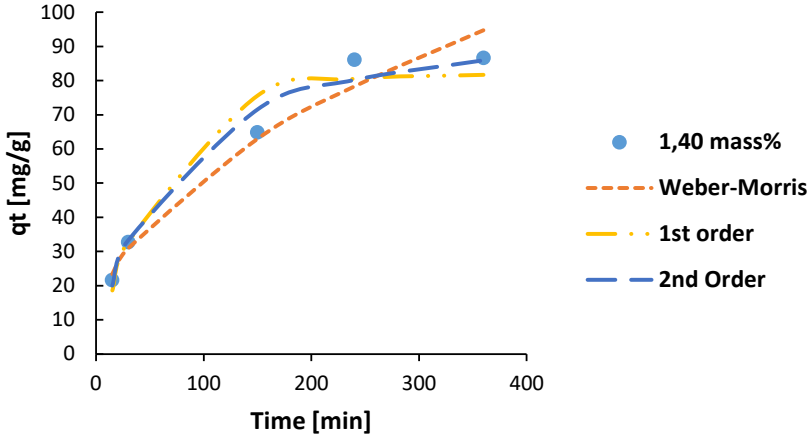

a) 1-hexanol kinetic model fits at 25 °C and 1,40 initial mass% of alcohol in solution

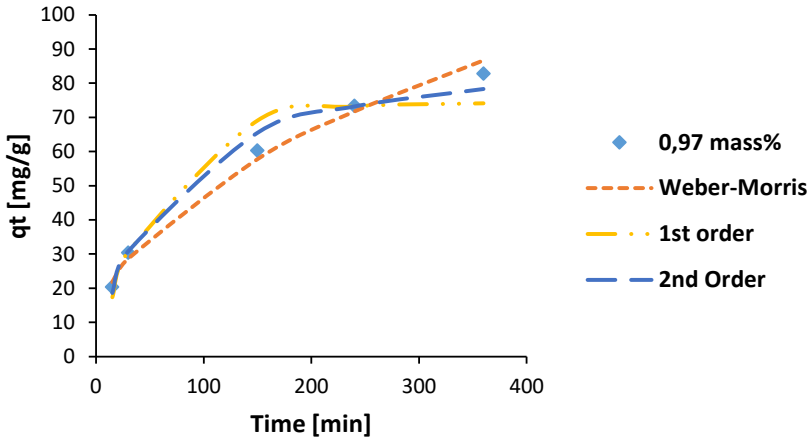

b) 1-hexanol kinetic model fits at 25 °C and 0,97 initial mass% of alcohol in solution

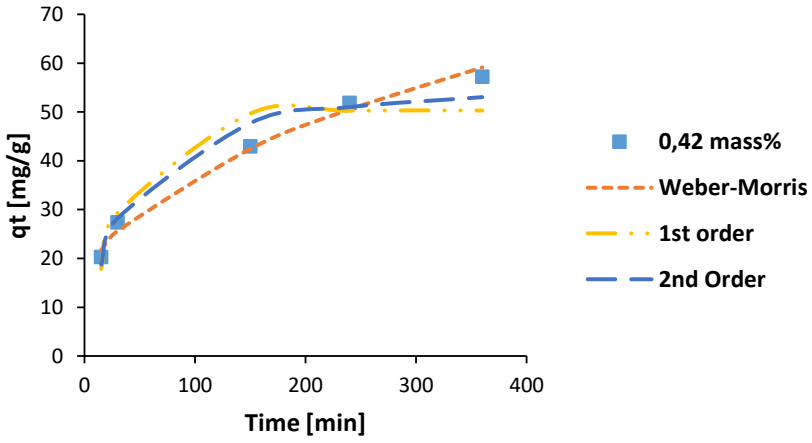

c) 1-hexanol kinetic model fits at 25 °C and 0,42 initial mass% of alcohol in solution

Figure 8-38: The kinetic modelling results for 1-hexanol at solution initial alcohol mass percentages of a) 1,40, b) 0,97 and c) 0,42 adsorbed onto Selexsorb® CDx at a temperature of 25 °C.

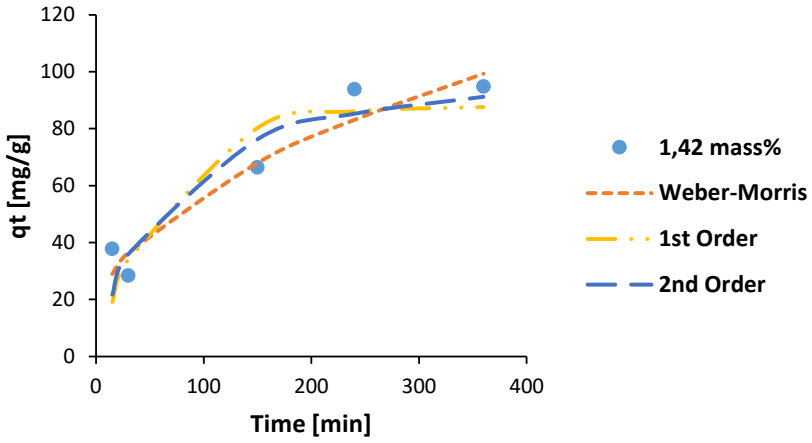

a) 1-hexanol kinetic model fits at 30 °C and 1,42 initial mass% of alcohol in solution

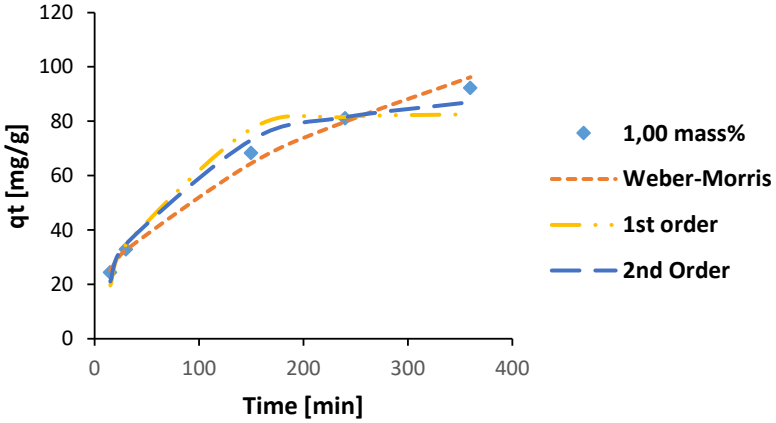

b) 1-hexanol kinetic model fits at 30 °C and 1,00 initial mass% of alcohol in solution

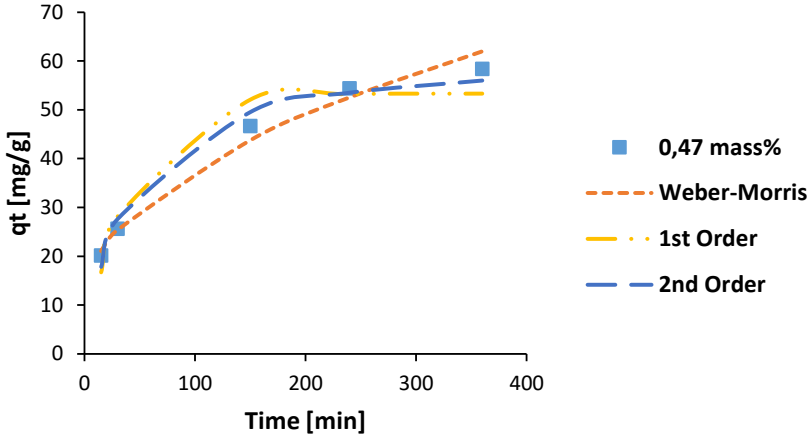

c) 1-hexanol kinetic model fits at 30 °C and 0,47 initial mass% of alcohol in solution

Figure 8-39: The kinetic modelling results for 1-hexanol at solution initial alcohol mass percentages of a) 1,42, b) 1,00 and c) 0,47 adsorbed onto Selexsorb® CDx at a temperature of 30 °C.

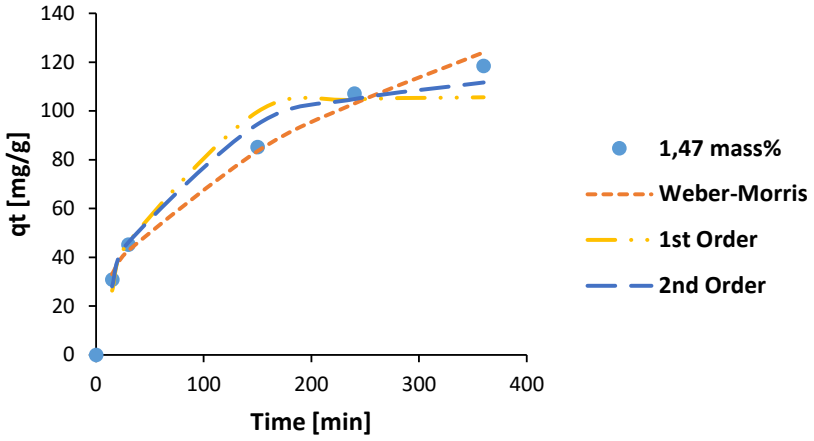

a) 1-hexanol kinetic model fits at 35 °C and 1,47 initial mass% of alcohol in solution

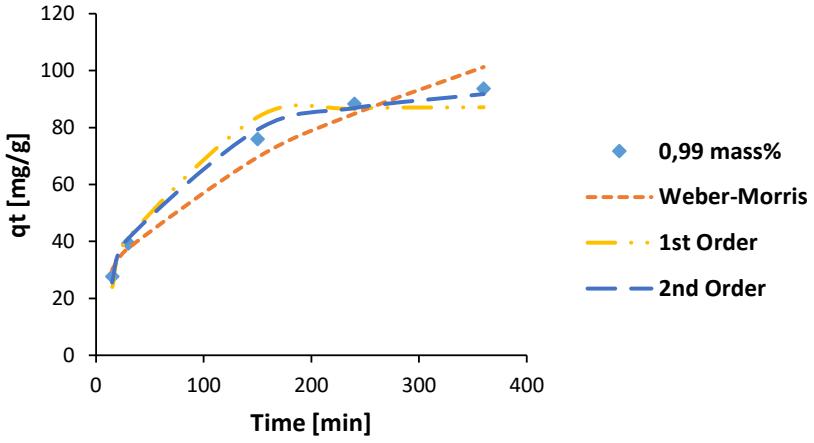

b) 1-hexanol kinetic model fits at 35 °C and 0,99 initial mass% of alcohol in solution

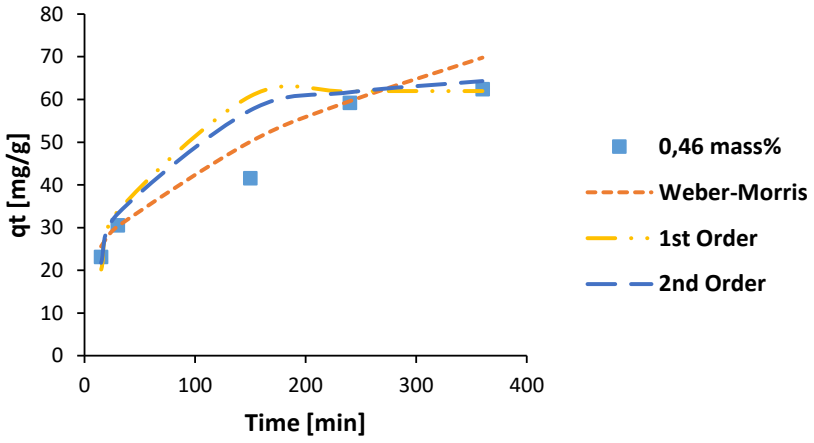

c) 1-hexanol kinetic model fits at 35 °C and 0,46 initial mass% of alcohol in solution

Figure 8-40: The kinetic modelling results for 1-hexanol at solution initial alcohol mass percentages of a) 1,47, b) 0,99 and c) 0,46 adsorbed onto Selexsorb® CDx at a temperature of 35 °C.

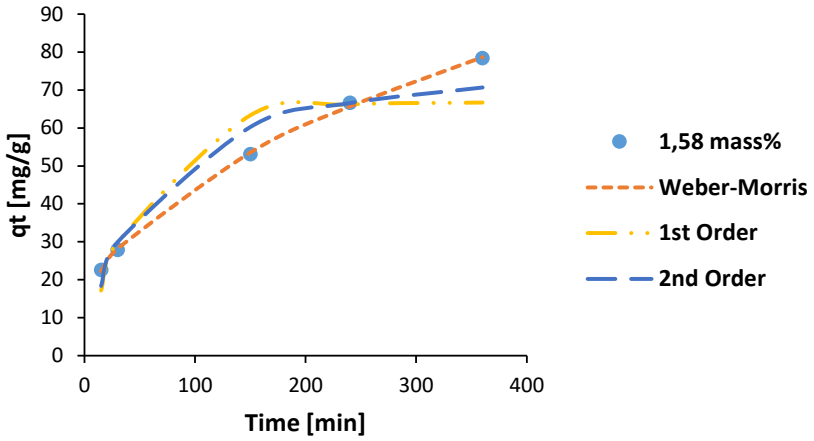

a) 1-octanol kinetic model fits at 25 °C and 1,58 initial mass% of alcohol in solution

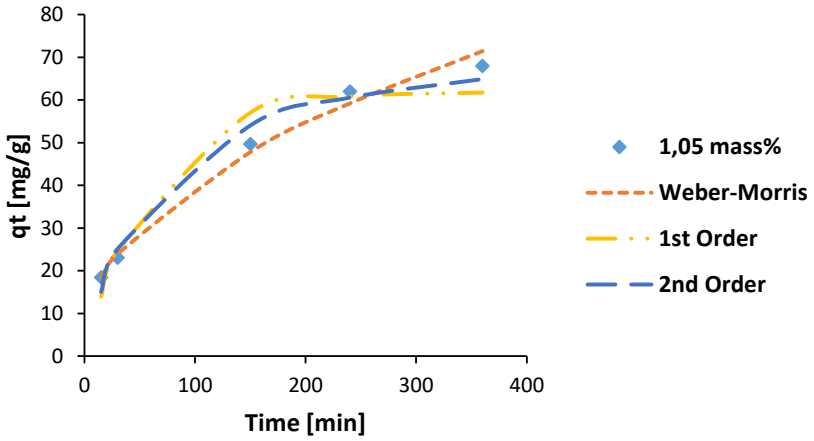

b) 1-octanol kinetic model fits at 25 °C and 1,05 initial mass% of alcohol in solution

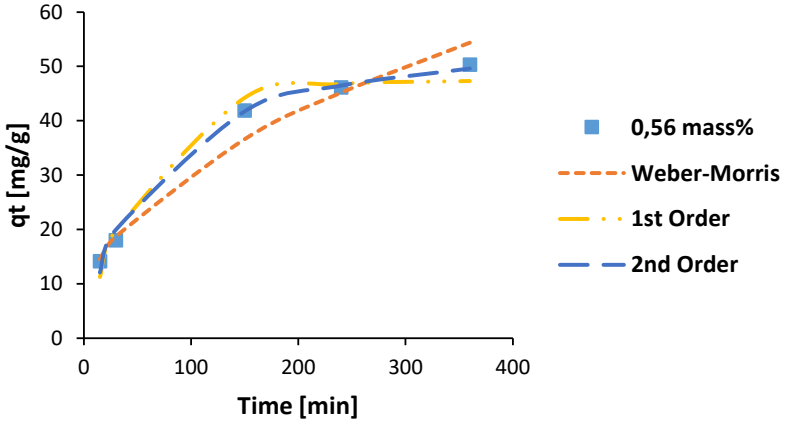

c) 1-octanol kinetic model fits at 25 °C and 0,56 initial mass% of alcohol in solution

Figure 8-41: The kinetic modelling results for 1-octanol at solution initial alcohol mass percentages of a) 1,58, b) 1,05 and c) 0,56 adsorbed onto Selexsorb® CDx at a temperature of 25 °C.

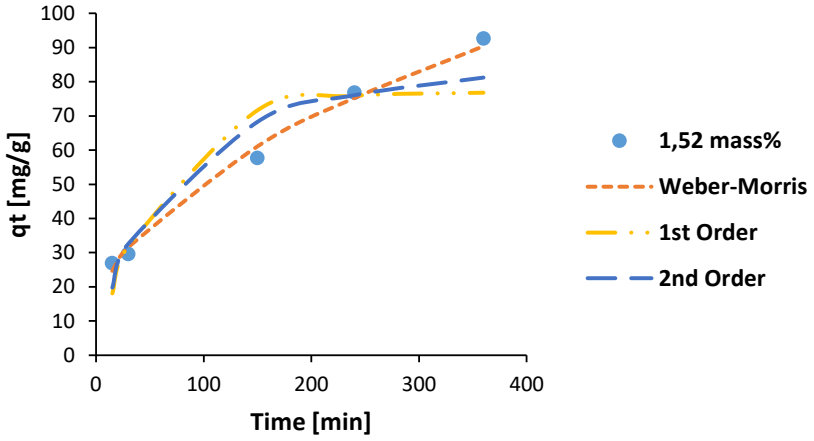

a) 1-octanol kinetic model fits at 30 °C and 1,52 initial mass% of alcohol in solution

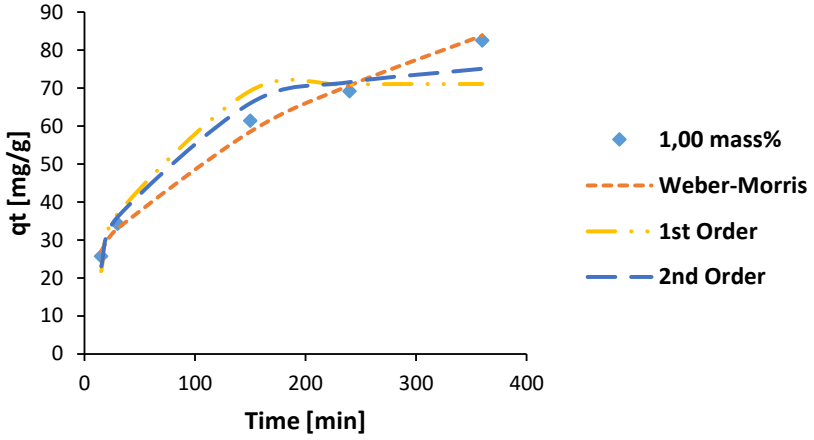

b) 1-octanol kinetic model fits at 30 °C and 1,00 initial mass% of alcohol in solution

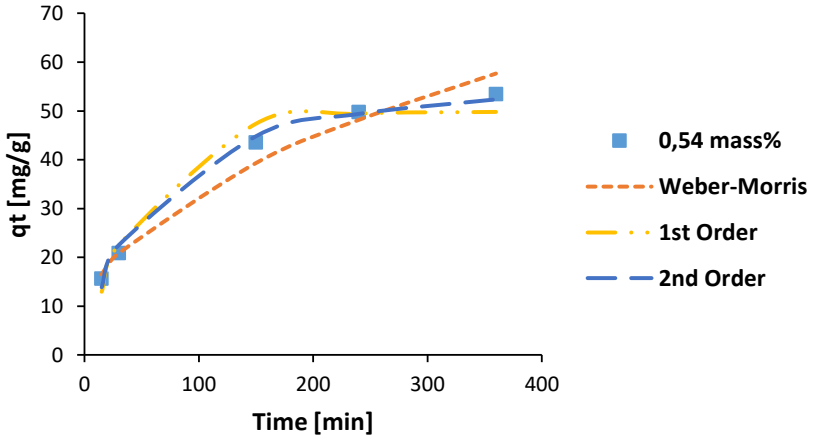

c) 1-octanol kinetic model fits at 30 °C and 0,54 initial mass% of alcohol in solution

Figure 8-42: The kinetic modelling results for 1-octanol at solution initial alcohol mass percentages of a) 1,52, b) 1,00 and c) 0,54 adsorbed onto Selexsorb® CDx at a temperature of 30 °C.

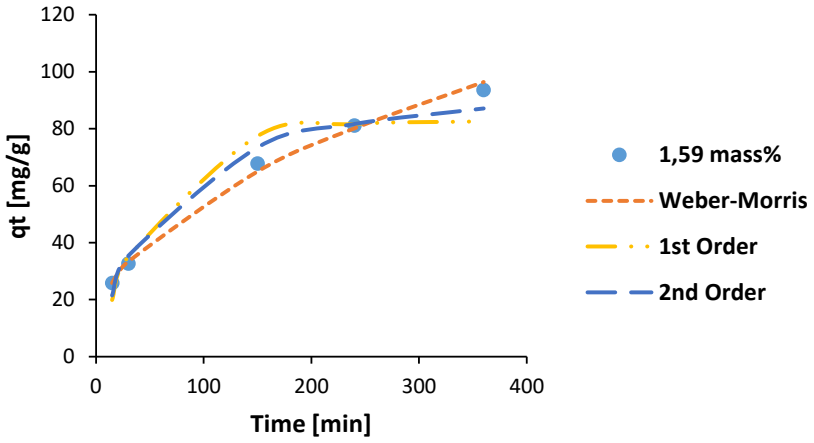

a) 1-octanol kinetic model fits at 35 °C and 1,59 initial mass% of alcohol in solution

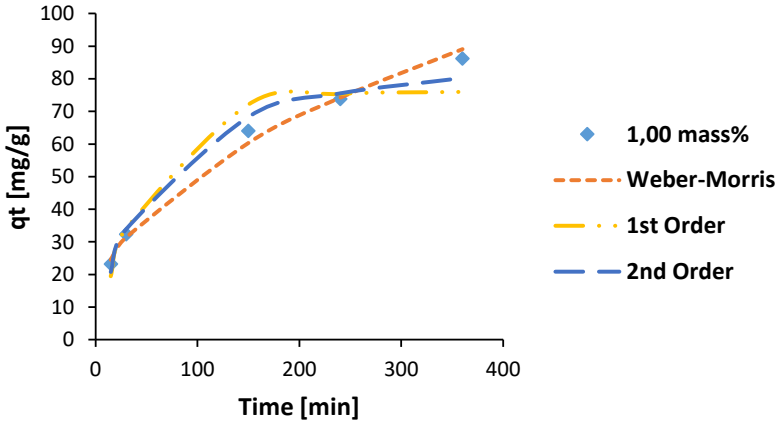

b) 1-octanol kinetic model fits at 35 °C and 1,00 initial mass% of alcohol in solution

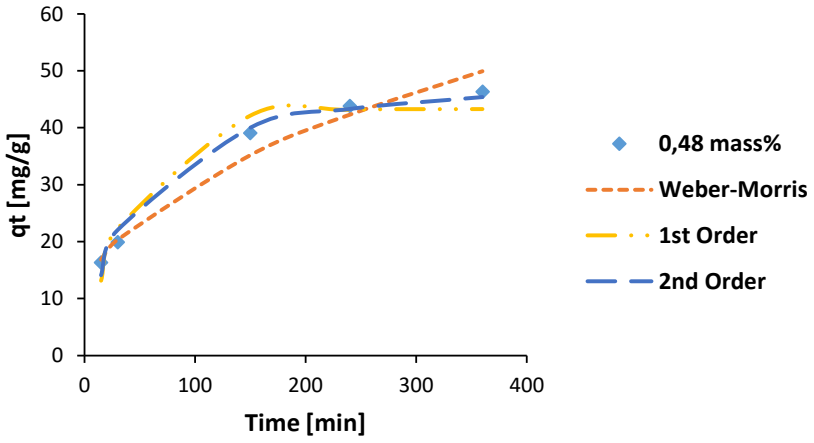

c) 1-octanol kinetic model fits at 35 °C and 0,48 initial mass% of alcohol in solution

Figure 8-43: The kinetic modelling results for 1-octanol at solution initial alcohol mass percentages of a) 1,59, b) 1,00 and c) 0,48 adsorbed onto Selexsorb® CDx at a temperature of 35 °C.

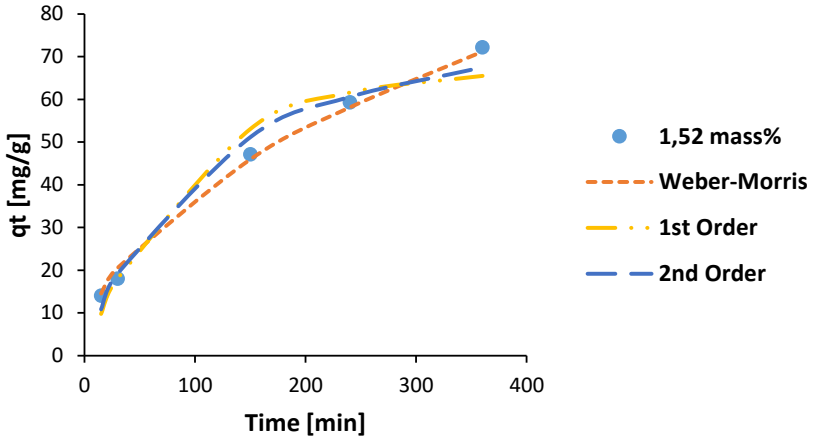

a) 1-decanol kinetic model fits at 25 °C and 1,52 initial mass% of alcohol in solution

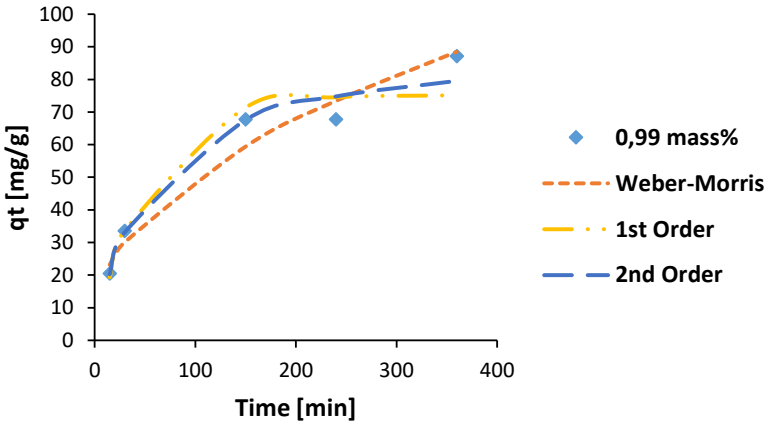

b) 1-decanol kinetic model fits at 30 °C and 0,99 initial mass% of alcohol in solution

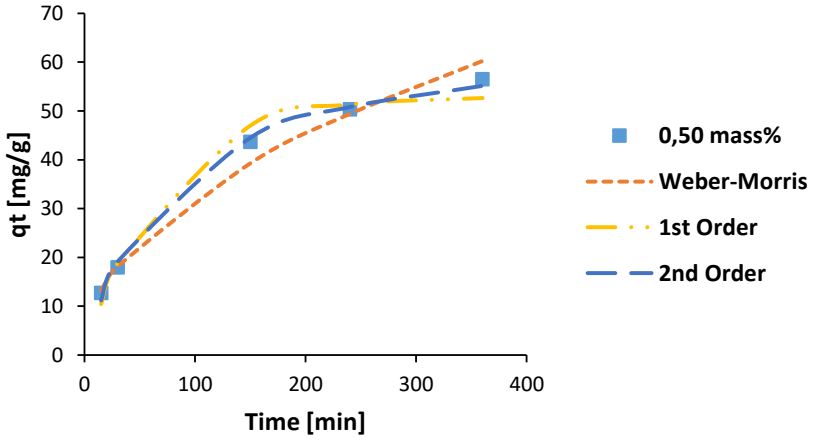

c) 1-decanol kinetic model fits at 25 °C and 0,50 initial mass% of alcohol in solution

Figure 8-44: The kinetic modelling results for 1-decanol at solution initial alcohol mass percentages of a) 1,52, b) 0,99 and c) 0,50 adsorbed onto Selexsorb® CDx at a temperature of 25 °C.

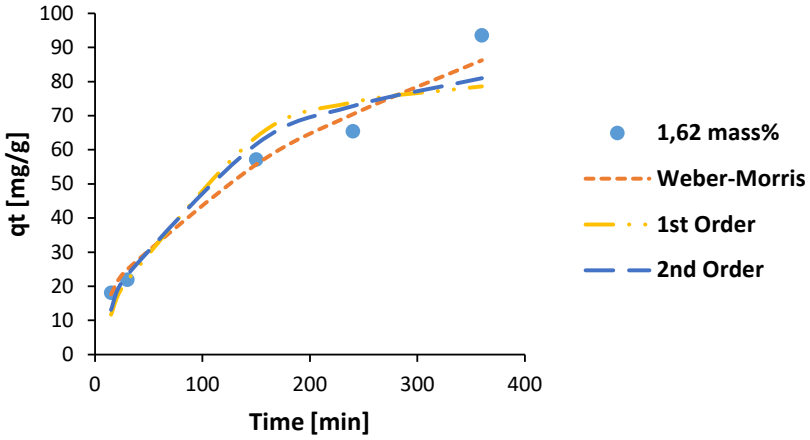

a) 1-decanol kinetic model fits at 30 °C and 1,62 initial mass% of alcohol in solution

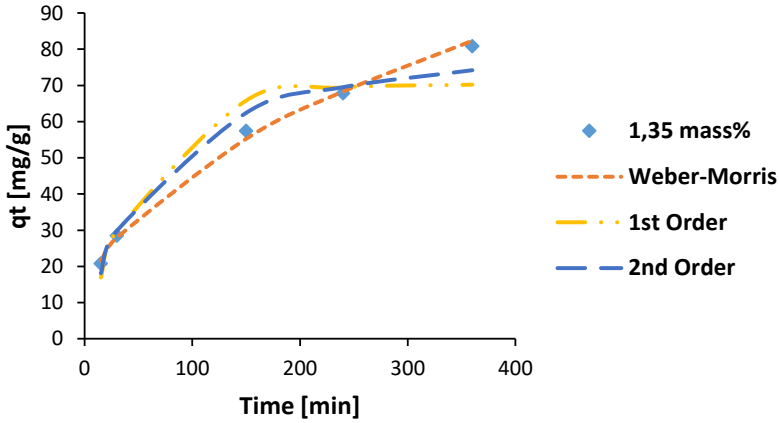

b) 1-decanol kinetic model fits at 30 °C and 1,35 initial mass% of alcohol in solution

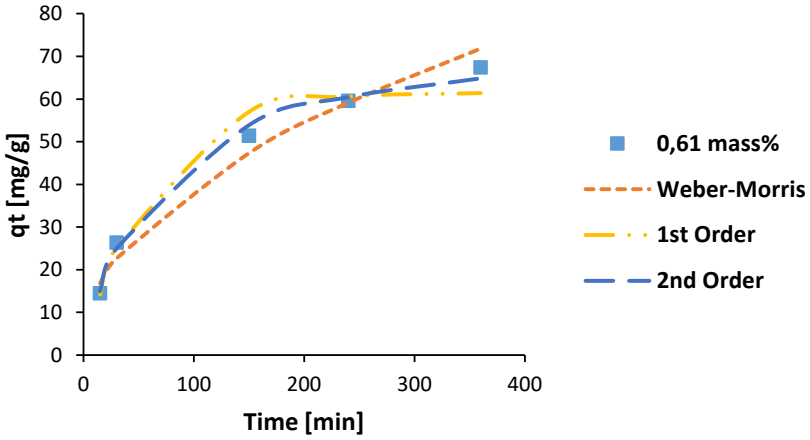

c) 1-decanol kinetic model fits at 30 °C and 0,61 initial mass% of alcohol in solution

Figure 8-45: The kinetic modelling results for 1-decanol at solution initial alcohol mass percentages of a) 1,62, b) 1,35 and c) 0,61 adsorbed onto Selexsorb® CDx at a temperature of 30 °C.

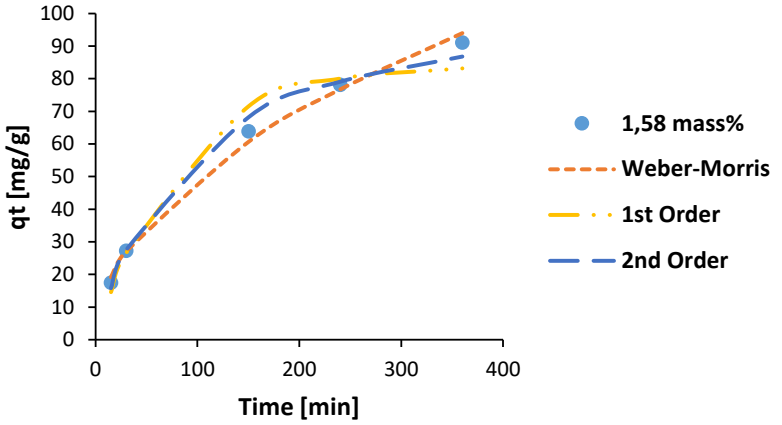

a) 1-decanol kinetic model fits at 35 °C and 1,58 initial mass% of alcohol in solution

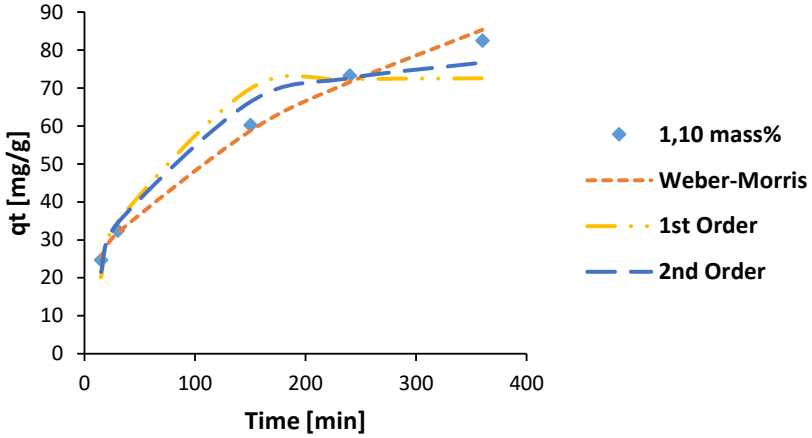

b) 1-decanol kinetic model fits at 35 °C and 1,10 initial mass% of alcohol in solution

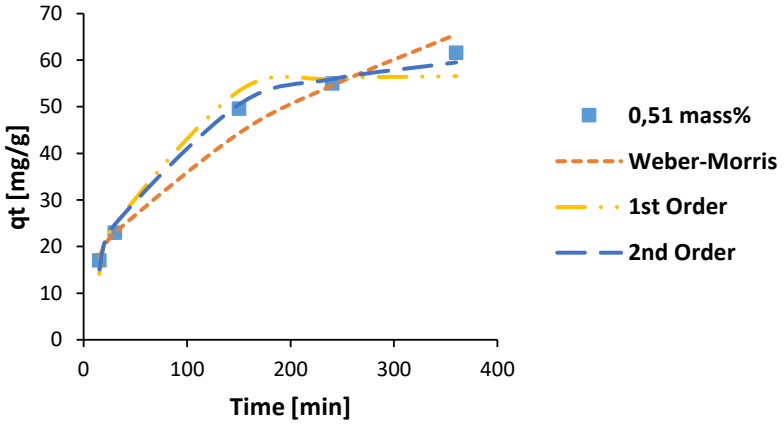

c) 1-decanol kinetic model fits at 35 °C and 0,51 initial mass% of alcohol in solution

Figure 8-46: The kinetic modelling results for 1-decanol at solution initial alcohol mass percentages of a) 1,58, b) 1,10 and c) 0,51 adsorbed onto Selexsorb® CDx at a temperature of 35 °C.

8.23 Adsorption-Regeneration Raw Experimental Data

The adsorption-regeneration raw experimental data is shown below. The adsorption GC results are given for each adsorbent after each adsorption cycle for each regeneration temperature.

8.23.1. 185 °C raw experimental adsorption data

Table 8-31, Table 8-32, Table 8-33, Table 8-34, Table 8-35, Table 8-36, Table 8-37 and Table 8-38 contain the raw experimental data for the adsorption runs in the 185 °C regeneration temperature runs for each cycle performed.

Table 8-31: Raw experimental data for adsorption cycle 1 in adsorption-regeneration experiments performed at 185° C

CYCLE 1	**SCDx**		**SCD**		**F-220**	
	n-decane	1-hexanol	*n*-decane	1-hexanol	*n*-decane	1-hexanol
Time (min)	**Mass (mg)**					
0	63,2122	0,9081	64,5768	0,9291	63,6541	0,9173
0	63,0703	0,9048	64,3894	0,9309	65,4685	0,9427
15	65,1028	0,8306	63,2176	0,8015	62,3885	0,7928
30	65,3767	0,7396	64,8852	0,7781	64,6982	0,6699
150	62,8524	0,5992	65,5190	0,6114	64,3382	0,6115
240	62,1666	0,5303	62,9202	0,5181	64,0741	0,5220
360	65,5936	0,5190	64,9546	0,4713	64,7476	0,4477
390	65,4453	0,5131	62,3550	0,4349	63,5593	0,4747
1244	64,4389	0,3656	64,1917	0,2534	64,5236	0,3257
1330	62,8841	0,3410	64,6073	0,2557	63,5316	0,3597
1350	63,1096	0,3599	63,6034	0,2523	64,3358	0,3650
1358	60,7145	0,3441	57,1081	0,2056	62,6764	0,3538

Table 8-32: Raw experimental data for adsorption cycle 2 in adsorption-regeneration experiments performed at 185° C

CYCLE 2	SCDx		SCD		F-220	
	n-decane	1-hexanol	*n*-decane	1-hexanol	*n*-decane	1-hexanol
Time (min)	**Mass (mg)**					
0	60,8564	0,9175	63,8564	0,9670	64,5738	0,9790
0	64,8993	0,9719	64,0290	0,9649	65,1021	0,9945
15	64,8375	0,8654	65,7297	0,8684	63,4346	0,8529
30	64,1147	0,6604	65,1509	0,8147	66,4658	0,8455
150	64,8603	0,6708	64,8275	0,6355	65,3036	0,6669
240	64,6184	0,6033	67,0220	0,5799	63,1477	0,5755
360	57,9839	0,4721	64,6647	0,4904	63,9741	0,5339
390	65,1944	0,5453	63,1872	0,4814	58,8035	0,4744
1245	64,6753	0,3808	64,5198	0,2836	64,3811	0,3971
1330	66,1183	0,3826	65,2183	0,2808	65,3567	0,3969
1380	64,0189	0,3707	64,7154	0,2722	63,8101	0,3918
1389	64,6989	0,3842	65,1556	0,2696	64,6789	0,3963

Table 8-33: Raw experimental data for adsorption cycle 3 in adsorption-regeneration experiments performed at 185° C

CYCLE 3	SCDx		SCD		F-220	
	n-decane	1-hexanol	*n*-decane	1-hexanol	*n*-decane	1-hexanol
Time (min)	**Mass (mg)**					
0	64,6446	0,9902	66,0080	0,9681	64,8544	0,9336
0	65,1420	1,0020	66,0964	0,9762	65,5614	0,9207
15	64,2972	0,8829	66,7964	0,8331	66,9722	0,8602
32	65,3740	0,8553	65,8902	0,8161	65,0761	0,7860
150	65,5167	0,6787	66,6284	0,6433	65,7317	0,6262
240	66,6175	0,6195	66,5688	0,5475	66,2478	0,6013
360	64,9616	0,5557	65,7495	0,4946	64,8841	0,4680
390	65,6123	0,5541	68,6208	0,5005	65,5189	0,4935
1230	62,5506	0,3700	66,7652	0,2798	66,0777	0,3858
1320	65,3668	0,3895	65,8206	0,2656	65,2942	0,3846
1400	64,5791	0,3833	65,2791	0,2459	66,3632	0,3963
1408	65,2197	0,3879	66,0601	0,2621	66,8510	0,4004

Table 8-34: Raw experimental data for adsorption cycle 4 in adsorption-regeneration experiments performed at 185° C

CYCLE 4	SCDx		SCD		F-220	
	n-decane	1-hexanol	*n*-decane	1-hexanol	*n*-decane	1-hexanol
Time (min)	**Mass (mg)**					
0	60,6487	0,9238	63,6216	0,9786	62,0258	0,9576
0	65,1416	0,9884	63,7612	0,9777	62,6833	0,9868
15	64,7468	0,8721	62,4679	0,8533	62,4070	0,8649
32	66,3425	0,8478	64,9056	0,8277	61,5426	0,8002
150	65,5346	0,6806	59,1156	0,5461	64,7433	0,6760
240	63,1983	0,6160	62,7040	0,5658	62,7047	0,4448
360	63,5110	0,5175	64,1565	0,5017	62,5811	0,5259
390	64,1102	0,5525	64,3430	0,4897	63,1718	0,5230
1280	64,9619	0,3988	62,9051	0,2816	62,3098	0,4078
1425	63,8384	0,3946	64,3494	0,2693	64,1822	0,3112
1492	63,7956	0,3988	61,3808	0,2551	63,8772	0,4017
1500	63,7364	0,3893	63,4842	0,2635	63,9611	0,4030

Table 8-35: Raw experimental data for adsorption cycle 5 in adsorption-regeneration experiments performed at 185° C

CYCLE 5	SCDx		SCD		F-220	
	n-decane	1-hexanol	*n*-decane	1-hexanol	*n*-decane	1-hexanol
Time (min)	**Mass (mg)**					
0	62,8730	0,9533	64,0683	0,9685	67,9969	1,0353
0	63,8337	0,9689	64,3177	0,9743	65,5266	1,0032
15	65,2688	0,8778	67,0557	0,9048	65,8320	0,9031
30	64,1982	0,8235	66,3059	0,8457	64,3353	0,8279
150	67,0275	0,6947	66,2884	0,6868	65,8283	0,6674
240	63,7564	0,6079	65,3791	0,5830	65,0398	0,5999
360	67,1955	0,5566	64,7281	0,5012	65,2248	0,5403
390	63,8562	0,5421	66,6218	0,5024	65,9516	0,5363
1280	65,6382	0,4639	64,9207	0,3184	69,2900	0,4657
1320	64,0397	0,4527	66,3438	0,3221	66,9839	0,4502
1360	65,6331	0,4615	67,0324	0,3251	64,1388	0,4270
1368	65,4350	0,4660	68,0894	0,3309	66,4452	0,4436

Table 8-36: Raw experimental data for adsorption cycle 6 in adsorption-regeneration experiments performed at 185° C

CYCLE 6	SCDx		SCD		F-220	
	n-decane	1-hexanol	*n*-decane	1-hexanol	*n*-decane	1-hexanol
Time (min)	**Mass (mg)**					
0	66,4650	1,0476	65,0177	1,0109	65,0743	1,0113
0	65,8029	1,0419	69,6332	1,0925	66,2632	1,0348
15	63,5540	0,8824	65,3042	0,8960	65,3156	0,9089
30	65,4444	0,8784	65,4069	0,8618	64,9221	0,8554
160	64,6633	0,6968	67,1227	0,6766	66,6001	0,6965
360	65,7882	0,6039	65,9706	0,5315	67,0998	0,5840
390	67,5477	0,6069	66,4982	0,5151	65,6986	0,5580
430	67,0533	0,5190	64,5655	0,4189	65,2432	0,5453
1340	67,7736	0,4211	65,9337	0,3330	65,5456	0,4632
1490	64,7100	0,4852	66,6149	0,2844	66,1908	0,4611
1510	67,2460	0,4985	66,9446	0,3277	66,4790	0,4606
1528	66,7820	0,4895	65,9287	0,3180	66,2979	0,4547

Table 8-37: Raw experimental data for adsorption cycle 7 in adsorption-regeneration experiments performed at 185° C

CYCLE 7	SCDx		SCD		F-220	
	n-decane	1-hexanol	*n*-decane	1-hexanol	*n*-decane	1-hexanol
Time (min)	**Mass (mg)**					
0	65,6327	1,0212	66,1871	1,0385	65,2364	1,0175
0	63,2914	0,9299	66,1201	1,0280	65,3613	0,9903
15	65,5135	0,9061	65,9130	0,9119	65,1187	0,7972
30	65,4193	0,8534	66,5993	0,8650	65,6936	0,8625
150	65,4193	0,6672	61,6396	0,6281	66,0745	0,6946
240	66,7082	0,6497	67,2155	0,6119	67,0829	0,6511
330	66,7223	0,6089	66,2529	0,5539	66,2979	0,6059
360	67,0504	0,5990	66,7715	0,4840	66,2228	0,5956
1295	66,7132	0,5508	67,3667	0,3654	64,2576	0,5342
1335	67,1258	0,5619	67,4735	0,3659	64,5902	0,5383
1385	66,5364	0,5665	65,5624	0,3546	64,9925	0,5426
1393	65,3458	0,5461	66,8419	0,3601	65,8795	0,5517

Table 8-38: Raw experimental data for adsorption cycle 8 in adsorption-regeneration experiments performed at 185° C

CYCLE 8	SCDx		SCD		F-220	
	n-decane	1-hexanol	*n*-decane	1-hexanol	*n*-decane	1-hexanol
Time (min)	**Mass (mg)**					
0	64,6669	0,9986	64,6012	0,9879	64,4093	1,0168
0	62,5977	0,9529	64,7166	0,9824	63,5422	0,9904
15	65,5969	0,8669	65,9260	0,8533	63,2621	0,8160
30	65,6097	0,8070	65,5860	0,7905	64,9164	0,7722
140	65,1980	0,6950	65,0885	0,6211	63,8625	0,6762
240	64,5410	0,6809	65,1525	0,5861	65,3975	0,6756
270	64,9502	0,6853	65,6980	0,5943	65,2218	0,6830
300	64,7094	0,6798	66,8154	0,3837	65,1038	0,6667
1400	65,7510	0,6298	66,7392	0,5100	64,4441	0,6012
1470	66,2437	0,6275	66,6571	0,5110	65,2641	0,6027
1525	66,0082	0,6291	65,0772	0,4986	63,9552	0,5959
1537	65,8091	0,6122	64,7022	0,4904	64,4212	0,5961

8.23.2. 205 °C raw experimental adsorption data

Table 8-39, Table 8-40, Table 8-42, Table 8-43, Table 8-44, Table 8-45 and Table 8-46 contain the raw experimental data for the adsorption runs in the 205 °C regeneration temperature runs for each cycle performed.

Table 8-39: Raw experimental data for adsorption cycle 1 in adsorption-regeneration experiments performed at 205° C

CYCLE 1	**SCDx**		**SCD**		**F-220**	
	n-decane	1-hexanol	*n*-decane	1-hexanol	*n*-decane	1-hexanol
Time (min)	**Mass (mg)**					
0	64,6451	0,9263	61,6224	0,8868	65,5950	0,9411
0	65,8608	0,9447	63,9895	0,9228	64,0606	0,9167
15	64,6622	0,8224	64,2502	0,7824	62,1716	0,7865
35	64,0946	0,7619	65,0788	0,7607	65,1715	0,7687
150	65,3152	0,6403	66,3814	0,6080	64,3750	0,5004
240	68,9566	0,5467	65,8598	0,5361	65,7781	0,5452
360	64,5925	0,5184	64,3003	0,4605	62,1835	0,4646
390	64,9816	0,5176	63,8887	0,4426	62,0535	0,4222
1350	63,7811	0,4644	64,9572	0,2833	65,1315	0,4196
1485	64,5047	0,4696	65,8409	0,2810	61,8900	0,3899
1526	64,7738	0,4677	65,9693	0,2450	53,5024	0,3332
1537	62,6550	0,4571	66,6087	0,2583	64,6889	0,4150

Table 8-40: Raw experimental data for adsorption cycle 2 in adsorption-regeneration experiments performed at 205° C

CYCLE 2	SCDx		SCD		F-220	
	n-decane	1-hexanol	*n*-decane	1-hexanol	*n*-decane	1-hexanol
Time (min)	**Mass (mg)**					
0	63,8349	0,9240	64,2779	0,9265	63,4938	0,9245
0	62,0147	0,8945	63,6594	0,9228	63,1737	0,8834
15	64,2338	0,7545	64,3180	0,8083	65,4738	0,8393
35	65,3016	0,8068	63,5815	0,7651	62,3367	0,7316
150	65,3150	0,6321	64,6451	0,6064	62,1986	0,5612
240	64,5628	0,5667	64,9952	0,5324	62,7856	0,5248
360	62,9139	0,5019	64,6755	0,4669	61,6676	0,4686
390	63,9229	0,5006	65,1511	0,4574	62,1436	0,4340
1350	65,8356	0,3968	63,7631	0,2458	64,4541	0,3784
1485	64,3971	0,3952	64,9192	0,2830	64,7559	0,3811
1525	64,7072	0,4006	63,5462	0,2830	65,6434	0,3879
1529	65,5226	0,4005	59,8231	0,2824	62,7644	0,3713

Table 8-41: Raw experimental data for adsorption cycle 3 in adsorption-regeneration experiments performed at 205° C

CYCLE 3	SCDx		SCD		F-220	
	n-decane	1-hexanol	*n*-decane	1-hexanol	*n*-decane	1-hexanol
Time (min)	**Mass (mg)**					
0	64,0641	0,9640	65,7475	0,9895	65,8319	0,9927
0	62,9987	0,9516	65,4899	0,9730	65,7782	0,9943
15	62,6914	0,8475	64,6552	0,8517	66,4330	0,8881
30	64,2523	0,8217	64,9536	0,8068	66,3596	0,8464
146	64,6753	0,6534	66,1663	0,6494	66,3824	0,6466
244	65,7411	0,5992	65,7642	0,5681	66,1968	0,6100
360	65,9400	0,5577	66,4125	0,5130	66,1621	0,5501
390	61,3922	0,5336	66,7946	0,5016	65,6098	0,5405
1335	64,9977	0,3892	65,6944	0,2767	65,9342	0,4177
1430	65,0853	0,3871	64,9836	0,2723	67,5013	0,4380
1465	64,9940	0,3986	62,9111	0,2511	65,1697	0,4214
1476	58,4305	0,3512	67,7256	0,2736	65,0153	0,4153

Table 8-42: Raw experimental data for adsorption cycle 4 in adsorption-regeneration experiments performed at 205° C

CYCLE 4	SCDx		SCD		F-220	
	n-decane	1-hexanol	*n*-decane	1-hexanol	*n*-decane	1-hexanol
Time (min)	**Mass (mg)**					
0	65,6636	0,8660	64,6236	0,9702	66,0961	0,9954
0	64,3590	0,9665	65,8612	0,8755	66,6041	0,8432
15	65,3796	0,8748	66,7648	0,8308	66,1187	0,8796
30	66,7260	0,7134	67,0070	0,8552	67,3093	0,8469
154	65,6572	0,6661	66,8629	0,6494	65,6408	0,6548
240	66,1173	0,5279	66,6060	0,5753	65,7836	0,6029
360	65,5798	0,5617	66,2203	0,5129	66,4567	0,5526
390	63,7662	0,4917	66,1024	0,4964	65,9394	0,5435
1203	65,9572	0,4409	66,0531	0,2511	66,1759	0,4079
1244	65,4695	0,4142	65,6248	0,2827	66,4106	0,4320
1350	66,6593	0,4432	66,8534	0,2804	65,2643	0,4201
1358	66,4561	0,4380	65,6366	0,2715	65,3152	0,4205

Table 8-43: Raw experimental data for adsorption cycle 5 in adsorption-regeneration experiments performed at 205° C

CYCLE 5	SCDx		SCD		F-220	
	n-decane	1-hexanol	*n*-decane	1-hexanol	*n*-decane	1-hexanol
Time (min)	**Mass (mg)**					
0	65,0468	0,9754	65,3815	0,7823	65,0786	0,7441
0	66,0524	0,9836	64,4588	0,7666	65,0484	1,0039
15	65,5634	0,8636	64,3107	0,6655	64,3191	0,8793
30	65,4008	0,8149	64,3813	0,5898	65,6498	0,8549
150	65,8820	0,6006	64,6888	0,4710	65,9147	0,5031
240	64,1307	0,5979	64,2876	0,3866	64,9997	0,4382
360	64,9913	0,5585	63,8818	0,3290	65,7888	0,4049
390	65,6227	0,5408	63,0030	0,3241	66,4890	0,3974
1210	66,7919	0,4543	63,8309	0,1837	65,7300	0,3358
1313	66,8729	0,4520	53,3835	0,1165	64,5146	0,2885
1427	65,9337	0,4611	64,6311	0,1657	65,6113	0,3190
1437	65,7876	0,4200	67,3500	0,2050	65,9700	0,3136

Table 8-44: Raw experimental data for adsorption cycle 6 in adsorption-regeneration experiments performed at 205° C

CYCLE 6	SCDx		SCD		F-220	
	n-decane	1-hexanol	*n*-decane	1-hexanol	*n*-decane	1-hexanol
Time (min)	**Mass (mg)**					
0	66,4262	1,0056	65,7855	0,9843	67,6233	1,0271
0	65,4401	0,9941	65,7904	0,9960	65,7218	0,9950
15	64,5458	0,8633	66,1060	0,8728	66,8795	0,8985
30	65,3996	0,8232	67,7350	0,8434	66,8281	0,8392
150	63,4623	0,6487	67,8076	0,6664	66,4585	0,6747
240	65,4306	0,6123	66,7592	0,5115	65,8351	0,6038
360	66,4315	0,5728	66,9699	0,4161	65,6700	0,5405
390	64,8787	0,5503	66,5148	0,4982	64,6248	0,5254
1260	64,8365	0,4981	65,8361	0,1921	57,8834	0,3876
1350	66,1634	0,4982	66,2799	0,3280	67,5773	0,4553
1380	65,7669	0,4965	62,5748	0,3061	65,2296	0,4450
1388	65,8699	0,4991	65,8211	0,3250	67,1725	0,4506

Table 8-45: Raw experimental data for adsorption cycle 7 in adsorption-regeneration experiments performed at 205° C

CYCLE 7	SCDx		SCD		F-220	
	n-decane	1-hexanol	*n*-decane	1-hexanol	*n*-decane	1-hexanol
Time (min)	**Mass (mg)**					
0	67,1396	0,9993	66,1338	0,9724	65,2187	0,9992
0	64,1156	0,9632	64,8259	0,9740	66,0734	1,0234
15	65,8856	0,8578	66,1798	0,8583	65,9343	0,8583
30	67,0972	0,8212	66,1884	0,7575	65,5187	0,7918
240	66,7881	0,6058	67,0132	0,5558	64,4918	0,5675
300	66,9869	0,5866	66,2347	0,5217	65,9353	0,5719
360	66,7700	0,5733	66,7939	0,5017	65,6383	0,5715
390	67,0967	0,5716	66,4272	0,4918	65,3333	0,5382
1350	66,9807	0,5970	65,6848	0,3996	66,4139	0,5573
1395	65,6202	0,5791	65,6247	0,4063	66,1252	0,5562
1480	66,4620	0,5800	65,3635	0,3999	66,0426	0,5387
1489	63,9215	0,5478	65,7829	0,4034	65,2220	0,5451

Table 8-46: Raw experimental data for adsorption cycle 8 in adsorption-regeneration experiments performed at 205° C

CYCLE 8	SCDx		SCD		F-220	
	n-decane	1-hexanol	*n*-decane	1-hexanol	*n*-decane	1-hexanol
Time (min)	**Mass (mg)**					
0	67,1308	0,8138	67,0583	1,0427	65,8209	1,0153
0	65,4223	1,0020	66,3112	1,0331	65,8788	0,6714
15	66,6648	0,8958	66,3743	0,9042	65,0841	0,8948
30	67,4491	0,8511	66,3994	0,8566	66,3582	0,6403
252	66,4686	0,4820	54,7799	0,5474	64,4925	0,6712
300	66,8784	0,6206	66,0300	0,5835	64,8020	0,6036
360	67,3837	0,5803	66,7548	0,5259	67,0705	0,5647
406	59,2164	0,4951	65,8548	0,5033	64,7715	0,5343
1305	59,5114	0,4186	67,0288	0,3196	66,3359	0,4617
1350	59,4115	0,4192	67,0458	0,3195	64,7823	0,4562
1365	59,9440	0,4212	64,4059	0,3030	66,5610	0,4613
1372	61,4122	0,4336	66,4522	0,3137	67,6233	0,1067